University of Wisconsin Milwaukee
UWM Digital Commons

Theses and Dissertations

May 2020

Development of a Hydrodynamic and Sediment Transport Model for Green Bay, Lake Michigan

Bahram Khazaei
University of Wisconsin-Milwaukee

Follow this and additional works at: https://dc.uwm.edu/etd

 Part of the Civil Engineering Commons, Environmental Engineering Commons, and the Hydrology Commons

Recommended Citation

Khazaei, Bahram, "Development of a Hydrodynamic and Sediment Transport Model for Green Bay, Lake Michigan" (2020). *Theses and Dissertations*. 2392.
https://dc.uwm.edu/etd/2392

This Dissertation is brought to you for free and open access by UWM Digital Commons. It has been accepted for inclusion in Theses and Dissertations by an authorized administrator of UWM Digital Commons. For more information, please contact open-access@uwm.edu.

DEVELOPMENT OF A HYDRODYNAMIC AND SEDIMENT TRANSPORT MODEL FOR GREEN BAY, LAKE MICHIGAN

by

Bahram Khazaei

A Dissertation Submitted in
Partial Fulfillment of the
Requirements for the Degree of

Doctor of Philosophy

in Engineering

at

The University of Wisconsin-Milwaukee

May 2020

ABSTRACT

DEVELOPMENT OF A HYDRODYNAMIC AND SEDIMENT TRANSPORT MODEL FOR GREEN BAY, LAKE MICHIGAN

by

Bahram Khazaei

The University of Wisconsin-Milwaukee, 2020
Under the Supervision of Professor Hector R. Bravo

Sediment dynamics are strongly linked with biogeochemical and physical changes in estuarine systems. Understanding the links between sediment processes and ecosystem responses is necessary for the restoration of degraded systems. Located in Northern US, and one of the largest freshwater estuaries on earth, Green Bay is a distinct example of these degraded systems. Rapid development and anthropogenic activities increased nutrient loading rates into the bay and led to a major disruption of the pre-existing biogeochemical regimes in the ecosystem. Contaminated and nutrient-rich sediments were discharged to the bay by the Fox River for almost half a century. Green Bay's seasonal-, morphological-, and physically-restricted mixing is unable to export a significant portion of the supplied materials to Lake Michigan, i.e., Green Bay behaves as an efficient retention basin for the lake. Therefore, several environmental and human-health related issues such as hypoxia, eutrophication, degraded water quality, and harmful algal blooms developed in Green Bay, turning the southern bay into a USEPA area of concern since the 1980s. Restoration programs were consequently developed,

including the development of monitoring programs and intensive collection of field data, research projects, and remedial action plans. Several of these efforts have highlighted the importance and usefulness of nutrient and toxic management practices as they relate to sediment processes. Robust models that simulate sediment transport and system biogeochemistry can be instrumental in the improvement of our understanding of these linked processes and the pace of restoration efforts. Previous research has studied the circulation, thermal regime and water quality in Green Bay, using models based on the Princeton Ocean Model and the Environmental Fluid Dynamics Code. Obstacles in those studies included shortage of field measurements and model limitations. Modeling challenges included the creation of boundary conditions for nested models, use of structured grids, modeling stratified flows in shallow areas, and limited model documentation. In this study, a state-of-the-art modeling platform, Finite-Volume Community Ocean Model (FVCOM), is adopted to investigate circulation patterns, surface waves, and 3D sediment dynamics in Lake Michigan, and Green Bay in particular. The FVCOM model runs in parallel mode, with notable advantages in computational efficiency. A well-calibrated and verified physically based hydrodynamic and sediment transport model has several practical applications for the management of the system, including but not limited to, explaining patterns and rates of sediment dynamics, predicting the short- and long-term effects of the restoration plans, providing simulations and early warning forecasts of the potential fate and transport of pollutants, and modeling the hypoxic dead zones within the bay.

Keywords: Green Bay, sediment, FVCOM, hydrodynamic modeling, fate and transport models, ecosystem restoration.

© Copyright by Bahram Khazaei, 2020
All Rights Reserved

To

my wife
for her patience, support, and endless love

TABLE OF CONTENTS

LIST OF FIGURES

LIST OF TABLES

LIST OF ABBREVIATIONS

T_{air}	Air Temperature
NH_3	Ammonia
AOC	Area of Concern
$\Delta\theta$	Average Angel Difference
BD	Bias Deviation
BBL	Bottom Boundary Layer
Cl^-	Chloride
Chl-a	Chlorophyll-a
CC	Correlation Coefficient
CMCST	Community Model for Coastal Sediment Transport
u	Currents Component in N-S Direction
v	Currents Component in E-W Direction
cyanoHABs	Cyanobacterial Harmful Algal Blooms
T_d	Dew Point Temperature
Q	Discharge
DO	Dissolved Oxygen
EFDC	Environmental Fluid Dynamics Code
FVCOM	Finite-Volume Community Ocean Model
FVCOM-SED	FVCOM-Sediment Transport Model
FVCOM-SWAVE	FVCOM Wave Model
F_n	Fourier norm

GLERL	Great Lakes Environmental Research Laboratory
GLCFS	Great Lakes Coastal Forecasting System
GLOFS	Great Lakes Operational Forecast System
GBMBS	Green Bay Mass Balance Study
NSE	Nash-Sutcliffe Efficiency
MPI	Message Passage Interface
NDBC	National Data Buoy Center
NOAA	National Oceanic and Atmospheric Administration
PCB	Polychlorinated Biphenyl
POM	Princeton Ocean Model
POMGL	Princeton Ocean Model Adapted for Greate Lakes
ROMS	Regional Ocean Modeling System
RMSE	Root Mean Squared Error
Hs	Significant Wave Height
SWAN	Simulating WAves Nearshore
T	Temperature
TKN	Total Kjeldahl Nitrogen
TMDL	Total Maximum Daily Load
TS	Total Solids
TSS	Total Suspended Solids
TU	Turbidity
USDA	United States Department of Agriculture

USEPA	United States Environmental Protection Agency
USGS	United States Geological Survey
UWM	University of Wisconsin-Milwaukee
WDNR	Wisconsin Department of Natural Resources

ACKNOWLEDGMENTS

Earning a Ph.D. has been the most exciting and challenging experience of my life and would not have been possible without the support and guidance I received from many individuals.

Firstly, I would like to express my sincere appreciation to my advisor Dr. Hector R. Bravo for his continuous support of my Ph.D. research. Without his patience, motivation, and guidance this dissertation would not have been achievable and I would give him most of the credit. Many thanks also to my Ph.D. committee members, Drs. J. Val Klump, Qian Liao, Eric J. Anderson, Changshan Wu, and Yin Wang for their contribution to my Ph.D. studies and invaluable suggestions in writing this dissertation.

During my journey at UWM, I had the opportunity to meet and work with many inspiring scientists, in particular, Dr. John Janssen who made my Ph.D. research a much more fun experience and Dr. Harvey A. Bootsma from whom I learned new concepts in limnology and biology. I would also like to recognize Jason Bacon and Jim Wagner for providing IT support and their help in troubleshooting the never-ending coding issues, as well as Jeff Houghton for his assistance in the fieldwork.

I have always been lucky to have great people in my life, especially my friends Amir, Amirali, Hossein, Mojtaba, Ramin, Saeed, Sina, and many, many others, Dr. Mohammadreza Tavakkolizadeh for his friendly and motivational mentorship during my undergraduate and master's studies at Ferdowsi University of Mashhad, and Mr. Shahrokhi, my fifth grade teacher, who had a remarkable impact on my personality with his passionate heart and thoughtfulness. I am also very grateful to Sarah and Adel Nasiri

for their emotional support that never let me feel thousands of kilometers away from my family.

In the end, I would like to express my deepest gratitude to my family, especially my wife, parents, and grandma (madar joon), whose unconditional love and support have given me the courage to face the challenges of life and learn/grow from them. I owe them every achievement in my life. Many thanks also to my aunt (khale Parvin), my in-laws, and my brother, Soroosh, for being an encouragement and helping me follow my dream of becoming a scientist.

I always had a passionate heart for nature. I've been lucky to find my career path in geophysical sciences that makes me able to study earth dynamics and its natural processes. I hope I can use that ability and dedicate my life to preserve the beauty of the earth.

"Water is sufficient…the spirit moves over water."

— Friedrich Nietzsche

Chapter 1:
Introduction, Review of Previous Work, and Problem Statement

1.1. Green Bay Area of Concern

The southern end of lower Green Bay and the northern end of the Fox River have been designated as an area of concern (AOC) by the Water Quality Board of the International Joint Commission since the 1980s due to several environmental and public health-related issues such as, but not limited to, hypoxia, excessive nutrients, toxic chemicals, harmful algal blooms, reduced water quality, lost or altered habitat. Green Bay conveys to Lake Michigan the flows from major tributary rivers that carry a significant amount of contaminated and nutrient-rich sediments to the bay. Fox River is one of the largest rivers discharging into Lake Michigan with an average annual discharge of 140 m^3/sec (based on records of United States Geological Survey gauge station at the mouth of Fox River during the 1989-2019 period) and perhaps the main supplier of sediments to the bay.

Figure 1.1 shows the location of Green Bay in Lake Michigan, Green Bay AOC, and the Fox River.

Figure 1.1. Locations of the lower Green Bay and the Fox River in the Lake Michigan basin. Upper left inset shows the location of Green Bay in the Great Lakes basin and the lower right inset shows Green Bay Area of Concern (AOC).

Sediments are introduced to the Fox River at its origin, Lake Winnebago, where the river picks up ~20% of the sediment and nutrient load entering the bay (Beversdorf et al., 2018). Along the 322-Km path from Lake Winnebago to Green Bay, Fox River drains an area of 16,395 km^2 and conveys sediment load from other sources through its tributaries. For decades, agricultural and industrial activities around the Lower Fox River watershed has increased the concentration of pollutants and nutrients in the river by intensifying soil erosion and introducing contaminants to the system. A distinctive example of such activities is the legacy of high concentration of Polychlorinated Biphenyl (PCB) in the Fox River and lower Green Bay due to activities and waste releases of paper companies into the Fox River between 1957 and 1971.

1.2. Green Bay Monitoring and Restoration

Under the critical environmental circumstances in Green Bay, development of a restoration program is necessary. Efforts that have been carried out to restore the Green Bay and Fox River system can be categorized into two major phases. Phase one includes monitoring different water quality aspects in the bay through research activities and fieldwork. These activities include computational and fieldwork efforts, in collaborations among different local and national organizations/institutes: University of Wisconsin (UW)-Milwaukee (UWM), UW-Madison, UW-Green Bay, University of Michigan, National Oceanic and Atmospheric Administration (NOAA) Great Lakes and Environmental Research Laboratory (GLERL), United States Geological Survey (USGS), United States Environmental Protection Agency (USEPA), Wisconsin Department of Natural Resources (WDNR), to name a few.

Researchers from the UWM Department of Civil and Environmental Engineering have

collaborated with UWM School of Freshwater Science (SFS; previously known as Great Lakes WATER Institute) to monitor water quality in Green Bay, develop models to simulate and predict the effects of circulation and biogeochemical processes in the bay water quality condition, and investigate the impacts of water degradation on ecosystems, aquatic creatures, and human life. Some of these studies are summarized in sections 1.3 through 1.6.

The Green Bay Mass Balance Study (GBMBS) was a four-year comprehensive monitoring and research program initiated by USEPA in 1989 to investigate toxic chemicals in the Fox River and Green Bay ecosystem. The program focused on the origin and transport of the PCB-contaminated sediments for which a mass balance approach was implemented to the Fox River system, from Lake Winnebago to Green Bay. The study also investigated the aquatic food web of the Fox River below the DePere dam and Green Bay (USEPA, 1989; Velleux et al., 1995). Figure 1.2 (Macksasitorn et al., 2015) shows the map of surface sediment PCB concentrations based on the analysis of sediment samples in Green Bay.

In a project funded by the University of Michigan Water Center and led by researchers at UWM and UW-Green Bay during the 2013-2015 period, the health of the Green Bay ecosystem was studied under current watershed, biogeochemical, and hydrodynamic conditions, and also under downscaled regional climate change scenarios. Hypoxia was investigated considering future climate scenarios such as warmer and wetter conditions with shorter winters, as well as, variabilities in ice cover, runoff, frequency of intense precipitation, wind speed and direction, and the stratification patterns and period. Local managers and stakeholders responsible for water treatment, soil conservation, land

use/cover change, watershed, and aquatic habitat management were involved in different stages of the project. An important output of this project was a management analysis tool that managers and stakeholders can use to monitor and visualize nutrient loadings into the bay and the way it responds to changes in climate conditions, land uses, and management/restoration actions (Klump et al., 2017).

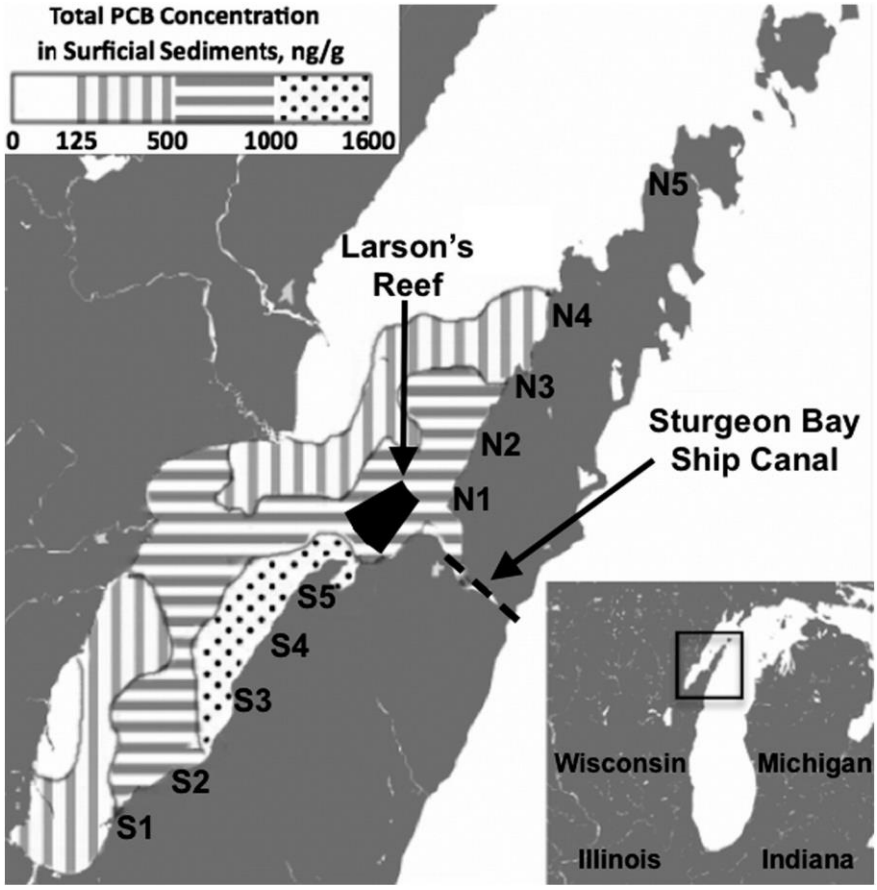

Figure 1.2. Map of the surface sediment PCB concentrations in Green Bay (Macksasitorn et al., 2015)

There is an ongoing project lead by UWM and UW-Green Bay researchers and funded by the UW Sea Grant Institute to develop a physical and hydrodynamic sediment transport model to complement the existing Green Bay sediment field database, improve the knowledge of the dynamics of the PCB-contaminated sediments, examine the

conditions leading to seasonal hypoxia, and contribute to the formulation of long-term solutions to those problems. The sediment transport model described in this dissertation proposal is a part of that project.

Phase two of restoration efforts includes fieldwork and engineering projects developed to improve the Green Bay ecosystem. The Green Bay Metropolitan Sewerage District (NEW Water) has carried out an aquatic monitoring program (NEW Water, 2017) since the 1980s that collects and analyzes water quality parameters in the Fox River, East River, and lower Green Bay. That program was developed to contribute to research focused on Fox River total maximum daily load (TMDL) assessments, restoration efforts for Green Bay AOC, and watershed management projects.

A dredging program was developed as a part of the Sediment Management Unit 56/57 remediation project to remove the PCB-contaminated sediment from the bed of the Fox River (Steuer 2000, WDNR 2001). Dredging operations are carried out in the reach of the Fox River between the De Pere dam and river mouth. WDNR reported that more than 2.5 million cubic meters of sediment were dredged between 2009 to 2014 from the Fox River (Wisconsin DNR, 2015). Analyses showed that dredging can permanently remove more than 95% of the PCBs in the sediment samples. PCB and suspended solids concentrations are subject to increase during and shortly after dredging activities in the mouth of the Fox River (Terta Tech Ec, 2019).

In 2012, Brown County started a construction project in the southwestern part of the bay that was planned to restore the Cat Islands to their historical positions with the objective of restoring aquatic vegetation and habitat associated with the islands. Clean dredged materials from the maintenance of the Green Bay Harbor were used to fill the islands and

the construction phase has made good progress to date (Brown County, 2018).

1.3. Linking Sediments, Water Quality, and Ecological Functioning of Green Bay

Large bays and estuarine systems are the most biologically productive ecosystems in the Great Lakes watershed, and they are heavily stressed. Excessive nutrients, highly concentrated and emerging contaminants, non-equilibrium dynamics, and disturbed food web have driven to risk the stability of these systems, requiring the development of direct management scenarios towards constraining nutrients loading. Development of a management scenario and restoration plan needs a comprehensive understanding of the governing biogeochemical and physical processes in the ecosystem. This understanding depends a great deal on the loading, recycling, and retention rates of the nutrients (Klump et al., 1997).

Research has shown that sediment processes play an important role in water quality. Chen et al. (2004) applied a 3D physical and biological model to Lake Michigan, to investigate the effects of circulation and mixing on biological activities in the lake. Their results showed that sediment resuspension has a significant impact on the spatial distribution and temporal variation of nutrients, in particular phosphorus, and plankton in southern Lake Michigan. Sediment resuspension can affect the ecosystem in two opposite ways. While resuspension events can increase the light attenuation coefficient, sediment plume increases nutrients availability after the plume appears. Due to the lack of a suspended sediment model Chen et al. used satellite-derived data to empirically estimate the sediment concentration in the lower trophic level food web model.

Other studies have also addressed the connections between sediment concentration and

the availability of nutrients that are crucial in modeling the aquatic habitats. Mussels scavenge phosphorus in the water column and release it in particulate and dissolved forms. The particulate phosphorus remains trapped in the sediments at the bottom of the lake and dissolved phosphorus is absorbed and consumed by *Cladophora* (Bootsma, 2009; Bravo et al., 2019a, 2017; Fillingham, 2015; Hecky et al., 2004). In the study of the connection between sediments and nutrients, hydrodynamic conditions are important in determining the bottom shear stress and estimating the resuspension events (Shen, 2016).

In a more recent study, Rowe et al. (2017) used a 3D biophysical model of Lake Michigan to investigate patterns of phytoplankton abundance and lake-wide productivity. Their results suggest that, although mussels play a great role in distributions of Chlorophyll-a (Chl-a), nutrient loading dominates lake-wide productivity even in the presence of mussels. However, they highlighted the need for additional effort to obtain more accurate water quality understanding of the eutrophic Green Bay.

Research focused on studying sediments in Green Bay has followed different frameworks. NEW Water is monitoring water quality parameters in Green Bay as a part of the restoration program. Analysis of these parameters indicates that sediments and suspended mater are a main driver of water quality and ecological health in the bay. Our preliminary analysis (Khazaei et al., 2018a, 2018b) shows that total solids (TS) and total suspended solids (TSS) are significantly and strongly correlated with water quality parameters, such as chloride (Cl^-), total phosphorus, ortho-phosphorus, total Kjeldahl nitrogen (TKN), ammonia (NH_3), Chl-a, and turbidity. Sediments are ideal attachment vehicles, i.e., pollutants and nutrients can be carried along or buried in the sediments

(Kordijazi and Silva, 2018).

Contaminants are introduced to the Fox River and Green Bay through different means, in particular, anthropogenic activities such as agricultural and industrial operations. A distinctive example of such activities in the Lower Fox River watershed was the release of PCBs during the 1957-1971 period into the river by the paper industry. The Fox River delivered about 85% of this compound to the bay, and atmospheric deposition contributed only a small portion of the load (Hermanson et al., 1991). The transport of PCBs can contaminate Green Bay and Lake Michigan fish and wildlife; thus, it is a public health issue.

Manchester-Neesvig et al. (1996), obtained sediment samples in 169 sampling stations across the bay during 1987 and 1990. They found that Green Bay contains approximately 8500 Kg of PCBs, mostly buried within three sedimentation zones in the bay. PCBs are not uniformly distributed across the bay and the most abundant PCB-contaminated sediments are found in the deposition zone that corresponds to the Fox River. That finding provided another evidence on the important role of the Fox River in transporting PCB-contaminated sediments into Green Bay. Based on the spatial distribution and vertical profiles of PCB concentrations in the Green Bay sediments, they recommended the removal of at least 20 cm of sediments at any location in the bay where dredging is done. That means that eliminating about 90% of the PCBs trapped in sediments of Green Bay requires the removal of 170,000,000 m^3 volume of sediments, which approximately cover 20% of the bay surface area. The relationship between sedimentation patterns and the spatial distribution of sediment-bound PCBs remained unanswered in that study due to the lack of a sediment transport model in the bay.

As a part of the GBMBS, the Fox River system was investigated (Velleux et al., 1995; Velleux and Endicott, 1994) during the 1988-1990 period to study the transport of PCBs from Lake Winnebago to Green Bay through the river. It was predicted that most of the PCBs are expected to stay in the Fox River in place; hence, in an extreme flow condition a significant resuspension and PCB export can be expected. Results of the Fox River PCB transport model could be linked in the future with a Green Bay mass balance model to complete the simulations of PCB transport in the Fox River/Green Bay ecosystem.

The open nature of Green Bay makes it difficult to establish a nutrient budget, especially for nitrogen and carbon, because they are constantly in exchange with the atmosphere. In one study, carbon and nitrogen budget analyses of Green Bay were carried out based on the direct measurements of input loads and depositions, complemented with estimates of exchange rates with Lake Michigan and production rates obtained indirectly based on the phosphorus cycle (Klump et al., 2009). River loadings are the major inputs to the carbon cycle, and the outputs are transported to upper Green Bay and/or exchange with Lake Michigan, burial in benthos, and exchanging CO_2 with the atmosphere. Although a big gap was found in the nitrogen cycle, it was roughly estimated that transport to Lake Michigan and sediment burial are the major output flux components in the cycle.

The phosphorus budget is often less complex in Green Bay since there are no significant interactions with the atmosphere. Klump et al. (1997) reported that Fox River provides about 70% of the annual phosphorus load to the bay. Green Bay acts as an efficient nutrient trap and retains almost 70-90% of the external phosphorus before flowing into the main body of Lake Michigan. Given that phosphorus is a limiting nutrient and a principal element of water quality in freshwater environments, it is important to obtain

comprehensive knowledge on phosphorus budget in these systems. The phosphorus cycle is dependent on the extent at which it will be held with the sediments or recycled back into the water column. To reach an equilibrium state, in terms of no significant increase in phosphorus concentrations in the bay, Klump et al. (1997) suggested that at least 50% of the annual input must be exported out of the bay. A robust transport model can help to improve our knowledge of nutrient recycling by providing accurate estimates of sediment conditions, deposition, and resuspension rate in the system.

The industrial release of Hg in the aquatic environment has led to the contamination of edible fish within the Great Lakes watershed (Macksasitorn et al., 2015). Hg emitted by coal-fired power plants has also contributed to the contamination of freshwaters and has been a public environmental health problem for decades. Analysis of the sediment cores in Green Bay has shown the existence of toxic substances in the bay sediments such as As, Pb, Zn, and Cd. Those substances are primarily introduced by anthropogenic sources and their level of concentration is governed by runoff and rivers flowing to the bay (Christensen and Chien, 1981).

Global freshwater systems are facing cyanobacterial harmful algal blooms (cyanoHABs). CyanoHABs have been detected in the Great Lakes, and in particular in Green Bay for a long time. Excessive nutrient loading into the bay and shallow water depth are known to be the major drivers of increasing the cyanoHABs situation in Green Bay. Given the reliance of HABs on nutrient availability, sediment transport regimes in Green Bay defines the spatial distribution of cyanoHABs across the bay. Analyses of the cruise samples collected in 2014 and 2015 at the mouth of Fox River and lower Green Bay indicates that the existence of the cyanoHABs is positively correlated with chlorophyll concentration

(Bartlett et al., 2018). However, as we move further away from the mouth of Fox River the mean concentration of the cyanoHABs decreases.

Recently, research has focused on the problem of hypoxia in Green Bay. Analysis of temperature and dissolved oxygen profiles during the 2009-2015 period indicates common summertime hypoxic zones in the southern Green Bay (Klump et al., 2018). During the May-September period, the hypoxic season could last two weeks to three months depending on thermal stratification, oxygen consumption near the bottom, organic carbon deposition, and other physical and meteorological forcing drivers of the bay.

Figure 1.3 (Klump et al., 2018) shows the spatial distribution of bottom-water dissolved oxygen concentration during the summers of the 2009-2015 period, based on near-monthly cruises of temperature and dissolved oxygen concentration samples. As shown in the figure, lower Green Bay is always facing hypoxic or in some cases anoxic zones. There are locations in the southern bay experiencing persistent dissolved oxygen concentrations lower than the water quality standard of 6 mg/L.

Figure 1.4 (Klump et al., 2017) shows the evolution of a dead zone in Green Bay. Excessive nutrient loading from the Fox River leads to persistent and massive algal blooms, including cyanobacteria. Shallow depths and rapid settling rates lead to the deposition of highly labile organic matter, which in turn supports high rates of benthic respiration, driving hypoxia under stratified conditions in the mid to late summer (Klump et al., 2017; Labuhn, 2017). The figure demonstrates the interactions between sediments, nutrients, and phytoplankton. Coldwater flows from Lake Michigan into Green Bay has also a significant role in the formation and developments of hypoxic zones and consequently biogeochemical processes in the benthos (Grunert et al., 2018).

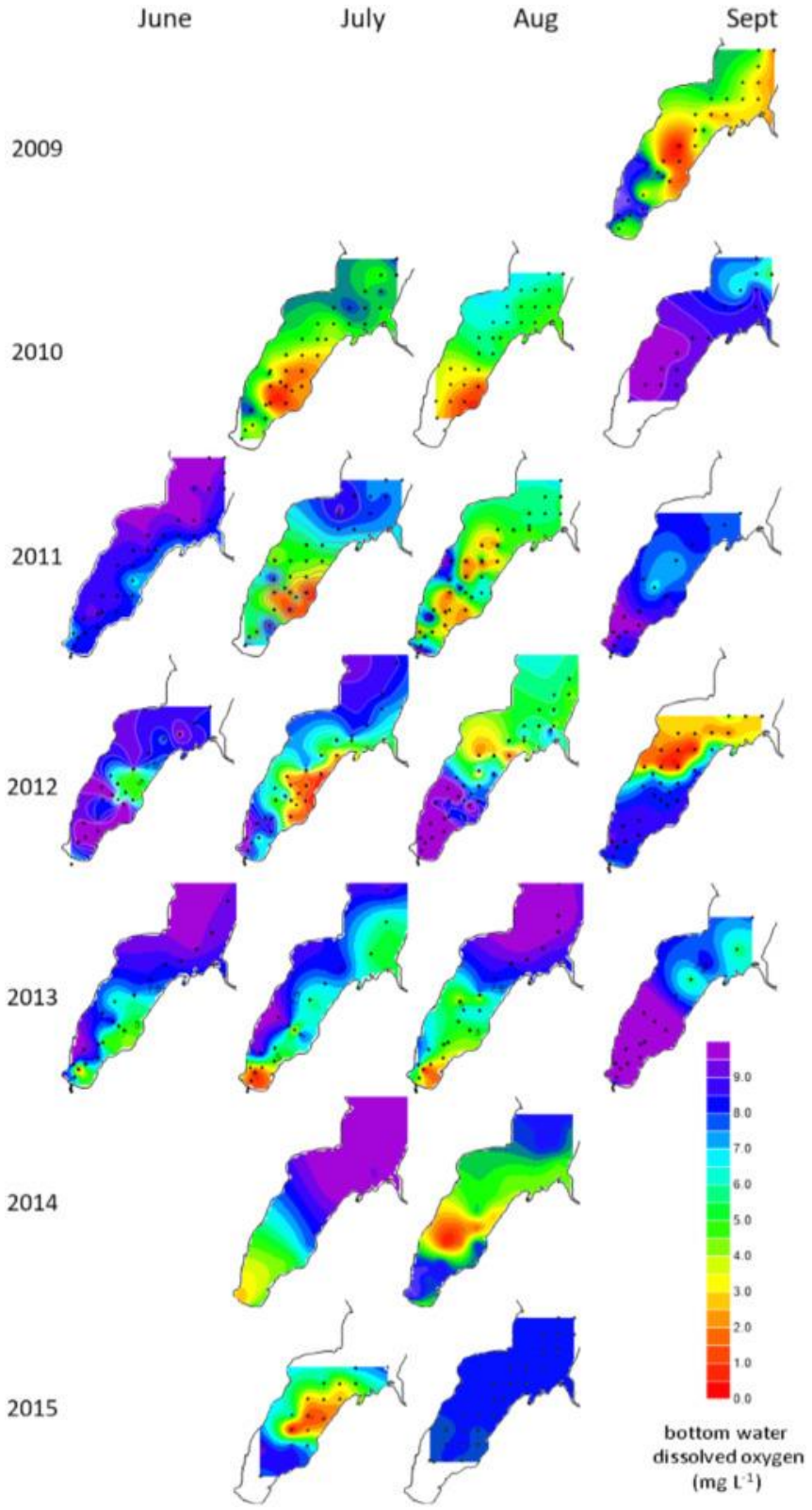

Figure 1.3. Spatial distribution of bottom dissolved oxygen concentration during the June-September of the 2009-2015 period (Klump et al., 2018)

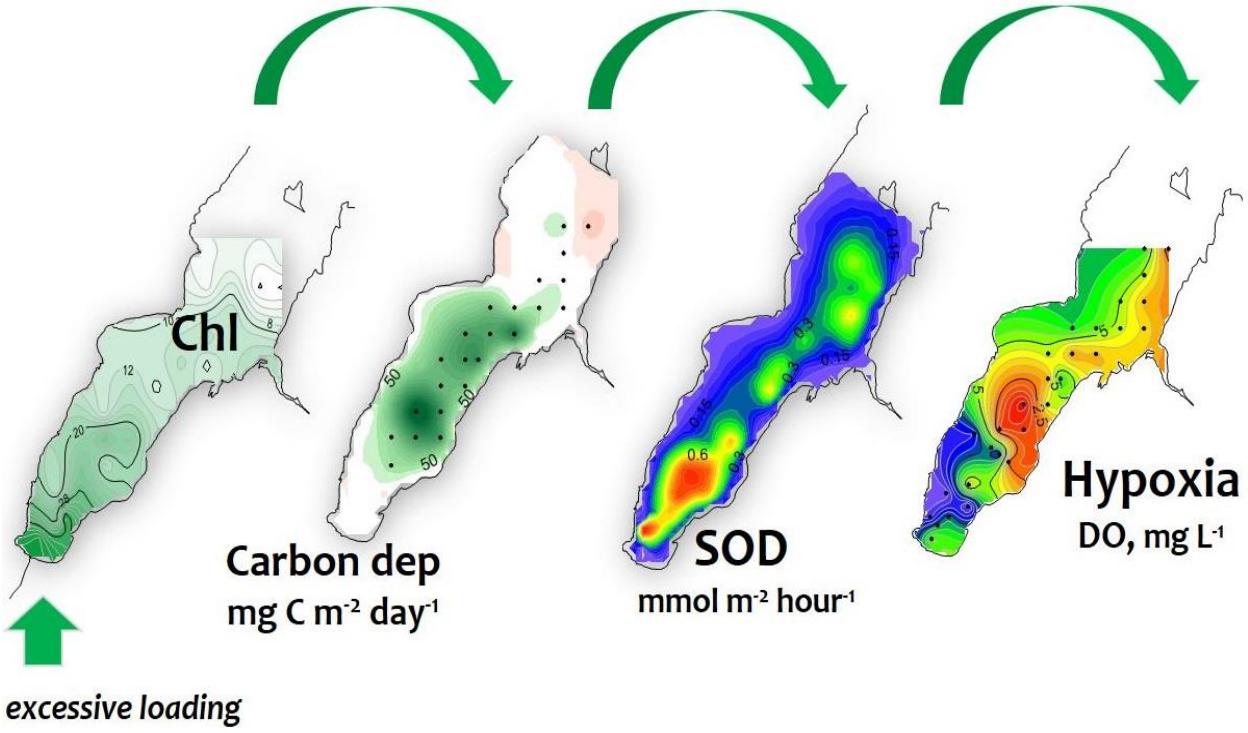

Figure 1.4. Evolution of a Dead Zone in Green Bay (Klump et al., 2017)

Primary production in an aquatic environment is a function of, but not limited to, light availability, nutrient availability in the system, algal biomass, and seasonal variability. LaBuhn and Klump (2016) showed that summertime primary production in Green Bay is a key driver of respiration in the benthos and at the sediment-water interface which is a dominant cause of hypoxia in Green Bay.

Change in water quality conditions of Green Bay has affected aquatic life and led to ecological degradation in the bay. Sampling the coastal wetlands and beach sites in Green Bay in the 1990s revealed that human development had affected the fish population by decreasing the fish diversity (Brazner, 1997). Invasion of the non-indigenous species such as Asian clam (Smith et al., 2018) or predatory cladoceran *Bythotrephes longimanus* (Merkle and De Stasio, 2018) disturbs the ecological balance of the systems and adds to the difficulties of the Green Bay restoration programs. On the

other hand, some native species that used to play a role in the life cycle of the bay ecosystem went extinct. For instance, *Hexagenia* mayfly provides an important food source for fish species, however, it has not been observed since 1955 in Green Bay (Kaster et al., 2018). Hypoxia and PCB-contaminated sediments are the most predominant barriers to mayfly egg stockings in Green Bay. Restoration of mayfly and other extinct species in Green Bay requires improvements in water quality and remediation of the benthos in the first place.

Water quality and the ecosystem of Green Bay have been the subject of a suite of studies for decades (e.g., DeVilbiss et al., 2016; Groff and Kaster, 2017; Lin et al., 2018, 2016; Maccoux et al., 2013; Qualls et al., 2007). All those researches have commonly pointed out to the importance of sediment loading into and transport across the bay. A robust sediment transport model can contribute to answering many questions on this matter and can help to improve management/restoration plans.

1.4. Hydrodynamics and Circulation in Green Bay

Early investigations of mixing dynamics in Green Bay were conducted by Modlin and Beeton (1970) based on differences in the conductivity between the bay, Fox River, and Lake Michigan. They showed that the exchange between the lake and the bay has decreased flushing time to six months compared to the flushing rate of two years based on Fox River loading rates only (Labuhn, 2017).

Before the development of computational hydrodynamic models, Miller and Saylor (1993, 1985) described circulation regimes in Green Bay based on field measurements of currents and water temperature at several stations including the four main passages between Green Bay and Lake Michigan: Death’s Door, Rock Island, St. Martin Island,

and Poverty Island. They also detected a counterclockwise circulation in the bay when dominant southwesterly winds are blowing. Another finding of that study was the identification of the two-layered currents in Green Bay and a stratified condition. The Fox River inflow runs at the surface layer, while cold hypolimnetic lake water flows into the bay and extends southward to maintain stratification and promotes flushing.

Wind-driven waves play an important role in the hydrodynamic patterns of Lake Michigan (Beletsky et al., 2006a). Waples and Klump (2002) showed that wind conditions can significantly affect water mass exchange between Green Bay and Lake Michigan, bottom water temperature, oxygen demand, and benthic biogeochemical processes. Extreme events can also affect the circulation and thermal regimes in Lake Michigan. There is evidence that extreme winter conditions during 2013-2014 may have imposed a shift in the thermal regime of Lake Michigan (Gronewold et al., 2015).

A 3D hydrodynamic model was developed by Hamidi et al. (2015) for Green Bay, based on the Princeton Ocean Model (POM; Blumberg and Mellor, 1987). That model was developed to examine the detailed spatiotemporal patterns of the interactions among the atmospheric heat flux across the water surface, the advective heat transport driven by the circulation, and cold lake water intrusion into the Green Bay bottom layer. Compared to the previous measurement-based models, that research provided more details of the circulation patterns all over Green Bay. For instance, their results showed that during July and August southwesterly winds drive three clockwise and two anticlockwise gyres inside the bay and further north of Chambers Island. Those results are compatible with cyclonic circulation patterns found for Lake Michigan in previous research (Beletsky and Schwab, 2008, 2001).

Analysis of the thermal regime by Hamidi et al. (2015, 2013) and Bravo et al. (2015) indicated continuous stratification between June and September in deeper areas of the bay. Mixing events occur due to wind blowing from the west, which increases bottom temperature and dissolved oxygen concentration. Wind fields are one of the main forcing factors of circulation patterns, which in turn drive biogeochemical processes in the bay such as sedimentation, water residence times, thermal stratification, and evolution of hypoxic zones.

Grunert et al. (2018) analyzed the thermal structure of Green Bay during 2012-2013. They showed that cold water intrusion from Lake Michigan affects significantly the thermal regime of the southern bay significantly and the stratification conditions. However, that effect depends on the climate conditions on a year-to-year basis. In Green Bay, a warming climate may not necessarily intensify the stratification in shallow seasonally stratified systems, while, atmospheric heat flux and wind can influence the thermal structure and/or stratification by changing the mixing regimes.

1.5. Review of Previous Studies Aiming at the Role of Sediment Transport in the Bay

Researchers have used different approaches to address the issue of sedimentation and sediment transport in Green Bay. The NOAA sediment trap study in Green Bay was one of the earliest programs aiming at sediment transport in Green Bay (Eadie et al., 1991). This was part of the GBMBS initiated and organized by USEPA with the primary objective of studying contaminant mass balance (USEPA, 1989). The sediment trap study by NOAA was developed with two main goals: 1) analysis of the seasonal flux of the suspended sediments, and 2) estimate net particle settling velocities in Green Bay. They

deployed sediment traps in five sites distributed in southern Green Bay in 1989 and collected samples of particulate material. Samples from near the bottom show high fluxes during the fall and minimum fluxes in summer. In the epilimnion, patterns of the seasonal fluxes are the same as the bottom, although mass flux is much less. During the stratified period, settling velocities range between 0.5 m/day in the epilimnion and 4-6 m/day in the bottom layer that implies the significance of horizontal transport or sediment resuspension events. Under the unstratified conditions settling velocities are about 12-18 m/day throughout the water column. At this rate, a sediment resuspension rate of 10 g/m^2/day is required to reach a steady state condition.

Hawley and Niester (1993) conducted a horizontal sediment transport analysis for southern Green Bay. They measured in the 1989 time series of water transparency at sampling stations located in the passages on both sides of Chambers Island. Water transparency data was first converted into total suspended material and then combined with current measurements made by Miller and Saylor (1993) to analyze the net sediment flux from and toward southern Green Bay. Analysis of the data showed that sediment flux at this boundary is primarily due to a counterclockwise circulation transport around Chambers Island. During the summertime, net transport of the sediments out of the southern bay is very small or negligible, i.e., significant portions of the sediment load discharged into the southern Green Bay by tributaries are probably deposited. However, roughly 10-33% of the mass loading by tributaries is flushed out into the northern bay in wintertime. The authors recommended more measurements and analysis to provide accurate estimates of the sediment transport in the bay.

Early topographic analysis of sedimentation rates by Manchester-Neesvig et al. (1996)

indicated non-uniform deposition patterns in the bay. They found three distinctive sedimentation zones with settling rates of more than 70 mg/cm^2/yr, mostly reflecting the sediment load by the Fox, Oconto, Peshtigo, and Menominee rivers. Sedimentation rates were found to be very negligible in the northern and central bay. That finding suggests that sediment load into the bay deposits mostly in the southern bay, and the rest of the load that moves to the northern bay is transported to Lake Michigan rather than being settled in the bay. Klump et al. (1997) also detected major depositional zones in the southern bay and characterized northern Green Bay as non-depositional zones of well-washed sands and glacial till.

WDNR funded a project to investigate the fate and transport of PCB-contaminated sediments in Green Bay (HydroQual Inc., 1999). A 3D sediment transport model was constructed upon a hydrodynamic model that accounts for transport in the water column and coupled with a wind-wave model to account for the effects of wind-driven waves on the transport of the sediments. They used a structured grid and discretized Green Bay into 2 Km grid cells, leading to more than 1000 cells. During the period of ice cover in the bay, heat exchange at the water surface was assumed as zero and no wind stress was applied at the surface. The sediment model included resuspension and deposition modules, which required bed shear stress simulations. Wave-induced shear stress at the bottom was simulated based on NOAA GLERL's wave model (Schwab et al., 1984). Sediment loading was considered from three major sources: 1) exchanges between Green Bay and Lake Michigan, 2) loadings from rivers, and 3) shoreline erosion. They calibrated the input parameters for the sediment transport model based on previous studies by Burban et al. (1990) in freshwater systems and Lick et al. (1995) for the Fox

River. Compared with the observations at the 25 sampling locations during the period of 1988-1990, HydroQual's model showed acceptable performance in simulating the patterns of suspended sediment concentration. They suggested that an ideal sediment transport model must be coupled with a eutrophication model to account for the internal loading processes rather than to only incorporate the loads due to hydrological and meteorological events. Such coupling could be implemented in a future version of the model presented in this dissertation.

Recently, a model was developed to investigate particle tracking in lower Green Bay with a focus on mixing time scales and flushing and residence times (Bravo et al., 2019b). A key finding of that study is that water exchange across Chambers Island transect plays an important role in the residence time of particles in the lower bay. Longest residence times are observed in the southern Green Bay near the mouth of the Fox River.

There have also been recent efforts in forecasting the sediment transport near the mouth of the Fox River based on the satellite imagery data (Hamidi et al., 2017). However, remote sensing approaches only provide estimations of sediment dynamics in surface layers of the water column and is limited to cloud-free atmospheric conditions, which is not very common in Green Bay.

Even though several other experimental or computational sediment transport models have been developed for Lake Michigan such as the Episodic Events Great Lakes Experiment (EEGLE) project (Hawley, 2004; Lee et al., 2007, 2005; Schwab et al., 2006), none of them focused on the simulation of the sediment transport in Green Bay.

1.6. Previous Hydrodynamic Models and Need for Development of a New Model

For decades Great Lakes researchers have conducted projects to improve the understanding of the circulation and thermal regime in Lake Michigan and Green Bay, and the associated transport of bacteria, pathogens, particles, and pollutants. NOAA GLERL developed and operated a Lake Michigan model (as well as models of all the Great Lakes) that is part of the Great Lakes Coastal Forecasting System (GLCFS). The model was developed based on the POM adapted to the Great Lakes (Schwab and Bedford, 1994).

As a part of a project funded by the University of Michigan Water Center, a hydrodynamic model based on the Environmental Fluid Dynamics Code (EFDC; Hamrick 1992) was developed for Green Bay. That model was coupled with a biogeochemical model, originally developed by HydroQual for the USEPA, and modified by LimnoTech (Klump et al., 2017). Figure 1.5 shows the model framework, including the integration of stakeholders, different model components (climate, watershed, hydrodynamic, and farm), and a management analysis tool.

Although POM and EFDC-based models were developed to model hydrodynamics of the Great Lakes, important obstacles faced on those models were the scarcity of simultaneous measurements of currents, temperature, and water quality observations (TSS, turbidity, etc.), required to validate models, and limitations of the models themselves. One relevant model limitation is the use of Cartesian structured rectangular grids in POM-based models that is not flexible enough to represent small-scale shoreline features. Additionally, those models had difficulties in modeling thermal structures and

stratified flows in shallow areas, especially, during upwelling or downwelling events. Insufficient documentation, simplified simulation of sediment transport, and neglected effects of the wind waves were some of the limitations in implementing the EFDC model. Those models might run slowly if a high-resolution grid is used in a large domain such as Lake Michigan.

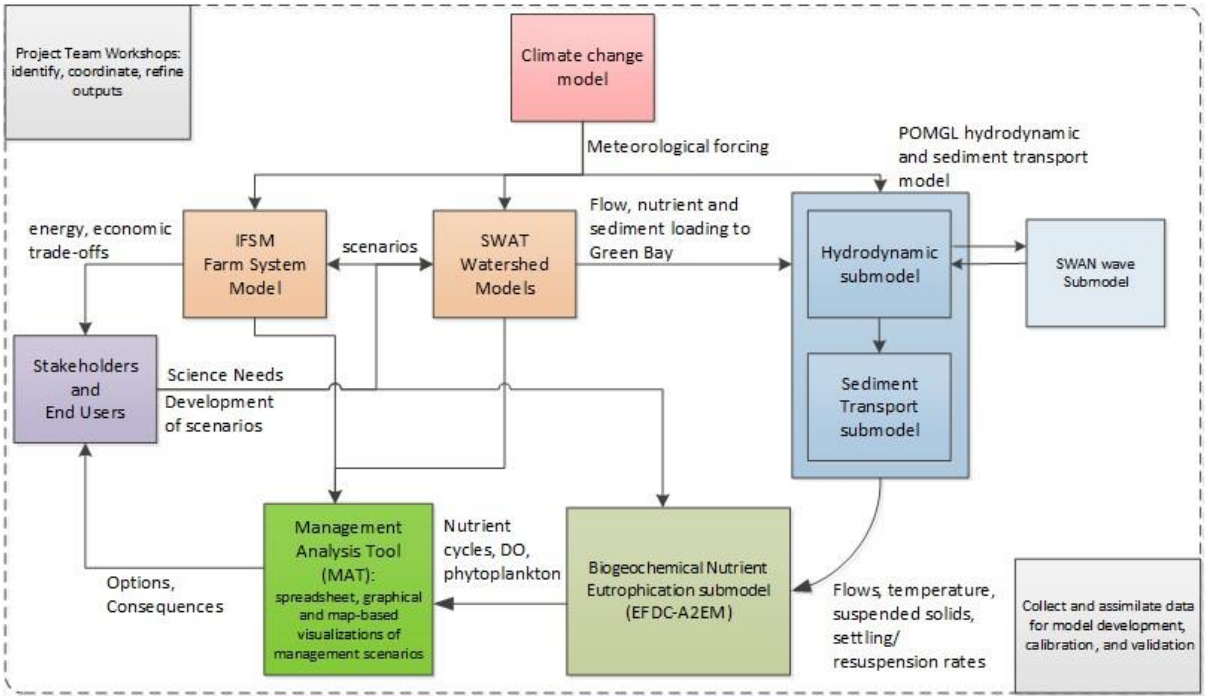

Figure 1.5. Green Bay Watershed Management Model Framework: Integration of stakeholders, multiple models (climate, watershed, hydrodynamic, and farm) and a management analysis tool (Klump et al., 2017)

The aforementioned obstacles pointed to the need to collect consistent sets of field data (e.g., recent observations of turbidity in the Green Bay AOC), and to develop a state-of-the-art modeling approach, such as that provided by Finite-Volume Community Ocean Model (FVCOM; Chen et al., 2013, 2003) as described in Chapter 2. FVCOM can run in parallel mode, uses an unstructured-grid, and is equipped with several water quality tools that can integrate different physical and biogeochemical processes efficiently.

During the past decades, significant accomplishments have been achieved in restoring Green Bay. Despite the efforts made, and as the existing literature reveals, there is a missing element in the development of a sustainable restoration plan for Green Bay. That important step is a robust and comprehensive sediment transport model that can contribute to a better understanding of the links between sediments, hydrodynamic circulation, and biogeochemical processes in the bay.

Not only a sediment transport model can benefit and enrich other related research projects, but it can help to evaluate the effectiveness of dredging the Fox River, Cat Island construction, and similar restoration plans by considering different loading scenarios. The sediment transport model can play an important role in understating nutrient-related processes and establishing nutrient budgets.

The main objective of this research is the development of a physically-based sediment transport model for Lake Michigan and Green Bay that a) complements the existing Green Bay sediment field database, b) contributes to the understanding of the ecological problems in the bay such as seasonal hypoxia, and harmful algal blooms, c) helps to recommend long-term solutions to those problems, and d) underpin a framework for development of a real-time sediment transport model for the Great Lakes as a supplementary feature of the Great Lakes Operational Forecast System (GLOFS) program.

This dissertation explains different steps of the hydrodynamic, wave, and sediment transport model developments, including details of the models' physics, initial and boundary conditions, external forcing preparation, and model validation. Also, the results of different model components are presented and sediment dynamics in Green Bay are

scrutinized based on the model results. TSS time series in lower Green Bay are available since 2018, therefore, 2018 and 2019 years were selected for the development of the Green Bay sediment transport model in this thesis. Simulations are limited to the period of May-October in each year because of ice conditions and field data availability.

Chapter 2:
Development of the Hydrodynamic and Wave Models based on the Finite-Volume Community Ocean Model (FVCOM)

2.1. Physical Model Description

As explained in Chapter 1, FVCOM is an efficient and robust computational tool and was selected in this study to develop the hydrodynamic model. FVCOM was developed by Chen et al. (2003) and is a prognostic free-surface ocean primitive-equation model that solves the continuity, momentum, and energy equations (including currents, temperature, salinity, and density calculations):

$$\frac{\partial u}{\partial t} + u\frac{\partial u}{\partial x} + v\frac{\partial u}{\partial y} + w\frac{\partial u}{\partial z} - fv = -\frac{1}{\rho_0}\frac{\partial p}{\partial x} + \frac{\partial}{\partial z}\left(A_H\frac{\partial u}{\partial z}\right) + F_u \quad (2.1)$$

$$\frac{\partial v}{\partial t} + u\frac{\partial v}{\partial x} + v\frac{\partial v}{\partial y} + w\frac{\partial v}{\partial z} + fu = -\frac{1}{\rho_0}\frac{\partial p}{\partial x} + \frac{\partial}{\partial z}\left(A_H \frac{\partial v}{\partial z}\right) + F_v \quad (2.2)$$

$$\frac{\partial w}{\partial t} + u\frac{\partial w}{\partial x} + v\frac{\partial w}{\partial y} + w\frac{\partial w}{\partial z} = -\frac{1}{\rho_0}\frac{\partial p}{\partial x} + \frac{\partial}{\partial z}\left(K_V \frac{\partial w}{\partial z}\right) + F_w \quad (2.3)$$

$$\frac{\partial u}{\partial x} + \frac{\partial v}{\partial y} + \frac{\partial w}{\partial z} = 0 \quad (2.4)$$

$$\frac{\partial T}{\partial t} + u\frac{\partial T}{\partial x} + v\frac{\partial T}{\partial y} + w\frac{\partial T}{\partial z} = \frac{\partial}{\partial z}\left(K_h \frac{\partial T}{\partial z}\right) + F_T \quad (2.5)$$

$$\rho = \rho(T, p) \quad (2.6)$$

where *(u, v, w)* are the three components of velocity in *(x, y, z)* Cartesian grid coordinates, A_H is the vertical eddy diffusion coefficient, K_V is the vertical eddy viscosity, p is the pressure, T is water temperature, ρ is water density, f is the Coriolis term, and F_u, F_v, F_w, and F_T represent the momentum and thermal diffusion terms.

Vertical mixing is calculated based on the MY-Level 2.5 turbulence closure scheme developed by Mellor and Yamada (1982) and modified by Galperin et al. (1988). Smagorinsky's eddy scheme is implemented in FVCOM for horizontal mixing calculations (Smagorinsky, 1963).

FVCOM runs in three dimensions based on finite volumes developed on an unstructured, sigma-coordinated grid; hence, FVCOM has high capabilities in representing complex geometry of the coastal environments such as islands and estuarine systems. This is very important in modeling Green Bay because of the highly irregular shorelines along the bay and the existence of several islands with uneven geometry. Therefore, FVCOM provides flexibility to preserve such small features on the generated grid. The model also can be run in either Cartesian or spherical coordinate systems.

Similar to POM, FVCOM is able to adopt a split mode numerical scheme in which it first calculates the surface elevation and currents based on a 2D external mode and then applies a 3D internal model to solve for the vertical diffusive transport. One of the most significant advantages of FVCOM is the ability of the program to run in parallel mode. A Message Passage Interface (MPI) is utilized to program the parallel operations. A substantial reduction in computation times can be achieved when FVCOM is used in parallelized mode. Cowles (2008) showed that by using 32 processors, a one-year hindcast of running FVCOM can be reduced to around a week of wall clock time. In addition, several FVCOM modules such as sediment transport and wave modules can run in offline mode which is an important feature for model development and calibration.

NOAA GLERL has adopted FVCOM to develop the latest version (3rd generation) of the GLOFS because its flexibility and also ability to model physical processes very well. FVCOM has been successfully implemented in modeling coastal oceanic applications (Chen et al., 2007, 2003; Huang et al., 2008; Li et al., 2017, 2018; Zhang et al., 2018), in modeling the Great Lakes (Anderson et al., 2010; Anderson and Schwab, 2011; Bai et al., 2013; Mao and Xia, 2017; Read et al., 2010; Shore, 2009; Xue et al., 2015), rivers and connecting channels (Anderson and Phanikumar, 2011; Anderson and Schwab, 2013; Guerra et al., 2017; Lai et al., 2018), as well as in water quality, ecological, and biogeochemical applications (Luo et al., 2012; Rowe et al., 2017, 2015; Safaie et al., 2016; Shen, 2016).

FVCOM was first written in Fortran 77 and then was updated to Fortran 90 (Chen et al., 2013) and its version 4.1 was used in this research. FVCOM is an efficient and powerful computational tool, and it is equipped with different modules that provide a reliable and

user-friendly platform for hydrodynamic research that aims to integrate the effects of physical and biogeochemical processes. Data assimilation and filtering modules can also improve the performance of the model and reduce the uncertainty of the simulations. Figure 2.1 provides a schematic overview of the FVCOM and its available modules.

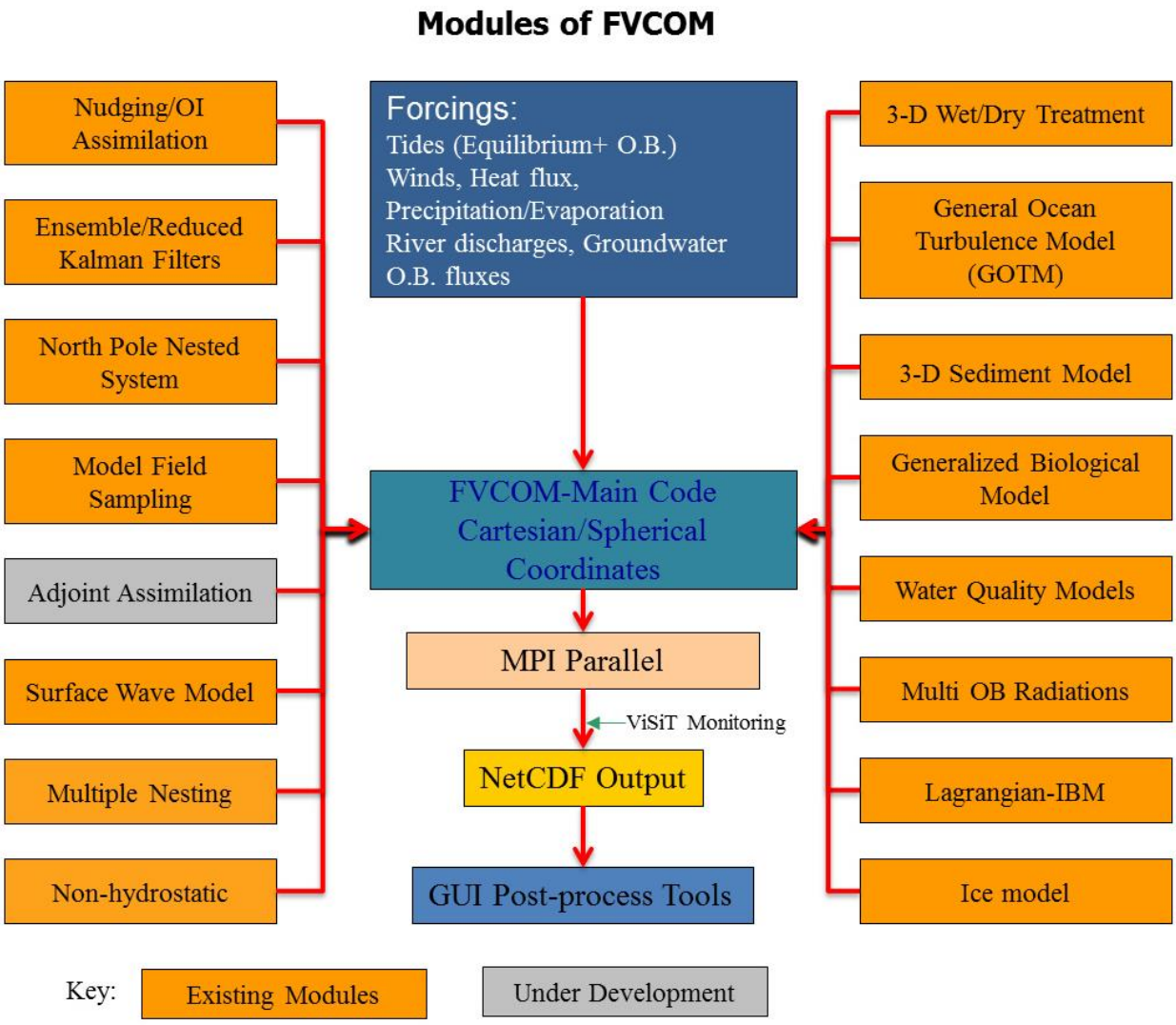

Figure 2.1. Schematic of the FVCOM and its modules (Chen et al., 2013)

2.2. Study Domain and Grid Specifications

In this research, the FVCOM model was developed for Lake Michigan, with a focus on Green Bay. Green Bay is the largest estuarine system in the Great Lakes basin and is

about 190 Km long and on average 22 Km wide. The area to the south of Chambers Island is known as lower Green Bay and north of that section is the upper Green Bay which connects to the main lake body. Green Bay receives flows from some major rivers such as Fox, Oconto, Peshtigo, and Menominee rivers in the lower Green Bay and Cedar, Escanaba, Rapid, and Whitefish rivers in the upper Green Bay.

The lower Fox River has a drainage basin of 16,395 km^2 and is the largest tributary to Green Bay. The lower Fox River originates in Lake Winnebago and is about 62 Km long before it discharges into southern Green Bay. The flow in the river is regulated by several dams along the Lower Fox River watershed and runs through the cities of Appleton and Green Bay, as well as some other smaller cities (Velleux et al., 1995). The Lower Fox River watershed is mostly covered with vegetation (Khazaei and Wu, 2018), but is also a heavily industrialized and developed area that hosts large industrial sites, in particular paper companies, as well as farmlands and urban life (Klump et al., 1997). The Fox River contributes up to about 70% of the nutrients and particulate loadings to Green Bay (Harris and Christie, 1987).

The first step in the development of the sediment transport model was the generation of a grid for the study area, i.e., the discretization of Lake Michigan and Green Bay control volume into finite elements. The SMS software version 10.1 (AQUAVEO, 2018) was used for the generation of the mesh and the development of the unstructured-grid for running the model in FVCOM. Mesh elements, location of nodes, and bathymetry of each element were triangulated based on a linear interpolation method. Bathymetry and shoreline of Lake Michigan were obtained from NOAA's bathymetry data extract tools (National Geophysical Data Centre, 2015; NOAA, 2017). The bathymetry data near the mouth of

the Fox River was also updated to include the bed alterations due to dredging.

Green Bay is a shallow water system with a maximum depth of ~50 m (near the exchange zone with Lake Michigan) and an average depth of ~20 m. The relatively small depth could affect the model performance, and hydrodynamic simulations could be significantly sensitive to the bathymetry and morphological characteristics of the bay. Therefore, a robust sediment transport model for Green Bay requires a high-resolution grid that can represent detailed bottom terrain variations, as well as the geometry of the complex shorelines in Green Bay. Figure 2.2 highlights the different characteristics of the bathymetries of Lake Michigan and Green Bay.

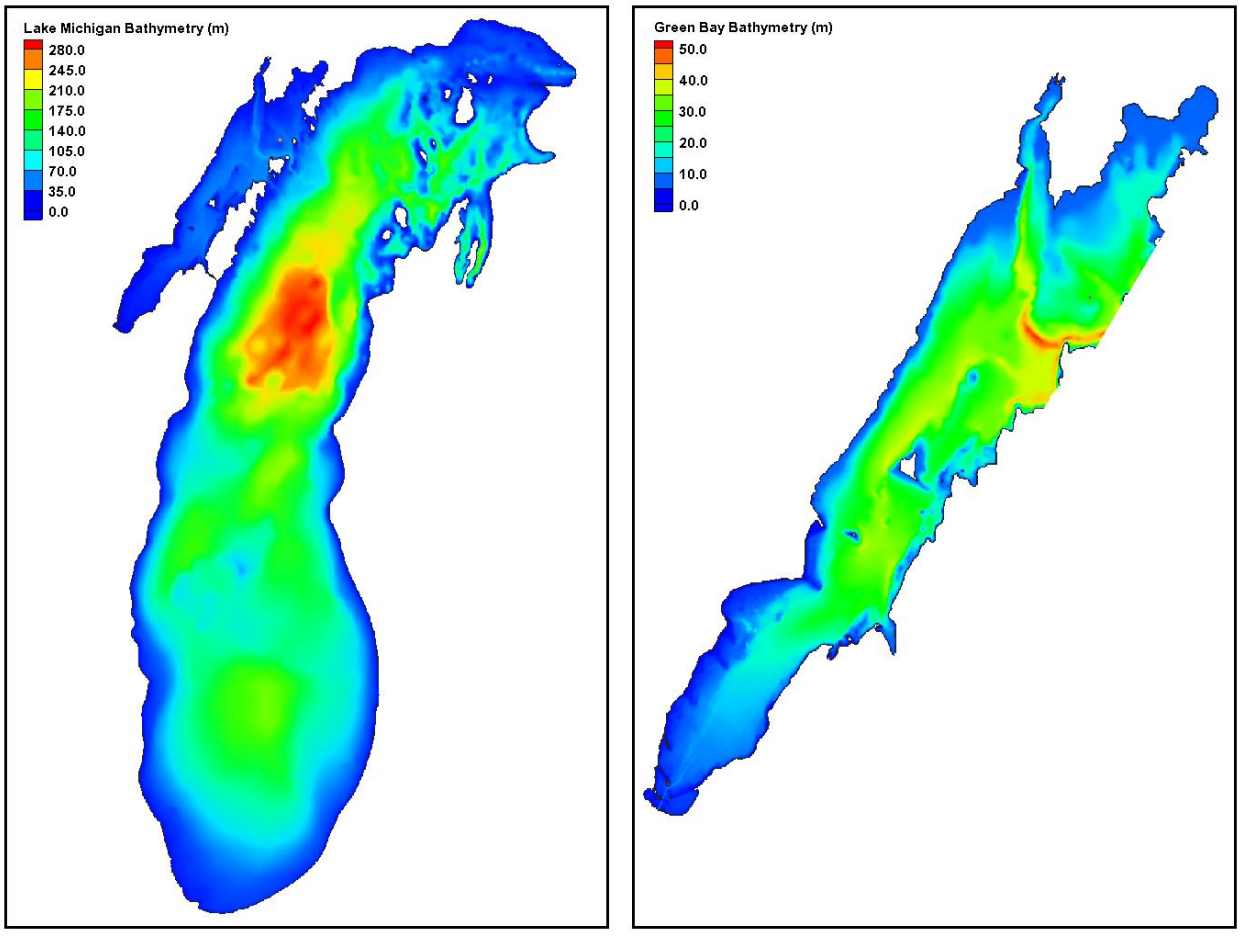

Figure 2.2. Bathymetry of Lake Michigan (left) and Green Bay (right)

Natural features with complex geometry that were incorporated in the grid include Long Tail Point and Little Tail Point Islands located on the west shore of lower Green Bay, Green and Chambers Islands in the center of the bay, and Plum, Detroit, Washington, Rock, St. Martin, Poverty, Summer, and Little Summer Islands in the exchange zone of the Lake Michigan and Green Bay. Also, the NOAA coastline data was updated to include the Cat Islands, a feature that is crucial in modeling the circulation and transport in the lower Green Bay. Figure 2.3 illustrates the Lake Michigan grid and the two left insets show the grid resolution in the Lake Michigan-Green Bay exchange area, and around the Cat Islands.

The unstructured-grid used in this research includes 28,985 nodes, 52,574 triangular elements, and 20 sigma layers with thickness proportional to the depth (i.e., following terrain variations). The grid is very dense in the lower Green Bay and at the mouth of Fox River with an element side length of ~100 m. Grid resolution decreases gradually toward the upper Green Bay, where the element side length increases to ~1500 m. The element side length in the Lake Michigan varies between ~1000 m near the shorelines and 10,000 m in the central lake areas. A dense grid for the exchange zone between Lake Michigan and Green Bay was constructed to better represent the fluxes into and out of the bay through the passages.

No open boundary conditions were defined for the grid because the flow from surrounding tributaries, the bi-directional flow at the Straits of Mackinac, and the outflow through the Chicago River diversion were neglected in this study. The time steps used in the simulations were 5 s. This time was determined by trial and error and based on the program stability conditions and computation time.

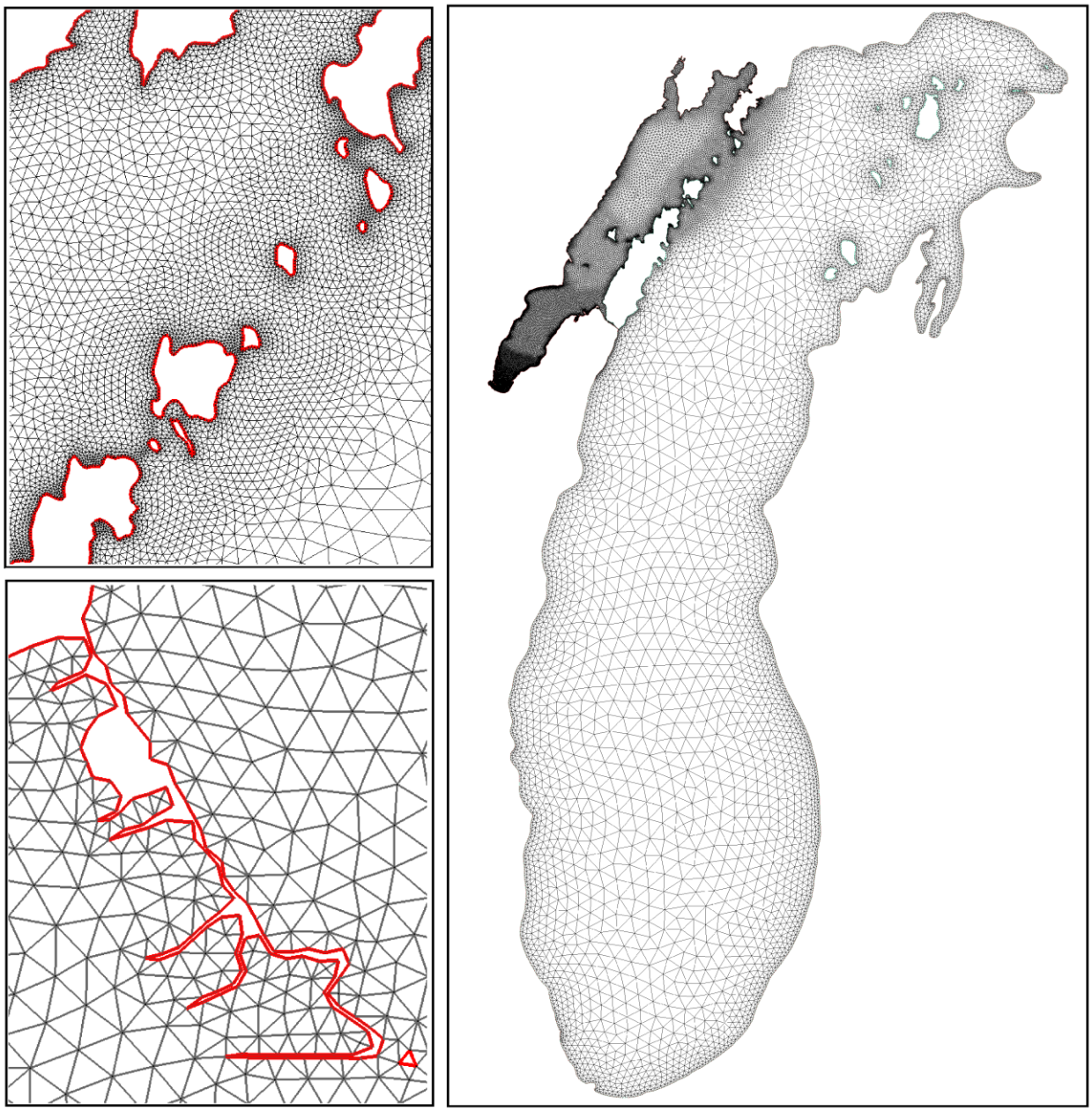

Figure 2.3. Lake Michigan grid resolution (right), Lake Michigan-Green Bay exchange area (top left), and Cat Islands (bottom left)

2.3. Wave Model

Sediment movement is primarily due to advective-diffusive transport and settlement of sediments in the water column; however, sediment processes near the bottom are affected by the wave interactions significantly. Therefore, construction of the sediment

transport model requires the implementation of a wave model in order to improve the simulation of current-wave-sediment interactions in the bottom boundary layer. These bottom shear stresses are calculated based on the current-wave interactions and incorporated in the sediment model to account for sediment resuspension and transport in the bottom layer.

FVCOM adopted the Simulating WAves Nearshore (SWAN) model to simulate wave actions (see Figure 2.1). SWAN has become popular in various applications including ocean wave simulations, engineering applications, modeling coastal and estuarine systems, and wave forecasting studies (Chen et al., 2018). SWAN wave model was developed by Booij et al. (1999) and models wave evolution using transport equations to solve for wave action density N as follows:

$$\frac{\partial N}{\partial t} + \frac{\partial c_x N}{\partial x} + \frac{\partial c_y N}{\partial y} + \frac{\partial c_\sigma N}{\partial \sigma} + \frac{\partial c_\theta N}{\partial \theta} = \frac{S_w}{\sigma} \tag{2.7}$$

where (c_x, c_y) are propagation velocities in (x, y) Cartesian grid coordinates, σ and θ are the intrinsic wave frequency and direction, C_σ is the propagation velocity due to variations in depth and currents, C_θ is the propagation in wave direction, and S_w is acting as a source/sink term to represent the effects of wind-wave generation, energy dissipation due to whitecapping, depth-induced wave breaking, and bottom friction, and nonlinear wave-wave interactions. Specific details of the SWAN model formulation and validation are described in the literature (Booij et al., 2004; Ris et al., 1999).

SWAN is a structured-grid wave model and was converted to an unstructured-grid finite-volume model by the FVCOM team (Chen et al., 2013), namely FVCOM-SWAVE. FVCOM-SWAVE was validated for different test problems that were used for SWAN

validation (Qi et al., 2009). FVCOM-SWAVE is fully coupled with FVCOM-SED to account for wave-sediment interactions and validated for a tidal inlet test case (Chen et al., 2013).

Chapter 3:
Development of the Sediment Transport Model based on the USGS Community Sediment Transport Model

3.1. Sediment Transport Model Description

In general, Green Bay provides a clear example of where refinements in sediment transport dynamics are essential. For example, settling rates for particulates are high (meters per day) and depths are relatively shallow, leading to the rapid delivery of fresh algal debris to the bottom. Sediment oxygen demand rates are highest in the southernmost end of Green Bay, while the flux of fresh algal detritus to the benthos is the highest, whereas longer-term organic carbon deposition is focused in the deeper portions of the mid-bay.

FVCOM is equipped with a built-in sediment transport model, namely FVCOM-SED,

which was used in the further development of the model for sediment interactions. FVCOM-SED utilizes the Community Model for Coastal Sediment Transport (CMCST) developed by Warner et al. (2008) in collaboration between USGS researchers and other institutions. The model was further improved with options for modeling cohesive and mixed sediment media (Sherwood et al., 2018).

FVCOM-SED simulates sediment transport by incorporating the effects of suspended sediment and bedload transport, layered bed dynamics, and cohesive sediment erosion/deposition algorithms for an unlimited number of bed layers. CMCST is originally developed to be run based on the Regional Ocean Modeling System (ROMS) which is a structured-grid solver. Major efforts were made by the FVCOM team to convert the RMOS-based sediment transport model into an unstructured-grid code to be consistent with the FVCOM circulation model (Chen et al., 2013).

FVCOM-SED is capable of modeling an unlimited number of cohesive and non-cohesive sediment classes in the sediment bed by defining attributes for each sediment class or sublayer. These attributes are determined in terms of each sediment class properties including grain diameter, sediment density, settling rates, critical shear stress for sediment resuspension, and bed erosion characteristics, which are used to determine bulk properties of individual bed layers.

Sediment bed consists of unlimited user-defined sediment layers beneath each hydrodynamic model cell as shown in Figure 3.1. Each sediment layer is initially defined with layer thickness, sediment class distribution, porosity, critical shear stress, and age. These parameters are used to estimate the grain density and occurrence of the last depositions in bed layers.

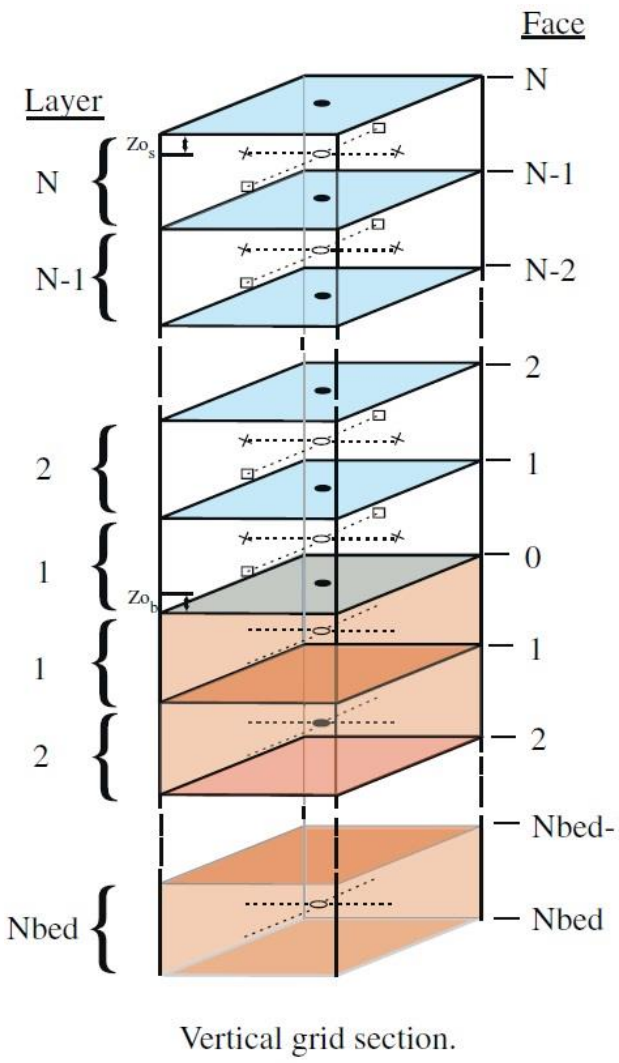

Figure 3.1. Vertical section of a grid cell component in the sediment transport model. Horizontal water column layers in FVCOM and bed layers in FVCOM-SED can vary from 1 to, respectively, N and Nbed (Warner et al., 2008).

The current version of the FVCOM sediment transport model defines initial distributions of sediment classes in bed uniformly for the entire domain. This assumption can lead to over-simplification of the initial conditions for the sediment transport model, in particular for complex and large-scale systems like Green Bay and Lake Michigan. In order to address that issue, the FVOM code was modified to define a non-uniform distribution of sediment classes in the study domain. Details of the new modifications and instructions

on how to define the initial bed fractions for a selected number of sediment classes are provided in Appendix A.

Erosion and deposition of sediments alter the bed layer characteristics, in particular the bed thickness. Therefore, an active layer is considered at the top of the bed layers to be adjusted accordingly and to keep the number of bed layers constant during the simulations. The thickness of the active layer can be estimated in each time step based on Harris and Wiberg (2001) empirical relationship:

$$z_a = max\left[k_1(\tau_{sf} - \tau_{ce}),\qquad 0\right] + k_2 D_{50} \tag{3.1}$$

where z_a is the active layer thickness (m), τ_{sf} is maximum bottom friction stress due to combined wave and currents interactions (N/m^2), τ_{ce} is critical stress for erosion (N/m^2), D_{50} is median grain diameter at the sediment-water interface (m), and k_1 and k_2 are empirical constants with values of 0.007 and 6.0, respectively.

The minimum thickness of the top layer is equal to z_a. During erosion events, if the thickness of the top layer decreases lower than this value, sediments from deeper layers are added to the top layer to meet the minimum depth criteria, and other layers are split accordingly to keep the number of layers constant. If continuous deposition of sediments increases the thickness of the top layer more than a user-defined threshold, a new layer is created for the deposition of suspended mass and two bottom layers are merged to have the same number of layers. Then the active layer thickness is calculated to avoid a thin layer of deposited sediments at the very top layer. Figure 3.2 demonstrates the bed layer modifications during the erosion and deposition events.

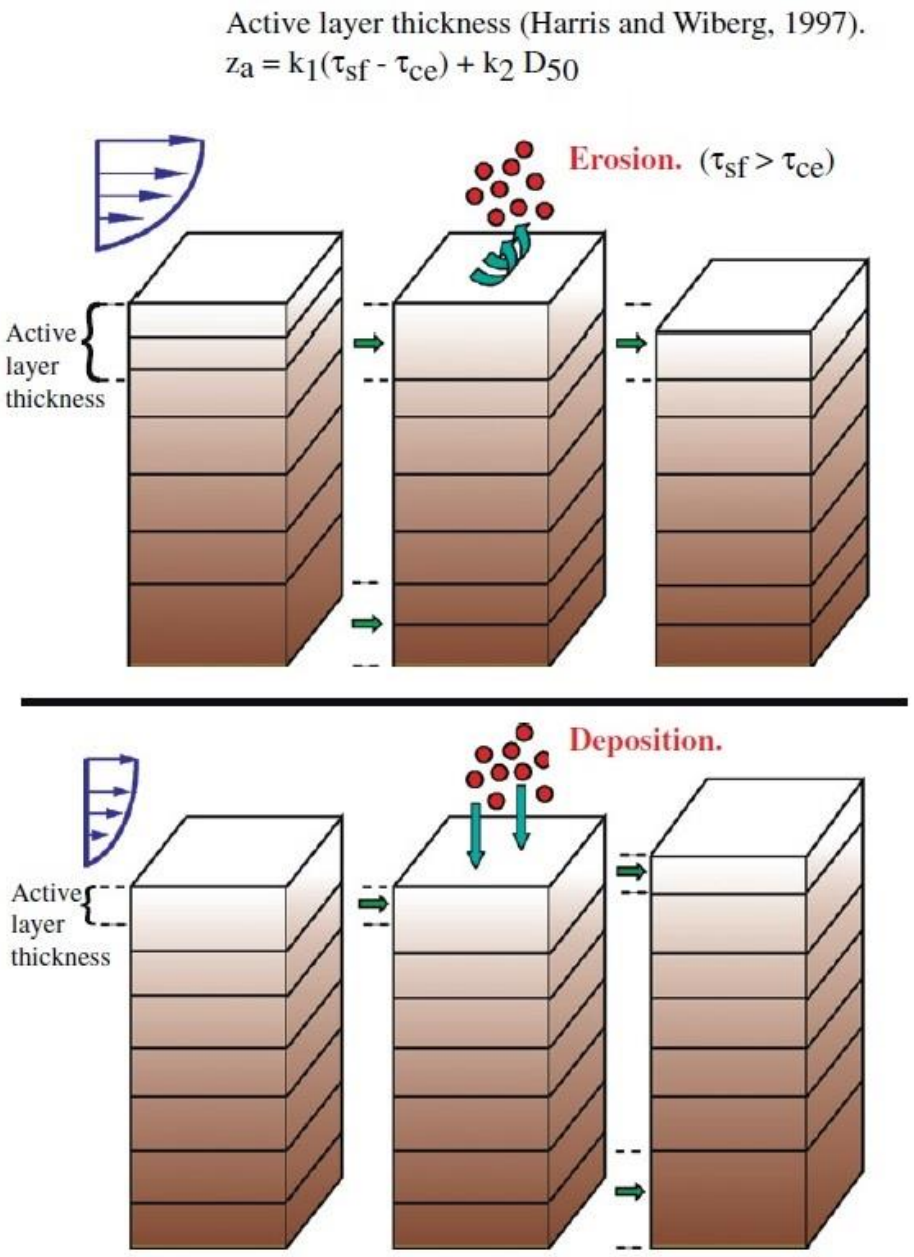

Figure 3.2. Bed layer modifications during bed erosion and sediment deposition events (Warner et al., 2008)

In the calculation of sediment transport fluxes, each sediment class can be considered as suspended load and/or bedload. While the suspended load is the vertical exchange of sediment mass between the top bed layer and water column, the bedload is considered as the horizontal exchange within the top layers of the bed. In each time step, transport

of sediment is limited to the mass available in the top bed layer, in which the bottom shear stress determines bedload transport rate and suspended load resuspension rate.

The erosion rate at the bottom is defined based on critical shear stress defined by the user and bottom shear stress. The sediment concentration profile in the water column is based on establishing a sediment budget between advection, vertical diffusion, introduction of new material due to erosion, and loss of material due to settling. FVCOM-SED computes suspended and bed loads separately and add them together to estimate the total load. More details regarding the suspended load and bedload calculations are provided in sections 3.3 and 3.4, respectively.

3.2. Current-Wave-Sediment Interactions in FVCOM

FVCOM, FVCOM-SWAVE, and FVCOM-SED are coupled to account for current-wave-sediment interactions in FVCOM as shown in Figure 3.3. Coupled circulation and wave model allows for combined calculations of shear stress at the bottom boundary layer (BBL). The FVCOM hydrodynamic model provides the flow fields required to simulate sediment transport in the Lake Michigan model by advection and diffusion. The FVCOM-SWAVE model includes wind-wave dynamics component to combine the shear stresses induced by both currents and waves.

In addition to hydrodynamic and wave model inputs, BBL calculations require information on bottom sediment characteristics such as median grain diameter, mean sediment density, and settling velocity (Warner et al., 2008). As shown in Figure 3.3, both currents and wave conditions are wind-driven and interacting with each other.

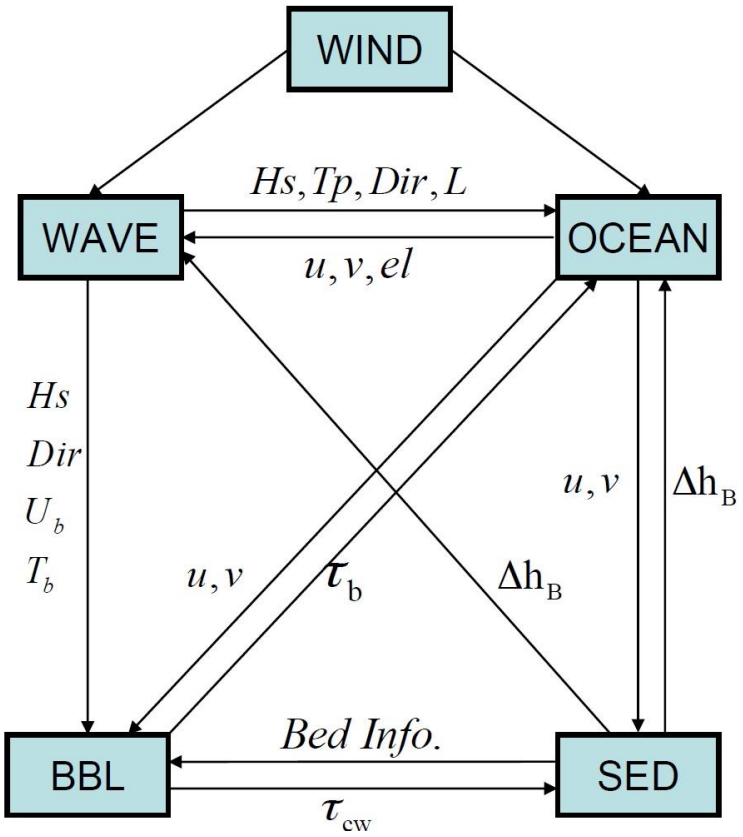

Figure 3.3. Schematic of coupling FVCOM circulation, wave, and sediment transport modules (Chen et al., 2013)

FVCOM-SWAVE takes current velocities, sea surface elevation, and bathymetry change as inputs when coupled with the FVCOM circulation model. FVCOM-SED is directly interacting by the circulation module, while wave actions affect sediments by changing shear stresses in the BBL.

3.3. Suspended Load

The suspended load is calculated by accounting for advective and diffusive concentration-based transport, using the following equation:

$$\frac{\partial C}{\partial t}+\frac{\partial uC}{\partial x}+\frac{\partial vC}{\partial y}+\frac{\partial wC}{\partial z}=\frac{\partial}{\partial x}\left(A_H\frac{\partial C}{\partial x}\right)+\frac{\partial}{\partial y}\left(A_H\frac{\partial C}{\partial y}\right)+\frac{\partial}{\partial z}\left(K_V\frac{\partial C}{\partial z}\right)+\frac{1}{H_z}C_{Source/sink} \quad (3.2)$$

where C is the sediment concentration, (u, v, w) are the three components of velocity in (x, y, z) Cartesian grid coordinates, A_H is the horizontal eddy viscosity, K_V is the vertical eddy viscosity, and H_z is the grid cell thickness. $C_{source/sink}$ also refers to additional exchange with water column through settling and resuspension as follows:

$$C_{source/sink} = -\frac{\partial \omega C}{\partial S} + E_s \tag{3.3}$$

where ω is the settling velocity positive in the upwards direction (m/s) and E_s is the erosion rate ($kg/m^2/s$) in the vertical sigma coordinate direction S. Ariathurai and Arulanandan (1978) defined erosion rates as:

$$E_s = E_0(1-\varphi)\frac{\tau_{sf} - \tau_{ce}}{\tau_{ce}}, \qquad if \qquad \tau_{sf} > \tau_{ce} \tag{3.4}$$

where E_0 is the bed erodibility constant ($kg/m^2/s$), φ is the porosity of the top bed layer. It should be noted that the suspended load is calculated for each individual sediment class, i.e., C, E_s, and ω are defined and calculated separately for each of those sediment classes.

At the surface of the water column, a no-flux boundary condition is considered for the sediment transport model:

$$K_V \frac{\partial C}{\partial z} = 0, \qquad z = 0 \tag{3.5}$$

The net sediment flux at the bottom is defined as the difference between erosion and deposition rates and is used for bottom boundary condition:

$$K_V \frac{\partial C}{\partial z} = E_s - D_s, \qquad z = -H \tag{3.6}$$

where D_s denotes the erosion rates at the bottom and H is the depth of the water column.

3.4. Bedload

Bedload transport rates are calculated based on Hans Albert Einstein's definition of non-dimensionalized volumetric sediment flux (q_{s*}):

$$q_{bl} = q_{s*} D_{50} \sqrt{(s-1) g D_{50}} \tag{3.7}$$

where q_{bl} is the horizontal bedload transport rate (m^2/s), D_{50} is the median size diameter (m), $s = \rho_s/\rho_w$ is the specific density in water, ρ_s is the sediment density (kg/m^3), and ρ_w is the water density (kg/m^3). q_{s*} is the magnitude of the non-dimensional transport rate for each sediment class and can be estimated in different ways, some of which are provided by FVCOM-SED.

In this study, bedload transport is calculated using the Meyer-Peter and Müller (1948) scheme based on the non-dimensional transport rate that can be estimated by the following equation:

$$q_{s*} = \max[8(\theta_{sf} - \theta_c)^{1.5}, \quad 0] \tag{3.8}$$

where $\theta_c = 0.047$ is the critical Shields parameter for skin stress and θ_{sf} is the Shields non-dimensional skin stress parameter defined as below:

$$\theta_{sf} = \frac{\tau_{sf}}{(\rho_s - \rho_w) g D_{50}} \tag{3.9}$$

The shear stresses due to pure currents in x and y directions ($\tau_{bx,c}$ and $\tau_{by,c}$) are estimated using the following equations:

$$\tau_{bx,c} = \frac{\kappa^2 \rho_w u \sqrt{u^2 + v^2}}{ln^2(z/z_0)} \tag{3.10}$$

$$\tau_{by,c} = \frac{\kappa^2 \rho_w v \sqrt{u^2 + v^2}}{ln^2(z/z_0)} \quad (3.11)$$

$$\tau_c = (\tau_{bx,c}^2 + \tau_{by,c}^2)^{0.5} \quad (3.12)$$

where $\kappa = 0.41$ is the von Karman's constant, z_0 is the constant bottom roughness length (m), z is the elevation of the center point of the bottom layer elements above the bed (m), and τ_c is the magnitude of the bottom shear stress due to currents (N/m^2). τ_{bx} and τ_{by} are calculated at the face of each element and then interpolated to the center of the cell. Shear stress due to waves is calculated based on:

$$\tau_w = 0.5\, f_w u_b^2 \quad (3.13)$$

Where u_b is the bottom wave orbital velocity (m/s) and f_w is the wave friction factor suggested by Madsen (1995). f_w is a function of wave excursion amplitude and bottom roughness length. Maximum bottom shear stress (τ_{sf}) is then calculated based on the vector sum of the shear stresses due to currents and waves.

Lesser et al. (2004) suggested a coefficient to modify bedload rates by accounting for local bed slope:

$$q_{bl,slope} = \frac{\tan \varphi_m}{(\tan \varphi_m - \tan \beta)\ \cos \beta} \quad (3.14)$$

$$\beta = \tan^{-1}\left(\frac{dz}{dx}\right) \quad (3.15)$$

where $q_{bl,slope}$ is the Lesser bedload correction coefficient, φ_m is the sediment friction angle, and β is estimated for each transport direction with a positive dz/dx in the downslope direction. To adjust the bedload transport, bedload rate is multiplied by the Lesser coefficient.

Previous studies (Lee et al., 2005) have shown that the most sensitive parameters in the sediment transport models of Lake Michigan are the fraction of fine-grained materials and sediment availability. Lee et al. (2005) also recommended that other re-suspension parameters such as settling velocity, critical shear stress, and erosion rate constant has been also found to be important and may cause up to a 40% difference in suspended sediment concentration. More details regarding the sediment classes in Green Bay and Lake Michigan, as well as estimation of sediment model parameters for those classes, are provided in sections 4.6 and 4.7.

3.5. Mixed Sediment

FVCOM-SED is capable of modeling cohesive (Sherwood et al., 2018) and/or non-cohesive (Warner et al., 2008) sediments. Mixed-sediment bed processes occur when both cohesive and non-cohesive sediments are present and considerable mud content is available in the sediment layer (Mitchener and Torfs, 1996). Critical shear stress of a mixed bed is calculated based on a weighted combination of cohesive and non-cohesive contents of the bed using the equation below:

$$\tau_{ce,eff} = max[P_c\tau_{cb} + (1 - P_c)\tau_{ce}, \tau_{ce}] \quad (3.16)$$

where $\tau_{ce,eff}$ is the effective critical shear stress for each sediment class, τ_{ce} is the particle shear stress for each sediment class, τ_{cb} is the bulk shear stress for sediment layer and is estimated based on Sanford's (2008) method, and P_c is the dimensionless cohesive behavior parameter. $P_c=0$ denotes a non-cohesive behavior, $P_c=1$ denotes cohesive behavior, and values between these limits changes based on the overall mud content in the bed layer (f_c) as follows:

$$P_c = \begin{cases} 0, & f_c \le f_{nc,thresh} \\ min\left[max\left(\dfrac{f_c - f_{nc,thresh}}{f_{c,thresh} - f_{nc,thresh}}\right), 0\right], & f_{nc,thresh} \le f_c \le f_{c,thresh} \\ 1, & f_c \ge f_{c,thresh} \end{cases} \quad (3.17)$$

$$f_c = \frac{\sum_{i=1}^{NCS} f_i \rho_i}{\sum_{i=1}^{NCS} f_i \rho_i + \sum_{i=1}^{NNS} f_i \rho_i} \quad (3.18)$$

where $f_{nc,thresh}$ and $f_{c,thresh}$ define thresholds of non-cohesive and cohesive bed behavior and typically have values of ~0.03-0.10 and ~0.2-0.3, respectively (Sherwood et al., 2018). f_i and ρ_i denote volume fraction and the sediment grain density of each sediment class i, respectively. NCS and NNS also indicate the number of cohesive and non-cohesive sediment classes in each bed layer.

There are different versions of sediment concentrations that can be used in the simulation of sediment fields in Green Bay. However, previous research has focused on the simulation of the TSS in Green Bay and Lake Michigan (e.g., Eadie et al., 1991; Hawley and Niester, 1993; Lee et al., 2005). There is also a rich TSS database available for lower Green Bay and mouth of the Fox River that can be used to estimate loadings in the bay and initiate the sediment transport model. More details are provided in Chapter 4.

Chapter 4:
Model Validation Criteria, External Forcings, and Field Data

4.1. Model Validation and Error Criteria

For validation of the scalar quantities in hydrodynamic and sediment transport models, four error criteria were selected: Root Mean Squared Error ($RMSE$), Bias Deviation (BD), Nash-Sutcliffe Efficiency (NSE) coefficient, and correlation coefficients (CC). Model skills for scalar variables can be assessed using the following formulation:

$$RMSE = \frac{1}{N}\left(\sum_{i=1}^{N}(e_i^2)\right)^{1/2} \tag{4.1}$$

$$BD = \frac{1}{N}\sum_{i=1}^{N}(e_i) \tag{4.2}$$

$$NSE = 1 - \frac{\sum_{i=1}^{N}(e_i^2)}{\sum_{i=1}^{N}(x_{i,O} - x_{ave,O})^2} \tag{4.3}$$

$$CC = \frac{\sum_{i=1}^{N}(x_{i,O} - x_{ave,O})(x_{i,P} - x_{ave,P})}{\left[\sum_{i=1}^{N}(x_{i,O} - x_{ave,O})^2\right]^{1/2}\left[\sum_{i=1}^{N}(x_{i,P} - x_{ave,P})^2\right]^{1/2}} \quad (4.4)$$

where N is the number of observations/predictions, e_i is the error of prediction (i.e., $e_i = x_{i,O}-x_{i,P}$; where $x_{i,O}$ and $x_{i,P}$ denote observation and prediction at point i, respectively) and $x_{ave,o}$ and $x_{ave,P}$ are the mean of observed and predicted data, respectively.

$RMSE$ represents model accuracy and the average error in the same unit of the variable (Wilks, 2011, p. 359). BD expresses the average deviations of prediction from observations (truth) and indicates an over- or underestimation of observations. Additionally, the NSE coefficient can be utilized to assess the predictive power of a model (Nash and Sutcliffe, 1970) and has been widely used to measure the accuracy of hydrological and water quality simulation models (Moriasi et al., 2007). Correlations between the observed and predicted data can also be taken into consideration in order to evaluate how well the simulations are producing the patterns of variabilities in the observations.

Clearly, lower $RMSE$ and BD values indicate better performance of the model. Also, NSE ranges from -∞ to 1, such that, $NSE = 1$ exhibits a perfect model, $NSE = 0$ indicates that the predictions are as accurate as the mean of the observational data, and negative values of NSE coefficient corresponds to the condition that the mean of observations can predict better than the model. Therefore, as the NSE gets closer to one, better results are expected from the model.

CC ranges between -1 and 1 with values close to 0 for the poor performance of the model in reproducing the patterns of change in observational data and values close to 1 for the best model performance. Correlations lower than zero will not be favorable for the

purpose of current model validation as they are basically indicating that the model is inversely simulating the observational data. It should also be mentioned that CC values are valid if they are significant. In the current study, CCs are reported if significant at $p\text{-}value <= 0.05$.

Model skills assessment for vector variables such as currents requires a different procedure. We use normalized Fourier norm (F_n) and average angle difference ($\Delta\theta$) to assess hydrodynamic model capability in the simulation of current vectors (Rowe et al., 2015; Schwab, 1983):

$$F_n = \frac{\|V_o, V_p\|}{\|V_0, 0\|} = \frac{\left(\frac{1}{N}\sum_{i=1}^{N}\left|V_{i,o} - V_{i,p}\right|^2\right)^{1/2}}{\left(\frac{1}{N}\sum_{i=1}^{N}\left|V_{i,o} - 0\right|^2\right)^{1/2}} \tag{4.5}$$

$$\Delta\theta = \frac{1}{\pi N}\sum_{i=1}^{N}\cos^{-1}\left(\frac{V_o . V_p}{|V_o||V_p|}\right) \tag{4.6}$$

where $V_{i,o}$ and $V_{i,p}$ denote observed and predicted currents vector at point i, respectively. $F_n = 0$ exhibits a perfect model, values between 0 and 1 are in the acceptable range and values greater than 1 indicate decreased model performance. $\Delta\theta = 0$ indicates a perfect directional agreement.

4.2. Meteorological Forcing

The external forcing was generated based on the interpolation of data obtained by land-based (and when available buoy) meteorological stations. Data of these meteorological stations are available at NOAA National Centers for Environmental Information (NCEI; NOAA, 2018). Figure 4.1 shows the location of these stations in the Great Lakes basin.

The interpolated forcing data was calculated based on a computer program developed to

generate metrological forcing for use in NOAA Great Lakes forecasting models (Beletsky et al., 2003; Schwab and Beletsky, 1998). The interpolation function utilizes a Natural Neighbor Method to interpolate forcing variables of air temperature, dew point temperature, cloud cover, wind direction, and wind speed. Empirical relationships were used to perform overland-overlake adjustments whenever land-based meteorological data was available and used (Beletsky and Schwab, 2001).

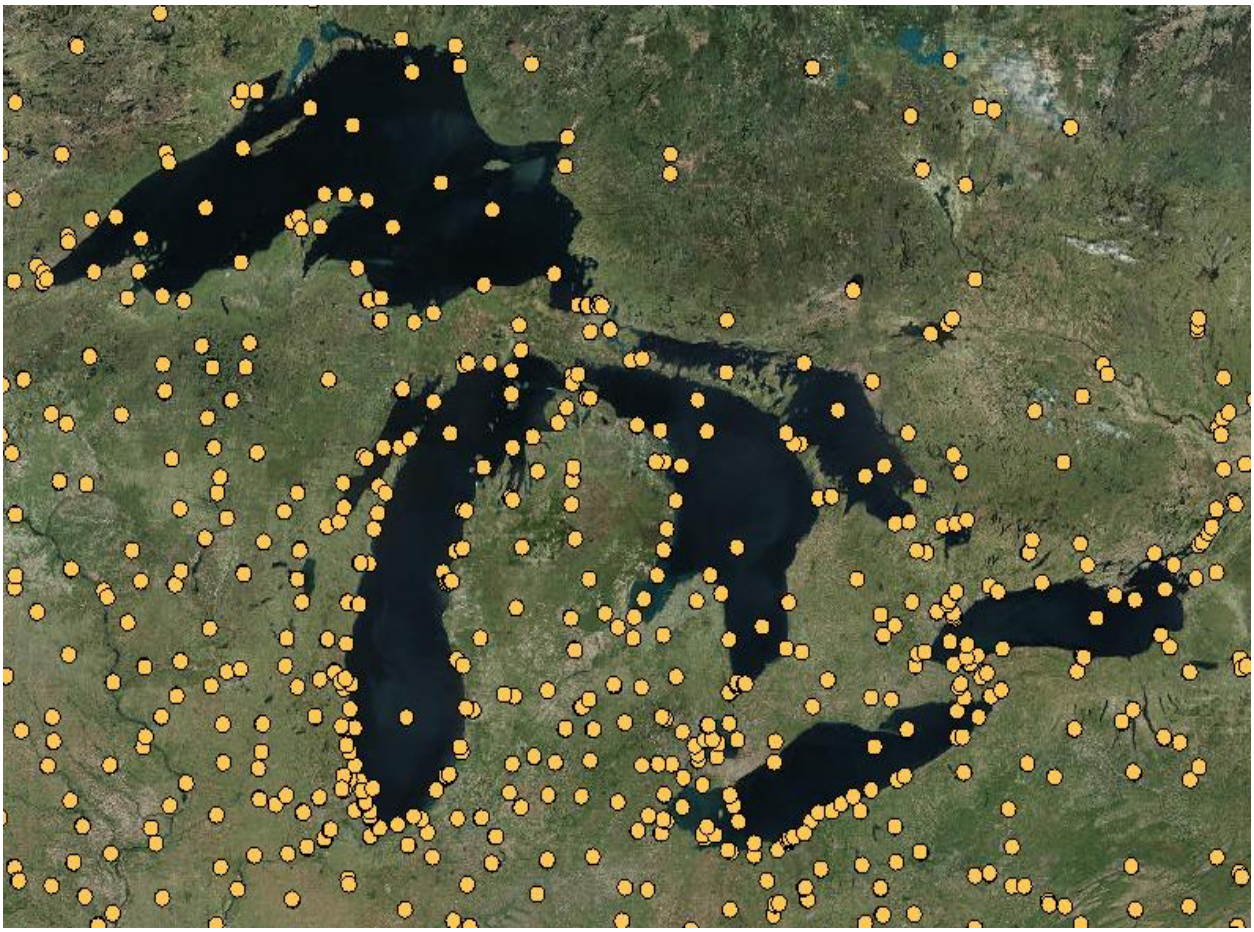

Figure 4.1. Location and distribution of the land-based and buoy meteorological stations available for use in the interpolation and generation of meteorological forcing (NOAA, 2018a)

Net heat flux was also calculated based on the balance of shortwave and longwave

radiative fluxes as well as sensible and latent heat flux components. The procedure is explained by McCormick and Meadows (1988) in detail. The interpolation function has been compared with other meteorological datasets such as North American Regional Reanalysis (NOAA, 2018b). Comparisons of the two datasets showed that the FVCOM works quite well when the interpolation procedure is used to generate the external forcing (Rowe et al., 2015). We limited our simulation to the period of May-October of each year because bottom layer interactions are maximum (Fillingham, 2015) and ice cover in Green Bay is zero during this period (Wang et al., 2012).

Comparisons of the interpolated meteorological forcing data with observations in 2018 and 2019 at buoy stations 45014 (southern Green Bay), 45013 (Milwaukee Atwater Beach), 45002 (northern Lake Michigan), and 45007 (southern Lake Michigan) were carried out to validate and double-check the process of external forcing preparation. Results of such comparison are presented in Appendix B. Figure 4.6 illustrates the locations of those buoy stations.

Figures 4.2 and 4.3 show interpolated air temperature, dew point temperature, and cloud cover over the Lake Michigan surface at the beginning of the simulation period, i.e., the initial condition for forcing on May 1st of 2018 and 2019. Also, Figures 4.4 and 4.5 show the interpolated wind field and general wind pattern over the surface of Lake Michigan at the beginning of the simulations in 2018 and 2019.

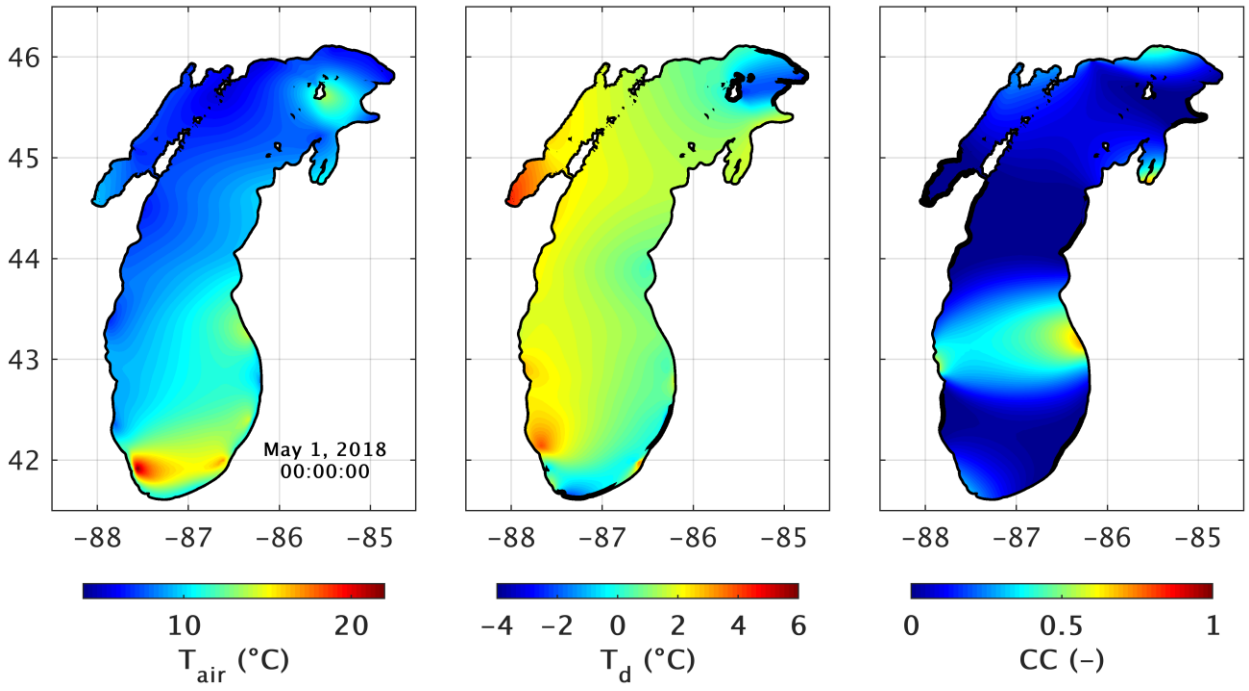

Figure 4.2. Interpolated air temperature (T_{air}), dew point temperature (T_d), and cloud cover (CC) at the beginning (May 1st) of simulations in the year 2018

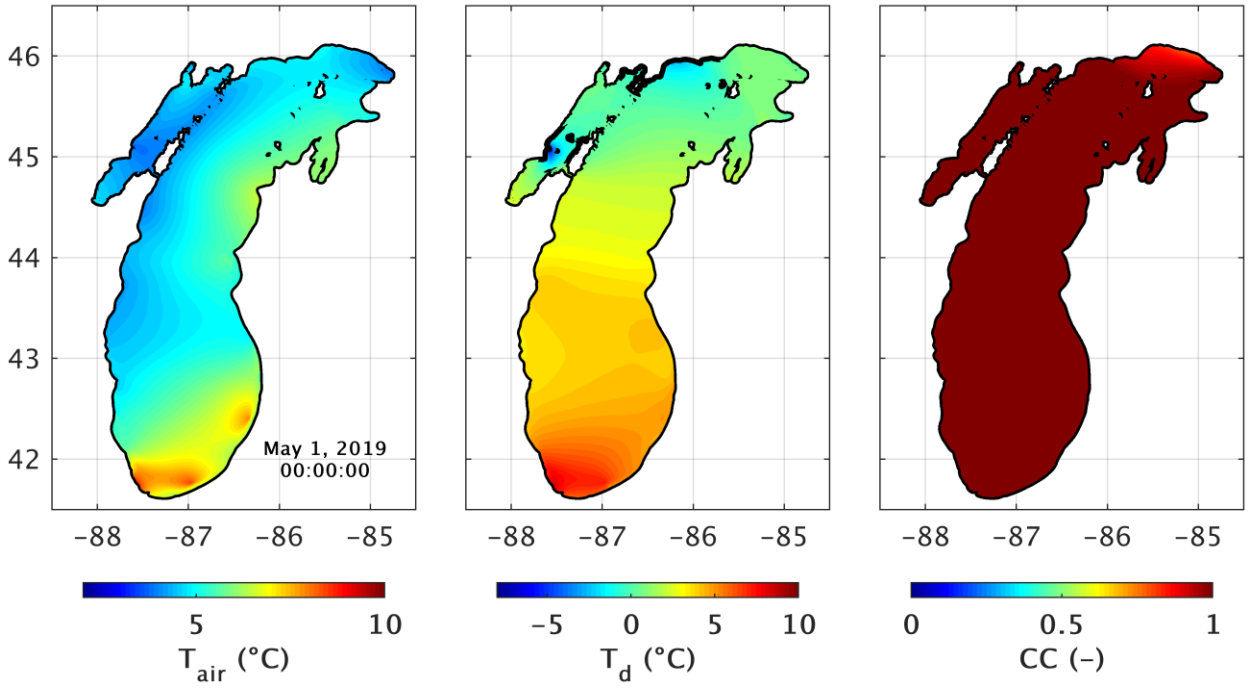

Figure 4.3. Interpolated air temperature (T_{air}), dew point temperature (T_d), and cloud cover (CC) at the beginning (May 1st) of simulations in the year 2019

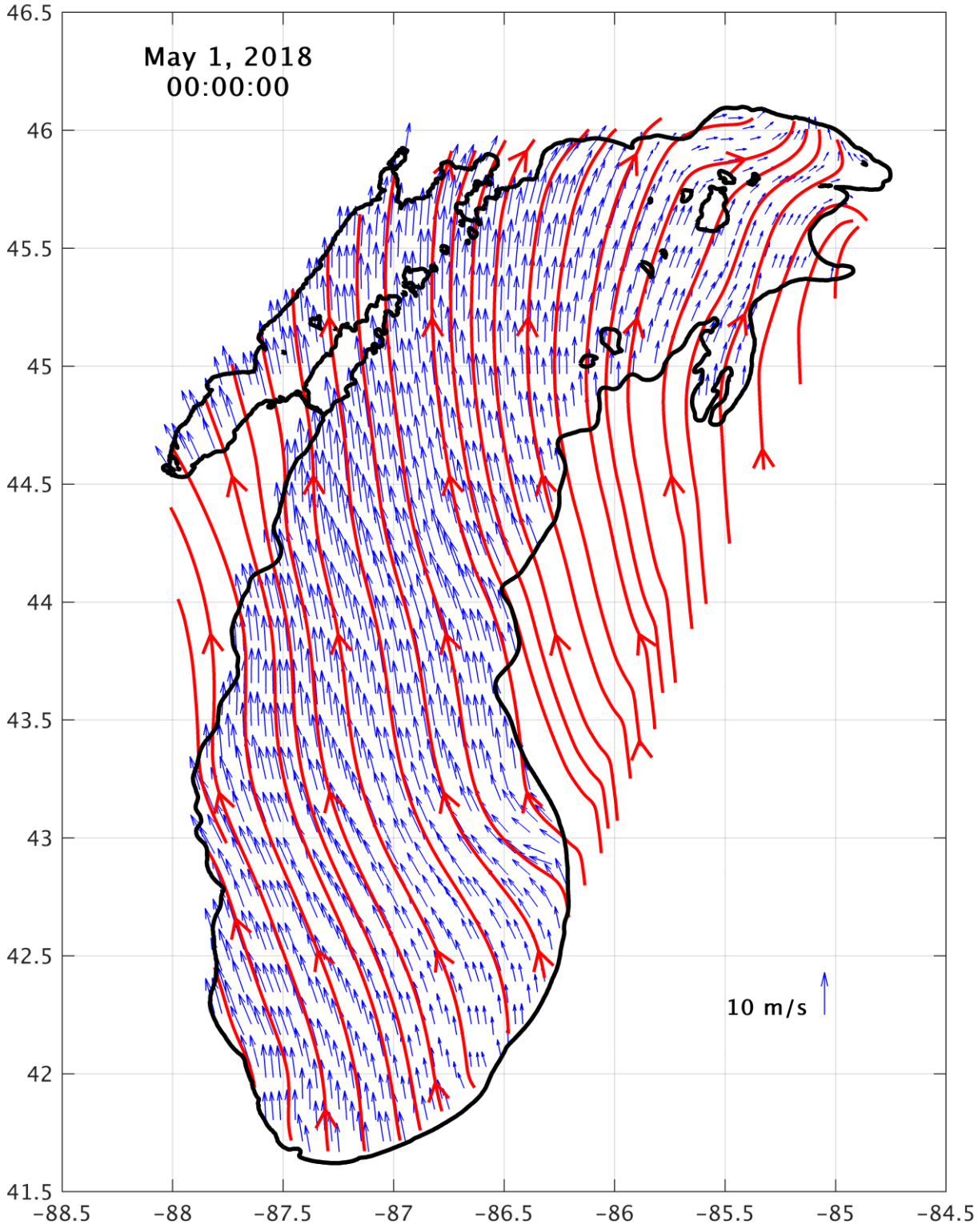

Figure 4.4. Interpolated wind fields (in blue) and general wind patterns (in red) at the beginning (May 1st) of simulations in the year 2018 over the Lake Michigan surface

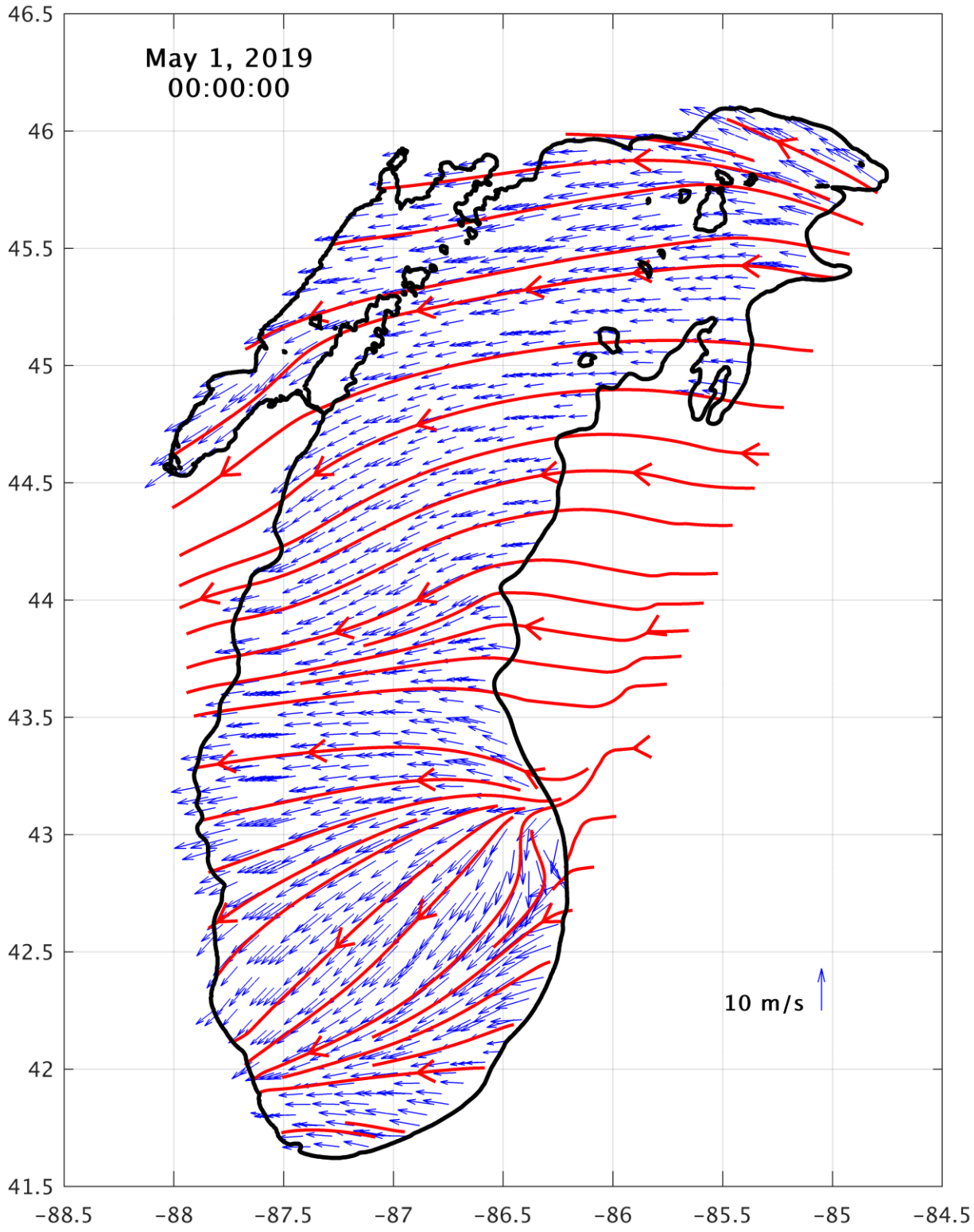

Figure 4.5. Interpolated wind fields (in blue) and general wind patterns (in red) at the beginning (May 1st) of simulations in the year 2019 over the Lake Michigan surface

4.3. Field Data

Data from different sources is required to construct a hydrodynamic and sediment transport model. The required dataset includes meteorological data, inflow rates and sediment loads into the system, and sediment characteristics of the study area. Field data is also required for model validation, and that dataset includes data on currents, temperature, wave data, and sediment concentration. Meteorological data used to generate the external forcing is the largest portion of the input data required for initializing and running the hydrodynamic model, and as explained in section 4.1, it is based on NOAA meteorological stations.

Four buoy stations located in different zones of Lake Michigan were selected to validate interpolated meteorological forcing data and the simulations of current and temperature. These stations are southern Green Bay (station ID: 45014), Atwater Beach in Milwaukee nearshore zone (station ID:45013), North Michigan (station ID: 45002), and South Michigan (station ID: 45007) central buoys. Table 4.1 shows the abbreviations used for these stations and their latitudes and longitudes. Locations of these buoy stations are also shown in Figure 4.6. Stations 45013 and 45014 are operated by UWM and the other two buoys are maintained and owned by the National Data Buoy Center (NDBC).

Field data from other sources was also obtained and used in this research. NEW Water TSS and turbidity observations in the Fox River and lower Green Bay are used for the estimation of loads from the Fox River. NEW Water measures water quality by analyzing samples taken in the Fox River and lower Green Bay AOC (shown in Figure 1.1). The NEW Water monitoring program provided a long-term time series of TSS and turbidity since 1991 and 2002, respectively, that was used in estimations of loading rates from

major rivers.

Table 4.1. List of buoy stations and sampling locations used in the study

Station Name	Station ID	latitude	longitude
Southern Green Bay Buoy	45014	44.80	-87.76
Milwaukee Atwater 20m Buoy	45013	43.10	-87.85
Northern Michigan Buoy	45002	45.34	-86.41
Southern Michigan Buoy	45007	42.67	-87.03
USGS Fox River Gauge	40851385	44.53	-88.01
USGS Menominee River Gauge	4067500	45.33	-87.66
Green Bay West Buoy	GBW	44.58	-87.99
Green Bay East Buoy	GBE	44.55	-87.96
NEW Water Station 13	NW 13	44.53	-88.01

In addition to the data obtained from the NEW Water monitoring program, there are other data collection efforts in the lower Green Bay that will provide data on turbidity and other water quality parameters (http://www.lakestat.com/). Those data collection efforts are operated by UWM researchers (Miller Lab in the School of Public Health, http://www.toddrexmiller.com/). Locations of the sampling sites GBW and GBE are shown in Figure 4.6.

As explained above, streamflow discharge into the lake and sediment loading data by inflowing rivers are essential in running a sediment transport model. Therefore, USGS data of discharge and turbidity at the mouth of Fox and Menominee Rivers are used for this purpose. The locations of the USGS gage stations at the mouth of the rivers are shown in Figure 4.6.

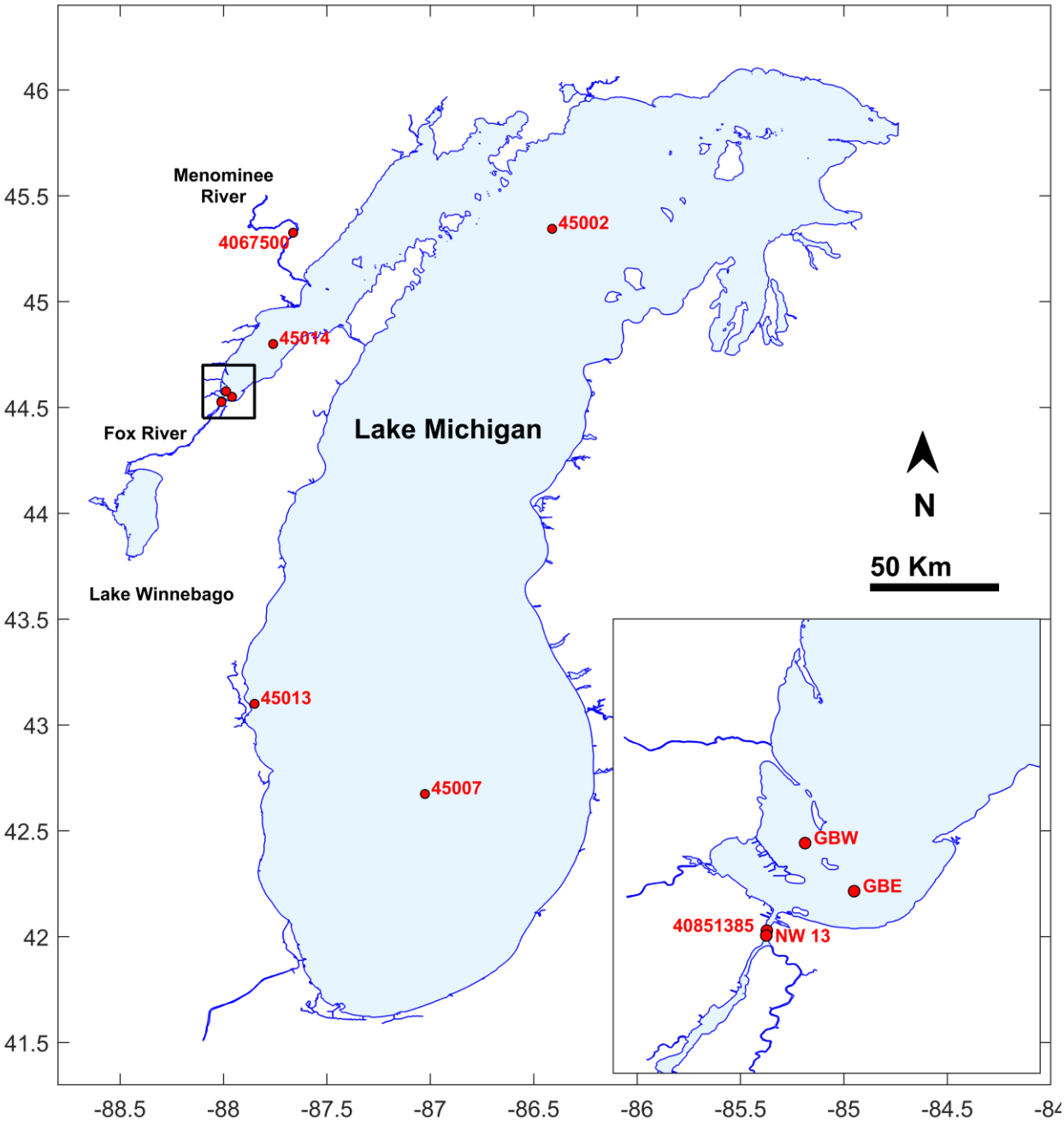

Figure 4.6. Locations of the selected buoy stations in Green Bay and Lake Michigan, USGS stations at Fox and Menominee Rivers, Green Bay West (GBW) and Green Bay East (GBE) buoys, and NEW Water Station 13 (NW 13)

It should be noted that there are always challenges in providing sufficient data to run a sediment transport model; scarcity of simultaneous measurements of currents,

temperature, and transported substances, inconsistent special and/or temporal resolution, outlier and/or erroneous field data, information on bed layer details and particle size distribution, to name a few. An important source of data that can be used to validate the sediment transport model and patterns/rates of sediment dynamics is the map of sediment accumulation rates (shown in Figure 4.7) in Green Bay compiled by Klump et al. (1997).

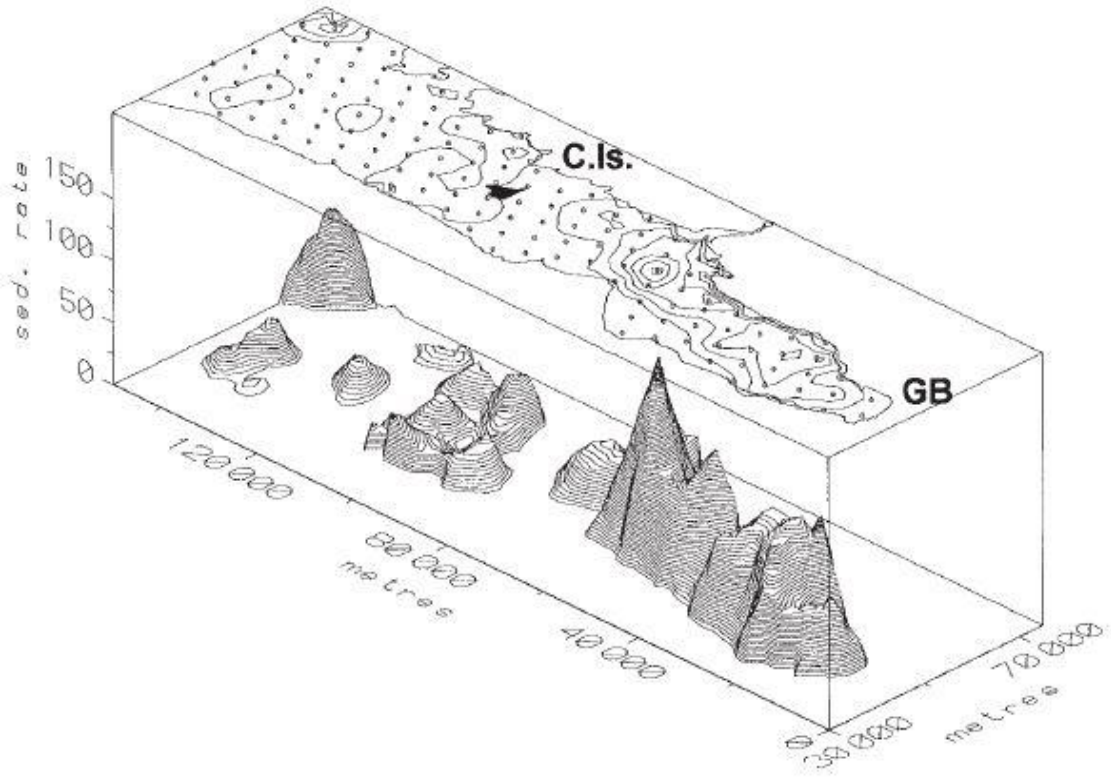

Figure 4.7. Mass sediment accumulation rates for Green Bay interpolated from ^{210}Pb-dated sediment cores. Contour intervals are 5 mg/cm^2/year in the lower plot and 30 mg/cm^2/year in the surface plot. Reproduced from Klump et al. (1997), data are from Manchester-Neesvig et al. (1996).

4.4. Initial Conditions

Initial conditions include three-dimensional values for water temperature, currents, and

turbulent variables for the hydrodynamic model and sediment class distribution for the sediment transport model. In this study, the model starts at rest, i.e., with zero values for current and turbulent variables. Water temperature is estimated based on the simulations of NOAA GLERL models mapped into the grid developed for current research. A 3D interpolation technique coded in MATLAB is used for the translation of temperature fields from NOAA's grid to the grid described in section 2.2. Also, the model started with zero sediment concentration in the water column and 1 m of sediment mass in the bed layer. More details regarding the sediment classes used in this study, as well as their characteristics and distribution throughout the lake, are provided in sections 4.6 and 4.7.

4.5. Boundary Conditions

As mentioned in section 2.2, no open boundary conditions were defined for the grid. Straits of Mackinac, Chicago River diversion, and water intakes around the lake are the main outflows from Lake Michigan. Those outflows were not considered for modeling in this research, as they do not have an important effect on the circulation regimes of Green Bay.

Among the several Green Bay tributaries, Fox River is the largest river flowing into the bay and one of the largest tributaries of Lake Michigan, and it plays an important role in the formation of the stratified flow conditions and circulation patterns in the bay. Also, the Fox River is the main source of sediment—and nutrient—loading into Green Bay; hence, it cannot be neglected in modeling the sediment transport in the bay. Another major tributary of Green Bay is the Menominee River which is located at the border of Wisconsin and the Upper Peninsula of Michigan. It provides more or less the same amount of volumetric water to Green Bay but much fewer sediment loads compared to the Fox River.

The Menominee river is also considered as an input boundary condition to the hydrodynamic and sediment transport models. Other tributaries are the Oconto and Peshtigo Rivers, but, their water and sediment input fluxes are minor comparing to Fox River and were neglected for this study. Table 4.2 shows the average and standard deviation of discharge and TSS concentration at the mouth of Fox, Menominee, Oconto, and Peshtigo Rivers based on the USGS measurements during the 2011-2019 period.

Table 4.2. Average and standard deviation of discharge (Q) and total suspended solids (TSS) concentration of Green Bay major tributaries based on the USGS measurements during the 2011-2019 period

River	Drainage area (Km^2)	Discharge (m^3/sec)		TSS (mg/L)	
		mean	std	mean	std
Fox	16,395	170	107	24	18
Oconto	2,500	24	20	0.24	0.30
Peshtigo	2,800	29	22	0.30	0.33
Menominee	10,180	106	77	3	2

As shown in Table 4.2, TSS loading by Peshtigo and Oconto Rivers is negligible, and therefore, is not included in the simulations. In addition to discharge and TSS concentration at the mouth of input tributaries, water temperature at these locations is also required for running the hydrodynamic model. Discharge and temperature time series were obtained based on the direct observations of USGS gauges. TSS concentration is estimated based on the relationship between TSS and turbidity in the lower Green Bay and USGS observations of turbidity. Sections 4.5.1 and 4.5.2 describe the procedure for estimations of the TSS time series in more detail. Figure 4.8 illustrates those time series at the mouths of Fox and Menominee Rivers for the period of 2011-

2019, when data for all required variables is available. Temperature, discharge, and TSS time series at the mouth of Fox and Menominee Rivers define the point source boundary conditions of the hydrodynamic and sediment transport models.

4.5.1. River Temperature and Discharge Inputs

USGS gauge stations 040851385 and 04067500 (locations are shown in Figure 4.6) monitor temperature at the mouth of Fox and Menominee Rivers, respectively, on a daily basis since 2011. Also, these two monitoring stations observe daily discharge from 1988 and 1981, respectively. Observations of temperature and discharge time series at these two stations were used as the river boundary conditions of the hydrodynamic model. Figure 4.8 illustrates these time series during the period of 2011-2019. There were a few gaps in the time series of both datasets which were filled using interpolation techniques.

4.5.2. Estimation of Sediment Loading Rates from Inflowing Rivers

Although rivers are the main supplier of sediments to Green Bay, in particular Fox River, there are no existing records of TSS loading time series from rivers. However, USGS observations of discharge and turbidity at the mouth of major inflowing rivers (i.e., Fox and Menominee Rivers) provides the opportunity for estimation of TSS time series at these locations given the strong relationship between turbidity and TSS. In addition, other parameters such as specific conductance, dissolved oxygen, and pH have also been observed during the past few years at the rivers' mouth that can be used in water quality studies of the lower Green Bay. The City of Green Bay Sewerage district, NEW Water, collects water quality samples along the Fox River, and measures TSS and turbidity at NEW Water station 13 (location is shown in Figure 4.6), very close to the location of USGS gauge station at the river mouth.

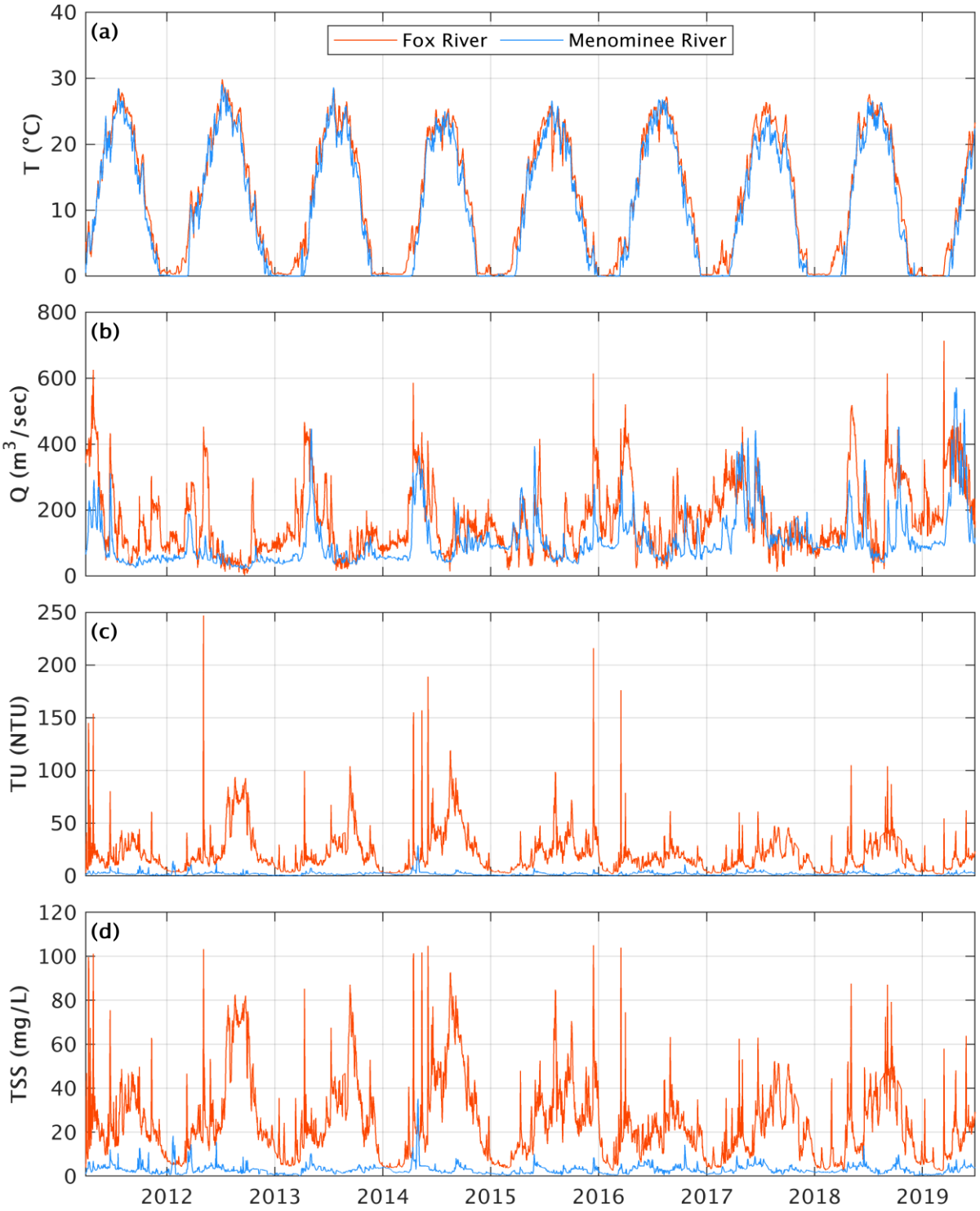

Figure 4.8. Daily temperature (T), discharge (Q), turbidity (TU), and total suspended solids (TSS) time series at the mouth of Fox and Menominee Rivers based on the observations at USGS gage stations 040851385 and 04067500, respectively, during the 2011-2019 period.

Different empirical relationships between turbidity and TSS, and between discharge and TSS were developed using data collected by NEW Water and USGS at the mouth of Fox River. The (turbidity, TSS) data pairs were based on NEW Water data collection. The (discharge, TSS) data pairs were based on discharge data collected by the USGS gauge and TSS data collected at the NEW Water station 13, respectively.

Different functional relations including linear, non-linear polynomials, power, and exponential functions were developed and tested between each pair of data. The 2nd order polynomial, power, and exponential functions showed the best performance. Those empirical relationships are formulated as below:

$$TSS = aX + bX^2 \quad (4.7)$$

$$TSS = aX^b \quad (4.8)$$

$$TSS = aXe^{bX} \quad (4.9)$$

where Equations 4.7, 4.8, and 4.9 represent the 2nd order polynomial, power, and exponential functions, respectively, X is the independent variable, i.e. turbidity or discharge here, and a and b are empirical coefficients. The intercept of the polynomial relationship was set to zero in order to avoid negative TSS estimations.

TSS and turbidity are highly correlated and can be used to accurately estimate TSS. Analyses of the available data in lower Green Bay also show that TSS can be estimated with good accuracy using the TSS-turbidity relationship. Figures 4.9 a, b, and c show comparison of the estimated and observed TSS based on the 2nd order polynomial, power, and exponential functions, respectively. According to the error criteria shown in Table 4.3, all of the three selected functions indicate good performance for this

relationship.

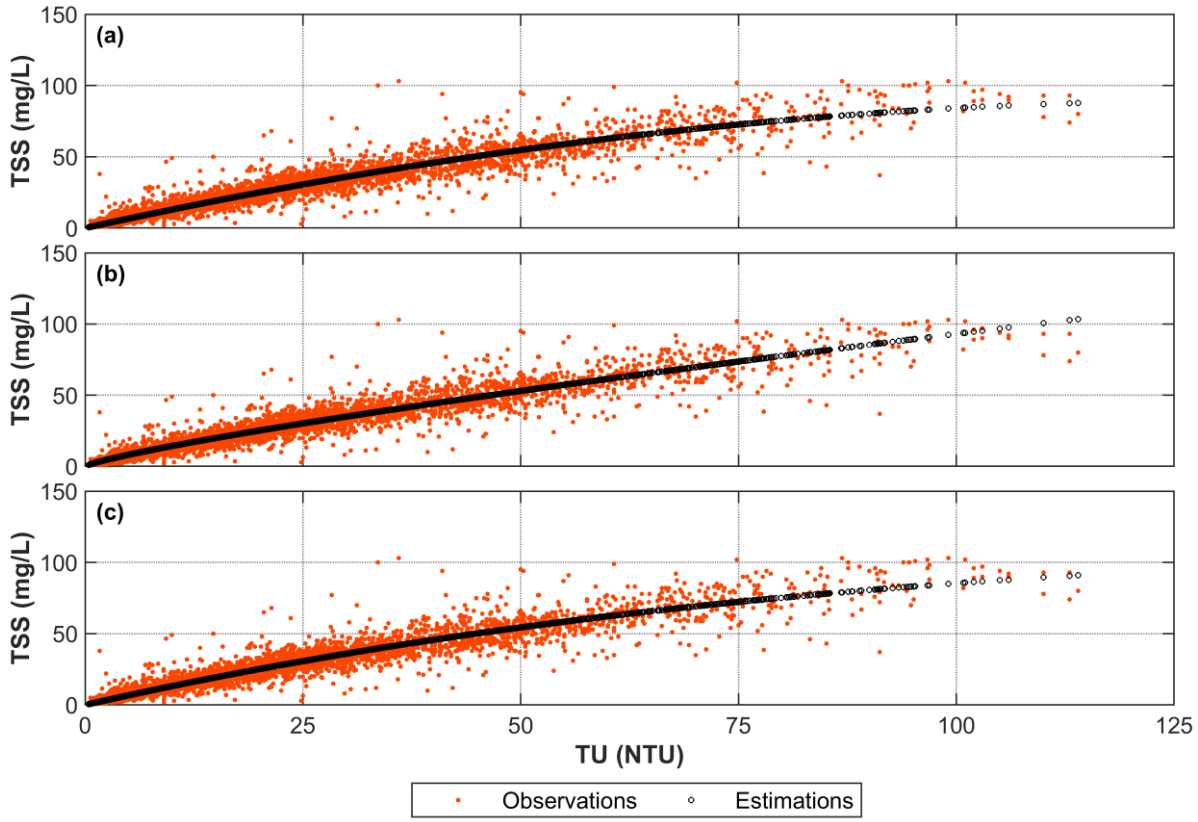

Figure 4.9. Empirical 2nd order polynomial (a), power (b), and exponential (c) functions used to estimate TSS based on the relationship between total suspended solids (TSS) and turbidity (TU) and using NEW Water observations during the 2002-2016 period

Table 4.3. Error criteria for total suspended solids (TSS) estimation based on the best selected empirical relationships for TSS-turbidity relationship

Empirical model	Coefficient a	Coefficient b	RMSE (mg/L)	BD (mg/L)	NSE
2nd order polynomial	1.349	-0.005	5.69	-0.29	0.92
power	2.200	0.813	5.71	0.20	0.92
exponential	1.387	-0.005	5.67	-0.19	0.92

Based on the available turbidity time series at the mouth of Fox River from the USGS gauge station and the suggested empirical models, TSS time series were generated and

illustrated in Figure 4.10. As can be seen in the figure, predictions are in good agreement with observations at this location.

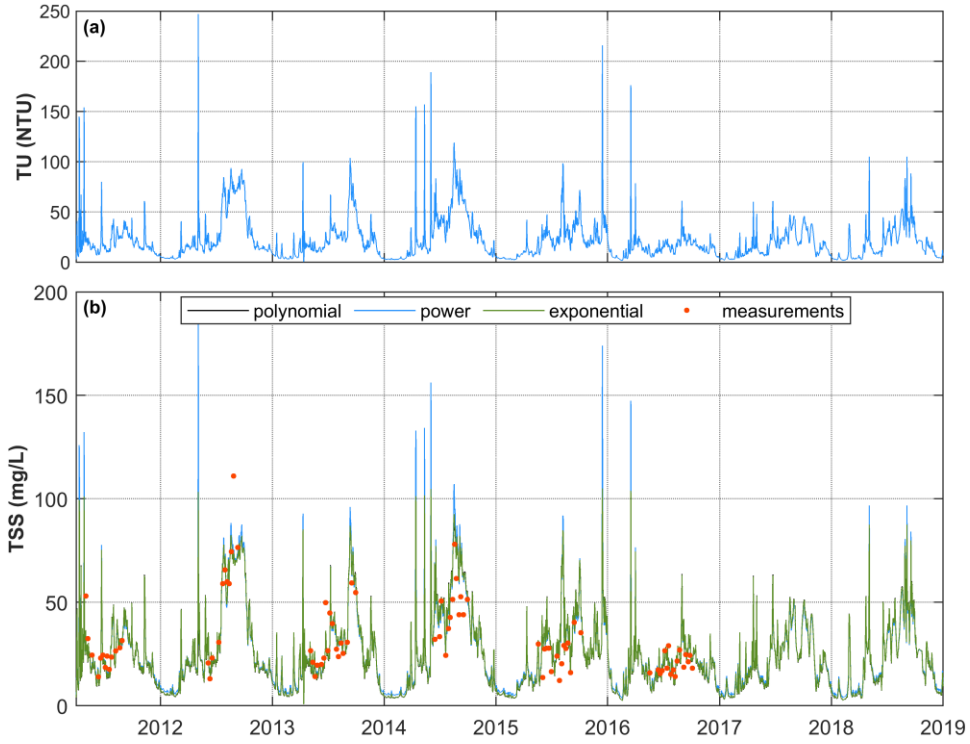

Figure 4.10. Turbidity (TU) time series based on USGS observations (a); and corresponding total suspended solids (TSS) time series estimated based on the suggested empirical relationships at the mouth of Fox River during the period of 2011-2019 (b). Red dots show NEW Water measurements at this location (station 13).

Another attempt was made to generate TSS time series at the mouth of Fox River based on the available TSS and discharge data pairs and the suggested empirical Equations 4.7 to 4.9. Figures 4.11 a, b, and c show comparison of the estimated and observed TSS based on the 2nd order polynomial, power, and exponential functions developed for the TSS-discharge relationship, respectively.

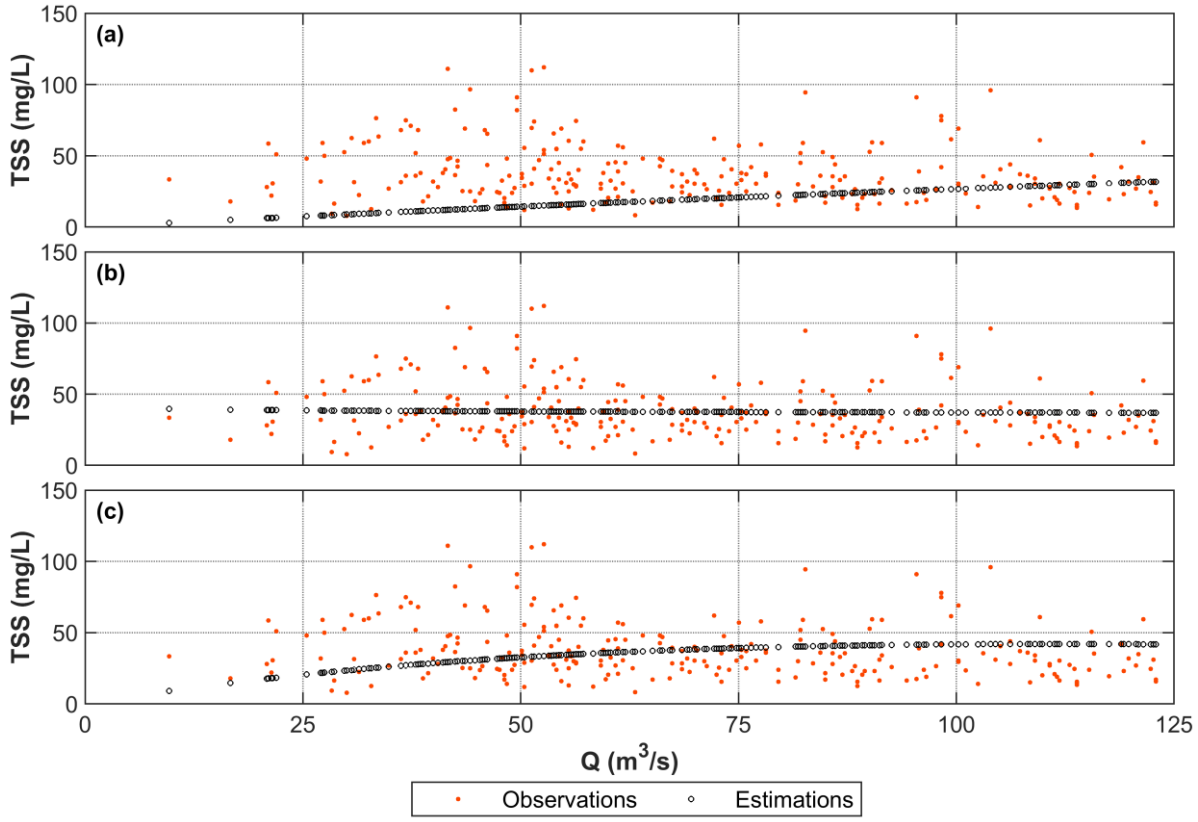

Figure 4.11. Empirical 2nd order polynomial (a), power (b), and exponential (c) functions used to estimate total suspended solids (TSS) based on the relationship between TSS and discharge (Q) and using NEW Water and USGS observations during the 1991-2016 period

As shown in the figure, TSS-discharge data is scattered, especially in low-flow events and requires more efforts to be considered for a legit relationship between the two variables. Table 4.4 also indicates that none of the functions was able to accurately predict TSS.

Based on the discharge time series at the mouth of Fox River from the USGS gauge station and the suggested empirical functions, TSS time series were generated and illustrated in Figure 4.12. As can be seen in the figure, selected empirical functions do not produce accurate results at the mouth of Fox River comparing to the observations.

Table 4.4. Error criteria for total suspended solids (TSS) estimation based on the best selected empirical relationships for TSS-discharge relationship

Empirical model	Coefficient a	Coefficient b	RMSE (mg/L)	BD (mg/L)	NSE
2nd order polynomial	0.307	-0.0003	29.67	-9.07	-0.72
power	42.205	-0.028	22.65	-0.001	0.01
exponential	1.025	-0.009	26.31	-3.50	-0.35

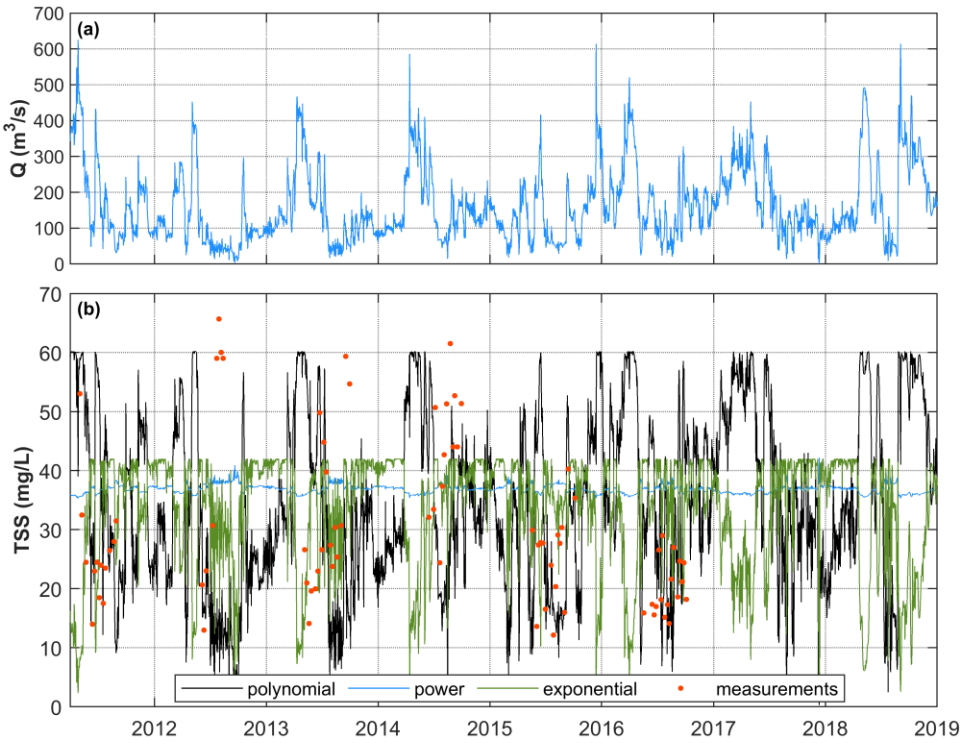

Figure 4.12. Discharge (Q) time series based on USGS observations (a); and corresponding total suspended solids (TSS) time series estimated based on the suggested empirical relationships at the mouth of Fox River during the period of 2011-2019 (b). Red dots show NEW Water measurements at this location (station 13).

To investigate the robustness of the suggested empirical relationships and their ability to predict new TSS data, a cross-validation analysis of different functions was conducted. In a cross-validation process, data is randomly split into two train and test data sets. Then

the train set is used to build a model while test data is used to verify if the model is generalizable to independent data sets. The cross-validation was repeated for 200 iterations here and in each iteration data is split into 80% training set and 20% test set. Results of the cross-validation analysis for all models are shown in Figure 4.13 in terms of the RMSE of TSS estimation in each iteration. In other words, in each iteration a model is developed based on the training set and the fitted TSS in both training and test sets was estimated based on the empirical model. Then RMSEs of these TSS estimations were calculated separately and are shown in the figure, i.e., red dots for the train set and blue dots for the test set.

Figure 4.13 shows that the average RMSEs for TSS-turbidity relationship (subplots a, b, and c) is relatively low and stay in a small range between 5 and 6 (mg/L) for both train and test sets. This indicates that the empirical models for TSS-turbidity relationship are robust and accurate enough in the estimation of TSS when new turbidity data is introduced to the model. Conversely, cross-validation of the TSS-discharge relationship shows high RMSE values in all three cases (subplots d, e, and f) and there are some cases the test data were estimated with very low accuracy.

Overall, the statistics and results presented above indicate that using the relationship between TSS and turbidity is a more reliable approach to generate the TSS time series at the mouth of the Fox River. In particular, the exponential function has the best performance and the least errors in estimation of TSS observations at this location. Therefore, this empirical relationship is selected to generate the loading rates of Fox and Menominee Rivers as shown in Figure 4.8. It should be noted that TSS observations are mostly collected during summer and early fall and there are no observations in winter and

early spring; therefore, it is difficult to assess the accuracy of estimations during winter and early spring.

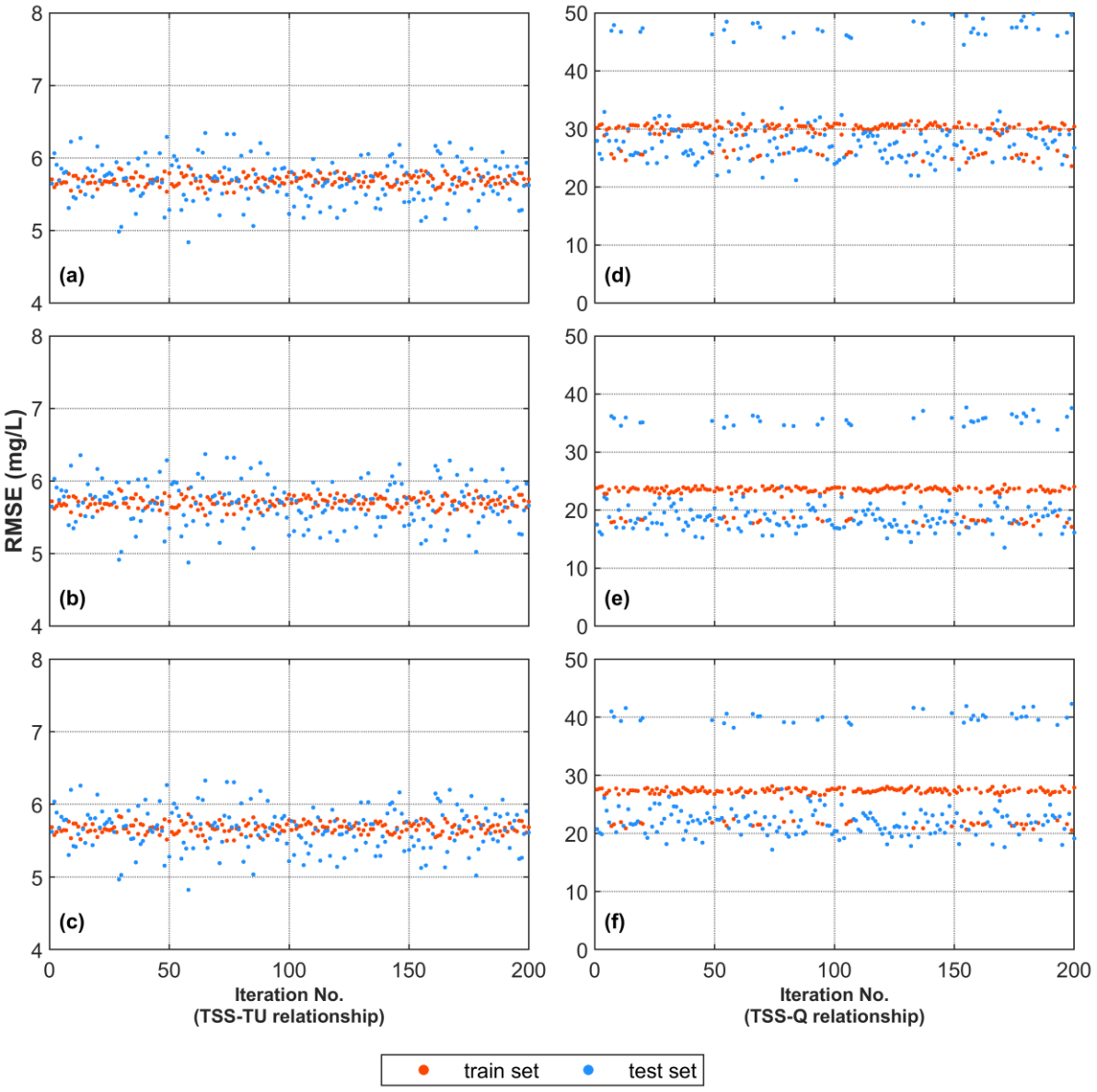

Figure 4.13. Cross-validation of the empirical polynomial (a and d), power (b and e), and exponential (c and f) functions suggested to estimate total suspended solids (TSS) based on the TSS-turbidity (left) and TSS-discharge (right) relationships. TU and Q indicate turbidity and discharge, respectively. The performance of each model is evaluated based on the calculation of RMSE in all cases and for each iteration of the cross-validation process.

TSS and discharge at the mouth of Fox River do not exhibit a simple relationship that could be described by the selected functions. Other efforts were made to find a meaningful relationship for the estimation of TSS based on discharge, such as detecting a lag between TSS and discharge data, considering precipitation and wind as additional variables and using multivariate analysis techniques such as multivariate regression and artificial neural networks, matching the cumulative distribution functions of the TSS and discharge datasets, and conducting a flow separation analysis on Fox River hydrograph to investigate relationship between TSS concentration and the quick runoff component of hydrograph. None of those trials led to a reasonable result for the TSS-discharge relationship. There is a possibility that sediment resuspension upstream of the USGS gauge due to dredging activities in the Fox River increases TSS concentration artificially without increasing the river flow. That could be a reason why TSS does not show a reliable relationship with discharge fluctuations in the Fox River, while in a natural condition such a relationship is expected.

4.6. Sediment Classes and Properties

As explained in Chapter 3, a sediment transport model requires information about sediment characteristics including sediment mean diameter size (D_{50}), density (ρ_s), and porosity (φ). Previous research and surveying of Green Bay sediment characteristics have provided this information, although such data is limited to a few locations in the Bay and/or does not represent the most recent conditions.

The available information was used in this study to obtain a general understanding and reasonable estimates of sediment characteristics in Green Bay. Then soil classification methods/standards and consultation with experts were utilized to narrow down the ranges

defined for each parameter in the literature. Finally, some of these model parameters were adjusted based on model calibration.

The first step in the determination of sediment characteristics is to explore the existing sediment classes and their distribution in Green Bay. Moore et al. (1973) and Wisconsin DNR (2000) are among the few major efforts that have studied the formation of Green Bay bed layer and distribution of different classes throughout the bay (Figures 4.14 and 4.15). Moore et al.'s classification is based on field notes and megascopic laboratory examinations and Wisconsin DNR's particle size fraction maps are based on the analysis of sediment samples.

They basically characterized the bottom of the bay with clay, silt, and sand, as well as gravel and rocky bed in the upper Green Bay near the exchange zone with Lake Michigan. Lee et al. (2007) also provided a spatial map of Lake Michigan fine-grained sediment distribution (Figure 4.16) which was compiled with the bottom sediment maps of Green Bay to produce the sediment distribution inputs for the current sediment transport model.

Jones (2000) defined three sediment classes for the lower Green Bay and Fox River system, which complement the gaps of previous classifications of the bed layer sediment composition in the southern Green Bay near the mouth of Fox River. According to the U.S. Department of Agriculture (USDA) soil classification standard (Table 4.5)—that categorizes particles based on their size—sediment classification of Jones in the Fox River systems corresponds to clay, silt, and sand particle types. This classification is also consistent with estimations of Moore et al. (1973) and Wisconsin DNR (2000) classifications of sediment characteristics in the southern Green Bay.

Given the details from these major studies, the distribution of four sediment classes in

Lake Michigan and Green Bay were determined for the current sediment transport model and the spatial patterns of different sediment classes are illustrated in Figure 4.17.

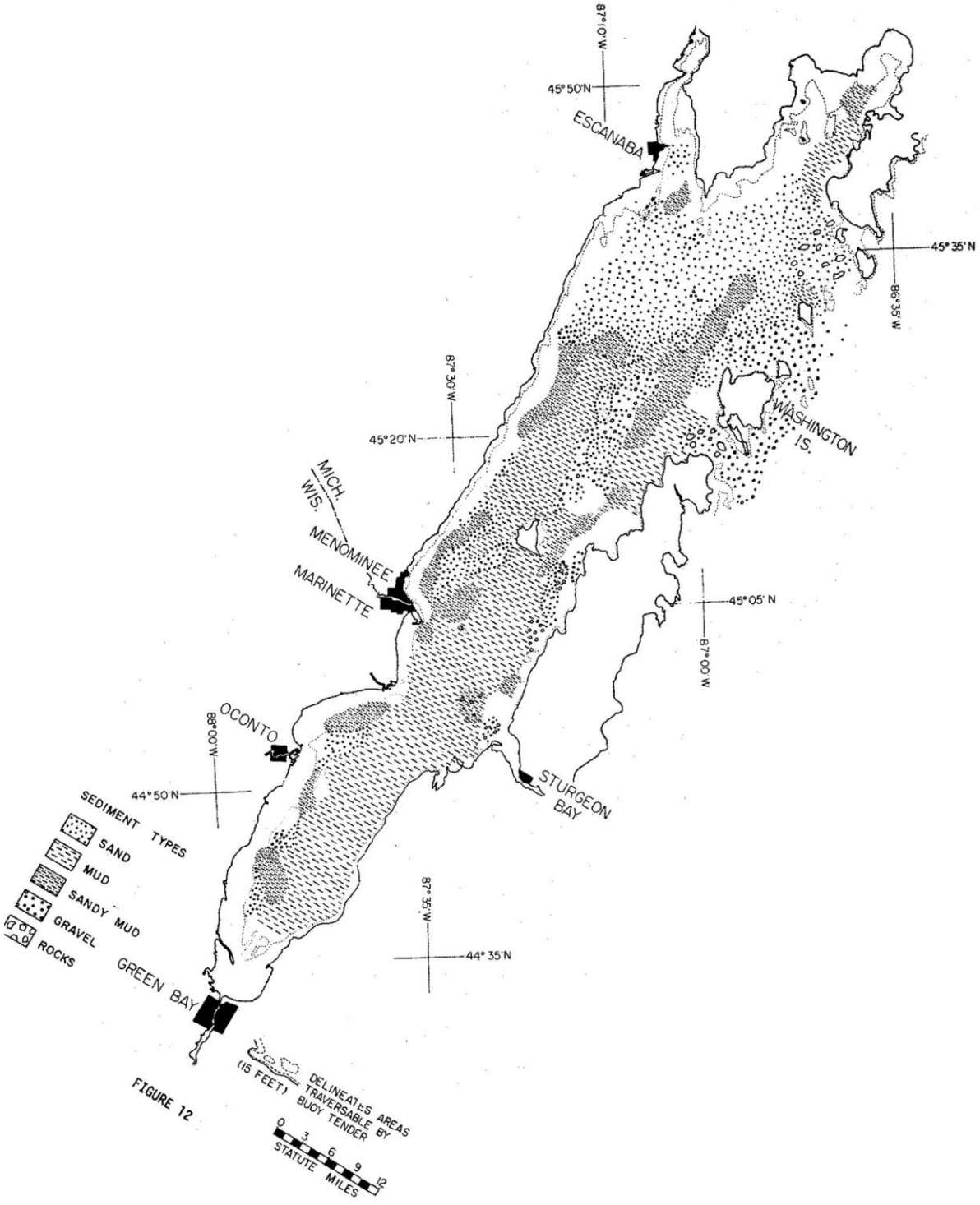

Figure 4.14. Green Bay sediment type classification (Moore et al., 1973)

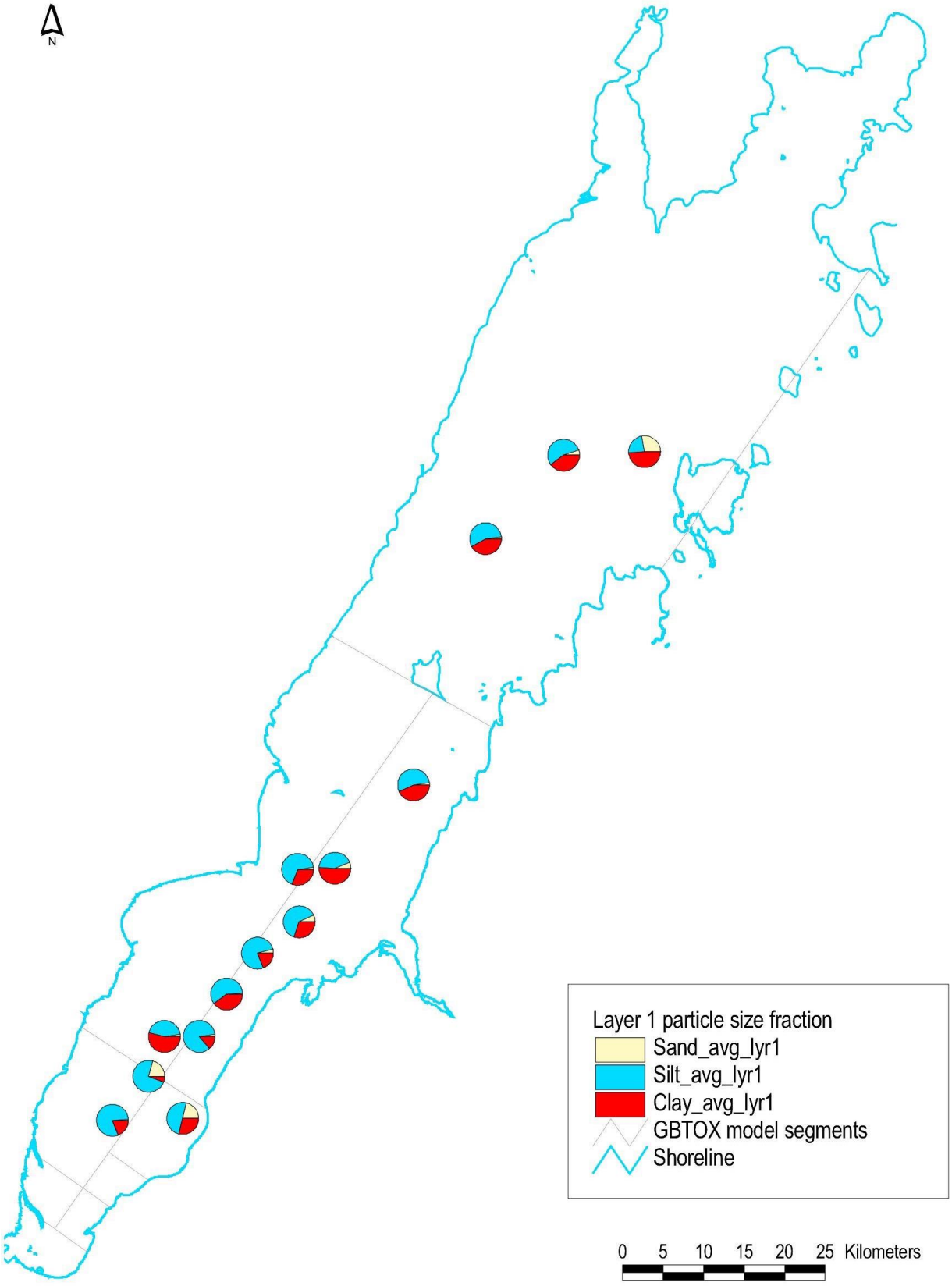

Figure 4.15. Particle size distribution in Green Bay bed layer (Wisconsin DNR, 2000)

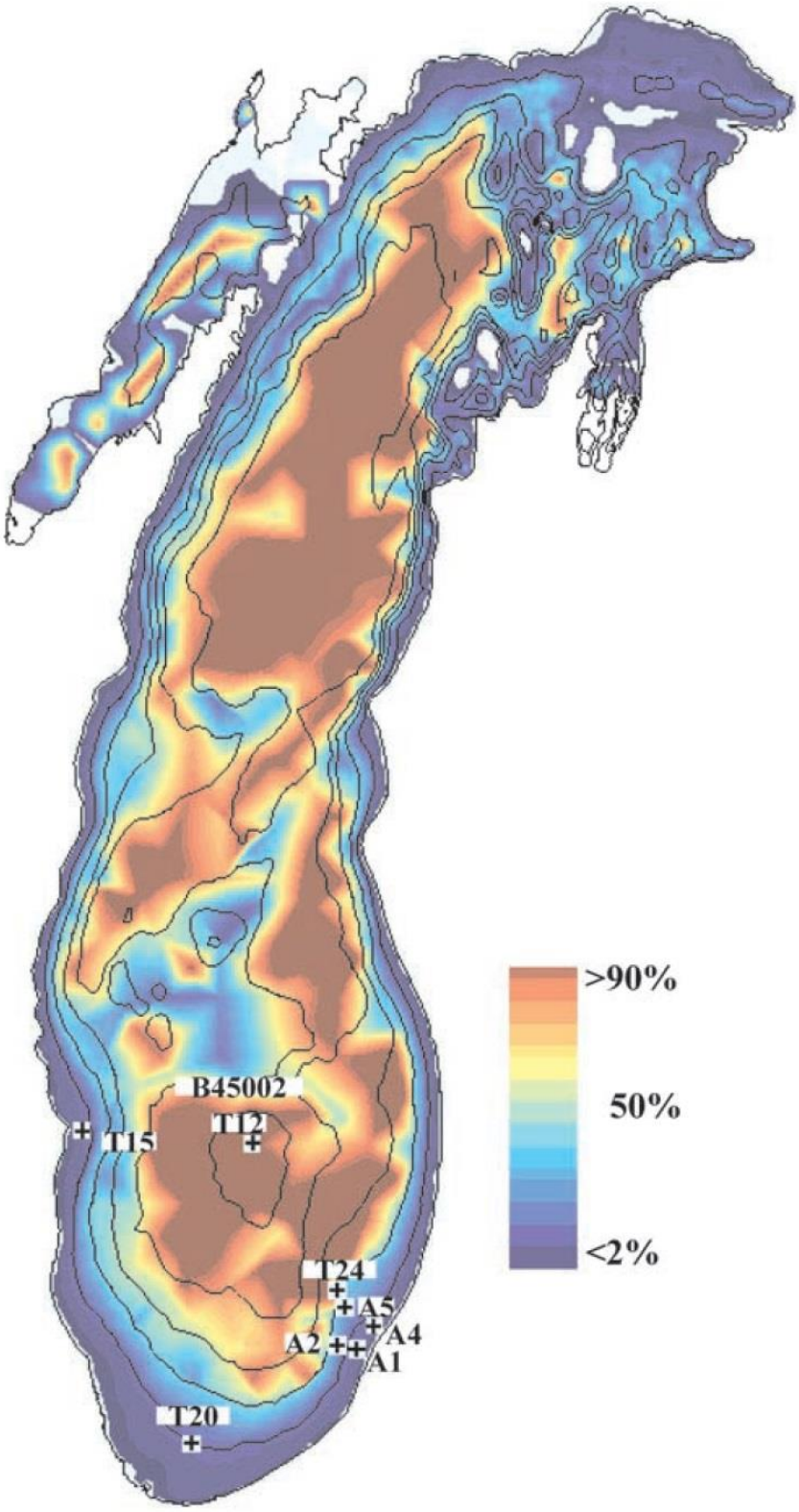

Figure 4.16. Lake Michigan spatial distribution of fine-grained sediment percentage (Lee et al., 2007)

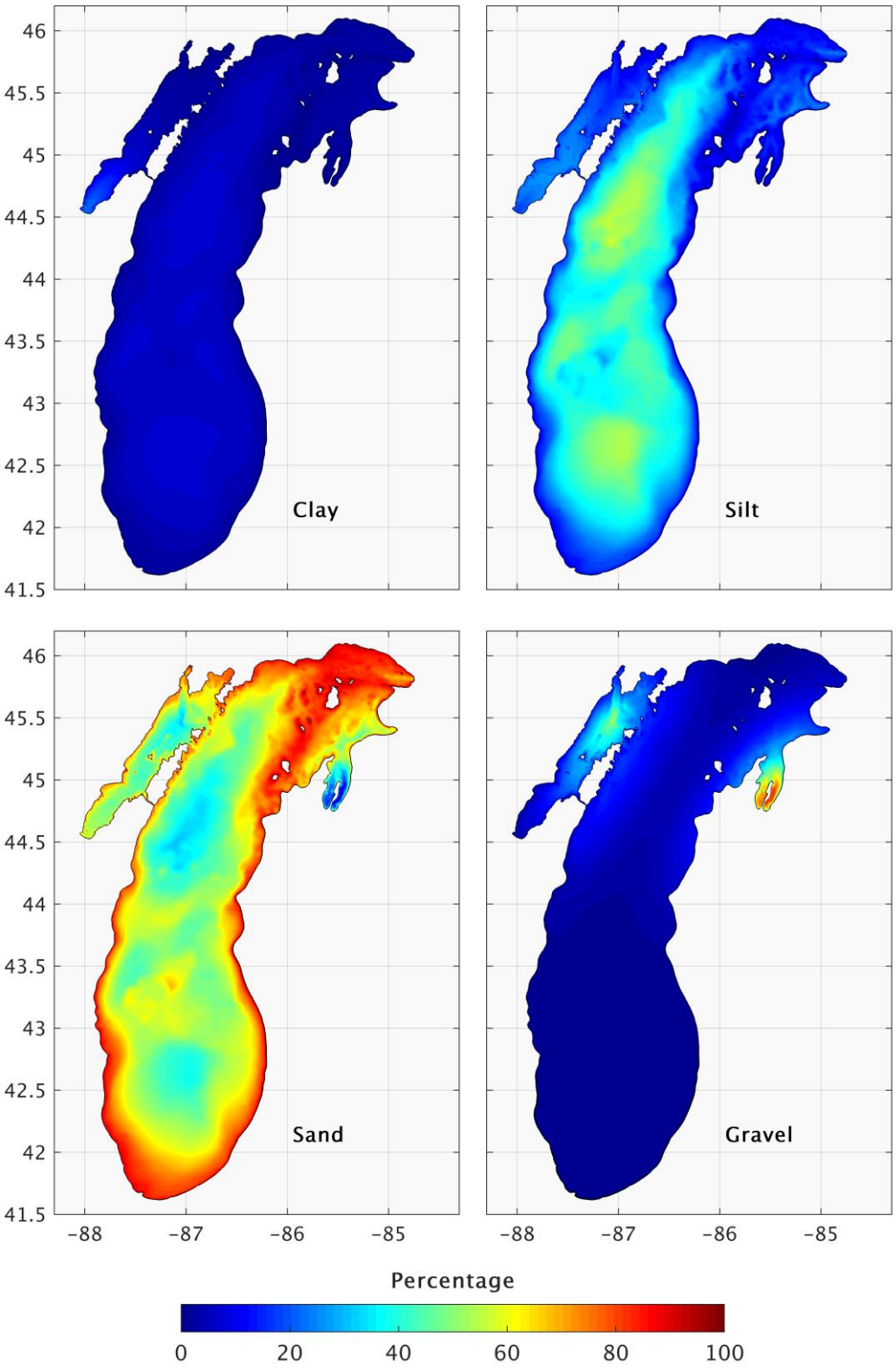

Figure 4.17. The initial distribution of different sediment classes in the FVCOM sediment transport model of Green Bay

Table 4.5. USDA soil classification based on particle size (Yolcubal et al., 2004)

Type	Diameter (mm)
gravel	> 2
sand	0.05–2
very coarse sand	1–2
coarse sand	0.5–1
medium sand	0.25–0.5
fine sand	0.10–0.25
very fine sand	0.05–0.10
silt	0.002–0.05
clay	< 0.002

Table 4.6 shows the sediment characteristics used for the Green Bay sediment transport model. The last column in the table indicates the source(s) referred to for selection of each sediment property.

Table 4.6. Sediment properties used for Green Bay sediment transport model

Sediment class	**1**	**2**	**3**	**4**	**Source**
Sediment type	Clay	Silt	Sand	Gravel	Moore et al. (1973), Wisconsin DNR (2000), and Lee et al. (2007)
D_{50} **(mm)**	0.002	0.025	0.050	2.00	Jones (2000) and Yolcubal et al. (2014)
ρ_s **(kg/m³)**	2300	2300	2450	2450	Klump (2019), Wisconsin DNR (2000)
Φ **(%)**	97.5	97.5	97.5	60.0	Manchester-Neesvig et al. (1996) and Klump (2019)

As reported in Table 4.6, a density of ~2350-2450 kg/m^3 is recommended for particles in Green Bay (Klump, 2019; Wisconsin DNR, 2000) that is used for fall velocity calculations

below.

4.7. Sediment Erosion and Deposition Characteristics

In addition to main sediment characteristics (D_{50}, ρ_s, φ), a sediment transport model is very sensitive to erosion and deposition characteristics of the particles. Previous studies in Green bay have provided such information based on fieldwork and lab analysis of sediment samples from lower Green Bay.

NOAA Sediment trap study in Green Bay has found a wide range of settling (or fall) velocity (ω) in Green Bay (Eadie et al., 1991), i.e., 6-70 mm/s in stratified period and 140-200 mm/s during the unstratified period. The selected simulation period of May-October mostly overlaps with the period of stratified conditions in Green Bay, therefore, low settling rates are expected. A recent analysis of lower Green Bay sediment samples has also shown values of 0.01-0.2 mm/s for settling velocity of fine particles (Klump, 2019).

To estimate consistent value for the settling velocity a method explained by García (2008) was used, which estimates fall velocity based on particle size and density. In this method, first a dimensionless parameter based on sediment properties is calculated:

$$R_{ep} = \frac{\sqrt{RgD_{50}}D_{50}}{\nu} \tag{4.10}$$

where R is the submerged specific gravity of the sediment and is calculated as $R=(\rho_s-\rho)/\rho$, g is the acceleration of gravity, and ν is the kinematic viscosity of water and is a function of water temperature. Considering an average value of 10 $^{\circ}C$ for water temperature in Lake Michigan (particularly near the bottom where most of the sediment interactions are occurring) during the simulation period, a value of 1.31×10^{-6} m^2/s is selected for ν in

Equation 4.10. Then Figure 4.18 is used to estimate the dimensionless sediment fall velocity parameter (R_f) for the selected sediment type.

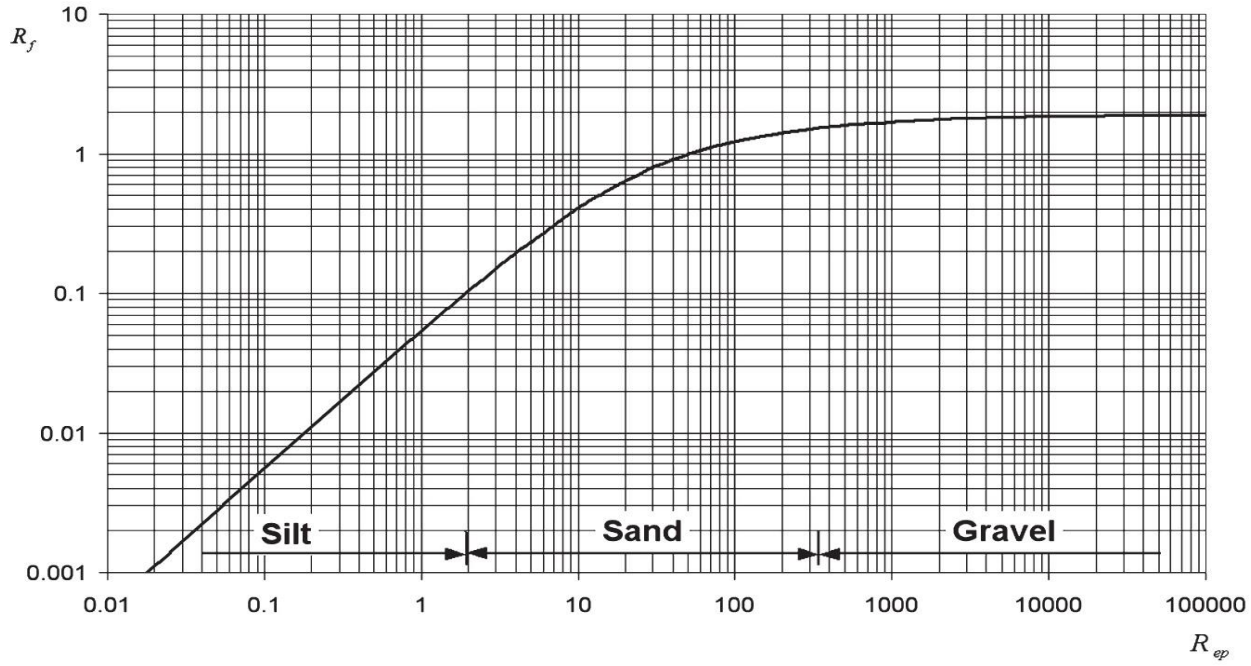

Figure 4.18. R_{ep} versus R_f diagram calculated based on drag coefficient for sphere shape sediments (García, 2008, p. 42)

Given the R_f from Figure 4.18, the settling velocity of particles is calculated using the equation below:

$$R_f = \frac{\omega}{\sqrt{RgD_{50}}} \tag{4.11}$$

Lower Green Bay bed layer is predominantly comprised of very fine sediments that lie outside of the range provided in Figure 4.18. Alternatively, a method proposed by Soulsby (1998) can be used to estimate the fall velocity in marine environment:

$$\omega = \frac{\nu}{D_{50}}\left[(10.36^2 + 1.049D_*^3)^{1/2} - 10.36\right] \tag{4.12}$$

where:

$$D_* = \left[\frac{gR}{\nu^2}\right]^{1/3} D_{50} \tag{4.13}$$

Both graphical and Soulsby's methods provide very similar estimations of the fall velocity of different sediment classes. For sediment classes 1, 2, and 3 Soulsby's method is used to estimate the fall velocity and for sediment class 4, the graphical method is used. Estimations of ω are reported in Table 4.7 for different sediment classes.

While fall velocity governs deposition, critical stress for erosion (τ_{ce}) defines erosion rates of the bottom, i.e., bed erosion is initiated when bottom critical shear stress exceeds that value. Therefore, an accurate estimation of those values is necessary for a reliable sediment transport model. A common way to define τ_{ce} is to use the modified Shields diagram shown in Figure 4.19.

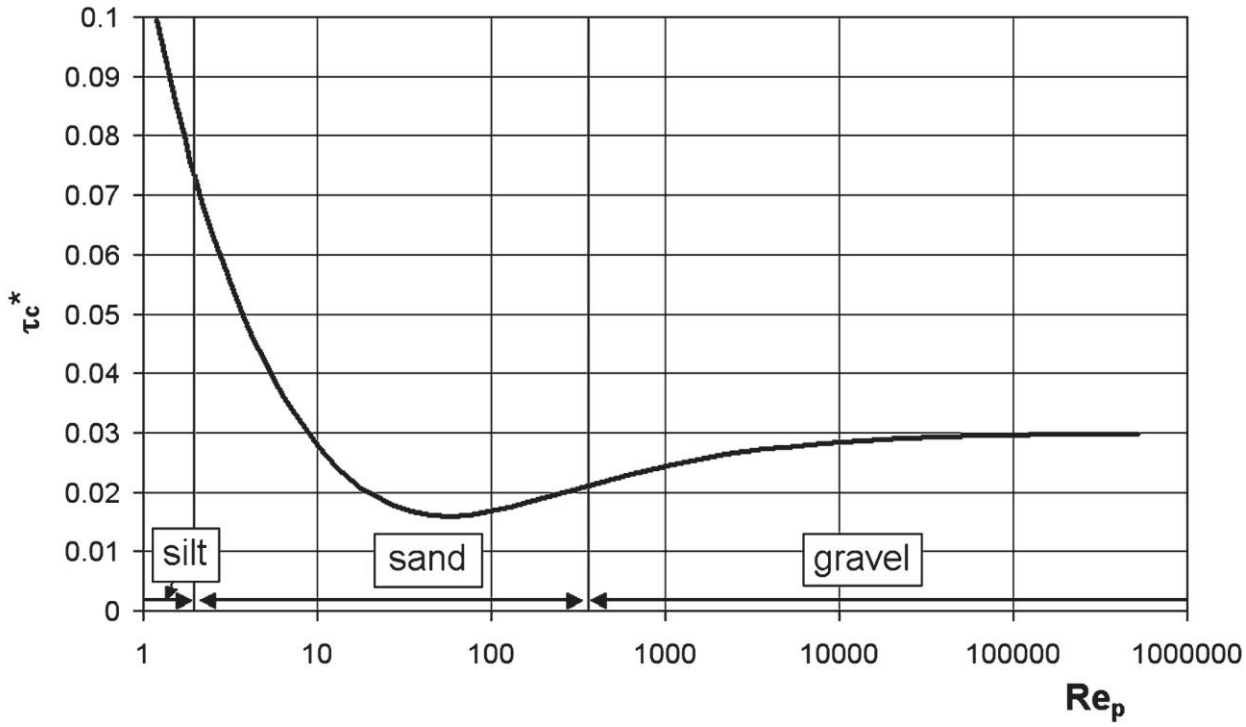

Figure 4.19. Modified Shields diagram (Parker, 2004)

Given the R_{ep} calculated based on Equation 4.10, non-dimensional critical Shields shear

stress (τ_c^*) can be found from Figure 4.19. Then, critical shear stress for erosion is estimated based on the Shields (1936) formulation:

$$\tau_c^* = \frac{\tau_{ce}}{\rho R g D_{50}} \tag{4.14}$$

For fine-grained sediments, that form most of the Green Bay bed layer, Shields diagram does not provide realistic results for critical Shields shear stress. Mantz (1977) proposed an empirical relationship that can estimate τ_c^* for fine-grained sediments:

$$\tau_c^* = R_{ep}^{-0.261} \tag{4.15}$$

For sediment classes 1, 2, and 3, Mantz's equation and for sediment class 4 modified Shields diagram were used to estimate the τ_{ce} and results are provided in Table 4.7.

Table 4.7. Sediment erosion and deposition properties used for Green Bay sediment transport model

Sediment class	**1**	**2**	**3**	**4**	**Source**
Sediment type	Clay	Silt	Sand	Gravel	Moore et al. (1973), Wisconsin DNR (2000), and Lee et al. (2007)
$\boldsymbol{\omega\ (mm/s)}$	0.002	0.260	1.160	165.0	Garcia (2008)
$\boldsymbol{\tau_{ce}\ (N/m^2)}$	0.013	0.060	0.100	0.950	Garcia (2008)
$\boldsymbol{E_0\ (kg/m^2/s)}$	0.001	0.010	0.01	0.1	Ariathurai and Arulanandan (1978)

Another important model parameter in Warner et al.'s (2008) formulation for erosion rates (Equation 3.4) is the bed erodibility constant (E_0). A wide range is suggested in the literature for erosion constant, however, Ariathurai and Arulanandan (1978) suggested a range between 5×10^{-4} and 5×10^{-3} $kg/m^2/s$ based on conducting tests on over 200 natural

and synthetic fine and cohesive sediment samples. Their experiments have shown that the slope of erosion rate curves increases with an increase in critical shear stress. Selected values for E_0 for different sediment classes are provided in Table 4.7.

Chapter 5:
Results of the Hydrodynamic and Wave Models

Model simulations were limited to the May-October period of each year to focus on ice-free and active bottom layer conditions in Lake Michigan. Modeling results of currents and temperature fields for the years 2018 and 2019 are presented in this chapter.

Four buoy stations shown in Figure 4.6 are selected for model validation. Those buoys are located in distinct areas in Lake Michigan and Green Bay that represent different climatic and geomorphological characteristics. Therefore, the validation of results at those locations indicates model performance under different conditions. Buoys 45002 and 45007 have measurements of water temperature and currents at the surface. Buoys 45013 and 45014 have temperature strings and currents along the water column and are useful to validate temperature profiles, in particular in stratified conditions in Green Bay.

5.1. Validation of Simulated Currents

Currents are one of the most important prediction results of a hydrodynamic model and are the major driver of sediments in the lake. Figures 5.1 and 5.2 show the comparison of surface currents in N-S (v component) and E-W (u component) directions during the May-October 2018, respectively, and at the location of buoys 45013 and 45014. As shown on both figures results of surface currents simulations in both locations are in fairly good agreement with the measurements in terms of the strength and direction of currents, in particular for bottom currents that might be crucial in estimations of bottom shear stresses and resuspension events. Tables 5.1 and 5.2 also show the error criteria for the surface and bottom currents at these two buoys, respectively. Fn less than 1 and small $\Delta\theta$ values also indicate that the model performs well in simulations of currents.

Table 5.1. Surface currents model skill error criteria in 2018 simulation

Buoy	Fn	Δθ
45014	0.94	0.39
45013	0.71	0.26

Table 5.2. Bottom currents model skill error criteria in 2018 simulation

Buoy	Fn	Δθ
45014	0.82	0.25
45013	0.80	0.32

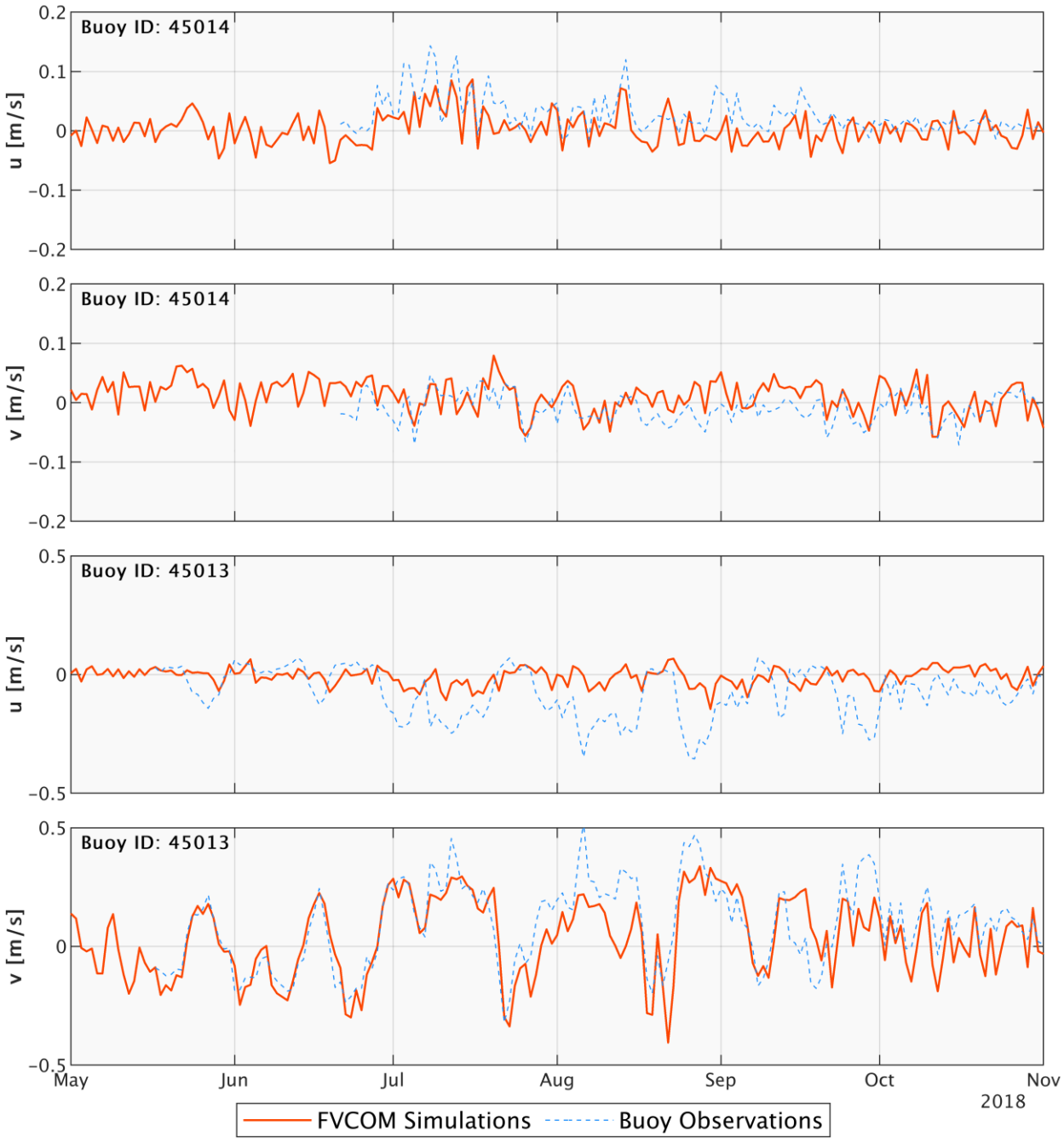

Figure 5.1. Comparison of the surface currents in N-S (v component) and E-W (u component) directions at the location of validation buoys 45014 in Green Bay and 54013 in Atwater beach in Milwaukee nearshore zone of Lake Michigan during the May-October 2018

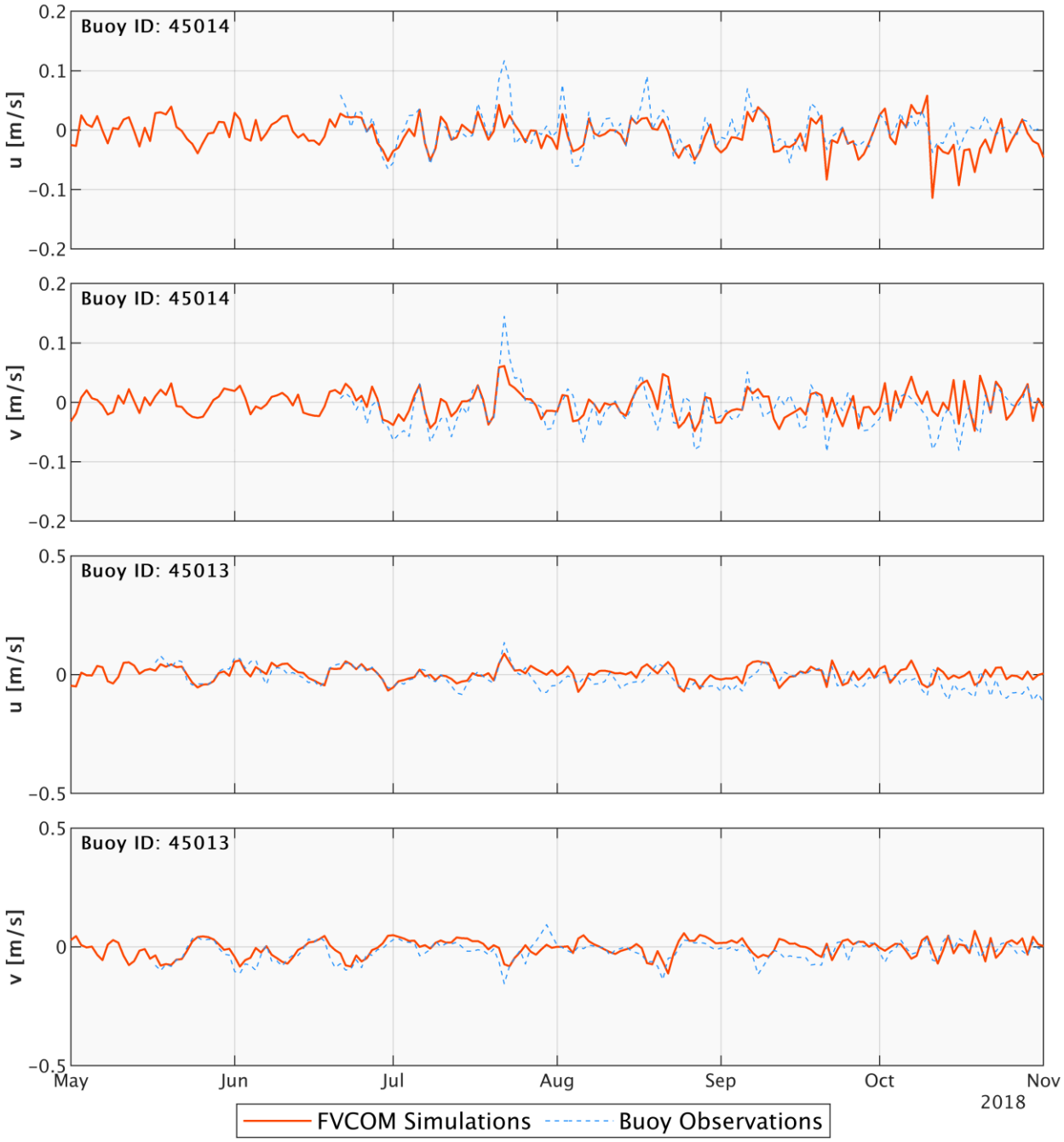

Figure 5.2. Comparison of the bottom currents in N-S (v component) and E-W (u component) directions at the location of validation buoys 45014 in Green Bay and 54013 in Atwater beach in Milwaukee nearshore zone of Lake Michigan during the May-October 2018

Tables 5.3 and 5.4 and Figures 5.3 and 5.4 show the comparison of the surface and bottom currents at the location of 45013 buoy for the simulation period May-October 2019 (data is not available for 45014 buoy in 2019 and only model simulations at this location are shown). Similar to 2018 results, model simulations of currents are in good agreement with observations given the complexity of the system and modeling conditions.

Table 5.3. Surface currents model skill error criteria in 2019 simulation (there is no data available for 45014 buoy)

Buoy	**Fn**	**Δθ**
45014	-	-
45013	0.53	0.14

Table 5.4. Bottom currents model skill error criteria in 2019 simulation (there is no data available for 45014 buoy)

Buoy	**Fn**	**Δθ**
45014	-	-
45013	0.7	0.27

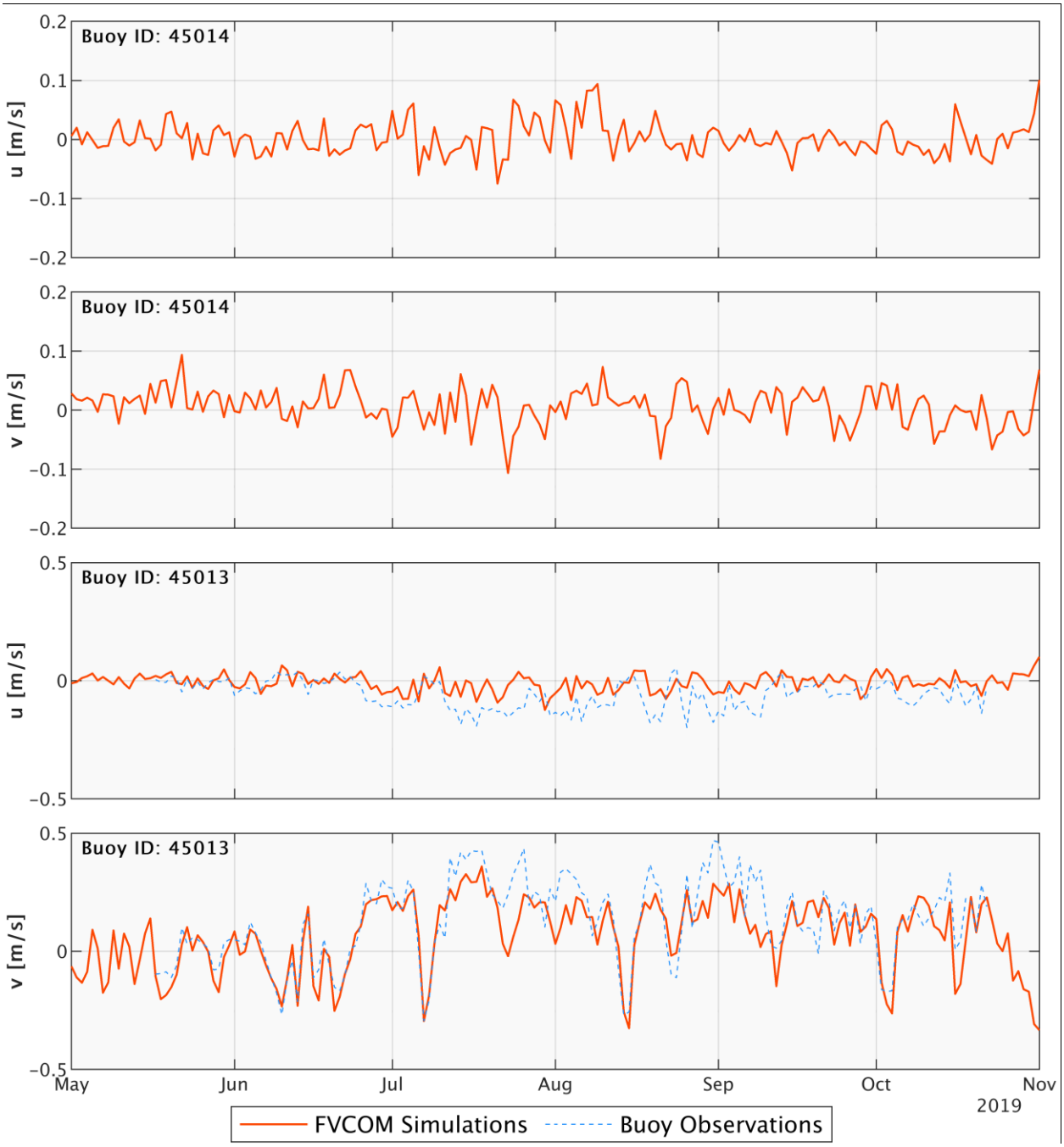

Figure 5.3. Comparison of the surface currents in N-S (v component) and E-W (u component) directions at the location of validation buoys 45014 in Green Bay and 54013 in Atwater beach in Milwaukee nearshore zone of Lake Michigan during the May-October 2019. 45014 buoy data is not available.

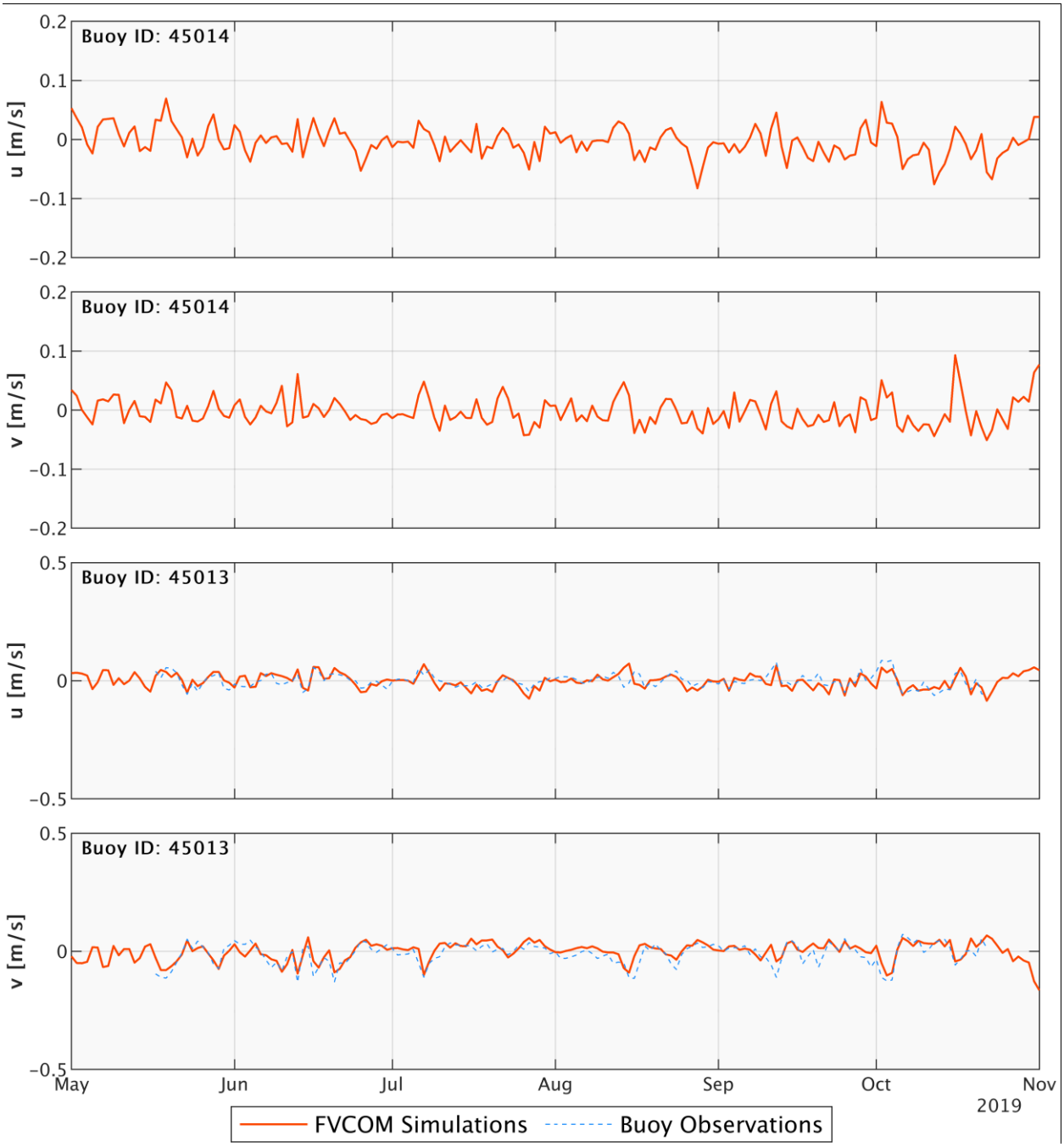

Figure 5.4. Comparison of the bottom currents in N-S (v component) and E-W (u component) directions at the location of validation buoys 45014 in Green Bay and 54013 in Atwater beach in Milwaukee nearshore zone of Lake Michigan during the May-October 2019. 45014 buoy data is not available.

5.2. Validation of Simulated Temperature

Figures 5.5 and 5.6 show surface temperature validations at the location of buoys during

May-October of 2018 and 2019, respectively. In both figures, the surface temperature is well estimated by the FVCOM model at the four locations. In particular, FVCOM shows a better performance compared to the POM-based models in capturing sudden changes in lake water temperature due to upwelling in nearshore areas. Comparison of the modeled lake temperature with observed values at buoy 45013, located in the nearshore zone of Lake Michigan, indicates such capability of the model. July and August upwellings, in terms of the sudden decrease of surface water temperature, were predicted with reasonable accuracy at this location. Tables 5.5 and 5.6 show error criteria for the surface temperature at validation buoys. Almost all of the error criteria indicate that the model performed well in estimations of surface temperatures in both years.

Table 5.5. Surface temperature model skill error criteria in 2018 simulation

Buoy	RMSE (°C)	BD (°C)	NSE	CC
45014	1.53	1.16	0.88	0.98
45013	2.59	-0.91	0.74	0.89
45002	3.87	0.99	0.63	0.85
45007	2.06	1.04	0.85	0.95

Table 5.6. Surface temperature model skill error criteria in 2019 simulation (there is no data available for 45014 buoy)

Buoy	RMSE (°C)	BD (°C)	NSE	CC
45014	-	-	-	-
45013	1.67	-0.16	0.85	0.92
45002	2.93	1.14	0.84	0.95
45007	2.74	2.23	0.86	0.98

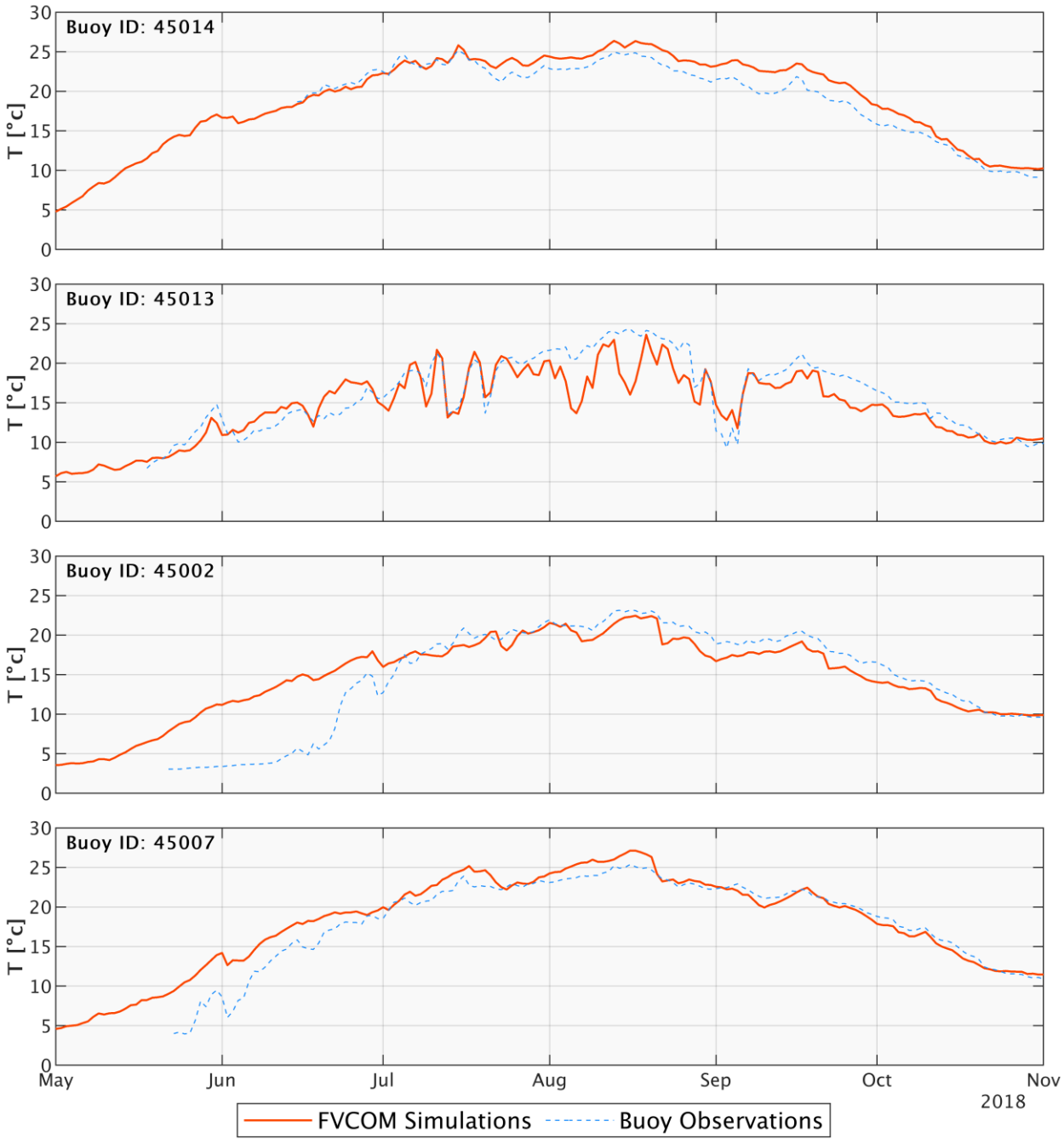

Figure 5.5. Comparison of the surface temperature at the location of four selected validation buoys during the May-October 2018

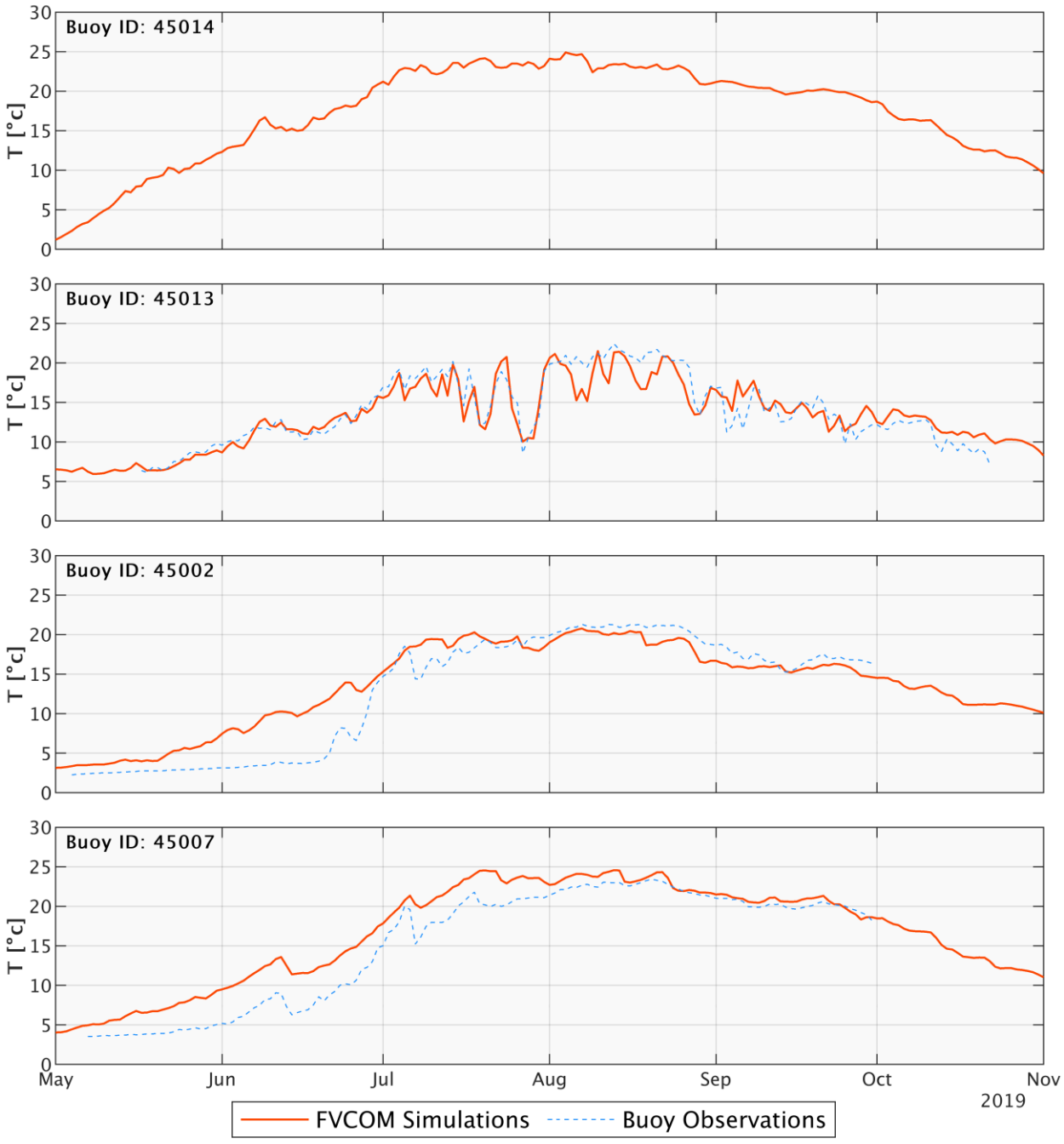

Figure 5.6. Comparison of the surface temperature at the location of four selected validation buoys during the May-October 2019. 45014 buoy data is not available.

Figures 5.7 and 5.8 and Tables 5.7 and 5.8 illustrate the comparison of bottom temperature predictions and measurements at the location of 45013 and 45014 buoys. The model performs better in the estimation of bottom temperature at buoy 45013

compared to previous POM-based models, yet it still shows difficulties in predicting the lake bottom temperature in Green Bay (buoy station 45014). The main reason for such a problem in the model is the stratified flow condition in Green Bay due to cold water intrusion from Lake Michigan into the bay. Coldwater from the lake is denser and flows close to the bottom of the bay while warmer water in the bay and from the rivers flows on top of this layer forming a two-layer flow condition in Green Bay.

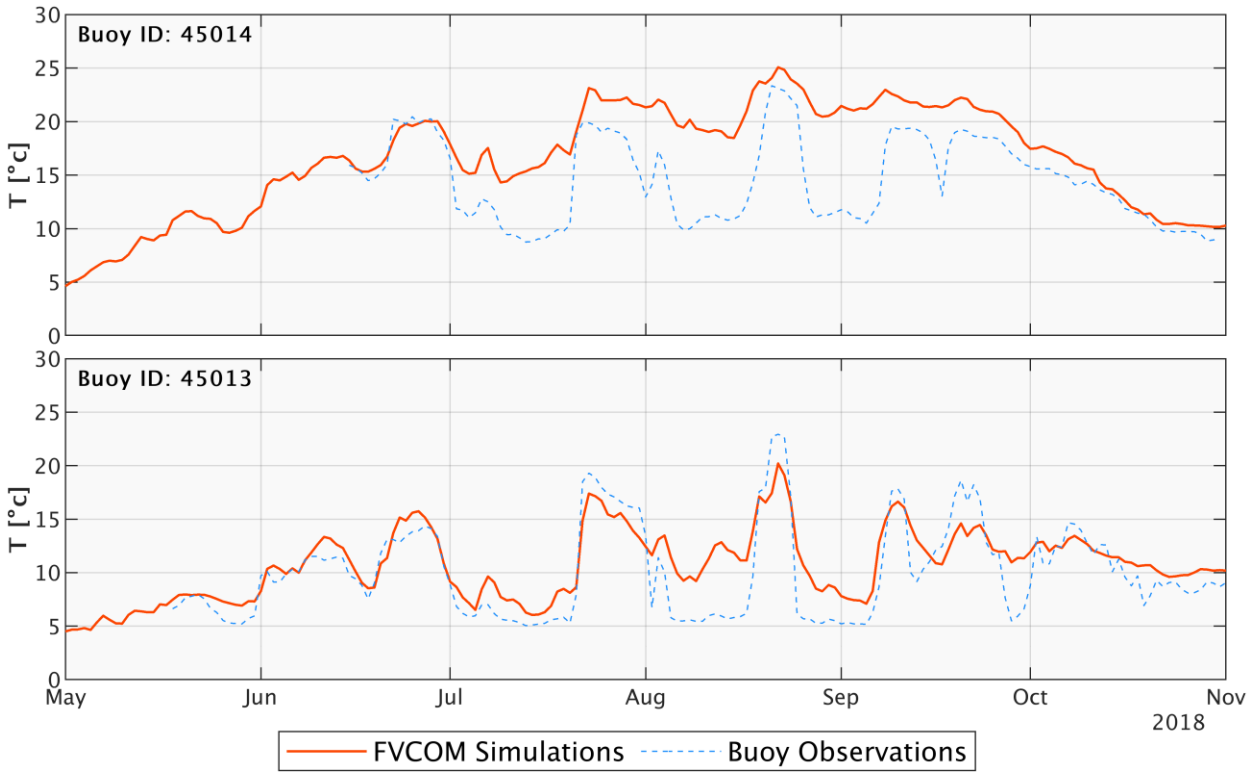

Figure 5.7. Comparison of the bottom temperature at the location of validation buoys 45014 in Green Bay and 54013 in Atwater beach in Milwaukee nearshore zone of Lake Michigan during the May-October 2018

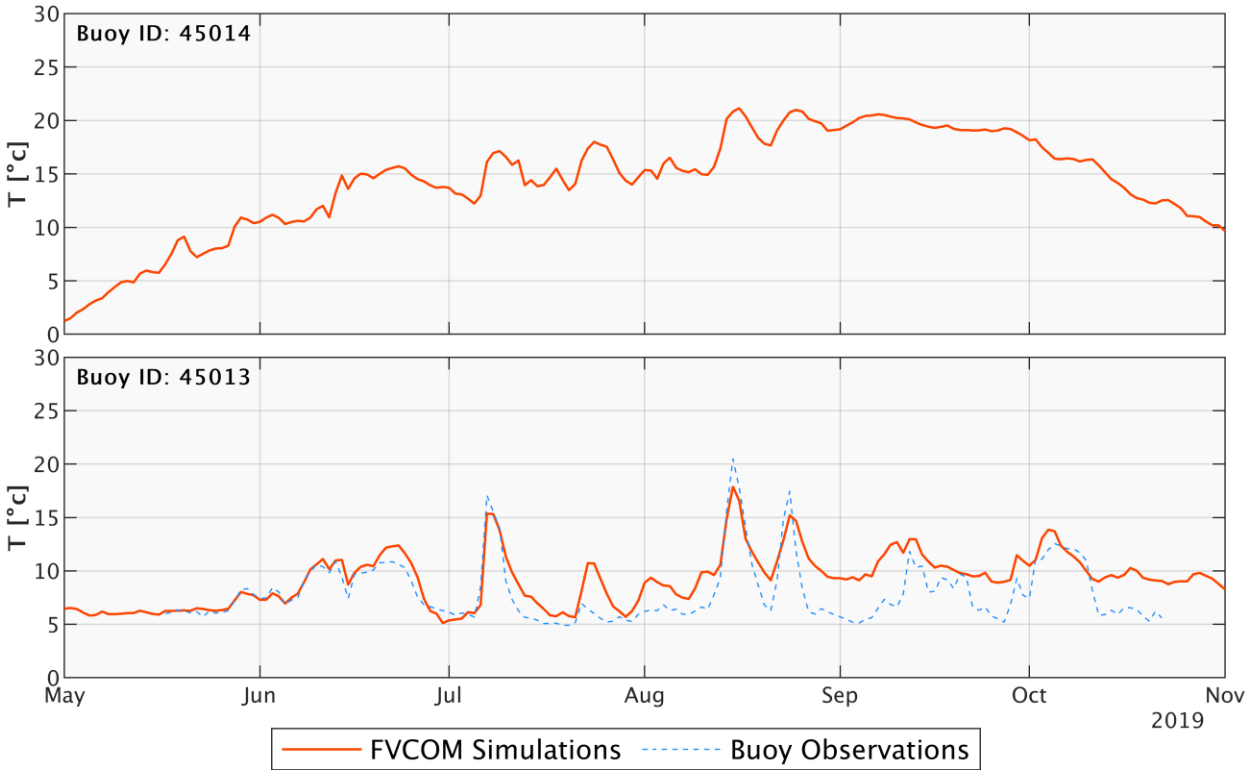

Figure 5.8. Bottom temperature at the location of validation buoys 45014 in Green Bay and 54013 in Atwater beach in Milwaukee nearshore zone of Lake Michigan during the May-October 2019. 45014 buoy data is not available.

Table 5.7. Bottom temperature model skill error criteria in 2018 simulation

Buoy	RMSE (°C)	BD (°C)	NSE	CC
45014	5.07	3.87	-0.64	0.65
45013	2.56	1.87	0.65	0.87

Table 5.8. Bottom temperature model skill error criteria in 2019 simulation (there is no data available for 45014 buoy)

Buoy	RMSE (°C)	BD (°C)	NSE	CC
45014	-	-	-	-
45013	2.29	1.51	0.36	0.80

Figures 5.9 and 5.10 show the water temperature profile comparisons at buoys 45013 and 45014, respectively, during the May-October 2018. The same comparison is also provided for the simulations in 2019 in Figure 5.11 for buoy 45013. Overall, the figures and correlations between the simulated and observed values suggest that the model is able to echo the patterns of temperature fields with reasonable accuracy. However, efforts need to continue in order to make predictions closer to measurements.

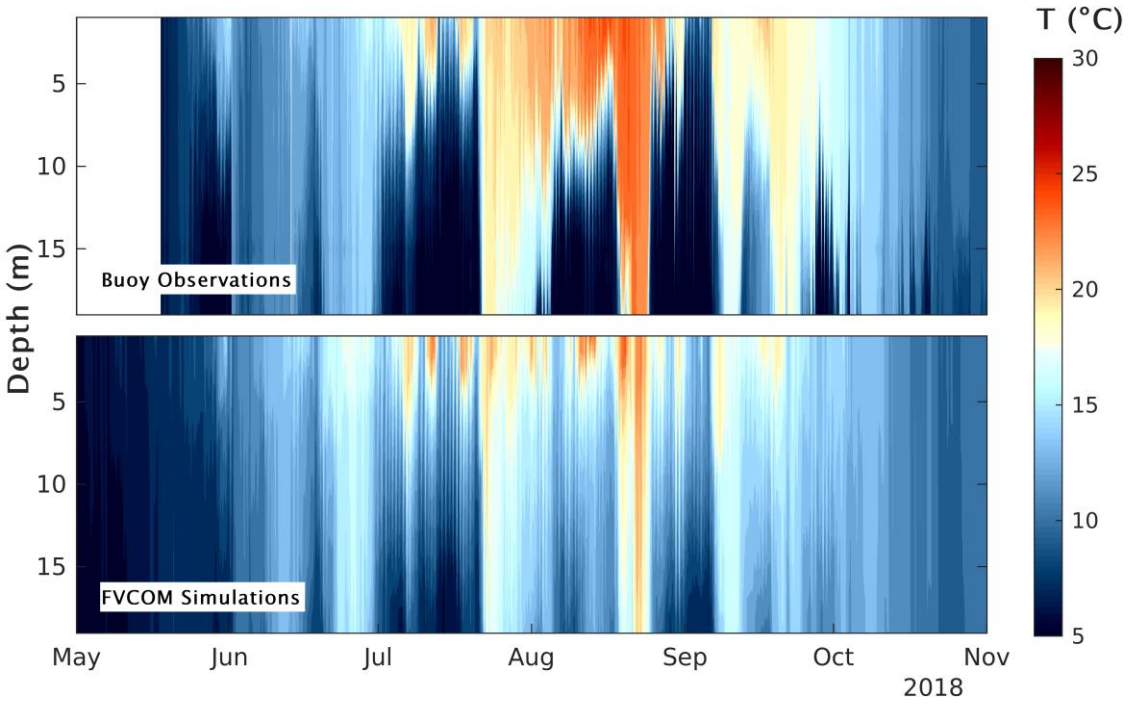

Figure 5.9. Comparison of the hourly temperature profiles at buoy 45013 in the Atwater beach in Milwaukee nearshore zone of Lake Michigan during May-October 2018

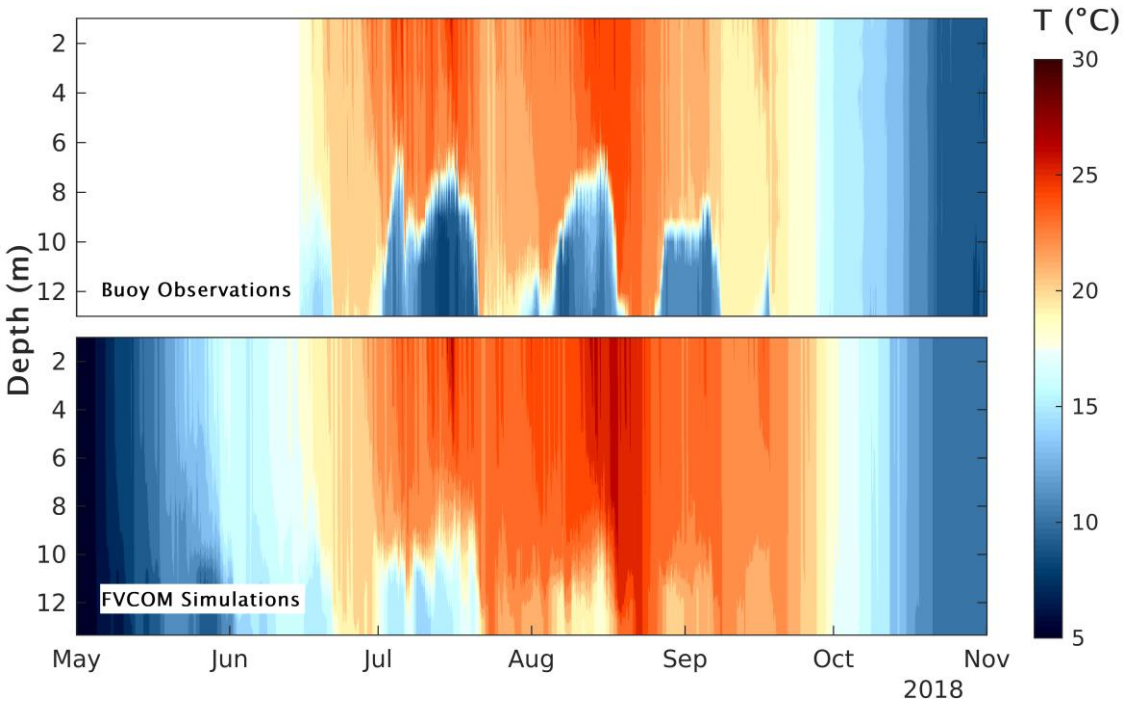

Figure 5.10. Comparison of the hourly temperature profiles at buoy 45014 in the lower Green Bay during May-October 2018

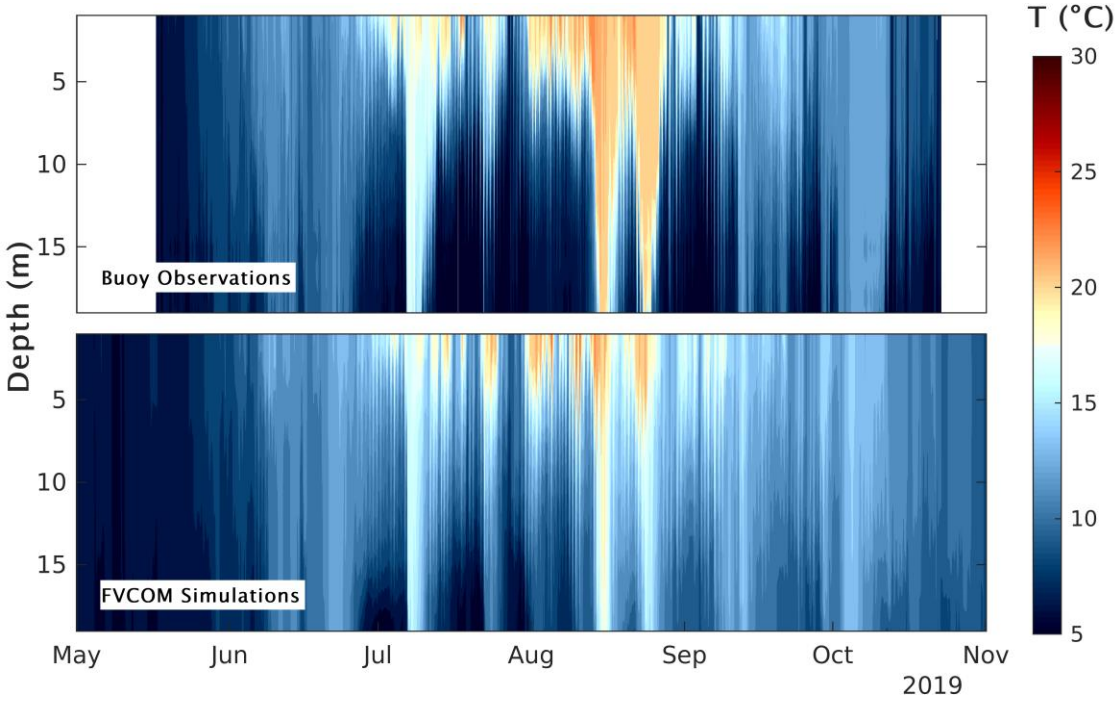

Figure 5.11. Comparison of the hourly temperature profiles at buoy 45013 in the Atwater beach in Milwaukee nearshore zone of Lake Michigan during May-October 2019

5.3. General Circulation and Thermal Patterns in Lake Michigan

Currents are wind-driven in Lake Michigan and they are the dominant driver of mass and heat transport in the lake. Figures 5.12 and 5.13 show monthly averages of depth-averaged currents in Lake Michigan during the May-October period of 2018 and 2019.

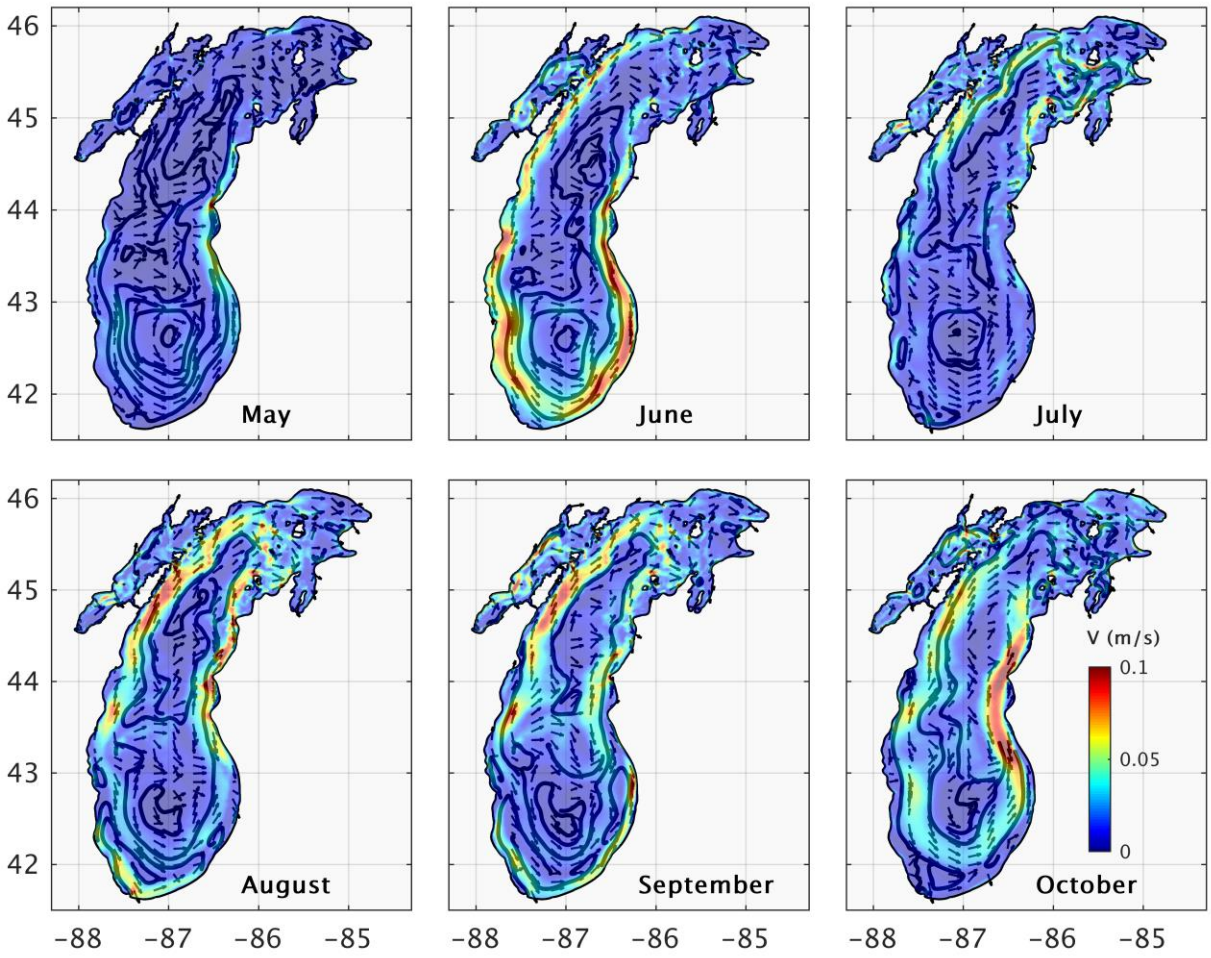

Figure 5.12. Monthly depth-averaged currents in Lake Michigan during the May-October 2018. Black arrows and black lines show the direction of flow and general circulation regimes, respectively.

According to both figures, a cyclonic (counterclockwise) circulation in the lake during the summertime is common. This is consistent with former analyses of the monthly average circulation patterns in Lake Michigan (Beletsky et al., 2006b). Also, currents form gyres

in the southern and northern basins, yet, the formation of gyres is more common in the southern basin than in the northern basin. Another important finding is that, as expected, nearshore currents are stronger than open lake currents and strong currents occur very often near the exchange zone with Green Bay.

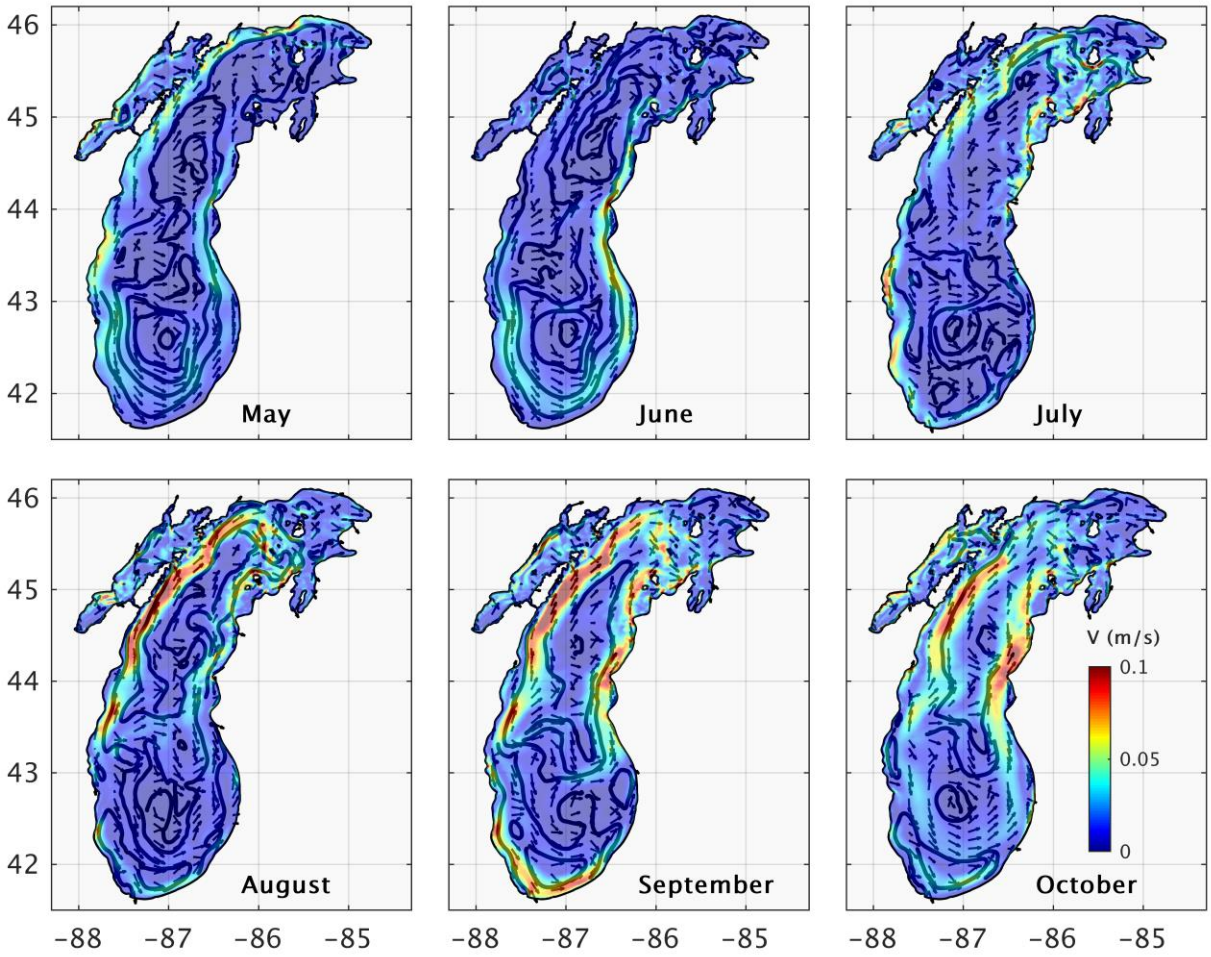

Figure 5.13. Monthly depth-averaged currents in Lake Michigan during the May-October 2019. Black arrows and black lines show the direction of flow and general circulation regimes, respectively.

The Lake Michigan surface temperature fields are illustrated in Figures 5.14 and 5.15 for 2018 and 2019 years. In short, southern and northern nearshore areas of Lake Michigan get warmer than the mid-lake coastal areas, and the thermal regimes of the lake are

similar in the two simulated years. Green Bay also gets warmer than the main body of the lake most probably due to weaker mixing and shallower morphological conditions.

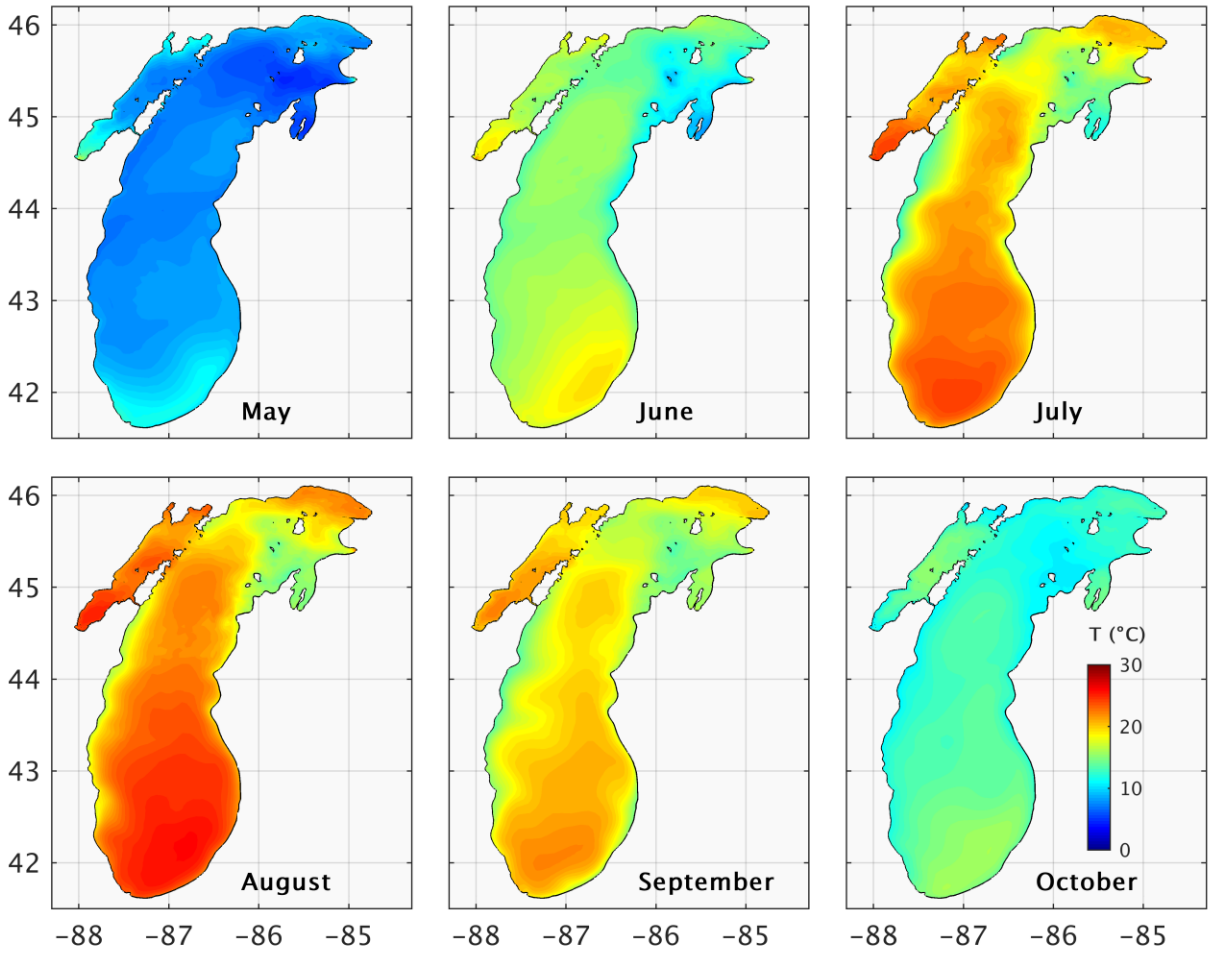

Figure 5.14. Monthly average surface temperature fields in Lake Michigan during the May-October 2018

One important finding is that the model is able to capture the upwelling events along the east and west coastlines. Comparing the simultaneous wind fields, surface currents, and surface temperature of Lake Michigan indicates that northerly and southerly winds in the west and east coasts, respectively, push the water offshore and cause the occurrence of upwellings in the nearshore zone. Figure 5.16 illustrates examples of three upwelling

events in Lake Michigan during the 2016 summertime simulated using the FVCOM hydrodynamic model. This figure clearly shows that N-S winds drive currents offshore and generate upwellings in Lake Michigan nearshore areas.

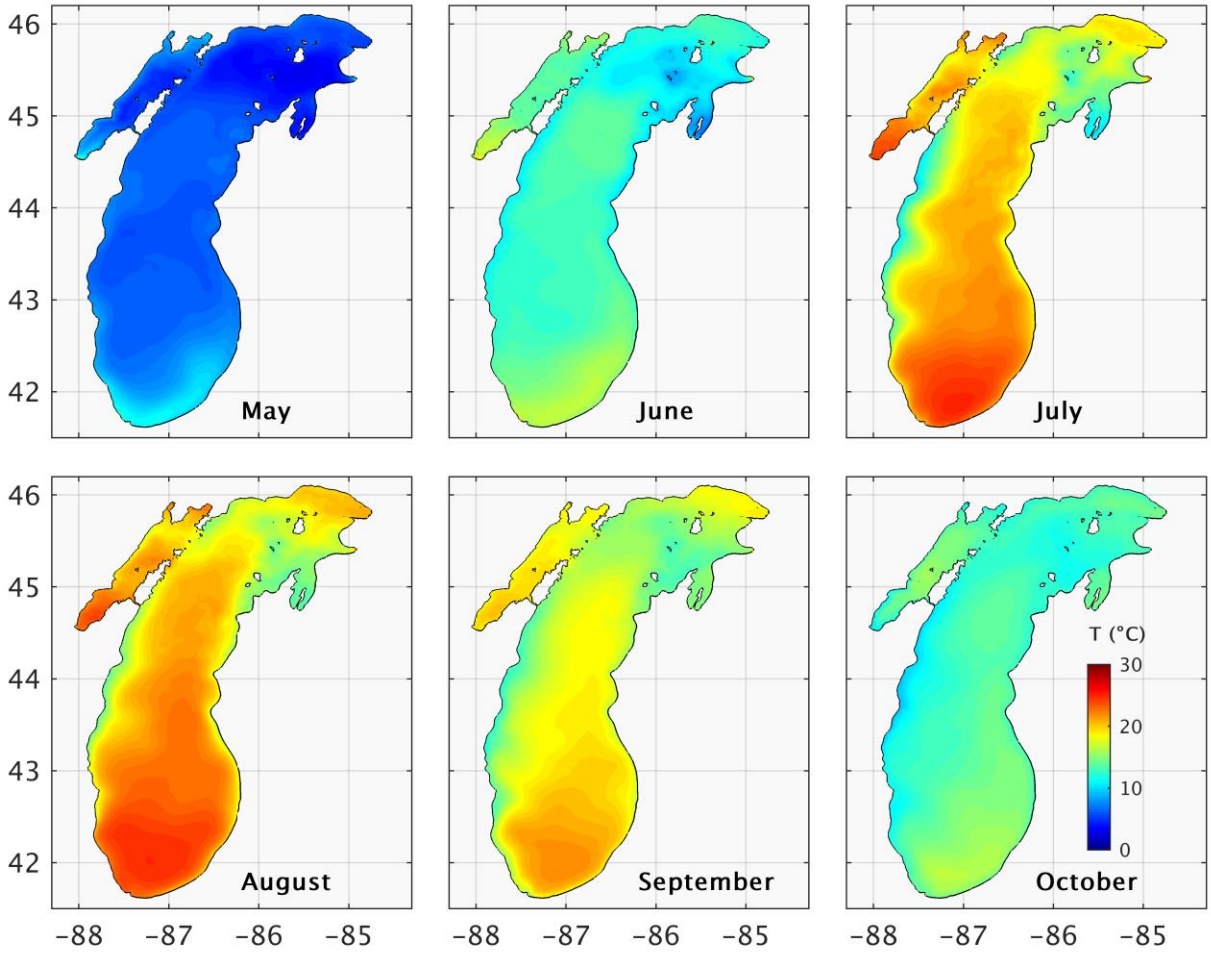

Figure 5.15. Monthly average surface temperature fields in Lake Michigan during the May-October 2019

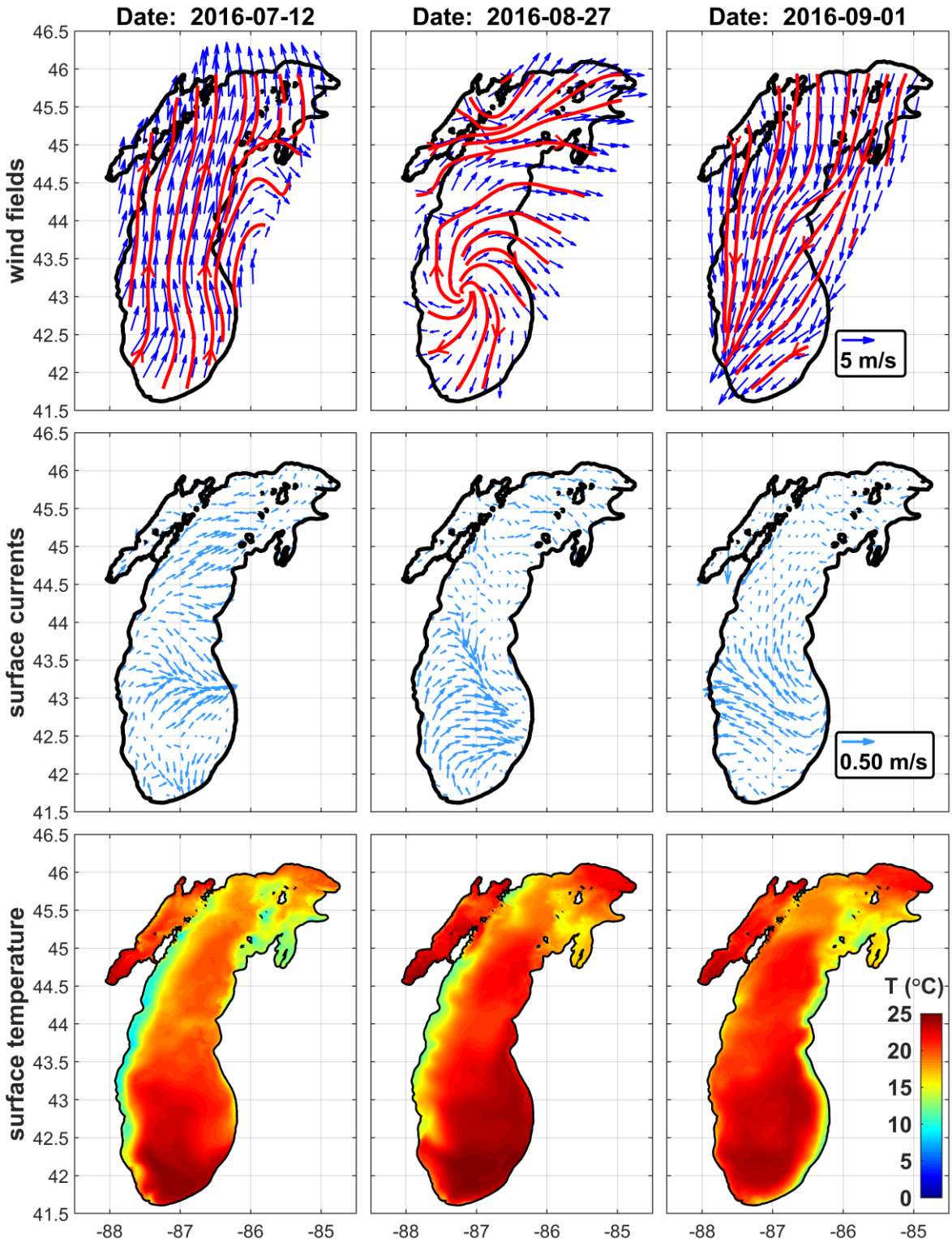

Figure 5.16. Three examples of the upwelling events in Lake Michigan in July, August, and September of 2016 (bottom row) with their corresponding surface currents (middle row) and wind fields (top row)

5.4. Circulation Patterns in Green Bay

Figures 5.17 and 5.18 illustrate the monthly-averaged circulation in Green Bay during the May-October 2018 and 2019, respectively. As shown in both figures, currents are more often northward in Green Bay. Also, larger currents occur along the western shoreline of upper Green Bay, south of Chambers Island, and near the connecting straits. Gyres also form in Green Bay, most commonly south or north of Chambers Island, and when currents are strong in the bay.

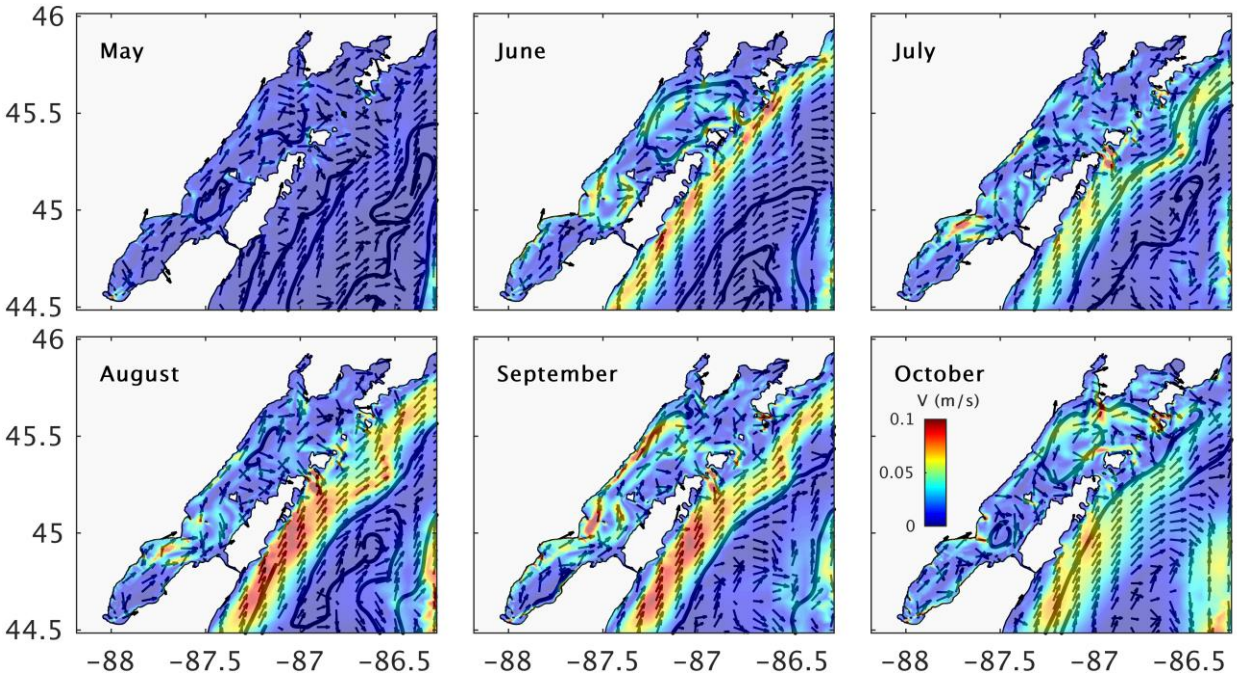

Figure 5.17. Monthly depth-averaged currents in Green Bay during the May-October 2018. Black arrows and black lines show the direction of flow and general circulation regimes, respectively.

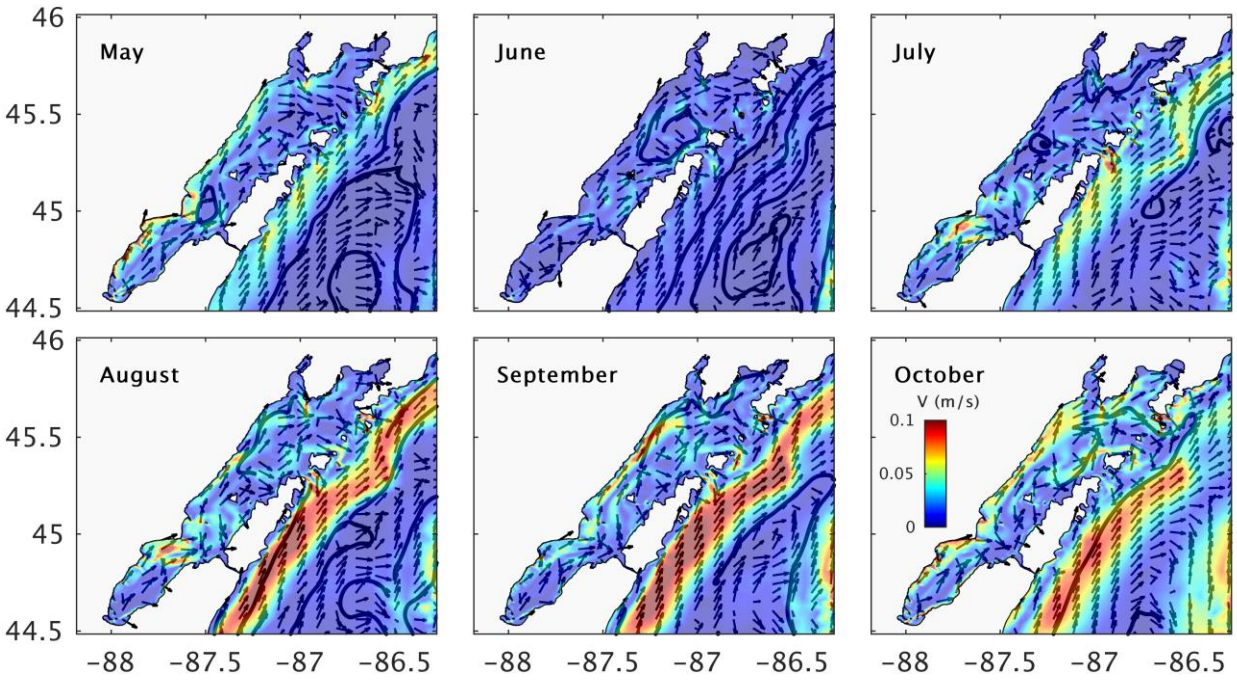

Figure 5.18. Monthly depth-averaged currents in Green Bay during the May-October 2019. Black arrows and black lines show the direction of flow and general circulation regimes, respectively.

5.5. Thermal Regimes and Stratification in Green Bay

Figures 5.14 and 5.15 clearly show that Green Bay follows different thermals regimes than those of Lake Michigan, i.e., warmer temperatures are expected in Green Bay compared to open lake waters. Higher-resolution versions of monthly average surface temperature fields are provided for Green Bay in Figures 5.19 and 5.20 for 2018 and 2019 simulations, respectively. Patterns are almost similar in both years, with some slight decrease in temperature of the bay in 2019. June-September is the time with most variability in temperature across the bay with higher temperatures occurring on southern and northern shallow areas and colder waters near the exchange zone with Lake Michigan, predominantly due to cold water intrusion from the lake.

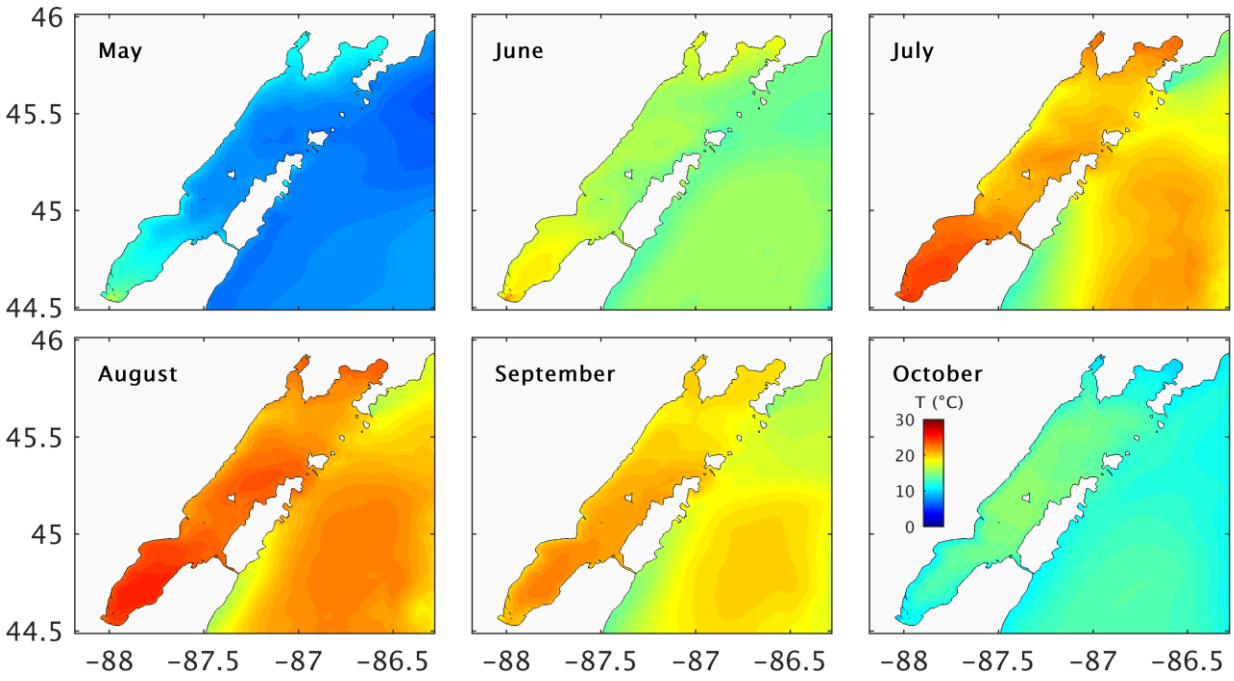

Figure 5.19. Monthly average surface temperature fields in Green Bay during the May-October 2018

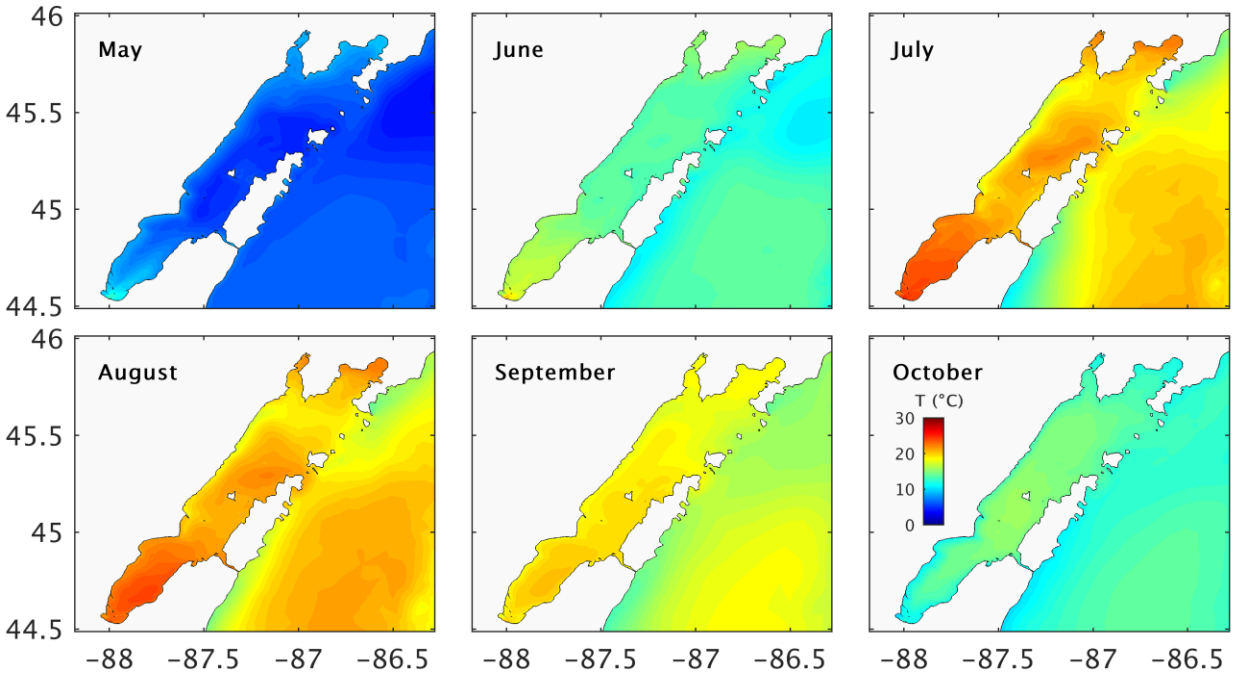

Figure 5.20. Monthly average surface temperature fields in Green Bay during the May-October 2019

Stratification plays, evidently, an important role in the formation of thermal structures and circulation regimes in Green Bay and thereby the ecological functioning of the bay. Three cross-sections were selected in this study to examine stratification in Green Bay (and also sediment dynamics along the water column in Chapter 6). Figure 5.21 shows the three selected cross-sections cutting through Green Bay in different locations.

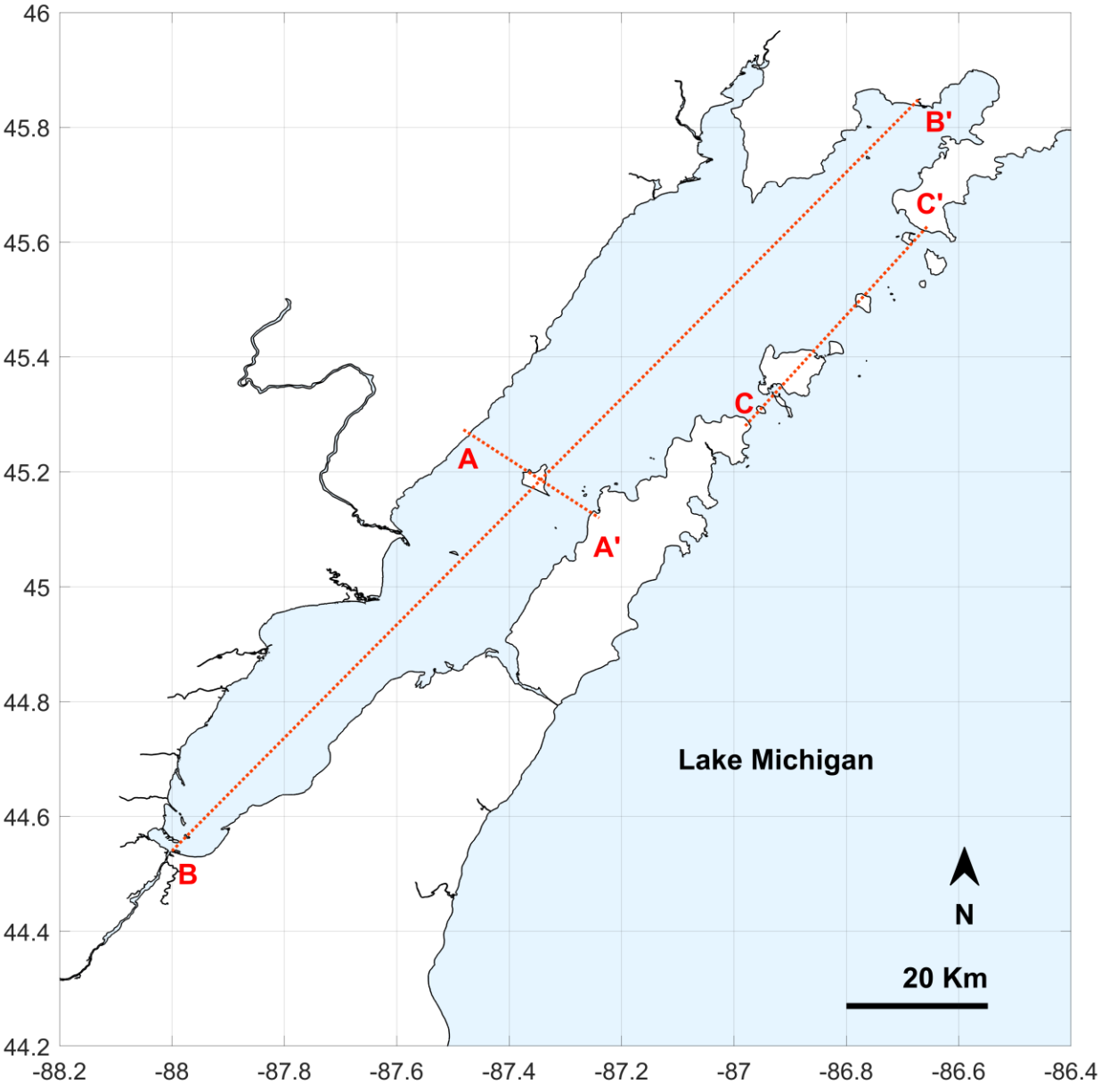

Figure 5.21. Three selected cross-sections for Green Bay

Cross-section A-A’ slices Green Bay across Chambers Island and is considered to investigate the fluxes in and/or out of lower Green Bay through western and eastern channels at that location. Cross-section B-B’ is a longitudinal-section of the bay from point B at the mouth of Fox River in lower Green Bay to point B’ located in Big Bay De Noc in upper Green Bay. This longitudinal-section was selected to investigate the thermal structure of the bay along its longitudinal direction and during the modeling period. Cross-section C-C’ passes through the area of exchange between Green Bay and Lake Michigan to investigate the patterns of transport through this important area.

Figures 5.22 and 5.23 show monthly-average temperature profile along the Green Bay’s longitudinal-section B-B’ in 2018 and 2019, respectively. The thermal structure of the bay is similar in the corresponding months of the two years. Consistent with findings of Hamidi et al. (2015, 2013) and Bravo et al. (2015), both figures show that stratification in Green Bay starts in June, peaks in July and August and fades in September. That implies stratification lasts about three months and for the entire summer in this system. Also, the mixing of temperature profiles occurs at faster rates in shallower areas, as expected. The Fox River has a significant effect on the thermal distribution of the southern part of Green Bay as shown in the first 50 Km section of the temperature profiles in both figures, closer to the mouth of the Fox River.

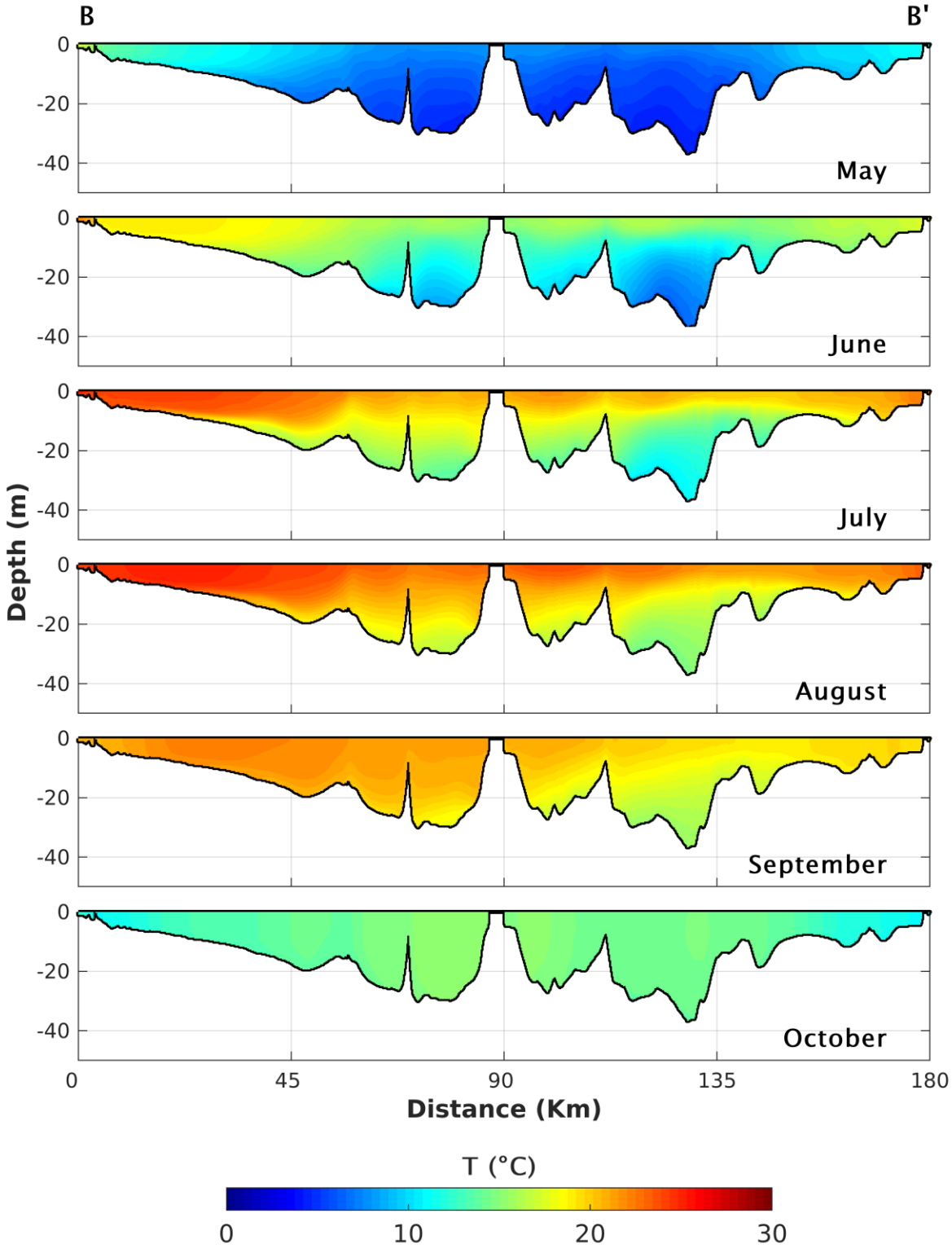

Figure 5.22. Monthly average temperature profiles along the B-B' cross-section in Green Bay during the period of May-October 2018 period. Distances are measured from point B at the mouth of the Fox River.

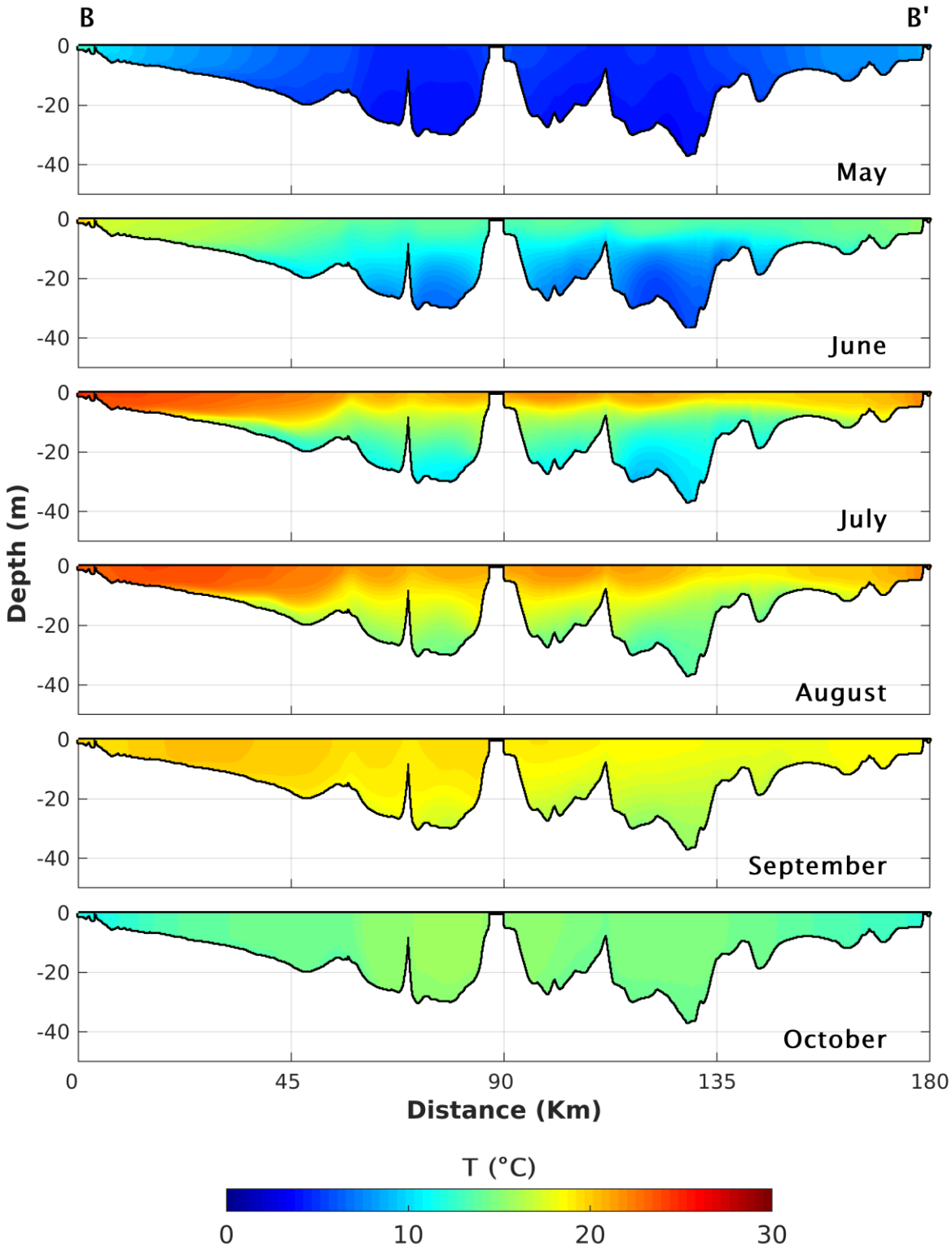

Figure 5.23. Monthly average temperature profiles along the B-B' cross-section in Green Bay during the period of May-October 2019 period. Distances are measured from point B at the mouth of the Fox River.

5.6. Validation of Simulated Waves

In addition to currents, wave actions play an important role in the sediment processes of the lake. In this study, the FVCOM-SWAN model was adopted for the simulation of waves. Three buoy stations of 45013, 45002, and 45007 (shown in Figure 4.6) were selected for validation of significant wave height (Hs) in the current study. These buoys are located in different areas of Lake Michigan which will provide the opportunity to validate model performance in different conditions. Buoys 45002 and 45007 represent deep open lake conditions at the center of northern and southern basins of Lake Michigan and buoy 45013 represent wave conditions in shallow coastal areas. It should be noted that significant wave height is defined as the average of the highest one-third of the waves, measured from wave trough to the crest.

Tables 5.9 and 5.10 also show the model skills for significant wave height at these three buoys. The model is biased in the buoy 45002 but almost all of the error criteria indicate that the model performed well in the simulation of waves in 2018 and 2019. Especially, high correlations between simulations and observations indicates that simulated results are producing the patterns of wave height variability with high accuracy.

Table 5.9. Significant Wave height model skill error criteria in 2018 simulation

Buoy	RMSE (m)	BD (m)	NSE	CC
45013	0.14	0.03	0.80	0.92
45002	0.22	0.15	0.74	0.96
45007	0.12	0.04	0.92	0.97

Table 5.10. Significant wave height model skill error criteria in 2019 simulation

Buoy	RMSE (m)	BD (m)	NSE	CC
45013	0.16	0.04	0.74	0.88
45002	0.23	0.18	0.58	0.95
45007	0.12	0.06	0.83	0.94

Figures 5.24 and 5.25 show comparisons of the significant wave height with buoy observations during May-October of 2018 and 2019, respectively.

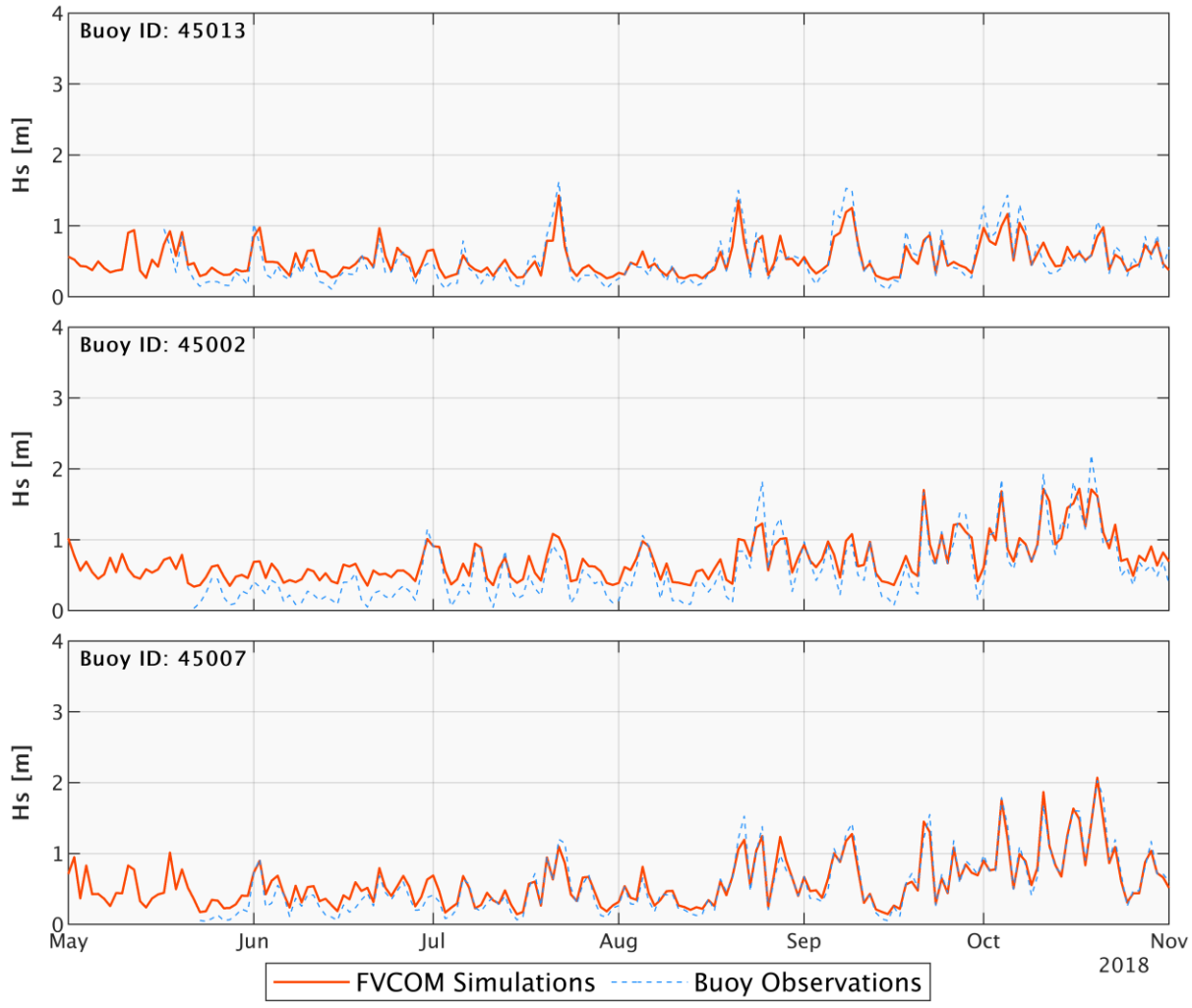

Figure 5.24. Comparison of the significant wave height (Hs) at the location of three selected validation buoys during the May-October 2018

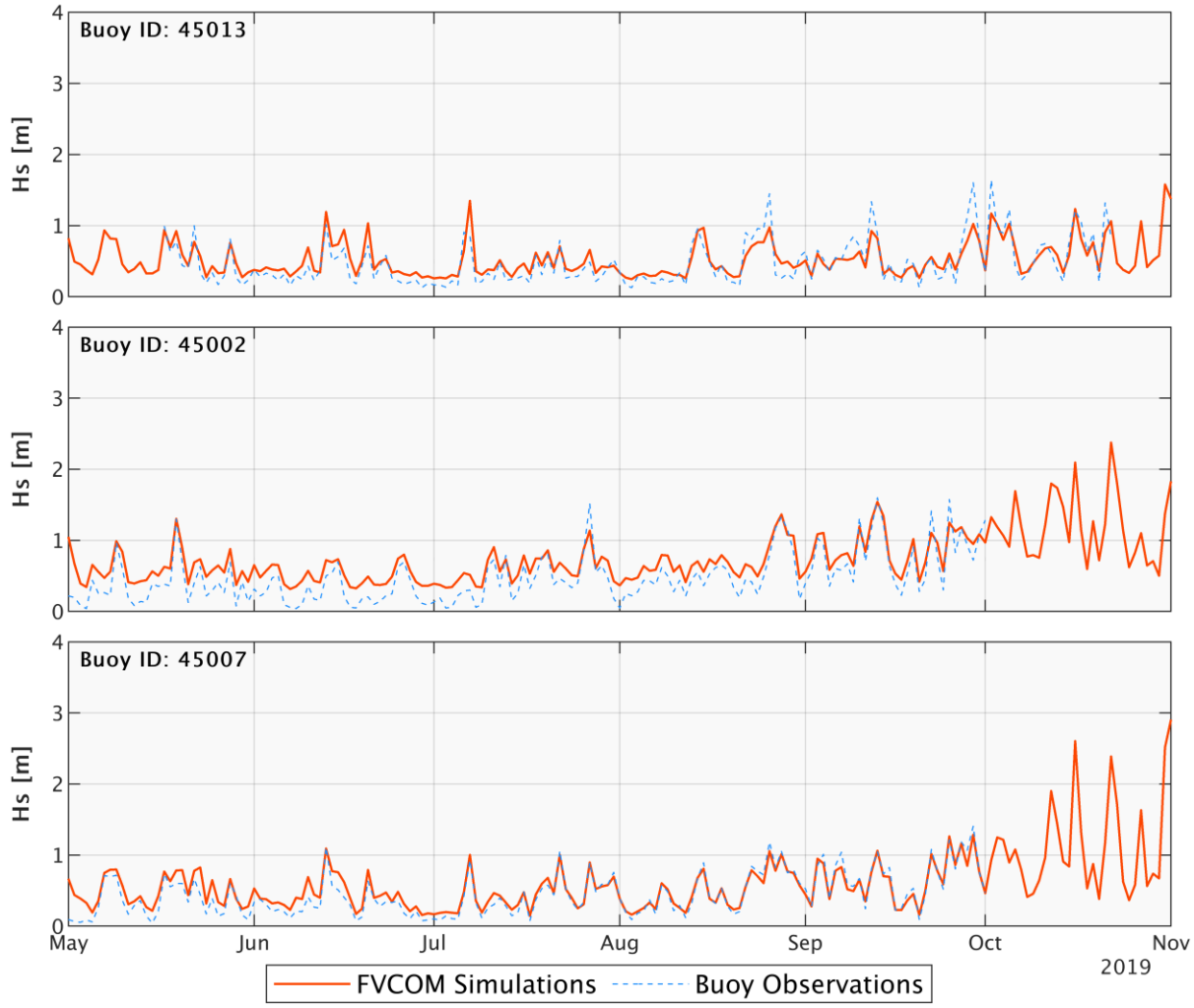

Figure 5.25. Comparison of the significant wave height (Hs) at the location of three selected validation buoys during the May-October 2019

5.7. Wave Fields in Lake Michigan and Green Bay

Figures 5.26 and 5.27 illustrate the monthly-averaged significant wave heights in Lake Michigan for 2018 and 2019 simulations, respectively. Wave patterns are pretty much similar in two years but different in different months. In general, the northern basin of Lake Michigan and the exchange zone with Green Bay experience stronger wave conditions. Waves are gradually increasing from May to September and there is a sharp increase in wave height from September to October.

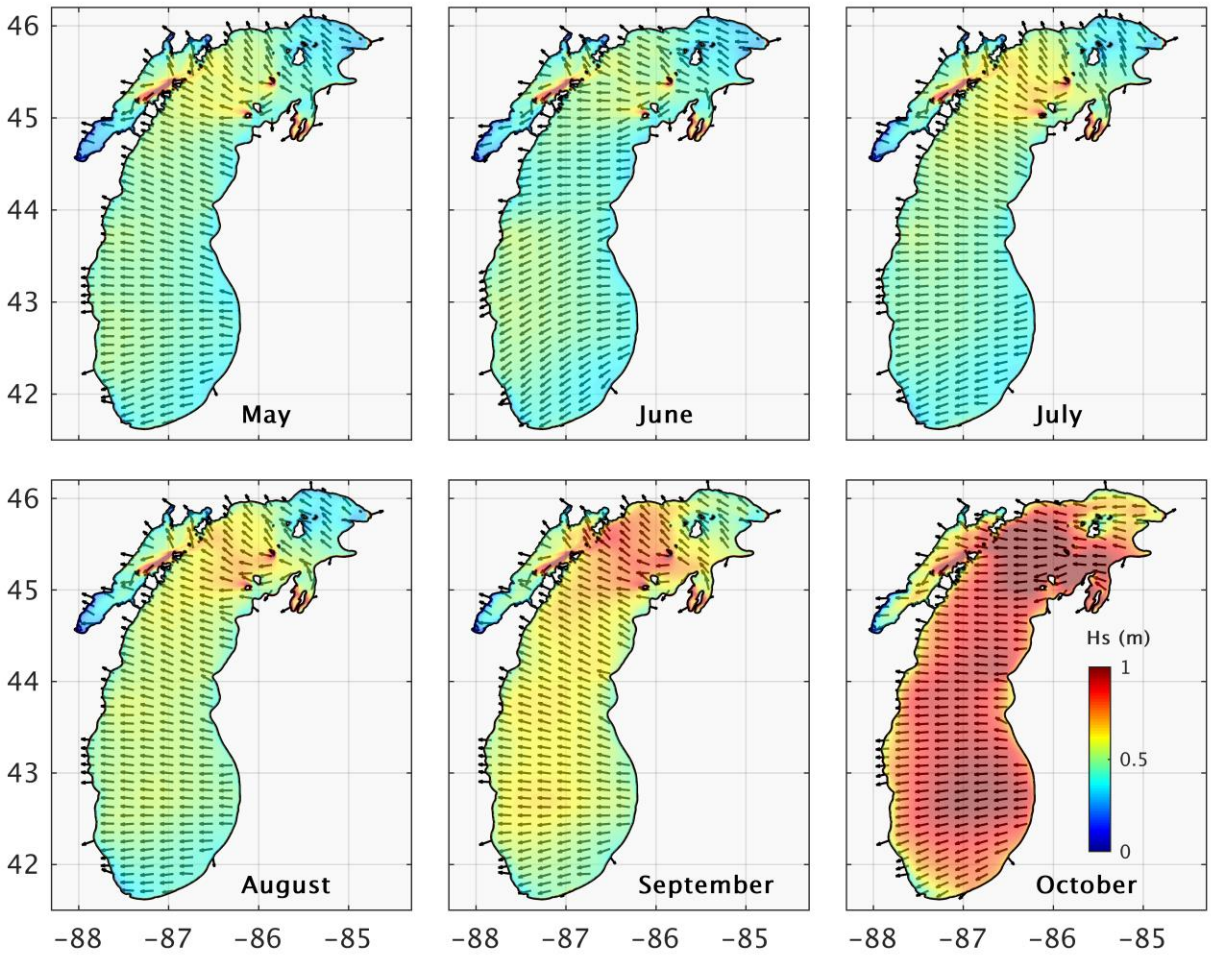

Figure 5.26. Monthly average significant wave heights (Hs) in Lake Michigan during the May-October 2018. Black arrows show wave direction.

More detailed patterns of wave fields for Green Bay are provided in Figures 5.28 and 5.29. As shown in both figures, high waves occur between the exchange zone and north of Chambers Island each month. Similar to Lake Michigan, waves are also stronger in September and October in the bay. In other months, strong waves southwest of the exchange zone were developed most probably due to intrusion of high waves from Lake Michigan into the bay and rapid change in bottom elevation in that area (see Figure 2.2). However, those strong wave actions require further investigations.

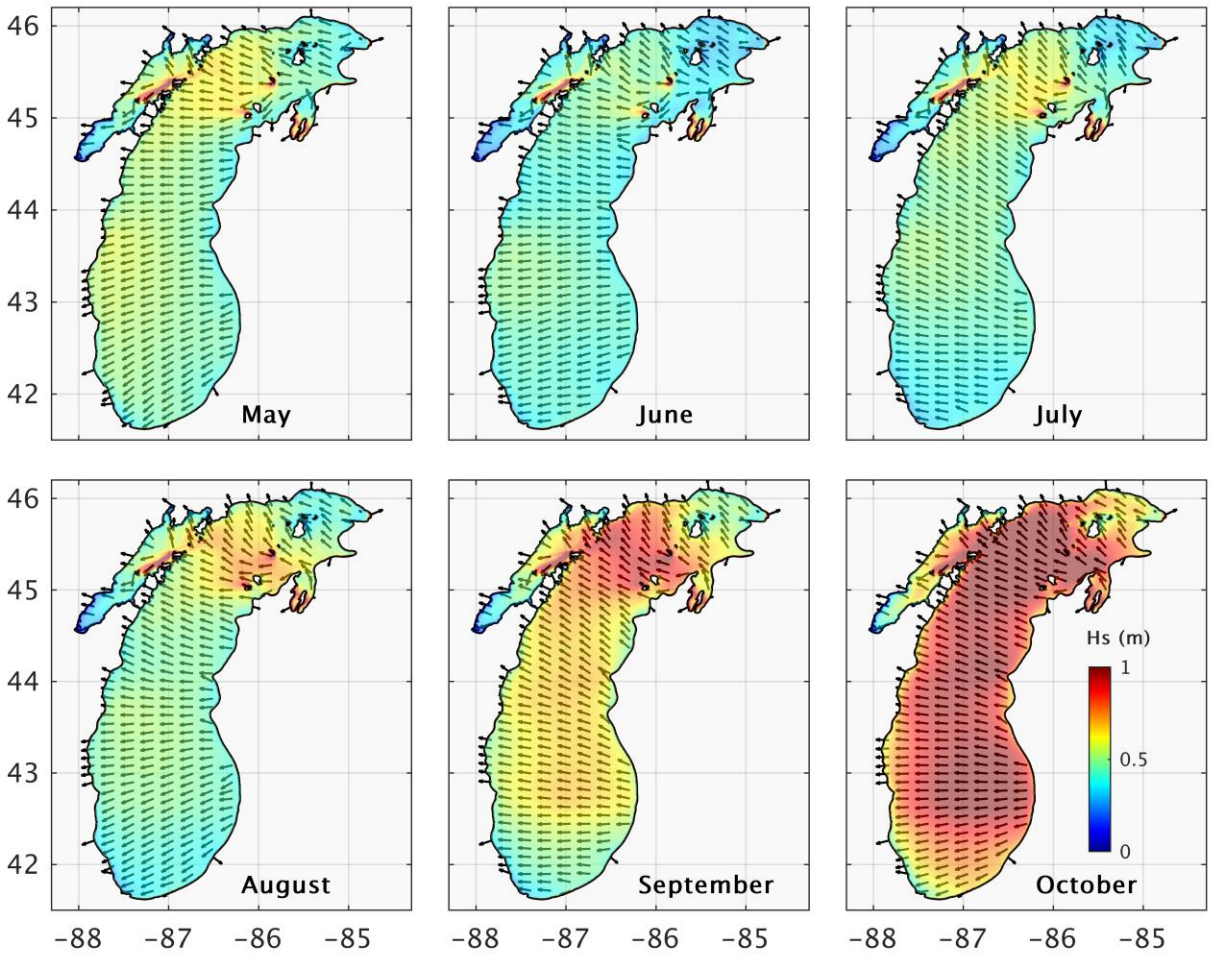

Figure 5.27. Monthly average significant wave heights (Hs) in Lake Michigan during the May-October 2019. Black arrows show wave direction.

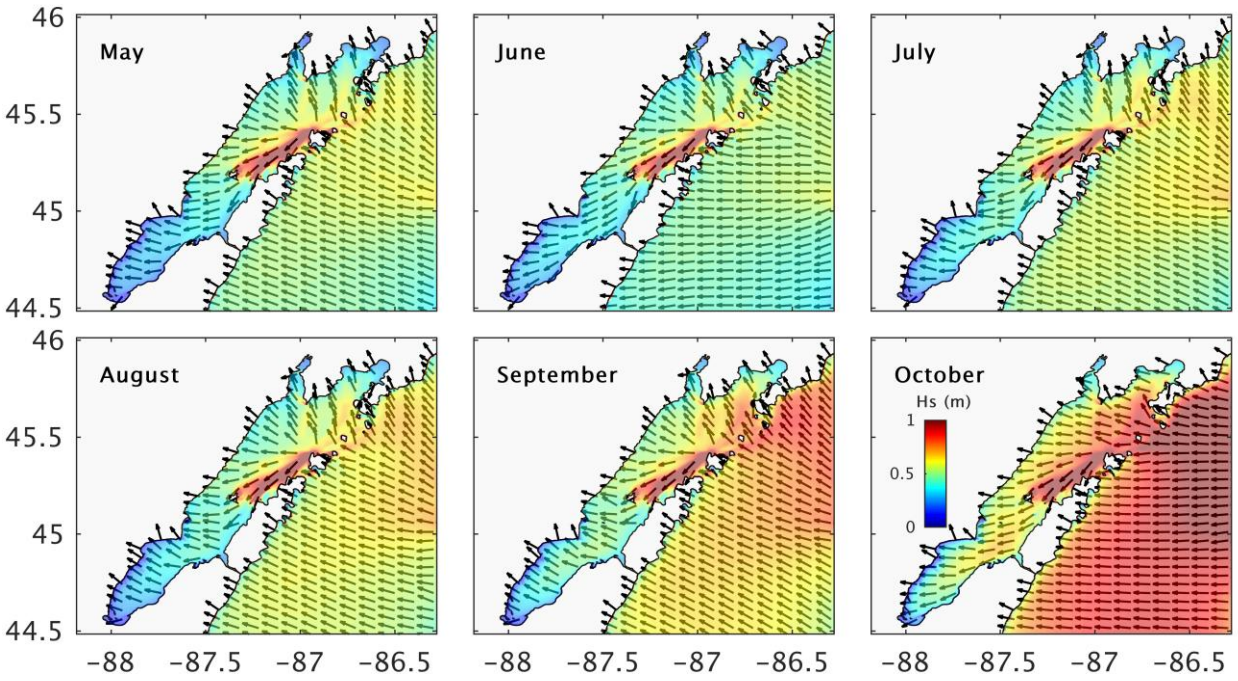

Figure 5.28. Monthly average significant wave heights (Hs) in Green Bay during the May-October 2018. Black arrows show wave direction.

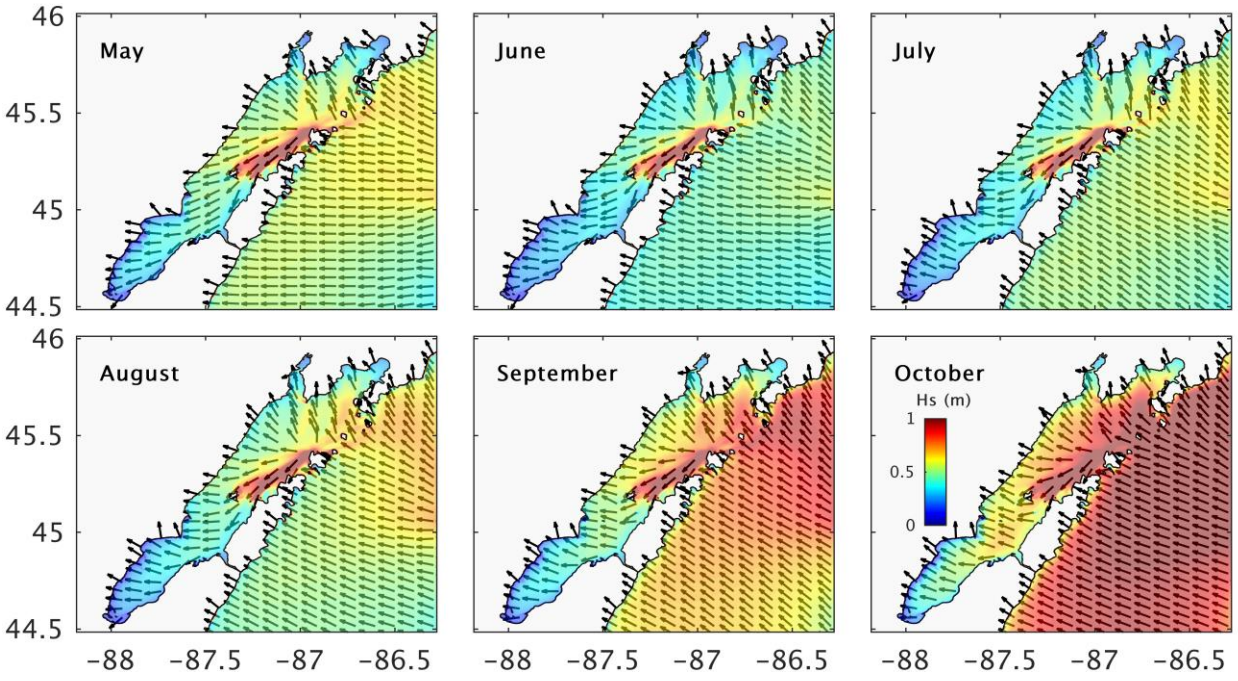

Figure 5.29. Monthly average significant wave heights (Hs) in Green Bay during the May-October 2019. Black arrows show wave direction.

Chapter 6:
Results of the Sediment Transport Model

6.1. Validation of Simulated Sediment Concentrations

Figures 6.1 and 6.2 provide comparisons of model simulations of TSS against the observations of GBW and GBE buoys located in the Green Bay AOC for 2018 and 2019 simulations, respectively. Figure 4.6 shows the location of the validation buoys. These buoys obtained time series of turbidity which was converted into TSS concentration based on the same relationship used for estimation of river loadings, based on USGS turbidity observations (explained in section 4.5.2). The sensor probes are placed at mid-depth of the water column. The sensors measurements represent the bottom conditions since the buoys are located in very shallow areas of Green Bay.

Figures indicate that the model simulates TSS with fairly good accuracy, given the complexity of the Green Bay system and sediment transport models. The model shows promising performance in simulation of storm events and resuspensions since major

peaks in both locations are captured quite well. There is a high TSS peak in early July in 2018 that has not been predicted by the model. That peak could also be explained by other assumptions such as sensor malfunction, a sudden increase in TSS concentrations due to construction activities near the GBW buoy (e.g., Cat Island project), dredging of Fox River, and navigation channel project. Also, the model does not show good performance in July and August of 2019 and was not able to reproduce some of the peaks during that period. Similar to the argument about the year 2018 model accuracy, those peaks could be due to other factors not included in the physical model.

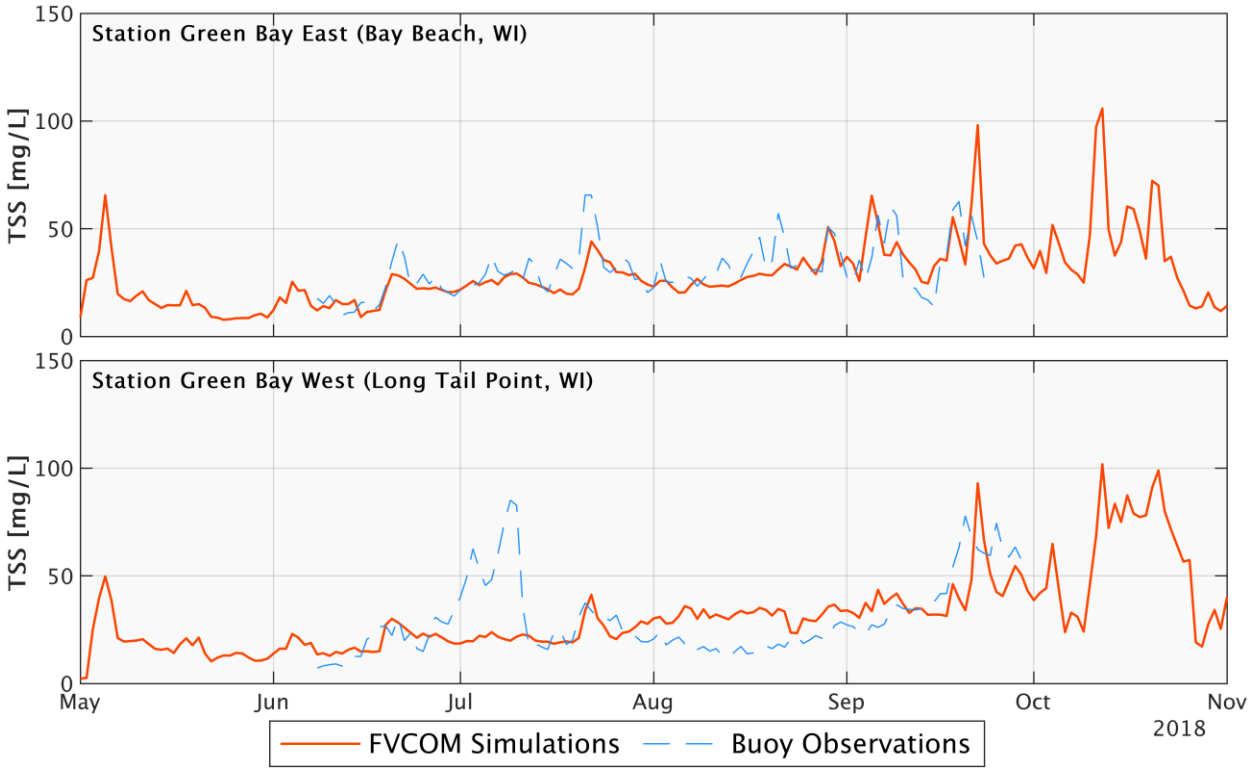

Figure 6.1. Comparison of the total suspended solids concentration (TSS) at the location of GBE and GBW validation buoys during the May-October 2018

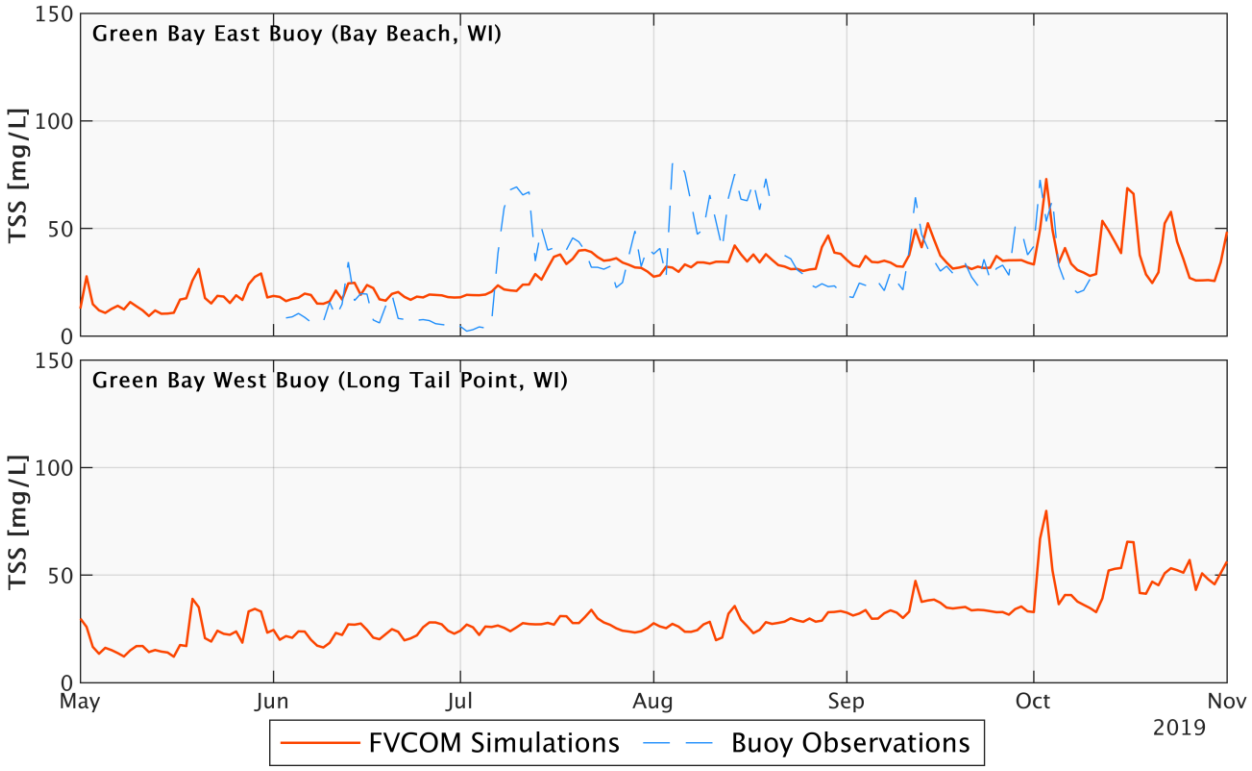

Figure 6.2. Comparison of the total suspended solids concentration (TSS) at the location of GBE and GBW validation buoys during the May-October 2019. GBW buoy data is not available.

Model skill statistics reported in Tables 6.1 and 6.2 also support the relatively good performance of the sediment transport model. Although the model showed some bias in the simulation of TSS concentrations, high correlations between observed and predicted values is another evidence that patterns of variability, in particular resuspension and sedimentation events, were simulated by the model.

Table 6.1. Sediment transport model skill error criteria in 2018 simulation

Buoy	RMSE (mg/L)	BD (mg/L)	NSE	CC
GBE	10.68	-2.35	0.22	0.63
GBW	16.82	-0.95	0.10	0.40

Table 6.2. Sediment transport model skill error criteria in 2019 simulation (there is no data available for GBW buoy)

Buoy	RMSE (mg/L)	BD (mg/L)	NSE	CC
GBE	17.2	-2.04	0.28	0.54
GBW	-	-	-	-

In the next sections, sediment transport regimes, erosion/deposition patterns and sedimentation rates of the lake, as well as sediment fluxes into and out of Green Bay are investigated. A sediment budget was also estimated for the different sections of Green Bay.

6.2. Patterns of Sediment Transport in Lake Michigan and Green Bay

Figures 6.3 and 6.4 provide monthly depth-averaged TSS concentration in Lake Michigan for the 2018 and 2019 May-October periods. Patterns of TSS variations throughout the lake are similar in corresponding months of the two years, consistent with their corresponding similar wave and current patterns. During May-September coastal areas in the southern basin of Lake Michigan, lower Green Bay, and coastal areas at the very northern parts of the lake are characterized with high TSS concentrations, a finding that is consistent with some of the previous Lake Michigan sediment transport models. In particular, Lee et al. (2007) have found similar patterns for TSS concentration in Lake Michigan using a sediment transport model, as well as remote sensing techniques (Figures 8 and 9 in that article). In October, the lake's sediment dynamics are at its highest peak predominantly due to strong wave actions during this month as shown in Figures 6.3 and 6.4.

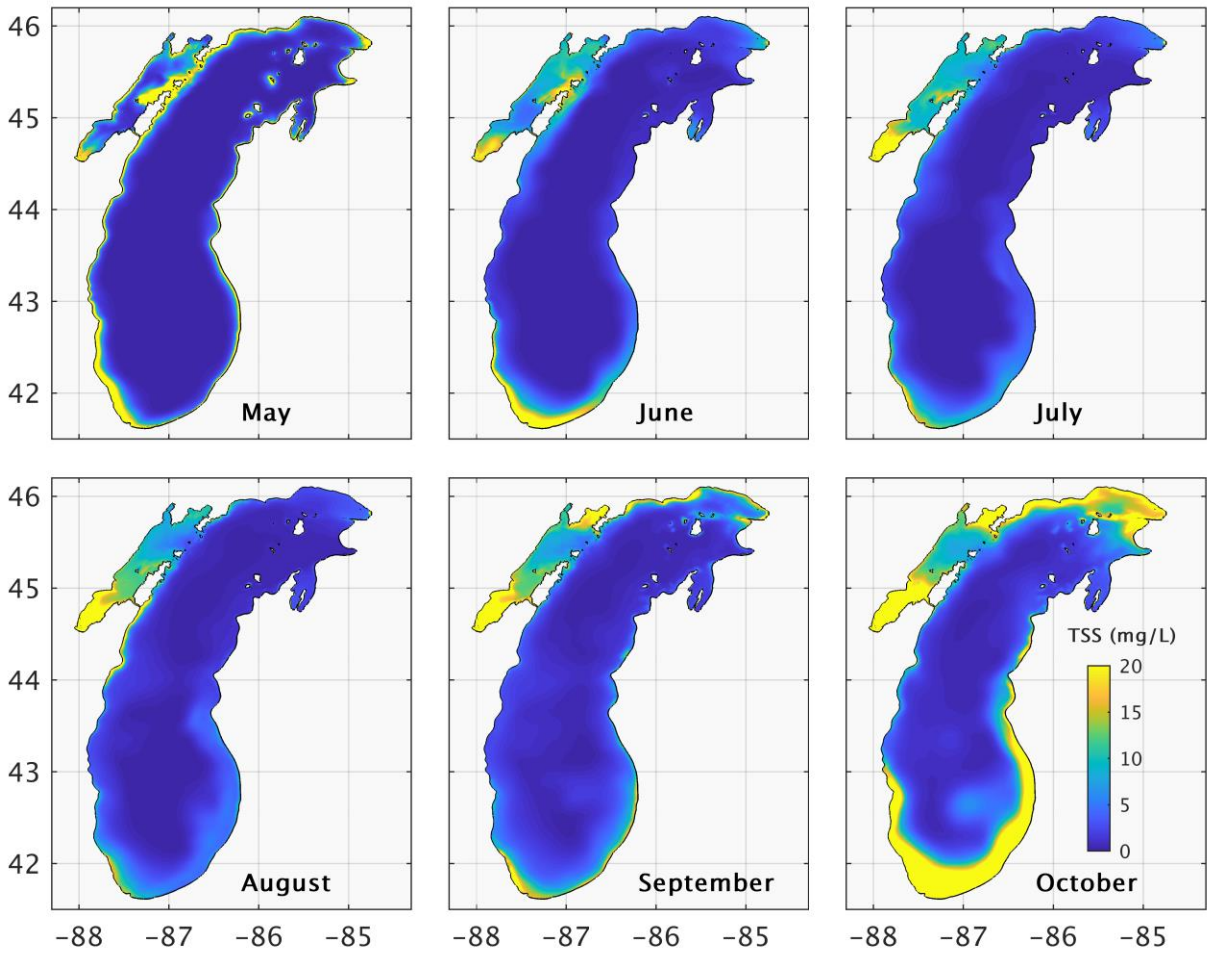

Figure 6.3. Monthly depth-averaged total suspended solids concentration (TSS) in Lake Michigan during the May-October 2018

Green Bay does not exactly follow the patterns of sediment transport in Lake Michigan (Figures 6.5 and 6.6). Southern bay is experiencing high TSS concentrations most of the time, while northern bay follows more or less the Lake Michigan patterns. Upper Green Bay sediment transport is mostly under the influence of circulations and waves as evidenced by the high TSS concentrations near the connecting straits where strong waves are present very often (as shown in Figures 5.28 and 5.29). However, variations in the southern bay seems to be affected by the Fox River persistent and excessive TSS loading and abundance of fine-grained sediments.

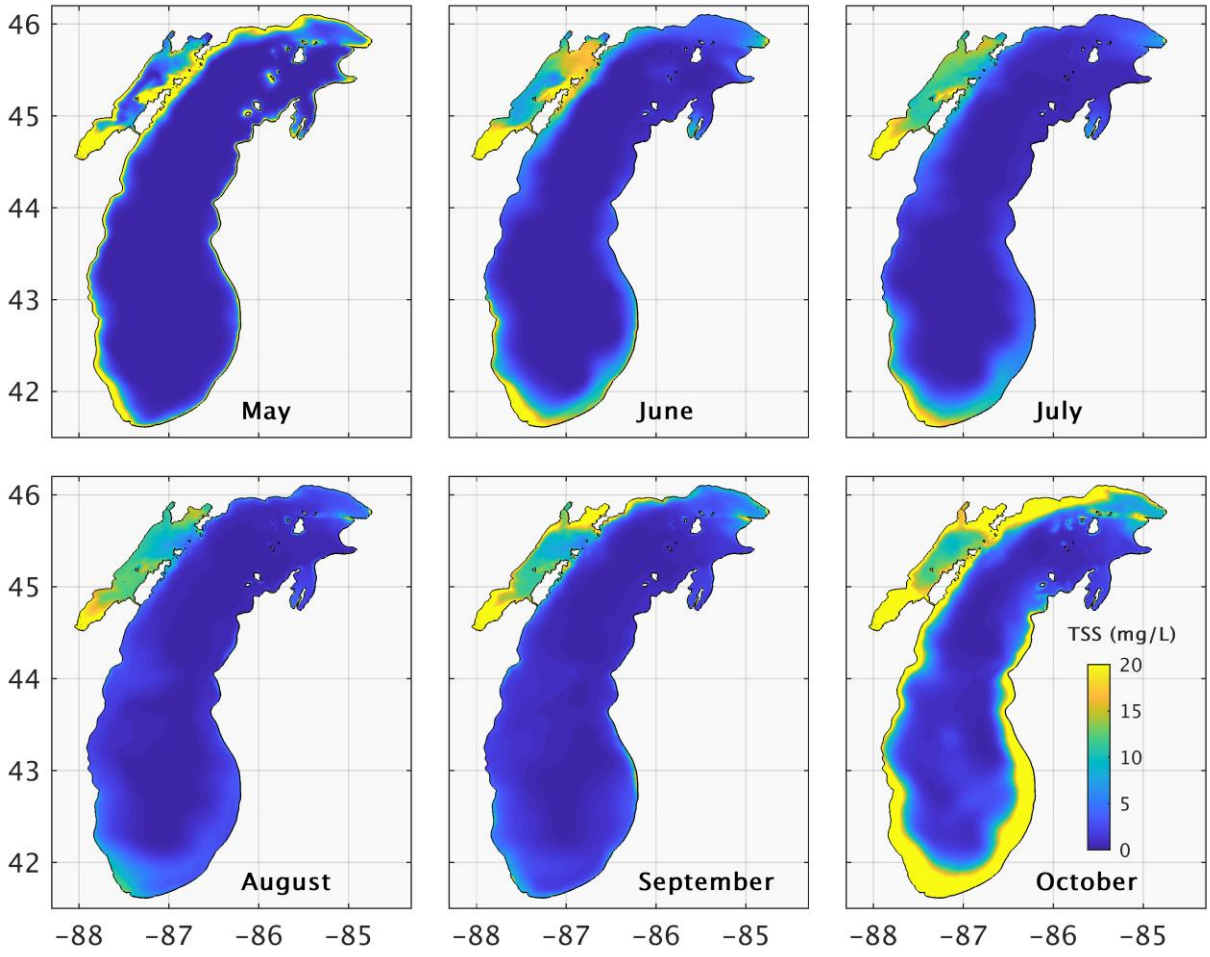

Figure 6.4. Monthly depth-averaged total suspended solids concentration (TSS) in Lake Michigan during the May-October 2019

TSS concentration patterns of lower Green Bay in corresponding months of each year are not very consistent comparing to the other areas of Lake Michigan and upper Green Bay. In particular, there is more TSS variability in May and June of 2019, while August and September 2019 have much less gradient compared to the same months in 2018. However, the model seems to overestimate TSS concentration during September and October in the offshore areas of lower Green Bay and north of AOC. That requires more investigations by obtaining time series of TSS (or turbidity) field data in those areas, in particular, during storm events when cruise sampling is not possible.

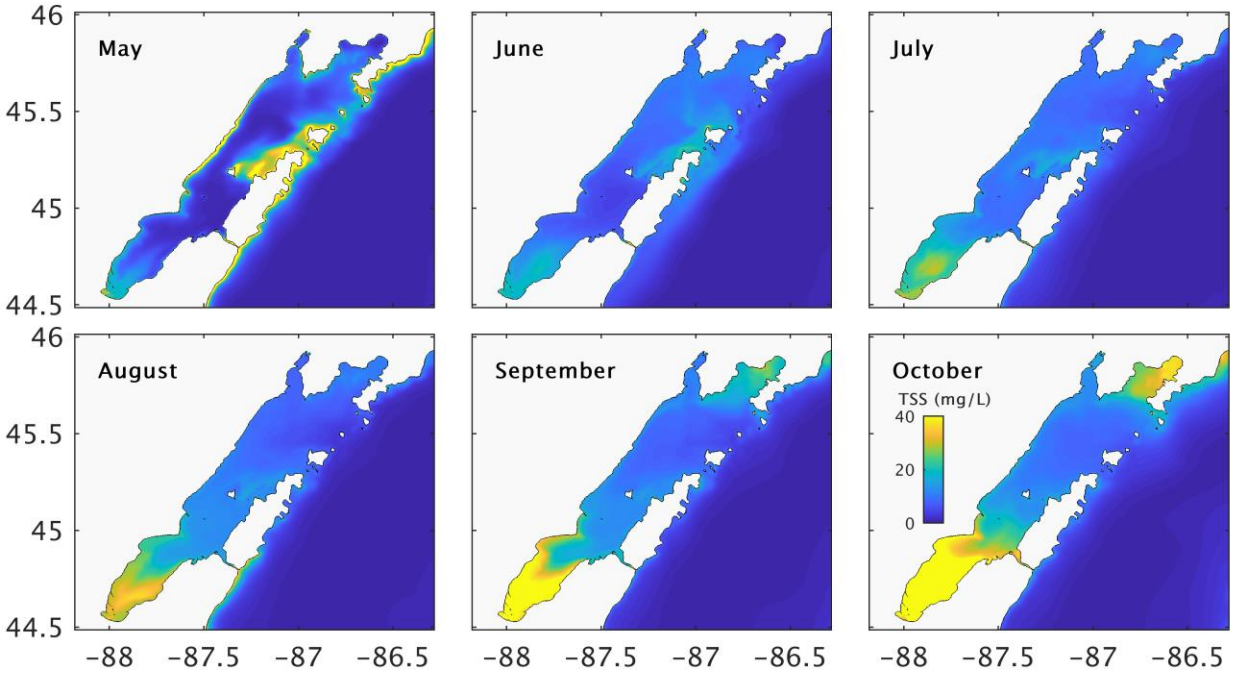

Figure 6.5. Monthly depth-averaged total suspended solids concentration (TSS) in Green Bay during the May-October 2018

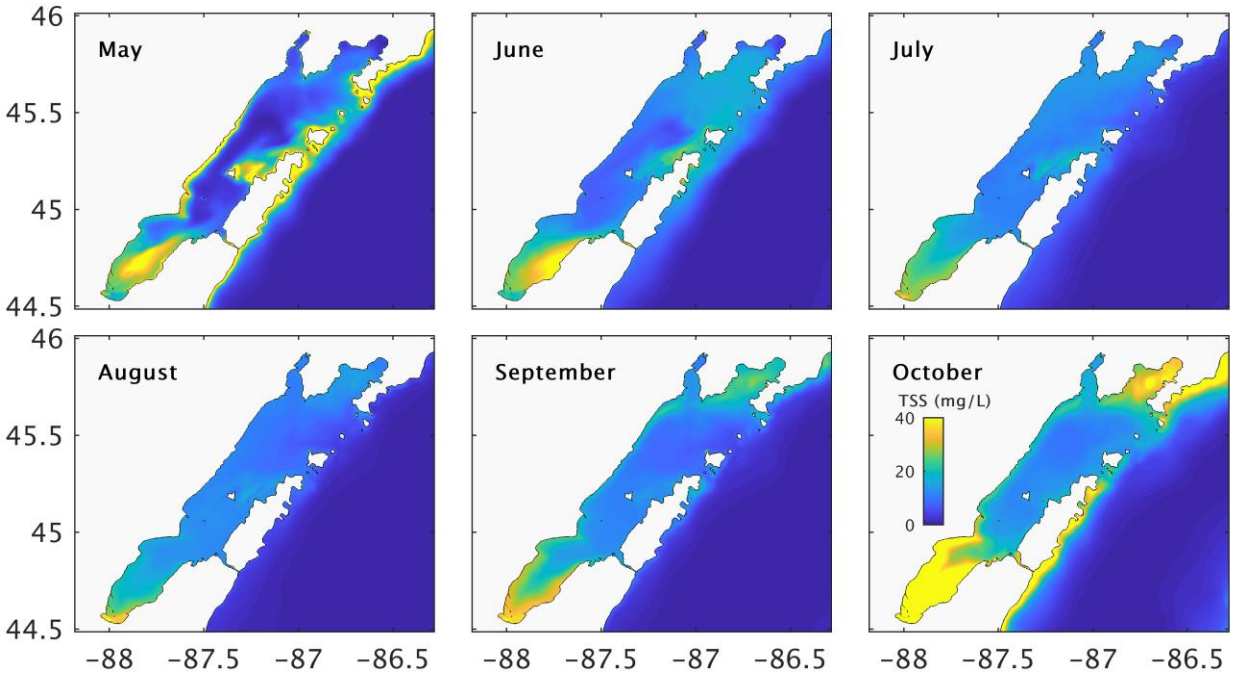

Figure 6.6. Monthly depth-averaged total suspended solids concentration (TSS) in Green Bay during the May-October 2019

TSS concentrations profiles along the B-B' longitudinal cross-section of Green Bay (see Figure 5.21), shown in Figures 6.7 and 6.8, also indicate similar patterns of change in the water column in upper Green Bay, although there is some discrepancy in the lower bay similar to the shift in patterns of depth-averaged TSS concentrations above. In 2019, TSS concentrations are higher in May and June and lower in August and September, compared to the corresponding months of 2018. This is another evidence that there are other factors involved in sediment dynamics of the lower Green Bay besides the meteorological forcing.

In general, there are more dynamics near the mouth of Fox River and higher TSS concentrations in the lower and upper ends of the bay at point B and B'. High TSS concentrations north of Chambers Island in May can be explained by strong wave actions in that area.

As discussed in Chapter 5, the FVCOM model and its modules FVCOM-SWAVE and FVCOM-SED provide a reliable and robust platform to simulate circulation and wave actions, and the corresponding sediment transport in Green Bay and Lake Michigan with reasonable accuracy. There are many applications for a sediment transport model in physical and biogeochemical studies of aquatic systems, some of which were elaborated in Chapter 1 of this study. In the next few sections, we investigate detailed patterns of sediment dynamics and interactions in Green Bay base on the results of the sediment transport model simulation in 2018 and explain those patterns with respect to their application in the development/evaluation of restoration scenarios and management plans.

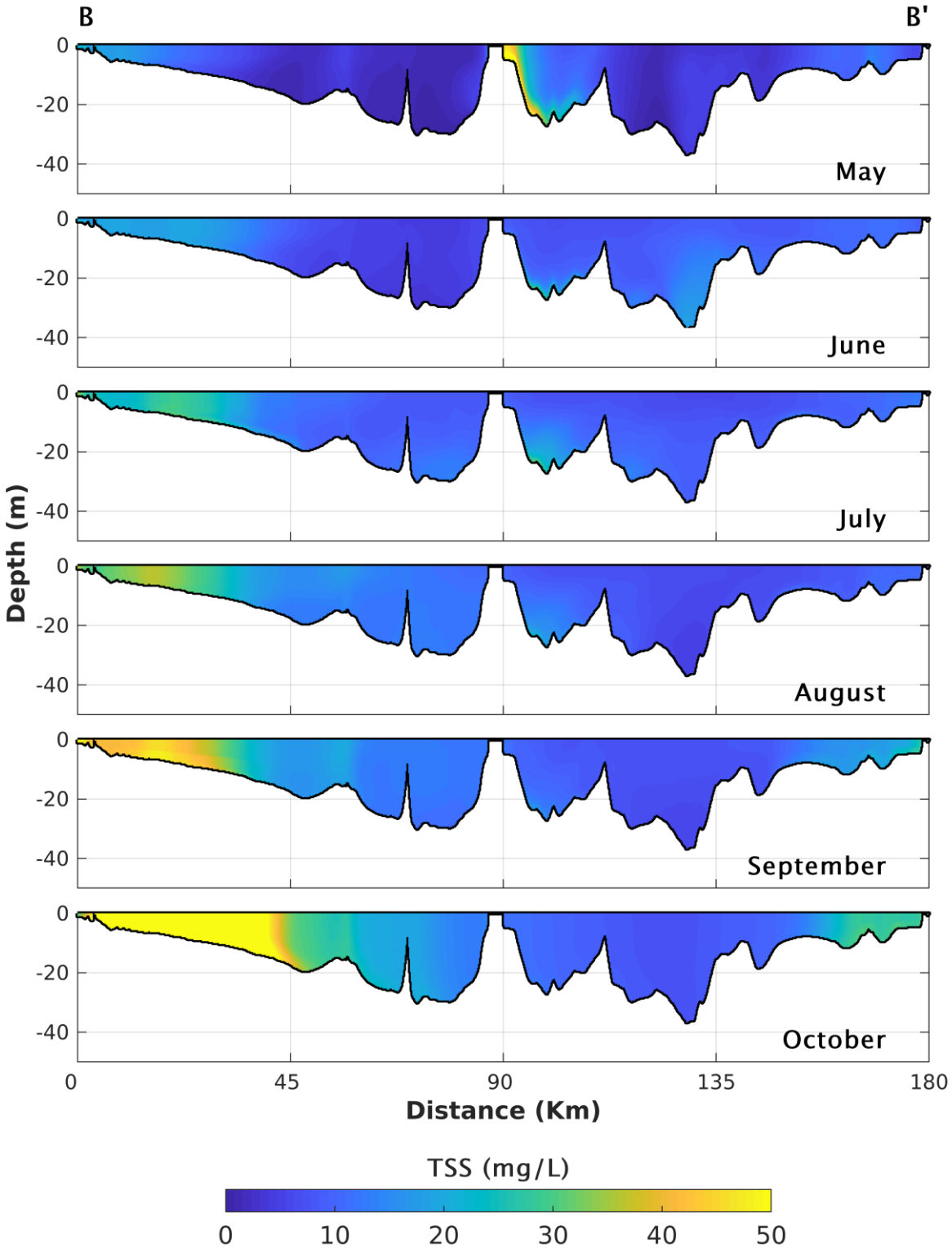

Figure 6.7. Monthly average profiles of total suspended solids (TSS) along the B-B' cross-section in Green Bay during the period of May-October 2018 period. Distances are measured from point B at the mouth of the Fox River.

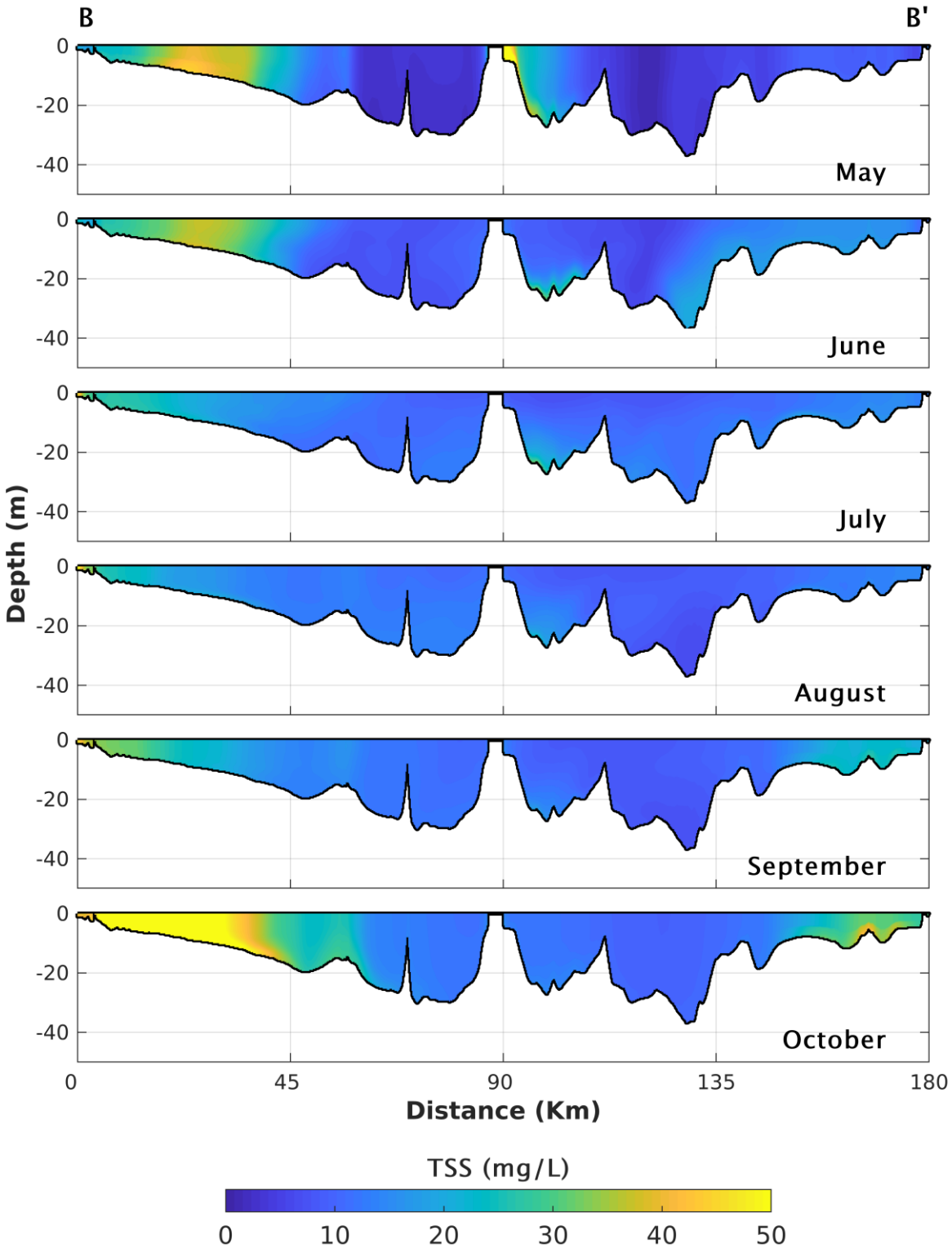

Figure 6.8. Monthly average profiles of total suspended solids (TSS) along the B-B' cross-section in Green Bay during the period of May-October 2019 period. Distances are measured from point B at the mouth of the Fox River.

6.3. Erosion, Deposition, and Sedimentation Rates in Lake Michigan, Green Bay, and Cat Island

The identification and explanation of the major areas of deposition and sedimentation rates in Green Bay have been an important question and subject of research for biologists. The current model can be used to investigate some of those patterns for the entire Green Bay. Figures 6.9 and 6.10 illustrate erosion and deposition in the surface bed layer of Lake Michigan and Green Bay based on sediment transport simulations in the six-month period of May-October 2018.

Overall, the general patterns of erosion and deposition are consistent with the circulation and wave averages in each month and follow the same spatiotemporal patterns as those of TSS simulations. Not surprisingly, most of the erosion and deposition occur in the nearshore zone and near the lake islands, predominantly due to strong wave actions and high bottom shear stress in these areas. Figure 6.9 shows similar patterns of bed erosion and deposition in Lake Michigan for most of the simulation period except for the months of May and October. In May, a significant trend of deposition in the nearshore zone is observed that may be attributed to the lake's weak currents and waves. Strongest alongshore currents and waves occur during October, producing strong shear stress near the shorelines and forcing sediment resuspension and transport with the currents.

During June-September, western coastlines of Lake Michigan seem to be more dynamic, which again is consistent with stronger wave-current regimes compared to the eastern side. During this period and on the western side of Michigan average currents are northward in the northern basin and southward in the southern basin of the lake. That has resulted in major erosions at the shoreline bends and major depositional areas north and

south of the bends in the northern and southern basins, respectively.

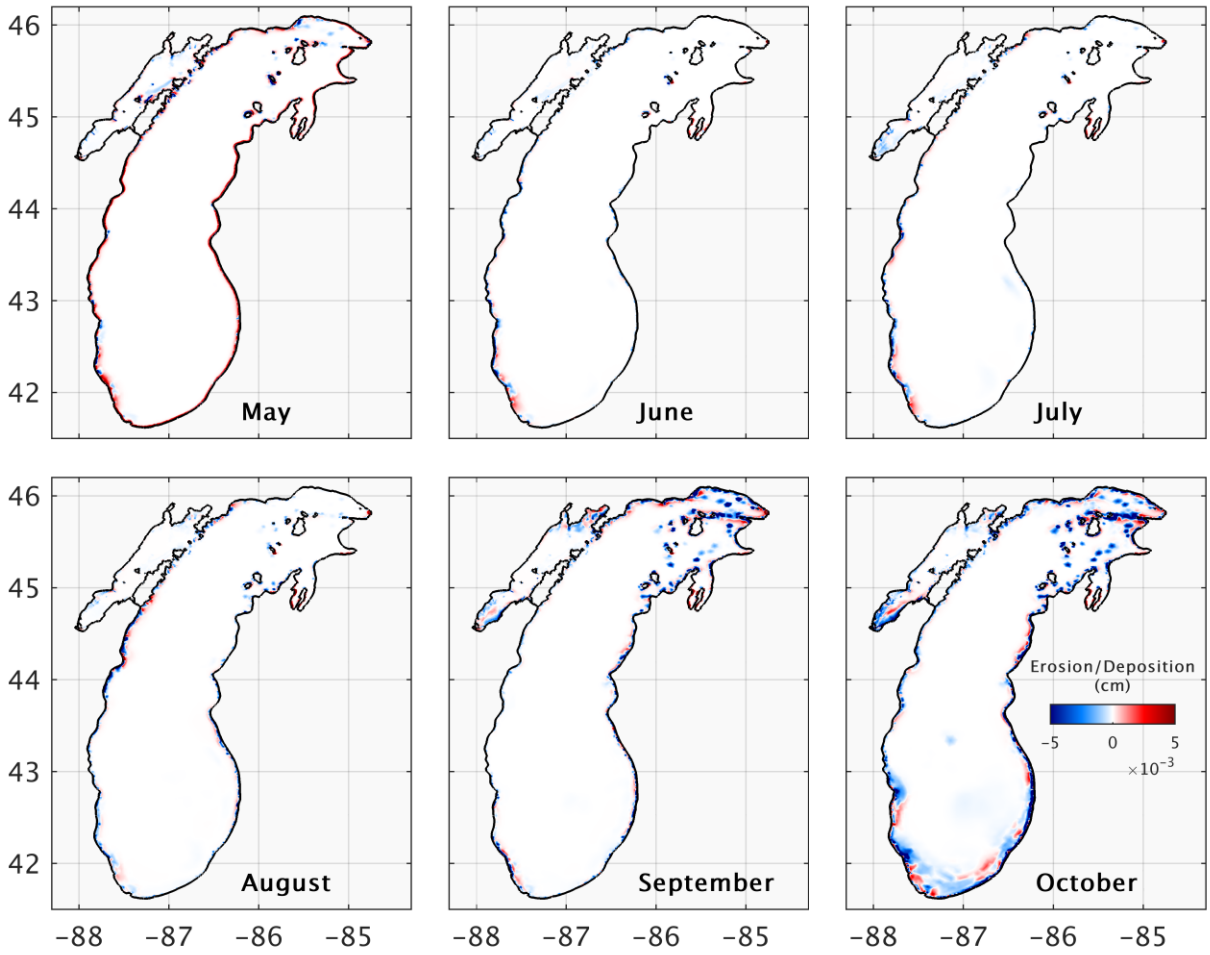

Figure 6.9. Monthly average erosion and deposition at the bottom of Lake Michigan during the period of the May-October 2018 period. Blue and red colors indicate erosion and deposition, respectively.

Frequent and noticeable erosion events in the western and southwestern Lake Michigan are driven by strong currents (see Figures 5.12 and 5.13) in the southern Lake Michigan basin. Sandy beaches on the east coast of Lake Michigan have most likely resulted from the transport of those eroded western shorelines along the counterclockwise currents in southern Lake Michigan basin. These findings are consistent with Lee et al.'s (2007) patterns of sedimentation in eastern Lake Michigan (Figure 13 of that article).

According to Figure 6.10, there seem to be additional drivers of erosion and deposition in Green Bay rather than waves and currents, in particular geometry of the bay, morphology, and Fox River loading. September and October are characterized with similar patterns of bed alterations, in which strong alongshore currents are eroding nearshore areas of lower Green Bay while the deeper central bay is receiving depositional materials that are either coming from eroded shorelines or river loading.

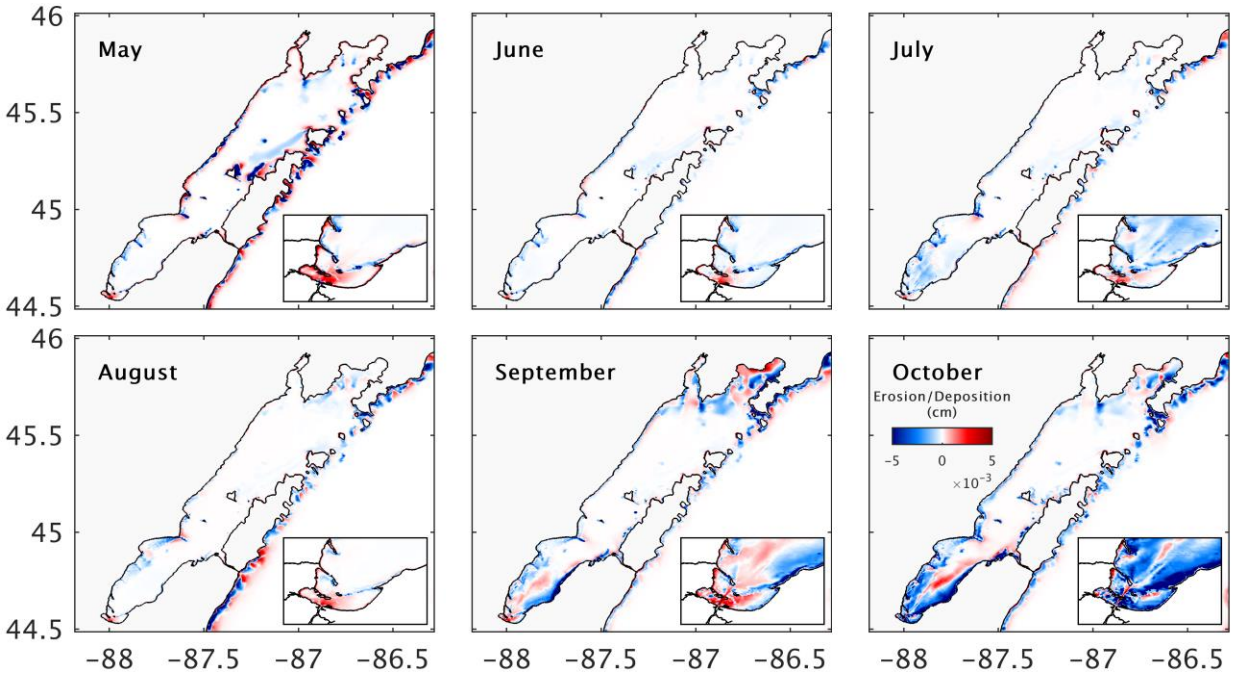

Figure 6.10. Monthly average erosion and deposition at the bottom of Green Bay during the period of May-October 2018 period. Blue and red colors indicate erosion and deposition, respectively. Bottom right insets in each month show the erosion and deposition in the Green Bay AOC.

The area near the exchange zone with Lake Michigan is more prone to erosion than depositions, as was expected because of strong currents and waves coming in from the lake. High PCB concentrations in the eastern nearshore zone of lower Green Bay (Figure 1.2) can be explained by strong erosion of deeply-buried and PCB-contaminated

sediments in that area. One important observation is the impact of several islands located on the western shoreline of the lower Green Bay on the deposition, especially the Cat Island. Except for October with high wave-current driven shear stress, the area south of Cat Island is characterized as a major area of deposition. This finding compares well with the analysis of spatial patterns of residence time found for lower Green Bay by Bravo et al. (2019b), i.e., the area near the mouth of Fox River shows the longest residence times.

Figure 6.11 provides estimates of sedimentation rates in Lake Michigan based on the six-month simulation period of May-October 2018. In those estimations initial conditions on May 1st, 2018 was considered as the baseline and sedimentation rates are calculated based on the difference in sediment mass between the beginning and end of simulations.

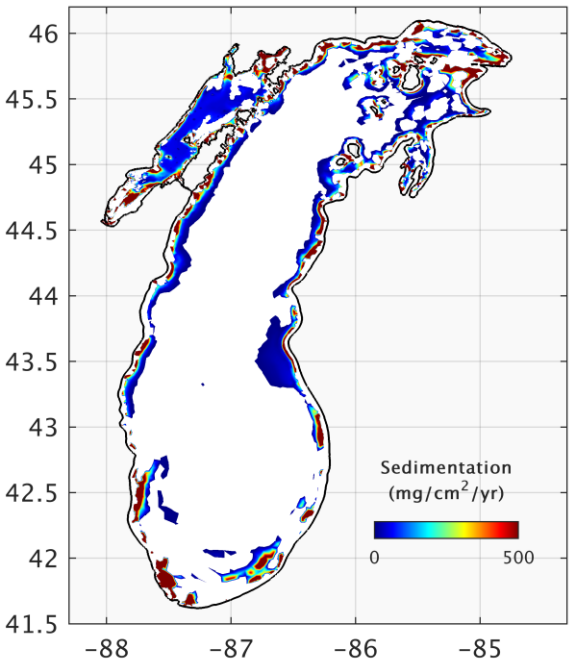

Figure 6.11. Sedimentation rates in Lake Michigan based on the six-month simulations of the May-October 2018 period. May 1st, 2018 is the baseline for calculations. White color indicates no sedimentation.

Lake Michigan sedimentation patterns, shown in Figure 6.11, are consistent with the

findings of previous research (Lee et al., 2007, Figure 13). In general sedimentation rates are higher in the boundary between deep open lake and nearshore areas and there is more sedimentation in the southern and eastern coastlines. Figure 6.12 shows sedimentation rates in Green Bay with more details. These results match fairly well with sedimentation patterns calculated based on the analysis of ^{210}Pb-dated sediment cores (Figure 4.7), in particular corresponding peaks of sedimentation in lower Green Bay and north of Chambers Island. However, the current study shows less sedimentation further north of Green Bay AOC, which could be explained by recent changes in lower bay bathymetry (dredging of navigation channel project) and construction of Cat Island. Also, the magnitude of sedimentation rates calculated based on the current model are higher than those estimated based on the biogeochemical methods.

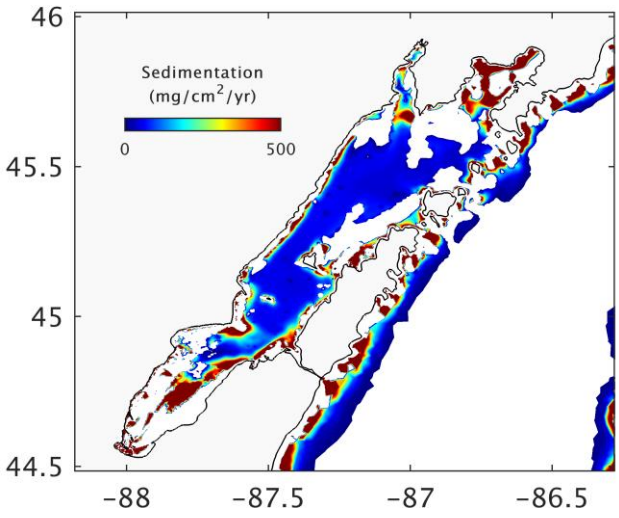

Figure 6.12. Sedimentation rates in Green Bay based on the six-month simulations of the May-October 2018 period. May 1st, 2018 is the baseline for calculations. White color indicates no sedimentation.

Figure 6.12 also suggests that the mouth of Sturgeon Bay and Peshtigo Point are other areas of high deposition in lower Green Bay and should be given consideration in

research focused on sedimentation in lower Green Bay. Another interesting observation is the agreement between spatial distribution of major deposition zones and areas of sedimentation shown in this dissertation and some of the patterns found for biogeochemical activities in the lower bay such as areas of high oxygen demand in lower Green Bay (Figure 1.3), Qualls et al.'s (2007) lower Green Bay classification based on the trophic conditions, and Bartlett et al.'s (2018) inverse relationship between distance from mouth of Fox River and availability of toxins in the lower Green Bay.

6.4. Green Bay Sediment Budget Analysis

One of the main applications of the Green Bay 3D sediment transport model is to establish sediment budgets for the bay. Major components of a sediment budget are river loading (i.e., Fox and Menominee Rivers in the case of the current study), changes in the bed layer including erosion and deposition events, and sediment flux into and out of the control volume. Cross-section A-A’ across the Chambers Island and C-C’ across the exchange zone with Lake Michigan in Figure 5.21 were considered to establish the sediment budgets for lower Green Bay and the entire bay, respectively. Sections 6.4.1 and 6.4.2 provide results of such analysis.

6.4.1. Sediment Fluxes across the Chambers Island Passage Zones

Green Bay is divided into lower- and upper Green Bay across Chambers Island. Therefore, the flux of sediment at that location determines the sediment budget for lower Green Bay. Figure 6.13 shows the monthly average patterns of TSS flux into and out of lower Green Bay through the eastern and western channels located on the sides of Chambers Island. In this dissertation, positive flux is defined as TSS flux into the control volume and vice versa.

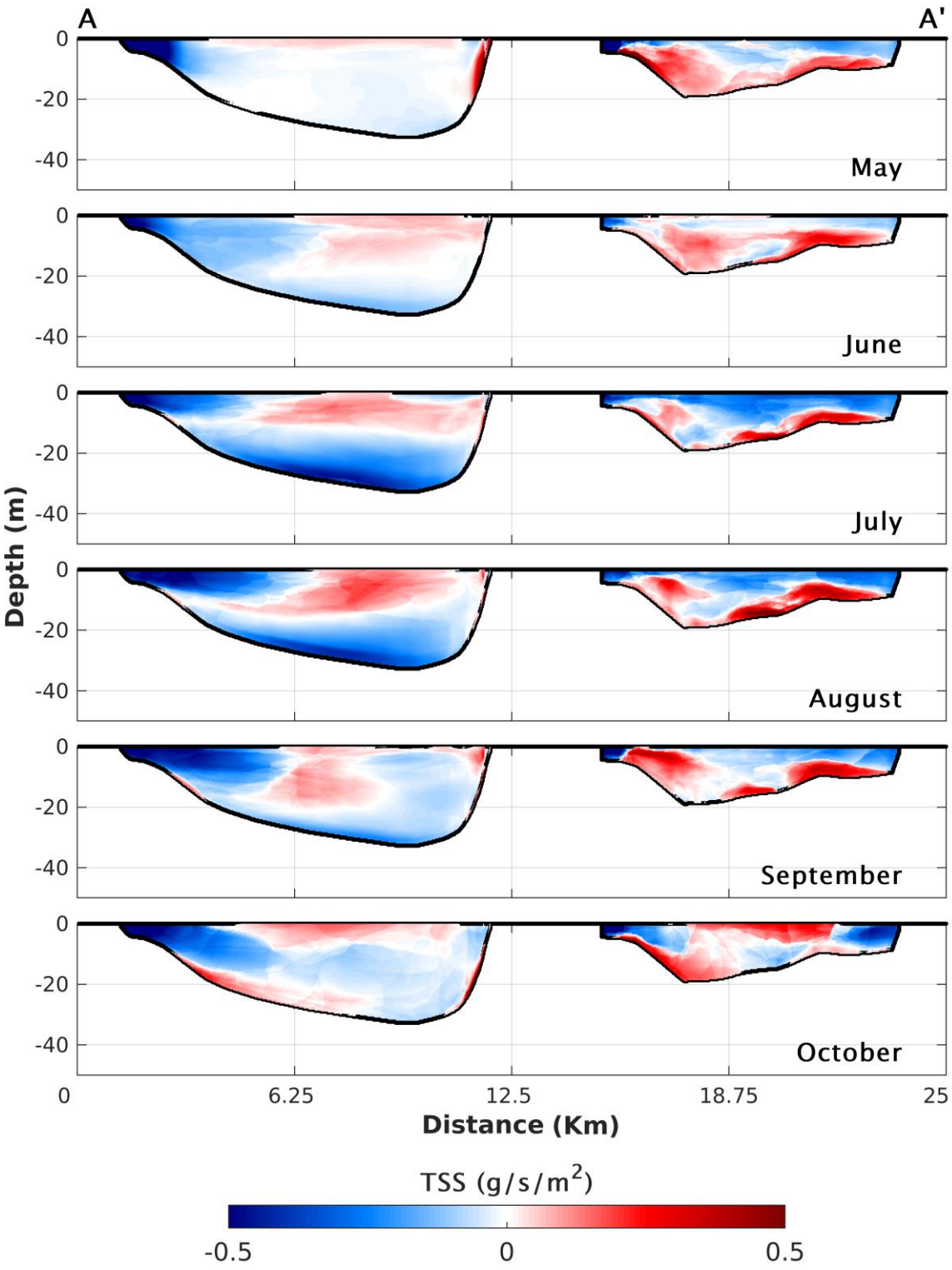

Figure 6.13. Monthly average total suspended solids (TSS) flux through cross-section A-A' across the Chambers Island during the May-October 2018. Blue and red colors indicate negative and positive fluxes of sediment out and into lower Green Bay, respectively.

As shown in the figure, both channels display a non-uniform regime of negative or positive flux. In general, the model predicted more negative flux through the western channel and more positive flux through the eastern channel. Currents are stronger and northward in the Green Bay western nearshore zone (as shown in Figures 5.17 and 5.18) which contributes to a negative and uniform TSS flux out of the lower bay. The general patterns of TSS flux provide evidence of the two-layered flow at this cross-section, in particular for the eastern channel with a persistent positive southward flux into the bay near the bottom and a negative northward flux out of the bay from the surface. That also provides more evidence for the lake-water intrusion from the bottom.

Figure 6.14 shows the results of the budget analysis for volume of water (V_W) and TSS through cross-section A-A' during the May-October 2018 period. Given the physical characteristics of the Lake Michigan basin and geomorphology of the system and simple rules of gravity, one would expect a negative flux of water and TSS out of lower Green Bay and towards Lake Michigan. However, a significant positive flux of water and TSS into lower Green Bay, as mentioned above and shown in Figure 6.14, provides evidence for the existence of two-layered flows that extend as far as lower bay.

The net flux of TSS in lower Green Bay is negative; indicating a net flux of TSS out of the lower bay. However, it almost equals the river loadings, as shown in Figure 6.14 that points out to two main facts; first at least for this time of the year 2018 lower Green Bay has not been an efficient sediment trap, however, that does not necessarily contradict the argument that lower Green Bay acts as retention basin for nutrients; and second, input rivers, especially Fox River, play an important role in sediment budget, contaminant transport, availability of nutrients, and ecological functioning of the bay. Section 6.5 will

address the impacts of river loading on some of the sediment activities in lower Green Bay and TSS budget analysis.

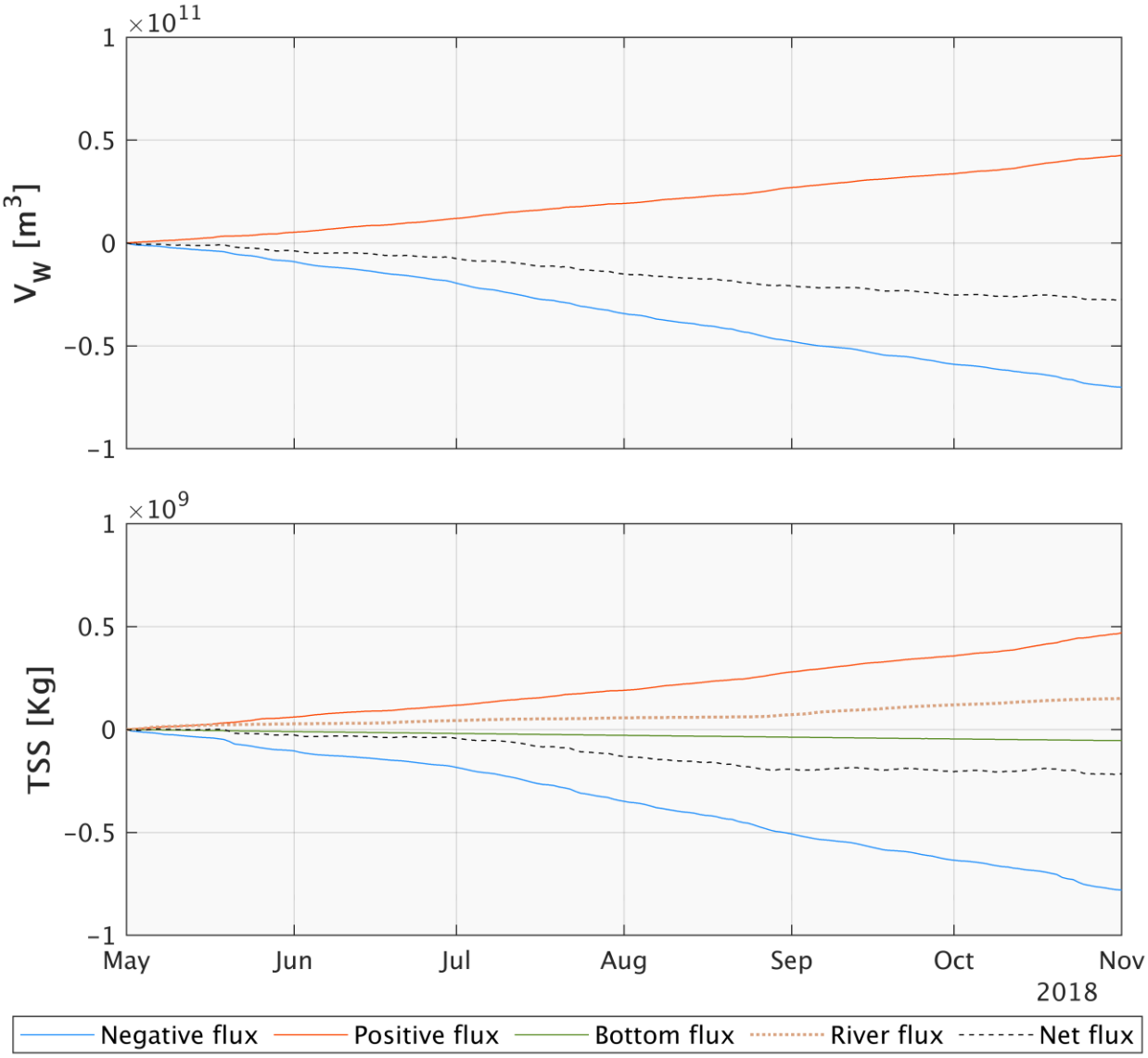

Figure 6.14. Lower Green Bay budget analysis for the volume of water (V_W) and total suspended solids (TSS) based on the May-October 2018 simulation. V_W is based on the currents only. Negative/positive flux is calculated with respect to A-A' cross-section.

Figure 6.14 shows bottom interactions, in terms of erosion and deposition activities, is not the major driver of sediment budget in the lower Green Bay, although they surely have

impacts on the water quality conditions by changing the concentration of organic particles and nutrients in the water column during a resuspension or settling event.

Hawley and Niester (1993) have found that the summertime net transport of sediment out of lower Green Bay is little and is not higher than tributary loadings. These findings are relatively consistent with the results presented in this section. However, the uniform assumption of transport in east and west channels in Hawley and Niester's study might have led to an oversimplification of water and sediment movement in this cross-section. The current 3D sediment transport model provided more realistic and detailed information of the transport from lower Green Bay and as evidenced by Figure 6.13, a two-layered flow considerably affects the net transport regime in both side channels. Klump et al. (1997), have found a greater northward transport from a geochemical budget standpoint, that is more consistent with findings of the current 3D model.

6.4.2. Sediment Fluxes across the Green Bay-Lake Michigan Exchange Zone

Although most of the sediment dynamics in Green Bay is limited to lower Green Bay, it is important to understand the sediment interactions between Green Bay and Lake Michigan. For that purpose, it is necessary to investigate the sediment budget of the entire Green Bay and fluxes through cross-section C-C' (see Figure 5.21), i.e., passage zones between the bay and main body of Lake Michigan. Figure 6.15 shows the average monthly TSS flux regimes through that cross-section and during the May-October 2018 period. It is not surprising that there is a net negative TSS flux out of the bay at this location, yet there is a significant influx towards Green Bay, in particular during the May-July period.

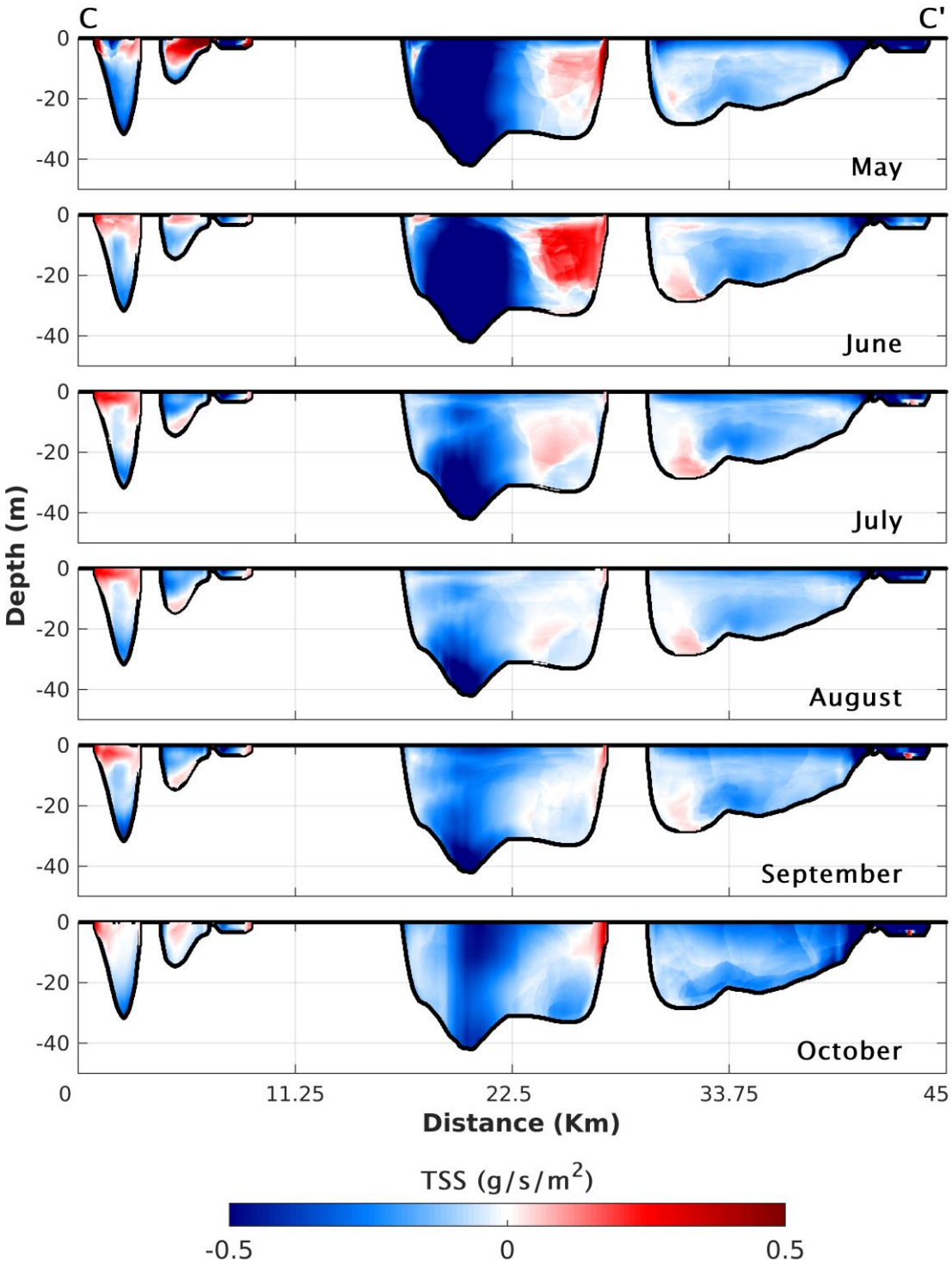

Figure 6.15. Monthly average total suspended solids (TSS) flux through cross-section C-C' across the Green Bay-Lake Michigan exchange zone during May-October 2018. Blue and red colors indicate negative and positive fluxes of sediment out and into Green Bay, respectively.

Figure 6.16 shows budget analysis estimations for V_W and TSS through cross-section C-C' during the May-October 2018 period. In general, results of budget calculations are consistent with those of lower Green Bay in terms of the net budget direction, i.e., V_W and TSS net fluxes are still negative and there are more outputs from the bay.

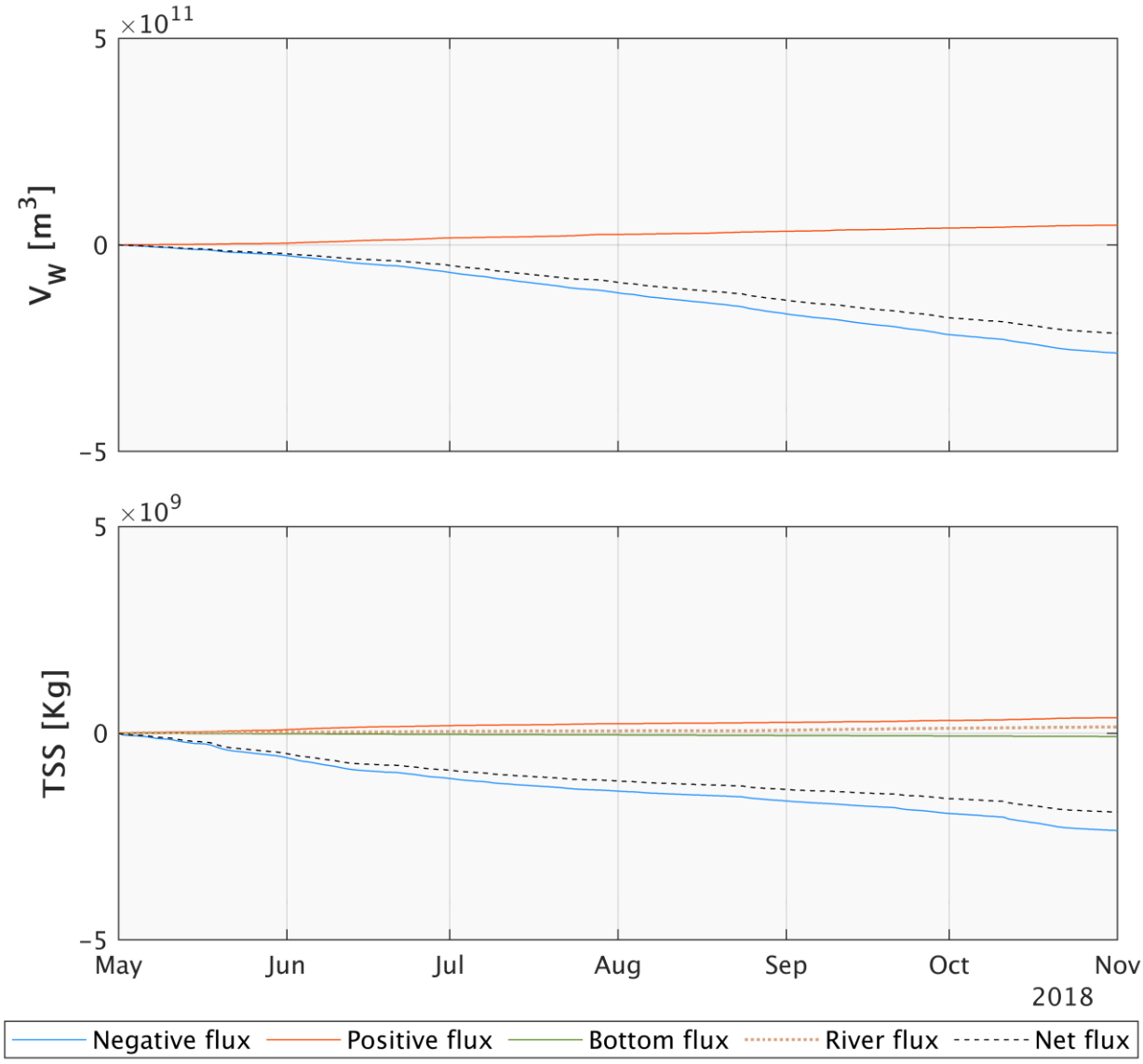

Figure 6.16. Green Bay budget analysis for the volume of water (V_W) and total suspended solids (TSS) based on the May-October 2018 simulation. V_W is based on the currents only. Negative/positive flux is calculated with respect to C-C' cross-section.

There is a significant difference in the balance between positive and negative fluxes here comparing to lower Green Bay and output flux governs the TSS budget of the bay. It can be implied from the difference between the budget patterns of the lower Green Bay and the whole bay, that those particles being introduced to upper Green Bay are very likely to leave the bay and end up in Lake Michigan. Therefore, the probability that a particle in the lower bay will be transported out of Green Bay depends on the likeness of that particle escaping lower Green Bay and reaching the area of exchange with Lake Michigan. These findings are in agreement with Bravo et al.'s (2019b) spatial distribution of residence times in lower Green Bay. They found that a significant number of particles released by Fox River into the bay remain in lower Green Bay after 120 days.

6.5. Green Bay Sediment Dynamics under Different Loading Scenarios

This section investigates the sensitivity of sediment transport to riverine loading rates by reducing the river TSS loadings by 50%. In that regard, TSS estimates from inflowing rivers were divided into half for the 2018 simulation. Figure 6.17 provides the monthly depth-averaged TSS estimates for the half loading scenario in 2018. Comparing this figure with Figure 6.5 does not show a significant difference in upper Green Bay, indicating that the Fox River load is not immediately transported to the upper Green Bay and affect the sediment interaction in the northern bay. However, the zone near the mouth of Fox River, Green Bay AOC, and the area south of Cat Island have been significantly impacted by reducing the loads. That impact is greater during the months of May-September with moderate currents and waves. In October, with strong wave dynamics, the area of impact is shrunk down, yet still, Green Bay AOC is simulated with much lower TSS concentrations.

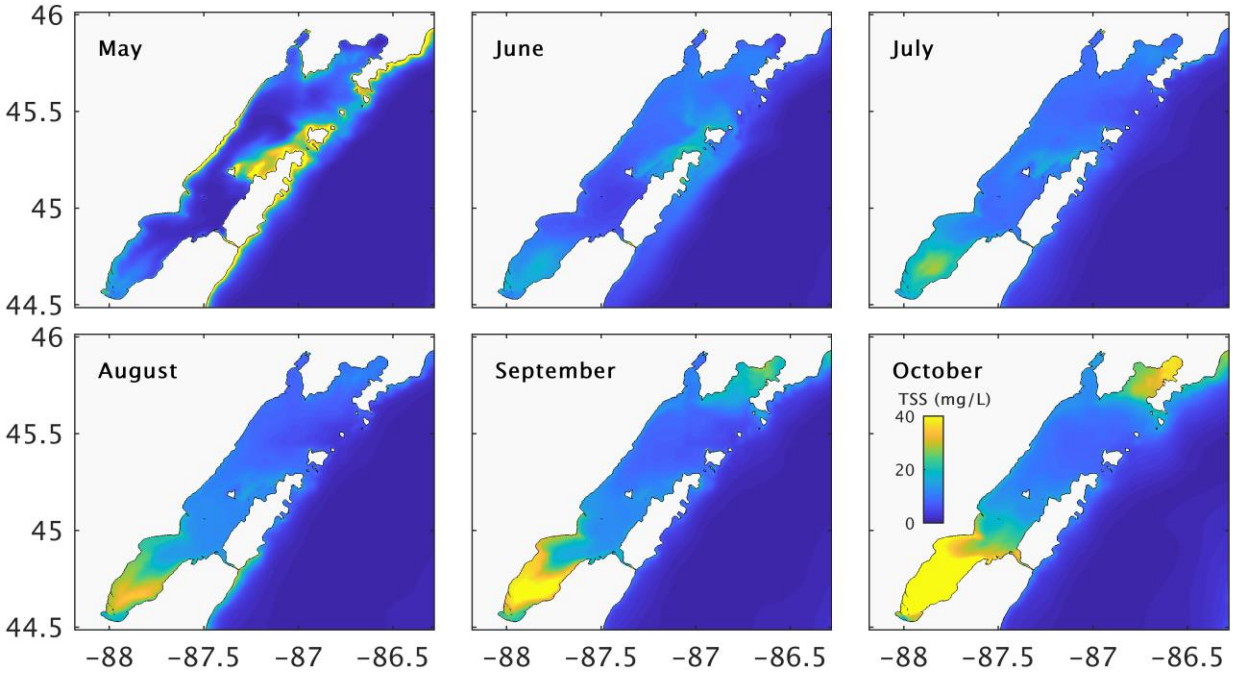

Figure 6.17. Monthly depth-averaged total suspended solids concentration (TSS) in Green Bay during the May-October 2018 under the half loading scenario

Figure 6.18 shows the monthly averaged profiles of TSS variations in the water column and along the B-B' cross-section. Similar to Figure 6.17, the area near the mouth of Fox River (point B) was impacted the most by reduced loadings, in particular during the May-September period.

Figures 6.17 and 6.18 show that change in loading rates affects the sediment availability/transport in a large area, which in turn further influences the erosion, deposition, and sedimentation rates in lower Green Bay. Figures 6.19 and 6.20 illustrate the erosion/deposition and sedimentation patterns in Green Bay and Cat Island predicted for the reduced loading rates. Comparison of Figures 6.19 and 6.10 shows a significant change in depositional patterns of Green Bay AOC and in the area south of Cat Island, in particular reduced loading has decreased deposition significantly.

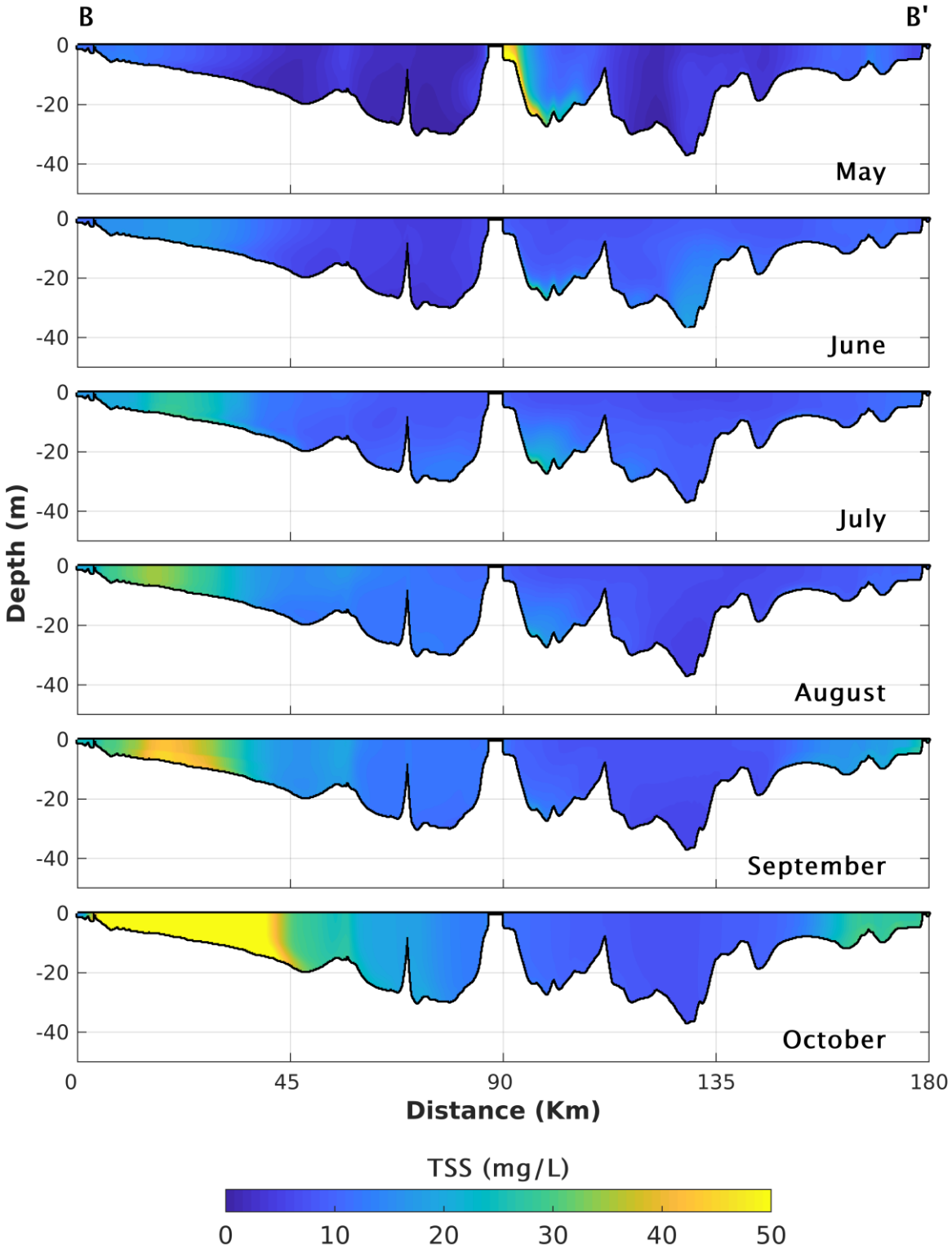

Figure 6.18. Monthly average profiles of total suspended solids (TSS) along the B-B' cross-section in Green Bay during the period of May-October 2018 period under the half loading scenario. Distances are measured from point B at the mouth of the Fox River.

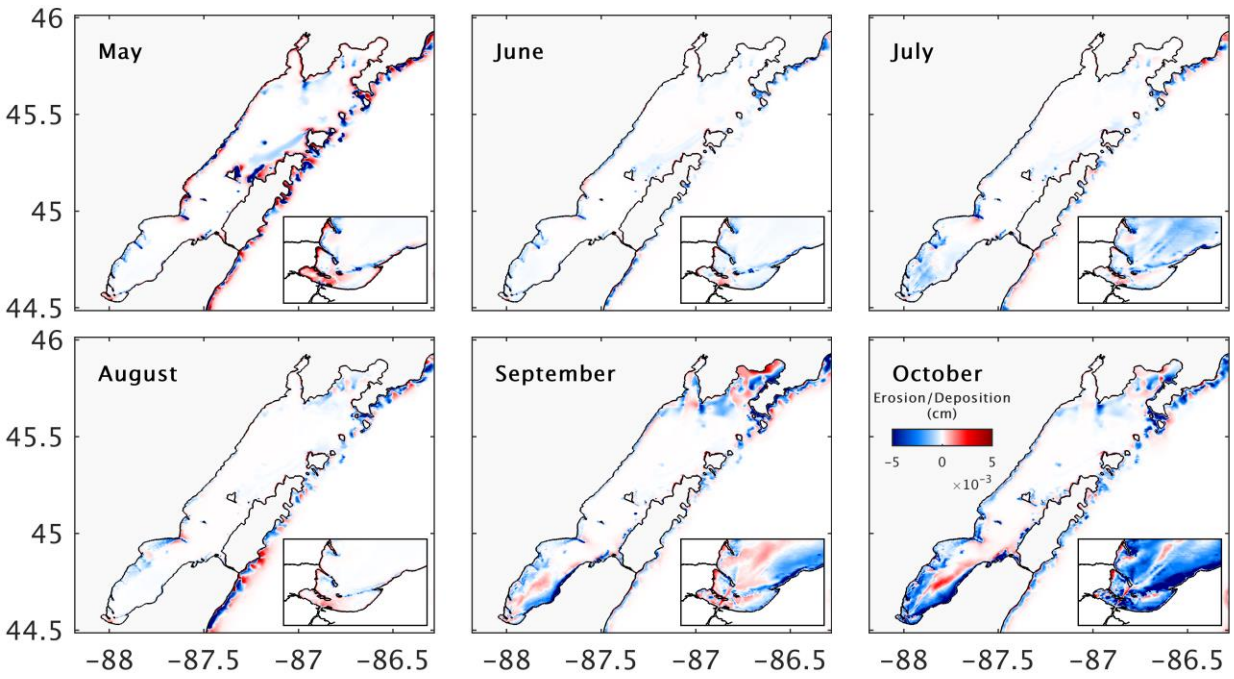

Figure 6.19. Monthly average erosion and deposition at the bottom of Green Bay during the May-October 2018 period under the half loading scenario. Blue and red colors indicate erosion and deposition, respectively. Bottom right insets in each month show the erosion and deposition in the Green Bay AOC.

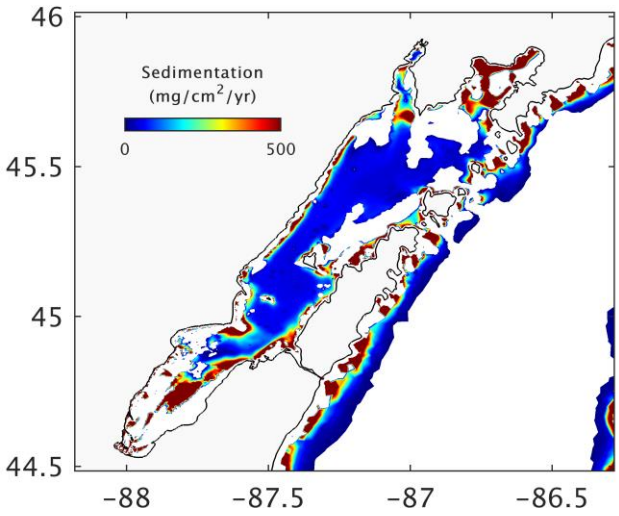

Figure 6.20. Sedimentation rates in Green Bay based on the six-month simulations of May-October 2018 period under the half loading scenario. May 1st, 2018 is the baseline for calculations. White color indicates no sedimentation.

Consistent with the change in deposition patterns, Figure 6.20 shows, in comparison with Figure 6.12 that sedimentation has also significantly decreased in the southern Green Bay near the mouth of the Fox River. These findings can improve our understanding of the immediate impacts of outflow and TMDL regulations, watershed management, and environmental/ecological flows assessment on Fox River and Green Bay AOC restoration plans.

Chapter 7:
Discussion and Conclusions

A well-calibrated and verified physically-based sediment transport model, coupled in the future with biogeochemical interactions, could have several useful applications for the management of the Green Bay system, including:

1. Explaining patterns and rates of sediment dynamics, including deposition, burial, resuspension and water clarity under different loading scenarios

2. Predicting the short- and long-term effects of the restoration plans

3. Providing simulations and early warning forecasts of the potential fate and tracking of contamination or material following a spill, accidental or deliberate discharges, or a lost object

4. Linking riverine loading and TMDL targets, and their impact on the bay

5. Modeling the sediment oxygen demand which will help better understanding the

formation and persistence of hypoxic dead zones

6. Improving nutrient transport and budget analysis in the system in terms of nutrient-sediment interactions once coupled with biogeochemical models

7. Anticipating the impacts of climate change, including the projections for warmer and wetter conditions, the increased frequency of intense precipitation events, and the loss of ice cover

8. Studying the transport and fate of contaminated sediments in the future

Several steps were taken in the current study in order to achieve the primary goals of the sediment transport model development. First, a new grid that has a fine resolution in Green Bay and includes some of the recent features of the system geometry such as Cat Islands and updated bathymetry based on the dredging channel project were created. A hydrodynamic model driven by the interpolated external forcing and coupled with the wave model for wave-current interactions was developed. The model includes the Fox and Menominee Rivers, as the main input tributaries to Green Bay.

Sediment transport was simulated using the coupled hydrodynamic and wave models. Other steps specific for the sediment transport model included estimation of sediment loadings by major input tributaries and determination of existing sediment types/classes in the bay, estimation of their erosion and deposition characteristics, and estimation of the spatial distribution of those sediment classes in the study area. The model was then calibrated by adjusting the related parameters, such as the sediment erosion rates and the portion of bed materials at the start of simulations.

Although the main focus of the current modeling platform is not to produce the

temperature fields for Green Bay, the simulations of temperature were not as good as those of currents. That can be a caveat in modeling biogeochemical interactions near the bottom such as hypoxia and algal blooms. However, that is a known problem for hydrodynamic models of shallow and complex estuarine systems such as Green Bay. There are other alternatives that can be taken into consideration in order to improve this feature of the model. Recent advancements in simulations of flow field based on machine learning techniques could be one of those alternatives, although that requires intensive observational data with reasonable seasonal and spatial variability. Any possible recent changes to the bathymetry of Green Bay, in particular near the area of exchange with Lake Michigan, could affect the physical circulation and lake water intrusion into the bay. An updated bathymetry of Green Bay could provide more realistic physical conditions for simulations of the hydrodynamics and make the lake water intrusion possible. Implementing data assimilation techniques, using other forcing models or datasets, and employment of other turbulent schemes could be other solutions to this obstacle.

The sediment transport model has produced promising results, given the complexity of the system, limited information about sediment distribution and characteristics in Green Bay and Lake Michigan, and uncertainties associated with the development of 3D sediment transport models. Future fieldwork can improve the performance of the current sediment transport model by providing more details and updated information about the characteristics of the bed sediment conditions, which are crucial in the assignment of sediment classes for the model initial conditions. Bathymetry data plays an important role in simulations of sediment dynamics and hydrodynamics of the system. Observations of sediment concentrations in different locations of the bay are another important

requirement for model development, calibration, and validation.

The model was run for two years, 2018 and 2019, in this study because of limited field data available for model validation. Results of the current model can help to improve understandings of the patterns and rates of sedimentation by running the model for several years, keeping track of bottom elevations, and comparing the modeled sedimentation rates with those estimated by other studies (e.g., Klump et al., 1997). In addition, the model can be used to explain patterns of resuspension by simulation of storm events and compare the calculated suspended sediment concentrations with existing measurements. The model was run to investigate the effects of one assumed reduced tributary loading. The model can also be used to evaluate sediment dynamics in the bay under different loading scenarios for river/watershed management and flow/TMDL regulation purposes. Another application of the model can be the evaluation of the Cat Island restoration by running the model with and without the restored Cat Islands and investigation of the effect of the restoration on the flow fields and sediment transport patterns under the two conditions.

This computer model investigation can be used to contribute to the design of future data collections and monitoring programs. In particular, modeling results can be used to recommend the locations appropriate for future fieldwork, including the collection of samples of bottom sediments, measuring currents, waves, and suspended sediment concentration during the summer season. Some specific areas of interest for that purpose would be connecting straits, east and west channels across the Chambers Island, and south of Cat Island, in which irregular patterns of sediment dynamics are observed. Updated characterization of bottom sediments is very important for reliable modeling.

Bottom sediment samples should be collected and used to determine sediment type (cohesive or non-cohesive), sediment class sizes, settling velocity, critical stress for resuspension, and erosion rates. Future deployments should be designed to capture sediment concentration during resuspension events, using the field data to calibrate the computer model.

REFERENCES

Anderson, E.J., Phanikumar, M.S., 2011. Surface storage dynamics in large rivers: Comparing three-dimensional particle transport, one-dimensional fractional derivative, and multirate transient storage models. Water Resour. Res. 47. https://doi.org/10.1029/2010WR010228

Anderson, E.J., Schwab, D.J., 2013. Predicting the oscillating bi-directional exchange flow in the Straits of Mackinac. J. Great Lakes Res. 39, 663–671. https://doi.org/10.1016/j.jglr.2013.09.001

Anderson, E.J., Schwab, D.J., 2011. Relationships between wind-driven and hydraulic flow in Lake St. Clair and the St. Clair River Delta. J. Great Lakes Res. 37, 147–158. https://doi.org/10.1016/J.JGLR.2010.11.007

Anderson, E.J., Schwab, D.J., Lang, G.A., 2010. Real-Time Hydraulic and Hydrodynamic Model of the St. Clair River, Lake St. Clair, Detroit River System. J. Hydraul. Eng. 136, 507–518. https://doi.org/10.1061/(ASCE)HY.1943-7900.0000203

AQUAVEO, 2018. SMS 13.0 Beta - The Complete Surface-water Solution | Aquaveo.com [WWW Document]. URL https://www.aquaveo.com/software/sms-surface-water-modeling-system-introduction (accessed 12.24.18).

Ariathurai, R., Arulanandan, K., 1978. Erosion Rates of Cohesive Soils. J Hydr Div, ASCE 101, 635–639.

Bai, X., Wang, J., Schwab, D.J., Yang, Y., Luo, L., Leshkevich, G.A., Liu, S., 2013. Modeling 1993–2008 climatology of seasonal general circulation and thermal structure in the Great Lakes using FVCOM. Ocean Model. 65, 40–63. https://doi.org/10.1016/J.OCEMOD.2013.02.003

Bartlett, S.L., Brunner, S.L., Klump, J.V., Houghton, E.M., Miller, T.R., 2018. Spatial analysis of toxic or otherwise bioactive cyanobacterial peptides in Green Bay, Lake Michigan. J. Great Lakes Res. 44, 924–933. https://doi.org/10.1016/J.JGLR.2018.08.016

Beletsky, D., Schwab, D., 2008. Climatological circulation in Lake Michigan. Geophys. Res. Lett. 35, L21604. https://doi.org/10.1029/2008GL035773

Beletsky, D., Schwab, D., McCormick, M., 2006a. Modeling the 1998–2003 summer circulation and thermal structure in Lake Michigan. J. Geophys. Res. 111, C10010. https://doi.org/10.1029/2005JC003222

Beletsky, D., Schwab, D., McCormick, M., 2006b. Modeling the 1998-2003 summer circulation and thermal structure in Lake Michigan. J. Geophys. Res. Ocean. 111, 1–18. https://doi.org/10.1029/2005JC003222

Beletsky, D., Schwab, D.J., 2001. Modeling circulation and thermal structure in Lake Michigan: Annual cycle and interannual variability. J. Geophys. Res. Ocean. 106, 19745–19771. https://doi.org/10.1029/2000JC000691

Beletsky, D., Schwab, D.J., Roebber, P.J., McCormick, M.J., Miller, G.S., Saylor, J.H.,

2003. Modeling wind-driven circulation during the March 1998 sediment resuspension event in Lake Michigan. J. Geophys. Res. Ocean. 108, n/a-n/a. https://doi.org/10.1029/2001JC001159

Beversdorf, L.J., Rude, K., Weirich, C.A., Bartlett, S.L., Seaman, M., Kozik, C., Biese, P., Gosz, T., Suha, M., Stempa, C., Shaw, C., Hedman, C., Piatt, J.J., Miller, T.R., 2018. Analysis of cyanobacterial metabolites in surface and raw drinking waters reveals more than microcystin. Water Res. 140, 280–290. https://doi.org/10.1016/J.WATRES.2018.04.032

Blumberg, A.F., Mellor, G.L., 1987. A description of a three-dimensional coastal ocean circulation model. American Geophysical Union (AGU), pp. 1–16. https://doi.org/10.1029/CO004p0001

Booij, N., Haagsma, I.J.G., Holthuijsen, L.H., Kieftenburg, A.T.M.M., Ris, R.C., van der Westhuysen, A.J., Zijlema, M., 2004. SWAN Cycle III version 40.51 Technical documentation. Delft, The Netherlands.

Booij, N., Ris, R.C., Holthuijsen, L.H., 1999. A third-generation wave model for coastal regions: 1. Model description and validation. J. Geophys. Res. Ocean. 104, 7649–7666. https://doi.org/10.1029/98JC02622

Bootsma, H. a, 2009. Causes, Consequences, and Management of Nuisance Cladophora. Report Submitted to the Environmental Protection Agency Great Lakes National Program Office, Project GL-00E06901. Chicago, Illinois.

Bravo, H.R., Bootsma, H., Khazaei, B., 2019a. Fate of phosphorus from a point source in the Lake Michigan nearshore zone. J. Great Lakes Res. 45, 1182–1196. https://doi.org/10.1016/j.jglr.2019.09.007

Bravo, H.R., Bootsma, H.A., Khazaei, B., 2017. Modeling the Transport and Fate of Phosphorus from a Point Source in the Lake Michigan Nearshore Zone, in: 37th International Association of Hydraulic Research World Congress. Kuala Lumpur, Malaysia.

Bravo, H.R., Hamidi, S.A., Anderson, E.J., Klump, J. V., Khazaei, B., 2019b. Timescales of Transport Through Lower Green Bay. J. Great Lakes Res.

Bravo, H.R., Hamidi, S.A., Klump, J.V., Waples, J.T., 2015. Currents and heat fluxes induce stratification leading to hypoxia in Green Bay, Lake Michigan. E-proceedings 36th IAHR World Congr. 1–10.

Brazner, J.C., 1997. Regional, Habitat, and Human Development Influences on Coastal Wetland and Beach Fish Assemblages in Green Bay, Lake Michigan. J. Great Lakes Res. 23, 36–51. https://doi.org/10.1016/S0380-1330(97)70883-9

Brown County, 2018. Cat Island Restoration Project — Port of Green Bay [WWW Document]. URL https://www.portofgreenbay.com/cat-island-restoration-project/ (accessed 10.12.18).

Burban, P.-Y., Xu, Y.-J., McNeil, J., Lick, W., 1990. Settling speeds of floes in fresh water and seawater. J. Geophys. Res. 95, 18213. https://doi.org/10.1029/JC095iC10p18213

Chen, C., Beardsley, R.C., Cowles, G., Qi, J., Lai, Z., Gao, G., Stuebe, D., Liu, H., Xu, Q., Xue, P., Ge, J., Hu, S., Ji, R., Tian, R., Huang, H., Wu, L., Lin, H., Sun, Y., Zhao, L., 2013. An Unstructured Grid , Finite-Volume Community Ocean Model FVCOM User Manual.

Chen, C., Huang, H., Beardsley, R.C., Liu, H., Xu, Q., Cowles, G., 2007. A finite volume numerical approach for coastal ocean circulation studies: Comparisons with finite difference models. J. Geophys. Res. 112, C03018. https://doi.org/10.1029/2006JC003485

Chen, C., Liu, H., Beardsley, R.C., 2003. An unstructured grid, finite-volume, three-dimensional, primitive equations ocean model: Application to coastal ocean and estuaries. J. Atmos. Ocean. Technol. 20, 159–186. https://doi.org/10.1175/1520-0426(2003)020<0159:AUGFVT>2.0.CO;2

Chen, C., Wang, L., Ji, R., Budd, J.W., Schwab, D.J., Beletsky, D., Fahnenstiel, G.L., Vanderploeg, H., Eadie, B., Cotner, J., 2004. Impacts of suspended sediment on the ecosystem in Lake Michigan: A comparison between the 1998 and 1999 plume events. J. Geophys. Res. 109, C10S05. https://doi.org/10.1029/2002JC001687

Chen, T., Zhang, Q., Wu, Y., Ji, C., Yang, J., Liu, G., 2018. Development of a wave-current model through coupling of FVCOM and SWAN. Ocean Eng. 164, 443–454. https://doi.org/10.1016/J.OCEANENG.2018.06.062

Christensen, E.R., Chien, N.-K., 1981. Fluxes of arsenic, lead, zinc, and cadmium to Green Bay and Lake Michigan sediments. Environ. Sci. Technol. 15, 553–558. https://doi.org/10.1021/es00087a004

Cowles, G.W., 2008. Parallelization of the Fvcom Coastal Ocean Model. Int. J. High Perform. Comput. Appl. 22, 177–193. https://doi.org/10.1177/1094342007083804

DeVilbiss, S.E., Zhou, Z., Klump, J.V., Guo, L., 2016. Spatiotemporal variations in the abundance and composition of bulk and chromophoric dissolved organic matter in seasonally hypoxia-influenced Green Bay, Lake Michigan, USA. Sci. Total Environ. 565, 742–757. https://doi.org/10.1016/J.SCITOTENV.2016.05.015

Eadie, B.J., Bell, G.L., Hawley, N., 1991. Sediment Trap Study in the Green Bay Mass Balance Program: Mass and Organic Carbon Fluxes, Resuspension, and Particle Settling Velocities. NOAA Technical Memorandum ERL GLERL-75. Great Lakes Environmental Research Laboratory Ann Arbor, Michigan July 1991.

Fillingham, J., 2015. Modeling Lake Michigan Nearshore Carbon and Phosphorus Dynamics. Theses Diss. University of Wisconsin-Milwaukee.

Galperin, B., Kantha, L.H., Hassid, S., Rosati, A., Galperin, B., Kantha, L.H., Hassid, S., Rosati, A., 1988. A Quasi-equilibrium Turbulent Energy Model for Geophysical Flows. J. Atmos. Sci. 45, 55–62. https://doi.org/10.1175/1520-0469(1988)045<0055:AQETEM>2.0.CO;2

García, M.H., 2008. Sediment Transport and Morphodynamics, in: García, M.H. (Ed.), Sedimentation Engineering: Processes, Measurements, Modeling, and Practice. American Society of Civil Engineers, Reston, VA, pp. 21–163. https://doi.org/10.1061/9780784408148.ch02

Groff, C.M., Kaster, J.L., 2017. Survival, growth, and production of Hexagenia bilineata mayflies in fluidized sediment from lower Green Bay, Lake Michigan. J. Great Lakes Res. 43, 102–107. https://doi.org/10.1016/J.JGLR.2016.10.008

Gronewold, a D., Anderson, E.J., Lofgren, B., Blanken, P.D., Wang, J., Smith, J., Hunter, T., 2015. Impacts of extreme 2013 – 2014 winter conditions on Lake Michigan ' s fall heat content , surface temperature ,. Geophys. Res. Lett. 3364–3370. https://doi.org/10.1002/2015GL063799.Received

Grunert, B.K., Brunner, S.L., Hamidi, S.A., Bravo, H.R., Klump, J.V., 2018. Quantifying the influence of cold water intrusions in a shallow, coastal system across contrasting years: Green Bay, Lake Michigan. J. Great Lakes Res. 44, 851–863. https://doi.org/10.1016/J.JGLR.2018.07.009

Guerra, M., Cienfuegos, R., Thomson, J., Suarez, L., 2017. Tidal energy resource characterization in Chacao Channel, Chile. Int. J. Mar. Energy 20, 1–16. https://doi.org/10.1016/J.IJOME.2017.11.002

Hamidi, S.A., Bravo, H.R., Klump, J.V., 2013. Evidence of Multiple Physical Drivers on the Circulation and Thermal Regime in the Green Bay of Lake Michigan, in: World Environmental and Water Resources Congress 2013. American Society of Civil Engineers, Reston, VA, pp. 1719–1726. https://doi.org/10.1061/9780784412947.169

Hamidi, S.A., Bravo, H.R., Val Klump, J., Waples, J.T., 2015. The role of circulation and heat fluxes in the formation of stratification leading to hypoxia in Green Bay, Lake Michigan. J. Great Lakes Res. 41, 1024–1036. https://doi.org/10.1016/j.jglr.2015.08.007

Hamidi, S.A., Hosseiny, H., Ekhtari, N., Khazaei, B., 2017. Using MODIS remote sensing data for mapping the spatio-temporal variability of water quality and river turbid plume. J. Coast. Conserv. 21, 939–950. https://doi.org/10.1007/s11852-017-0564-y

Harris, C.K., Wiberg, P.L., 2001. A two-dimensional, time-dependent model of suspended sediment transport and bed reworking for continental shelves. Comput. Geosci. 27, 675–690. https://doi.org/10.1016/S0098-3004(00)00122-9

Harris, V.A., Christie, J., 1987. The lower Green Bay Remedial Action Plan: nutrient and eutrophication management. Technical Advisory Committee report. Publication No. WR-167-87. Wisconsin Department of Natural Resources. Madison, WI.

Hawley, N., Lesht, B.M., Schwab, D.J., 2004. A comparison of observed and modeled surface waves in southern Lake Michigan and the implications for models of sediment resuspension. J. Geophys. Res. 109, C10S03. https://doi.org/10.1029/2002JC001592

Hawley, N., Niester, J., 1993. Measurement of Horizontal Sediment Transport in Green Bay, May-October, 1989. J. Great Lakes Res. 19, 368–378. https://doi.org/10.1016/S0380-1330(93)71225-3

Hecky, R.E., Smith, R.E., Barton, D.R., Guildford, S.J., Taylor, W.D., Charlton, M.N., Howell, T., 2004. The nearshore phosphorus shunt: a consequence of ecosystem engineering by dreissenids in the Laurentian Great Lakes. Can. J. Fish. Aquat. Sci. 61, 1285–1293. https://doi.org/10.1139/f04-065

Hermanson, M.H., Christensen, E.R., Buser, D.J., Chen, L.-M., 1991. Polychlorinated Biphenyls in Dated Sediment Cores from Green Bay and Lake Michigan. J. Great Lakes Res. 17, 94–108. https://doi.org/10.1016/S0380-1330(91)71345-2

Huang, H., Chen, C., Cowles, G.W., Winant, C.D., Beardsley, R.C., Hedstrom, K.S., Haidvogel, D.B., 2008. FVCOM validation experiments: Comparisons with ROMS for three idealized barotropic test problems. J. Geophys. Res. 113, C07042. https://doi.org/10.1029/2007JC004557

HydroQual Inc., 1999. Hydrodynamics, Sediment Transport, and Sorbent Dynamics in Green Bay. Report to Wisconsin Department of Natural Resources, Madison, Wisconsin.

Jones, C.A., 2000. An Accurate Model of Sediment Transport. University of California, Santa Barbara.

Kaster, J.L., Groff, C.M., Klump, J.V., Rupp, D.L., Iyer, S., Hansen, A., Barbour, S., Hall, L., 2018. Evaluation of lower Green Bay benthic fauna with emphasis on re-ecesis of Hexagenia mayfly nymphs. J. Great Lakes Res. 44, 895–909. https://doi.org/10.1016/J.JGLR.2018.06.006

Khazaei, B., Hamidi, S.A., Houghton, S., Bartlett, S., Bravo, H.R., 2018a. On the Relation between Sediment Concentration and Water Quality Parameters in the Green Bay of Lake Michigan, in: ASLO 2018 Summer Meeting. Victoria, Canada, 10-15 Jun.

Khazaei, B., Hamidi, S.A., Nabizadeh, A., 2018b. An Empirical Approach to Estimate Total Suspended Sediment using Observational Data in Fox River and Southern Green Bay, WI, in: World Environmental and Water Resources Congress. Minneapolis, MN, USA.

Khazaei, B., Wu, C., 2018. Estimation of Vegetation Coverage Based on Seasonal Variabilities in MODIS-Based Vegetation Indices, in: World Environmental and Water Resources Congress 2018. American Society of Civil Engineers, Reston, VA, pp. 11–20. https://doi.org/10.1061/9780784481400.002

Klump, J.V., 2019. Lab analysis of the Green Bay Sediment Samples. University of Wisconsin-Milwaukee, Unpublished data.

Klump, J.V., Brunner, S.L., Grunert, B.K., Kaster, J.L., Weckerly, K., Houghton, E.M., Kennedy, J.A., Valenta, T.J., 2018. Evidence of persistent, recurring summertime hypoxia in Green Bay, Lake Michigan. J. Great Lakes Res. 44, 841–850. https://doi.org/10.1016/J.JGLR.2018.07.012

Klump, J.V., Edgington, D.N., Sager, P.E., Robertson, D.M., 1997. Sedimentary phosphorus cycling and a phosphorus mass balance for the Green Bay (Lake Michigan) ecosystem. Can. J. Fish. Aquat. Sci. 54, 10–26. https://doi.org/10.1139/cjfas-54-1-10

Klump, J.V., Fitzgerald, S.A., Waplesa, J.T., 2009. Benthic biogeochemical cycling, nutrient stoichiometry, and carbon and nitrogen mass balances in a eutrophic freshwater bay. Limnol. Oceanogr. 54, 692–712. https://doi.org/10.4319/lo.2009.54.3.0692

Klump, V., Vimont, D., Fermanich, K., Kennedy, J., Richmond, N., 2017. Green Bay Hypoxia: Biogeochemical Dynamics, Watershed Inputs and Climate Change. Milwaukee, Wisconsin. Grant#NA10NOS4780139.

Kordijazi, A., Silva, M., 2018. Advancing Systematic and Fundamental Changes in Agricultural Water Resources Management, in: 2018 IEEE Conference on Technologies for Sustainability (SusTech). IEEE, pp. 1–2. https://doi.org/10.1109/SusTech.2018.8671352

Labuhn, S.L., 2017. Dissolved oxygen dynamics within Green Bay in an effort to understand hypoxia Table of Contents. University of Wisconsin-Milwaukee.

Lai, W., Pan, J., Devlin, A.T., 2018. Impact of tides and winds on estuarine circulation in the Pearl River Estuary. Cont. Shelf Res. 168, 68–82. https://doi.org/10.1016/J.CSR.2018.09.004

Lee, C., Schwab, D.J., Beletsky, D., Stroud, J., Lesht, B., 2007. Numerical modeling of mixed sediment resuspension, transport, and deposition during the March 1998 episodic events in southern Lake Michigan. J. Geophys. Res. Ocean. 112, 1–17. https://doi.org/10.1029/2005JC003419

Lee, C., Schwab, D.J., Hawley, N., 2005. Sensitivity analysis of sediment resuspension parameters in coastal area of southern Lake Michigan. J. Geophys. Res. C Ocean. 110, 1–16. https://doi.org/10.1029/2004JC002326

Lesser, G.R., Roelvink, J.A., van Kester, J.A.T.M., Stelling, G.S., 2004. Development and validation of a three-dimensional morphological model. Coast. Eng. 51, 883–915. https://doi.org/10.1016/j.coastaleng.2004.07.014

Li, B., Tanaka, K.R., Chen, Y., Brady, D.C., Thomas, A.C., 2017. Assessing the quality of bottom water temperatures from the Finite-Volume Community Ocean Model (FVCOM) in the Northwest Atlantic Shelf region. J. Mar. Syst. 173, 21–30. https://doi.org/10.1016/J.JMARSYS.2017.04.001

Li, J., Pan, S., Chen, Y., Fan, Y.-M., Pan, Y., 2018. Numerical estimation of extreme waves and surges over the northwest Pacific Ocean. Ocean Eng. 153, 225–241. https://doi.org/10.1016/J.OCEANENG.2018.01.076

Lick, W., Xu, Y.-J., McNeil, J., 1995. Resuspension Properties of Sediments from the Fox, Saginaw, and Buffalo Rivers. J. Great Lakes Res. 21, 257–274. https://doi.org/10.1016/S0380-1330(95)71036-X

Lin, P., Klump, J.V., Guo, L., 2018. Variations in chemical speciation and reactivity of phosphorus between suspended-particles and surface-sediment in seasonal hypoxia-influenced Green Bay. J. Great Lakes Res. https://doi.org/10.1016/j.jglr.2018.05.022

Lin, P., Klump, J.V., Guo, L., 2016. Dynamics of dissolved and particulate phosphorus influenced by seasonal hypoxia in Green Bay, Lake Michigan. Sci. Total Environ. 541, 1070–1082. https://doi.org/10.1016/J.SCITOTENV.2015.09.118

Luo, L., Wang, Jia, Schwab, David J, Vanderploeg, Henry, Leshkevich, George, Bai, Xuezhi, Hu, Haoguo, Wang, Dongxiao, Luo, C.:, Wang, J, Schwab, D J,

Vanderploeg, H, Leshkevich, G, Bai, X, Hu, H, Wang, D, 2012. Simulating the 1998 spring bloom in Lake Michigan using a coupled physical-biological model. J. Geophys. Res 117, 10011. https://doi.org/10.1029/2012JC008216

Maccoux, M.J., Dolan, D.M., Chapra, S.C., 2013. Chloride and total phosphorus budgets for Green Bay, Lake Michigan. J. Great Lakes Res. 39, 420–428. https://doi.org/10.1016/J.JGLR.2013.06.012

Macksasitorn, S., Janssen, J., Gray, K.A., 2015. PCBs refocused: Correlation of PCB concentrations in Green Bay legacy sediments with adjacent lithophilic, invasive biota. J. Great Lakes Res. 41, 215–221. https://doi.org/10.1016/J.JGLR.2014.12.021

Madsen, O.S., 1995. Spectral wave-current bottom boundary layer flows, in: Proceedings of the Coastal Engineering Conference. ASCE, pp. 384–398. https://doi.org/10.1061/9780784400890.030

Manchester-Neesvig, J.B., Andren, A.W., Edgington, D.N., 1996. Patterns of Mass Sedimentation and of Deposition of Sediment Contaminated by PCBs in Green Bay. J. Great Lakes Res. 22, 444–462. https://doi.org/10.1016/S0380-1330(96)70969-3

Mantz, P.A., 1977. Incipient transport of fine grains and flakes by fluids-extended Shields diagram. J. Hydraul. Div. 103.

Mao, M., Xia, M., 2017. Dynamics of wave–current–surge interactions in Lake Michigan: A model comparison. Ocean Model. 110, 1–20. https://doi.org/10.1016/J.OCEMOD.2016.12.007

McCormick, M.J., Meadows, G.A., 1988. An intercomparison of four mixed layer models in a shallow inland sea. J. Geophys. Res. 93, 6774. https://doi.org/10.1029/JC093iC06p06774

Mellor, G.L., Yamada, T., 1982. Development of a turbulence closure model for geophysical fluid problems. Rev. Geophys. 20, 851. https://doi.org/10.1029/RG020i004p00851

Merkle, C.A., De Stasio, B.T., 2018. Bythotrephes longimanus in shallow, nearshore waters: Interactions with Leptodora kindtii, impacts on zooplankton, and implications for secondary dispersal from southern Green Bay, Lake Michigan. J. Great Lakes Res. 44, 934–942. https://doi.org/10.1016/J.JGLR.2018.02.013

Meyer-Peter, E., Müller, R., 1948. Formulas for Bed-Load transport. IAHSR 2nd Meet. Stock. Append. 2.

Miller, G.S., Saylor, J.H., 1993. Low-Frequency Water Volume Transport Through the Midsection of Green Bay, Lake Michigan, Calculated From Current and Temperature Observations. J. Great Lakes Res. 19, 361–367. https://doi.org/10.1016/S0380-1330(93)71224-1

Miller, G.S., Saylor, J.H., 1985. Currents and Temperatures in Green Bay, Lake Michigan. J. Great Lakes Res. 11, 97–109. https://doi.org/10.1016/S0380-1330(85)71749-2

Mitchener, H., Torfs, H., 1996. Erosion of mud/sand mixtures. Coast. Eng. 29, 1–25. https://doi.org/10.1016/S0378-3839(96)00002-6

Modlin, R.F., Beeton, A.M., 1970. Dispersal of Fox River Water in Green Bay, Lake Michigan, in: Proceedings of the 13th Conference of Great Lakes Research. Buffalo, NY, pp. 468–476.

Moore, J.R., Meyer, R.P., Morgan, C.L., 1973. Investigation of the Sediments and Potential Manganese Nodule Resources of Green Bay, Wisconsin. University of Wisconsin, Sea Grant College Program. Technical Report-WIS. WISCU-T-73-001.

Moriasi, D.N., Arnold, J.G., Van Liew, M.W., Bingner, R.L., Harmel, R.D., Veith, T.L., 2007. Model evaluation guidelines for systematic quantification of accuracy in watershed simulations. Trans. ASABE.

Nash, J.E., Sutcliffe, J.V., 1970. River flow forecasting through conceptual models part I — A discussion of principles. J. Hydrol. 10, 282–290. https://doi.org/10.1016/0022-1694(70)90255-6

National Geophysical Data Centre, 2015. Bathymetric Data Viewer [WWW Document]. URL http://maps.ngdc.noaa.gov/viewers/bathymetry/ (accessed 1.1.17).

NEW Water, 2017. Aquatic Monitoring Program › NEW Water [WWW Document]. URL http://newwater.us/programs-initiatives/aquatic-monitoring-program/ (accessed 10.1.18).

NOAA, 2018a. National Centers for Environmental Information (NCEI) [WWW Document]. URL https://gis.ncdc.noaa.gov/maps/ncei/cdo/hourly (accessed 11.1.18).

NOAA, 2018b. ESRL : PSD : NCEP North American Regional Reanalysis (NARR) [WWW Document]. URL https://www.esrl.noaa.gov/psd/data/gridded/data.narr.html (accessed 12.24.18).

NOAA, 2017. Bathymetry of Lake Michigan [WWW Document]. URL https://ngdc.noaa.gov/mgg/greatlakes/michigan.html (accessed 1.1.17).

Parker, G., 2004. 1D Morphodynamics of Rivers and Turbidity Currents. Saint Anthony Falls Lab., Univ. of Minn., Minneapolis. [Available at http://hydrolab.illinois.edu/people/parkerg/morphodynamics_e-book.htm].

Qi, J., Chen, C., Beardsley, R.C., Perrie, W., Cowles, G.W., Lai, Z., 2009. An unstructured-grid finite-volume surface wave model (FVCOM-SWAVE): Implementation, validations and applications. Ocean Model. 28, 153–166. https://doi.org/10.1016/J.OCEMOD.2009.01.007

Qualls, T.M., Dolan, D.M., Reed, T., Zorn, M.E., Kennedy, J., 2007. Analysis of the Impacts of the Zebra Mussel, Dreissena polymorpha, on Nutrients, Water Clarity, and the Chlorophyll-Phosphorus Relationship in Lower Green Bay. J. Great Lakes Res. 33, 617–626. https://doi.org/10.3394/0380-1330(2007)33[617:AOTIOT]2.0.CO;2

Read, J., Klump, V., Johengen, T., Schwab, D., Paige, K., Eddy, S., Anderson, E., Manninen, C., 2010. Working in Freshwater: The Great Lakes Observing System Contributions to Regional and National Observations, Data Infrastructure, and Decision Support. Mar. Technol. Soc. J. 44, 84–98. https://doi.org/10.4031/MTSJ.44.6.12

Ris, R.C., Holthuijsen, L.H., Booij, N., 1999. A third-generation wave model for coastal regions: 2. Verification. J. Geophys. Res. Ocean. 104, 7667–7681. https://doi.org/10.1029/1998JC900123

Rowe, M.D., Anderson, E.J., Vanderploeg, H.A., Pothoven, S.A., Elgin, A.K., Wang, J., Yousef, F., 2017. Influence of invasive quagga mussels, phosphorus loads, and climate on spatial and temporal patterns of productivity in Lake Michigan: A biophysical modeling study. Limnol. Oceanogr. 62, 2629–2649. https://doi.org/10.1002/lno.10595

Rowe, M.D., Anderson, E.J., Wang, J., Vanderploeg, H.A., 2015. Modeling the effect of invasive quagga mussels on the spring phytoplankton bloom in Lake Michigan. J. Great Lakes Res. 41, 49–65. https://doi.org/10.1016/J.JGLR.2014.12.018

Safaie, A., Wendzel, A., Ge, Z., Nevers, M.B., Whitman, R.L., Corsi, S.R., Phanikumar, M.S., 2016. Comparative Evaluation of Statistical and Mechanistic Models of *Escherichia coli* at Beaches in Southern Lake Michigan. Environ. Sci. Technol. 50, 2442–2449. https://doi.org/10.1021/acs.est.5b05378

Sanford, L.P., 2008. Modeling a dynamically varying mixed sediment bed with erosion, deposition, bioturbation, consolidation, and armoring. Comput. Geosci. 34, 1263–1283. https://doi.org/10.1016/j.cageo.2008.02.011

Schwab, D., Bedford, K., 1994. Initial implementation of the Great Lakes Forecasting System: A real-time system for predicting lake circulation and thermal structure. Water Pollut. Res. J. Can 292, 203–220.

Schwab, D.J., 1983. Numerical Simulation of Low-Frequency Current Fluctuations in Lake Michigan. J. Phys. Oceanogr. 13, 2213–2224. https://doi.org/10.1175/1520-0485(1983)013<2213:NSOLFC>2.0.CO;2

Schwab, D.J., Beletsky, D., 1998. Lake Michigan Mass Balance Study: Hydrodynamic Modeling Project. ERL GLERL-108. NOAA GLERL, Ann Arbor, MI.

Schwab, D.J., Bennett, J.R., Liu, P.C., Donelan, M.A., 1984. Application of a simple numerical wave prediction model to Lake Erie. J. Geophys. Res. 89, 3586. https://doi.org/10.1029/JC089iC03p03586

Schwab, D.J., Eadie, B.J., Assel, R.A., Roebber, P.J., 2006. Climatology of Large Sediment Resuspension Events in Southern Lake Michigan. J. Great Lakes Res. 32, 50–62. https://doi.org/10.3394/0380-1330(2006)32[50:COLSRE]2.0.CO;2

Shen, C., 2016. Modeling of dreissenid mussel impacts on Lake Michigan. ProQuest Diss. Theses. University of Wisconsin-Milwaukee.

Sherwood, C.R., Aretxabaleta, A.L., Harris, C.K., Paul Rinehimer, J., Verney, R., Ferré, B., 2018. Cohesive and mixed sediment in the Regional Ocean Modeling System (ROMS v3.6) implemented in the Coupled Ocean-Atmosphere-Wave-Sediment Transport Modeling System (COAWST r1234). Geosci. Model Dev. 11, 1849–1871. https://doi.org/10.5194/gmd-11-1849-2018

Shields, A., 1936. “Anwendung der Aechichkeits-Mechanic und der Turbuleng Forschung auf dir Geschiebewegung’ Mitt Preussische,” Versuchsanstalt für Wasserbau and

Schiffbau. Berlin, Germany (translated to English by W. P. ott and J. C. van Uchelen, California Institute of Technology, Pasadena, California).

Shore, J.A., 2009. Modelling the circulation and exchange of Kingston Basin and Lake Ontario with FVCOM. Ocean Model. 30, 106–114. https://doi.org/10.1016/J.OCEMOD.2009.06.007

Smagorinsky, J., 1963. General circulation experiments with the primitive equations, I. The basic experiment. Mon. Weather Rev. 91, 99–164. https://doi.org/10.1175/1520-0493(1963)091<0099:GCEWTP>2.3.CO;2

Smith, B.J., Harris, B.S., Harris, T.J., LaBudde, L.A., Hayer, C.-A., 2018. Status and trends of the Asian clam (Corbicula fluminea) in the lower Fox River and Green Bay. J. Great Lakes Res. 44, 943–949. https://doi.org/10.1016/J.JGLR.2018.02.012

Soulsby, R.L., 1998. Dynamics of marine sands.

Steuer, J.J., 2000. A Mass-Balance Approach for Assessing PCB Movement During Remediation of a PCB-Contaminated Deposit on the Fox River , Wisconsin.

Terta Tech Ec, I., 2019. Lower Fox River Remediation of OPerable Units 2-5.

USEPA, 1989. Green Bay/Fox River Mass Balance Study. US EPA Great Lakes National Program. EPA-905/8-89/001, Chicago, Illinois.

Velleux, M., Endicott, D., 1994. Development of a Mass Balance Model for Estimating PCB Export from the Lower Fox River to Green Bay. J. Great Lakes Res. 20, 416–434. https://doi.org/10.1016/S0380-1330(94)71159-X

Velleux, M., Endicott, D., Steuer, J., Jaeger, S., Patterson, D., 1995. Long-Term Simulation of PCB Export from the Fox River to Green Bay. J. Great Lakes Res. 21, 359–372. https://doi.org/10.1016/S0380-1330(95)71047-4

Wang, J., Bai, X., Hu, H., Clites, A., Colton, M., Lofgren, B., Wang, J., Bai, X., Hu, H., Clites, A., Colton, M., Lofgren, B., 2012. Temporal and Spatial Variability of Great Lakes Ice Cover, 1973–2010*. J. Clim. 25, 1318–1329. https://doi.org/10.1175/2011JCLI4066.1

Waples, J.T., Klump, J.V., 2002. Biophysical effects of a decadal shift in summer wind direction over the Laurentian Great Lakes. Geophys. Res. Lett. 29, 43-1-43–4. https://doi.org/10.1029/2001GL014564

Warner, J.C., Sherwood, C.R., Signell, R.P., Harris, C.K., Arango, H.G., 2008. Development of a three-dimensional, regional, coupled wave, current, and sediment-transport model. Comput. Geosci. 34, 1284–1306. https://doi.org/10.1016/J.CAGEO.2008.02.012

Wilks, D.S., 2011. Statistical methods in the atmospheric sciences. Academic Press.

Wisconsin DNR, 2015. The Lower Green Bay & Fox River Great Lakes Area of Concern Highlights from the Lower Green Bay & Fox River Area of Concern.

Wisconsin DNR, 2000. Model Evaluation Workgroup Technical Memorandum 2f: Estimation of Sediment Bed Properties for Green Bay.

Xue, P., Schwab, D.J., Hu, S., 2015. An investigation of the thermal response to

meteorological forcing in a hydrodynamic model of Lake Superior.

Yolcubal, I., Brusseau, M.L., Artiola, J.F., Wierenga, P., Wilson, L.G., 2004. ENVIRONMENTAL PHYSICAL PROPERTIES AND PROCESSES. Environ. Monit. Charact. 207–239. https://doi.org/10.1016/B978-012064477-3/50014-X

Zhang, J., Xiong, M., Yin, C., Gan, S., 2018. Inner shelf response to storm track variations over the east LeiZhou Peninsula, China. Int. J. Appl. Earth Obs. Geoinf. 71, 56–69. https://doi.org/10.1016/J.JAG.2018.03.011

APPENDIX A. Modifications of the FVCOM Sediment Transport Module (FVCOM-SED)

The current version of FVCOM-SED is only able to define the uniform distribution of sediment classes at the bottom layers, i.e., the model will start the simulations with the same initial bed fractions defined for sediment classes all over the domain. In this study, the FVCOM code was modified such that it can accept different proportions of sediment classes in grid nodes. Subroutines “init_sed.F”, “mod_sed_cstms.F”, and “mod_input.F” were modified for this purpose and the modified version of these subroutines are provided as follows. New modifications of the codes are bolded.

Also, the distribution of initial bed fractions has to be defined in the NetCDF format. An example of the input NetCDF data with details about the definition of initial bed fractions is included at the end of this Appendix. If “SEDIMENT_PARAMETER_TYPE” in the run nml file is defined as “uniform”, then the initial bed fractions will be read from the sediment input file (*.inp), otherwise the non-uniform distribution of initial bed fraction will be obtained from the NetCDF file called based on the filename defined in the run nml file (SEDIMENT_PARAMETER_FILE).

It should also be noted that the proportions of sediment classes in each bed layer and for every node of the grid have to be checked and the sum of all bed fractions must be equal to one before writing data into the input NetCDF file.

Subroutine “init_sed.F”

```
!=======================================================================
! FVCOM Sediment Initialization Routine (User Defined)
!   Configuration:  default
!=======================================================================
  Subroutine Init_Sed
# if defined (SEDIMENT)
  USE MOD_UTILS
  USE MOD_NCTOOLS
  USE MOD_INPUT
  USE ALL_VARS
  USE EQS_OF_STATE


# if defined (ORIG_SED)
  Use Mod_Prec
  Use Mod_Sed
  Use Lims, only: m,kbm1,kb
  implicit none
  integer :: i,k,ised
  real(sp) :: bed_thickness
  real(sp), allocatable :: tmp(:)

   TYPE(NCVAR),  POINTER :: VAR
   TYPE(NCDIM),  POINTER :: DIM
   LOGICAL :: FOUND

  if(dbg_set(dbg_sbr)) write(ipt,*) "Start: Init_Sed"

  if(SEDIMENT_PARAMETER_TYPE/=UNIFORM)then
   ! bkhazaei <
   ! in the new veersion non-uniform distribution distribution of sediments
   ! is implemented in the model based on a new apporach using the subroutine:
   !         "LOAD_SEDIMENT_PARAMETER_DIST"
   ! So the following call to older version is commented out here.
   ! do i=1,nsed
   !   call LOAD_SEDIMENT_PARAMETER(sed(i)%t_cd,sed(i)%t_ce,sed(i)%rate)
   ! end do
   ! bkhazaei >
  else
    do i=1,nsed
      sed(i)%t_cd = sed(i)%tau_cd
      sed(i)%t_ce = sed(i)%tau_ce
      sed(i)%rate = sed(i)%erate
    end do
  end if
```

```
 !set up the bedflag
 ! bedflag = 0. => deactive erosion/deposition
 ! bedflag = 1. => normal erosion/deposition
 if(BEDFLAG_TYPE/=CNSTNT)then
   allocate(tmp(0:mt)) ; tmp = 0.0
   call LOAD_BEDFLAG(tmp)
   bottom(0:mt,bflag) = tmp(0:mt)
   deallocate(tmp)
 else
   do i=1,m
     bottom(i,bflag) = 1.0
   end do
 endif;


 !-------------------------------------------------
 !Initialize critical shear stress for erosion
 !-------------------------------------------------
! do i=1,nsed
!   if(sed(i)%stype=='cohesive')then
!     VAR => FIND_VAR(NC_START,'tce',FOUND)
!     IF(.not. FOUND) CALL FATAL_ERROR("COULD NOT FIND VARIABLE 'tce'&
!          & IN THE STARTUP FILE OBJECT")
!     CALL NC_CONNECT_AVAR(VAR, sed(i)%t_ce)
!     CALL NC_READ_VAR(VAR)
!     CALL NC_DISCONNECT(VAR)
!   end if
! end do
 !-------------------------------------------------
 !Initialize critical shear stress for deposition
 !-------------------------------------------------
! do i=1,nsed
!   if(sed(i)%stype=='cohesive')then
!     VAR => FIND_VAR(NC_START,'tcd',FOUND)
!     IF(.not. FOUND) CALL FATAL_ERROR("COULD NOT FIND VARIABLE 'tcd'&
!        & IN THE STARTUP FILE OBJECT")
!     CALL NC_CONNECT_AVAR(VAR, sed(i)%t_cd)
!     CALL NC_READ_VAR(VAR)
!     CALL NC_DISCONNECT(VAR)
!   end if
! end do
 !-------------------------------------------------
 !Initialize surface erosion rate
 !-------------------------------------------------
! do i=1,nsed
!   VAR => FIND_VAR(NC_START,'ero',FOUND)
!   if(sed(i)%stype=='cohesive')then
!     IF(.not. FOUND) CALL FATAL_ERROR("COULD NOT FIND VARIABLE 'ero'&
!        & IN THE STARTUP FILE OBJECT")
!     CALL NC_CONNECT_AVAR(VAR, sed(i)%rate)
```

```
!     CALL NC_READ_VAR(VAR)
!     CALL NC_DISCONNECT(VAR)
!   end if
! end do
 !-------------------------------------------------
 !Initialize Bed Properties
 !-------------------------------------------------

 Do k=1,Nbed
   Do i=1,m
      bed(i,k,iaged) = 0.00
      bed(i,k,ithck) = init_bed_thickness(k)
      bed(i,k,iporo) = init_bed_porosity
    End Do
  End do

 !-------------------------------------------------
 !Initialize Bed_Frac properties
 !-------------------------------------------------

 !Do k=1,Nbed
 !  Do i=1,m
 !     Do ised=1,Nsed
 !       sed(ised)%frac(i,k)=1.0/float(nsed)
 !     End Do
 !   End Do
 !End Do
 !-------------------------------------------------
 !Initialize Bed_Frac properties
 !Version 2.0 Skagit Sediment Setup
 !Mostly fine sand (dominant size class on flats)
 !-------------------------------------------------

 Do k=1,Nbed
   Do i=1,m
      Do ised=1,Nsed
        ! bkhazaei <
        ! sed(ised)%frac(i,k)=init_bed_fraction(ised)  !1.0/float(nsed)
                       sed(i)%frac(i,k)=init_bed_fraction(i,ised)
        ! bkhazaei >
      End Do
    End Do
 End Do

 !-------------------------------------------------
 ! store the fraction at bed surface
 !-------------------------------------------------
 !do ised=1,nst
 !   sed(ised)%frac(1:m,1:nbed)=sedbed%bed_frac(1:m,1:nbed,ised)
 !end do
```

```
  !-------------------------------------------------
  !Initialize Sediment Concentrations
  !-------------------------------------------------
  Do k=1,Kb
    Do i=1,m
      Do ised=1,Nsed
            ! bkhazaei < 1/22/2019
            ! sed(ised)%conc(i,k) = 0.0
            sed(ised)%conc(i,k) = sed(ised)%Csed_initial
            ! bkhazaei >
        sed(ised)%cnew(i,k) = sed(ised)%conc(i,k)

      End Do
    End do
  End do

  if(dbg_set(dbg_sbr)) write(ipt,*) "End: Init_Sed"

  Return


# elif defined (CSTMS_SED)

  Use Mod_Prec
  Use Mod_Sed_CSTMS
  Use Lims, only: m,kbm1,kb
  implicit none
  integer  :: i,k,ised,kbed,j
  real(sp) :: cff1
  ! bkhazaei <
  real(sp),allocatable:: nsttmp(:)
  ! bkhazaei >
!
!-----------------------------------------------------------------------
!  Initialize sediment bed properties.
!-----------------------------------------------------------------------
!
  if(dbg_set(dbg_sbr)) write(ipt,*) "Start: Init_Sed"

  nnew=1
  nstp=2

  Do k=1,Nbed
     bed(1:m,k,iaged) = init_bed_age(k)
     bed(1:m,k,ithck) = init_bed_thickness(k)
     bed(1:m,k,iporo) = init_bed_porosity(k)
     if(COHESIVE_BED.or.SED_BIODIFF.or.MIXED_BED)then
       bed(1:m,k,ibtcr) = init_bed_tau_crit(k)
     endif
```

```
     if(SED_BIODIFF)then
       bed(1:m,k,idiff) = init_bed_biodiff(k)
     end if
     do i=1,nst

           ! bkhazaei <
           IF(SEDIMENT_PARAMETER_TYPE/=UNIFORM)then
            sedbed%bed_frac(1:m,k,i) = init_bed_fraction(1:m,(k-1)*nst+i)
           ELSE
            sedbed%bed_frac(1:m,k,i)     = init_bed_fraction(i,k)
           END IF
           ! bkhazaei >

!   sedbed%bed_mass(1:m,k,i) = init_bed_mass(i,k)
!
!           Calculate mass so it is consistent with density, thickness, and
!           porosity.
!
           ! bkhazaei <
           IF(SEDIMENT_PARAMETER_TYPE/=UNIFORM)then
            do j=1,m,1
              sedbed%bed_mass(j,k,1:2,i)=init_bed_thickness(k)*sed(i)%Srho&
               &*(1.0-init_bed_porosity(k))*init_bed_fraction(j,(k-1)*nst+i)
            end do
           ELSE
            sedbed%bed_mass(1:m,k,1:2,i)=init_bed_thickness(k)*sed(i)%Srho&
               &*(1.0-init_bed_porosity(k))*init_bed_fraction(i,k)
           END IF
           ! bkhazaei >

     end do
  End do

  !-------------------------------------------------
  !Initialize Sediment Concentrations
  !-------------------------------------------------
  Do ised=1,Nsed
    ! BK < 1/22/2019
    !sed(ised)%conc = 0.0_sp
    sed(ised)%conc = sed(ised)%Csed_initial
    ! BK >
    sed(ised)%cnew = sed(ised)%conc
  End do

!
!-----------------------------------------------------------------------
!  Compute initial total thickness for all sediment bed layers.
!-----------------------------------------------------------------------
!
  if(SED_MORPH)then
```

```
    do i=1,m
       sedbed%bed_thick0(i)=0.0_sp
       DO kbed=1,Nbed
         sedbed%bed_thick0(i)=sedbed%bed_thick0(i)+sedbed%bed(i,kbed,ithck)
       END DO
       sedbed%bed_thick(i,nnew)=sedbed%bed_thick0(i)
    end do

  end if

  if(dbg_set(dbg_sbr)) write(ipt,*) "End: Init_Sed"

  Return

# endif


# endif
  End Subroutine Init_Sed
!=======================================================================
```

Subroutine “mod_sed_cstms.F”

Note: Only sections of this subroutine that includes subroutine introduction and new modifications are reported here. These sections are separated with “…”.

```
!/===========================================================================/
! Copyright (c) 2007, The University of Massachusetts Dartmouth
! Produced at the School of Marine Science & Technology
! Marine Ecosystem Dynamics Modeling group
! All rights reserved.
!
! FVCOM has been developed by the joint UMASSD-WHOI research team. For
! details of authorship and attribution of credit please see the FVCOM
! technical manual or contact the MEDM group.
!
!
! This file is part of FVCOM. For details, see http://fvcom.smast.umassd.edu
! The full copyright notice is contained in the file COPYRIGHT located in the
! root directory of the FVCOM code. This original header must be maintained
! in all distributed versions.
!
! THIS SOFTWARE IS PROVIDED BY THE COPYRIGHT HOLDERS AND CONTRIBUTORS "AS IS"
! AND ANY EXPRESS OR IMPLIED WARRANTIES, INCLUDING, BUT NOT LIMITED TO,
! THE IMPLIED WARRANTIES OF MERCHANTABILITY AND FITNESS FOR A PARTICULAR
! PURPOSE ARE DISCLAIMED.
!
!/---------------------------------------------------------------------------/
! CVS VERSION INFORMATION
! $Id$
! $Name$
! $Revision$
!/===========================================================================/

!=======================================================================
! FVCOM Sediment Module
!
! Copyright:    2005(c)
!
! THIS IS A DEMONSTRATION RELEASE. THE AUTHOR(S) MAKE NO REPRESENTATION
! ABOUT THE SUITABILITY OF THIS SOFTWARE FOR ANY OTHER PURPOSE. IT IS
! PROVIDED "AS IS" WITHOUT EXPRESSED OR IMPLIED WARRANTY.
!
! THIS ORIGINAL HEADER MUST BE MAINTAINED IN ALL DISTRIBUTED
! VERSIONS.
!
```

```
! Contact:      G. Cowles
!               School for Marine Science and Technology, Umass-Dartmouth
!
! Based on the Community Sediment Transport Model (CSTM) as implemented
!     in ROMS by J. Warner (USGS)
!
! Comments:     Sediment Dynamics Module
!
! Current FVCOM dependency
!
!   init_sed.F:  - user defined sediment model initial conditions
!   mod_ncdio.F: - netcdf output includes concentration/bottom/bed fields
!   fvcom.F:     - main calls sediment setup
!   internal.F:  - calls sediment advance
!
! History
!   Feb 7, 2008: added initialization of bottom(:,:) to 0 (w/ T. Hamada)
!               : fixed loop bounds in hot start and archive for conc (w/ T.
Hamada)
!              : added comments describing theoretical bases of dynamics
!   Feb 14,2008: added non-constant settling velocity for cohesive sediments
(w/ T. Hamada)
!             : updated vertical flux routine to handle non-constant vertical
velocity (w/ T. Hamada)
!               : added a user-defined routine to calculate settling velocity
based on concentration (w/ T. Hamada)
!            : added a user-defined routine to calculate erosion for a general
case (w/ T. Hamada)
!
!  PLEASE NOTE!!!!!!!!!!
!  Do NOT USE INTEL FORTRAN COMPILER VERSION 11.0 IT HAS KNOWN BUGS WHEN DEALING
WITH TYPES WITH ALLOCATABLE
!    COMPONENTS.  YOU WILL SEE WEIRD BEHAVIOR.  VERSION 11.1 IS OK.
!
!
!  Later
!   1.) Modify vertical flux routines to work with general vertical coordinate
!   2.) Add divergence term for bedload transport calc
!   3.) Add ripple roughness calculation
!   4.) Add morphological change (bathymetry + vertical velocity condition)
!   5.) Eliminate excess divisions and recalcs
!
!==============================================================================
Module Mod_Sed_CSTMS
#if defined (SEDIMENT) && (CSTMS_SED)
Use Mod_Par
Use Mod_Prec
Use Mod_Types
Use Mod_wd
Use Control, only : seddis
```

```
Use all_vars,only : CNSTNT,UNIFORM,SEDIMENT_PARAMETER_TYPE
# if defined (WAVE_CURRENT_INTERACTION)
USE MOD_WAVE_CURRENT_INTERACTION
# endif
# if defined (MULTIPROCESSOR)
Use Mod_Par
# endif
# if defined (FLUID_MUD)
USE MOD_FLUID_MUD
# endif

Use Mod_CSTMS_vars

Use Mod_FlocMod

implicit none



…



!========================================================================
!Read Sediment Parameters From Sediment Input File
!========================================================================
Subroutine Read_Sed_Params
  Use Input_Util
  ! bkhazaei <
  USE MOD_UTILS
  USE MOD_NCTOOLS
  USE MOD_INPUT
  USE ALL_VARS
  USE EQS_OF_STATE
  USE MOD_INPUT
  ! bkhazaei >
  Implicit None


  ! bkhazaei <
  integer :: ibedf,jbedf,nodenum
  TYPE(NCVAR),  POINTER :: VAR
  TYPE(NCDIM),  POINTER :: DIM
  LOGICAL :: FOUND
  ! bkhazaei >
  integer linenum,i,k1,iscan
  real(sp)           :: ftemp
  character(len=120) :: stemp

  real(sp),allocatable:: ncstmp(:)
```

```
  real(sp),allocatable:: nnstmp(:)
  real(sp),allocatable:: nsttmp(:)
  logical, allocatable:: nswitch(:)
  character(len=80),allocatable:: strtmp(:)

  !
  !  Imported variable declarations
  !

  !
  !  Local variable declarations.
  !
  integer :: iTrcStr, iTrcEnd
  integer :: ifield, igrid, itracer, itrc, nline


  !-----------------------------------------------------------------------
  !  Initialize.
  !-----------------------------------------------------------------------
```

…

```
  !read in initial bed fraction
  ! bkhazaei <
  IF(SEDIMENT_PARAMETER_TYPE/=UNIFORM)then
            allocate(init_bed_fraction(mt,nst*nbed))
            call LOAD_SEDIMENT_PARAMETER_DIST(init_bed_fraction)
            write(*,*) 'Non-uniform distribution of sediment in bed:'
            write(*,*) '             --> Data obtained from NC file'

  ELSE
  ! bkhazaei >

              allocate(init_bed_fraction(nst,nbed))
              allocate(nsttmp(nst*nbed))
              Call
Get_Val_Array(nsttmp,sedfile,'INIT_BED_FRACTION',nst*nbed,echo=.true.)
              do i=1,nbed
                        init_bed_fraction(1:nst,i)=nsttmp((i-1)*nst+1:(i-
1)*nst+nst)
                        if(sum(init_bed_fraction(1:nst,i))/=1.0)then
                                  write(*,*)'error in init_bed_fraction in
sed param file'
                                  write(*,*)'also  error  in  your  chosen
career'
                                  write(*,*)'in bed layer:',i
```

```
                                    write(*,*)'you                  entered:
',init_bed_fraction(1:nst,i)
                                    write(*,*)'must have the summary = 1'
                                    stop
                            end if
                    end do
                    if(minval(init_bed_fraction)         <         0.         .or.
maxval(init_bed_fraction) > 1.)then
                            write(*,*)'error in init_bed_fraction in sed param
file'
                            write(*,*)'also error in your chosen career'
                            write(*,*)'you entered: ',init_bed_fraction
                            write(*,*)'must be >= 0 and <= 1'
                            stop
                    endif
                    deallocate(nsttmp)

  ! bkhazaei <
  ENDIF
  ! bkhazaei >
```

Subroutine “mod_input.F”

Note: Only sections of this subroutine that includes subroutine introduction and new modifications are reported here. These sections are separated with “…”.

```
!/============================================================================/
! Copyright (c) 2007, The University of Massachusetts Dartmouth
! Produced at the School of Marine Science & Technology
! Marine Ecosystem Dynamics Modeling group
! All rights reserved.
!
! FVCOM has been developed by the joint UMASSD-WHOI research team. For
! details of authorship and attribution of credit please see the FVCOM
! technical manual or contact the MEDM group.
!
!
! This file is part of FVCOM. For details, see http://fvcom.smast.umassd.edu
! The full copyright notice is contained in the file COPYRIGHT located in the
! root directory of the FVCOM code. This original header must be maintained
! in all distributed versions.
!
! THIS SOFTWARE IS PROVIDED BY THE COPYRIGHT HOLDERS AND CONTRIBUTORS "AS IS"
! AND ANY EXPRESS OR  IMPLIED WARRANTIES, INCLUDING,  BUT NOT  LIMITED TO,
! THE IMPLIED WARRANTIES OF MERCHANTABILITY AND  FITNESS FOR A PARTICULAR
! PURPOSE ARE DISCLAIMED.
!
!
!/----------------------------------------------------------------------------/
! CVS VERSION INFORMATION
! $Id$
! $Name$
! $Revision$
!/============================================================================/

MODULE MOD_INPUT
  USE MOD_NCTOOLS
  USE MOD_UTILS
  IMPLICIT NONE

  PUBLIC
  SAVE


  TYPE(NCFILE), POINTER ::NC_DAT
```

```
  TYPE(NCFILE), POINTER ::NC_AVG
  TYPE(NCFILE), POINTER ::NC_RST
  TYPE(NCFILE), POINTER ::NC_START


…


  ! bkhazaei <
  SUBROUTINE LOAD_SEDIMENT_PARAMETER_DIST(init_bed_frac)

    USE CONTROL
    IMPLICIT NONE

    REAL(SP),ALLOCATABLE :: init_bed_frac(:,:)

    TYPE(NCFILE), POINTER :: NCF
    TYPE(NCVAR),  POINTER :: VAR
    TYPE(NCDIM),  POINTER :: DIM1
    TYPE(NCDIM),  POINTER :: DIM2
    integer status,I,IERR

    LOGICAL FOUND

    ! FIND THE Sediment Parameter FILE OBJECT
    NCF => FIND_FILE(FILEHEAD,trim(SEDIMENT_PARAMETER_FILE),FOUND)
    IF(.not. FOUND) CALL FATAL_ERROR &
         & ("COULD NOT FIND SEDIMENT_PARAMETER_FILE OBJECT",&
         & "FILE NAME: "//TRIM(SEDIMENT_PARAMETER_FILE))

    DIM1 => FIND_DIM(NCF,'node',FOUND)
    IF(.not. FOUND) CALL FATAL_ERROR &
         & ("COULD NOT FIND SEDIMENT_PARAMETER_FILE DIMENSION 'node' in:",&
         & "FILE NAME: "//TRIM(SEDIMENT_PARAMETER_FILE))
    IF (DIM1%DIM /= MGL)CALL FATAL_ERROR &
         & ("Dimension 'node' in the SEDIMENT_PARAMETER_FILE does not match
MGL for this model?",&
         & "FILE NAME: "//TRIM(SEDIMENT_PARAMETER_FILE))

            ! FIND THE 'initial bed fraction' variable
    VAR => FIND_VAR(NCF,'init_bed_frac',FOUND)
    IF(.not. FOUND) CALL FATAL_ERROR &
         & ("COULD NOT FIND SEDIMENT_PARAMETER_FILE VARIABLE 'init_bed_frac'
in:",&
         & "FILE NAME: "//TRIM(SEDIMENT_PARAMETER_FILE))

    CALL NC_CONNECT_AVAR(VAR,init_bed_frac)
    CALL NC_READ_VAR(VAR)
    CALL NC_DISCONNECT(VAR)
```

```
END SUBROUTINE LOAD_SEDIMENT_PARAMETER_DIST
! bkhazaei >
```

Example of a “SEDIMENT_PARAMETER_FILE” in NetCDF format:

Note: “init_bed_frac” is the variable name that includes the sediment distribution inputs. This variable should be written in a matrix that the number of rows is equal to node number and the number of columns is equal to the number of sediment classes (nst) times number of bed layers (nbed). For example, if there are 3 sediment classes, 2 bed layers, and 28985 nodes in the domain, then “init_bed_frac” will have the following format (nst, nbed, node):

1, 1, 1 2, 1, 1 3, 1, 1 1, 2, 1 2, 2, 1 3, 2, 1

1, 1, 2 2, 1, 2 3, 1, 2 1, 2, 2 2, 2, 2 3, 2, 2

…

1, 1, 28985 2, 1, 28985 3, 1, 28985 1, 2, 28985 2, 2, 28985 3, 2, 28985

It is important to note that the sum of each row should be equal to 1.

```
$ ncdump -h sediment_distribution.nc
netcdf sediment_distribution {
dimensions:
            node = 28985 ;
            nele = 52574 ;
            nst_nbd = 4 ;
            three = 3 ;
variables:
float x(node) ;
                        x:long_name = "nodal x-coordinate" ;
                        x:units = "meters" ;
            float y(node) ;
                        y:long_name = "nodal y-coordinate" ;
                        y:units = "meters" ;
            float lon(node) ;
                        lon:long_name = "nodal longitude" ;
                        lon:standard_name = "longitude" ;
                        lon:units = "degrees" ;
            float lat(node) ;
                        lat:long_name = "nodal latitude" ;
                        lat:standard_name = "latitude" ;
                        lat:units = "degrees" ;
```

```
            float xc(nele) ;
                        xc:long_name = "nodal x-coordinate" ;
                        xc:units = "meters" ;
            float yc(nele) ;
                        yc:long_name = "nodal y-coordinate" ;
                        yc:units = "meters" ;
            float lonc(nele) ;
                        lonc:long_name = "nodal longitude" ;
                        lonc:standard_name = "longitude" ;
                        lonc:units = "degrees" ;
            float latc(nele) ;
                        latc:long_name = "nodal latitude" ;
                        latc:standard_name = "latitude" ;
                        latc:units = "degrees" ;
            int nv(three, nele) ;
                        nv:long_name = "nodes surrounding element" ;
            float init_bed_frac(nst_nbd, node) ;
                        init_bed_frac:long_name = "Distribution of Sediment
                        Classes" ;
                        init_bed_frac:units = "%" ;
                        init_bed_frac:grid = "fvcom_grid" ;
                        init_bed_frac:coordinates = "lat lon" ;
                        init_bed_frac:type = "data" ;

// global attributes:
                        :Title = "Initial Distribution of Sediment Classes" ;
                        :Institution = "University of Wisconsin-Milwaukee" ;
                        :source = "Matlab program: FVCOM_write_IC_Sed" ;
                        :Updated by = "Bahram Khazaei and Hector R. Bravo" ;
                        :History = "NetDCF File created on 2019-11-13
11:06:57" ;
}
```

APPENDIX B. Validation of Meteorological Forcings

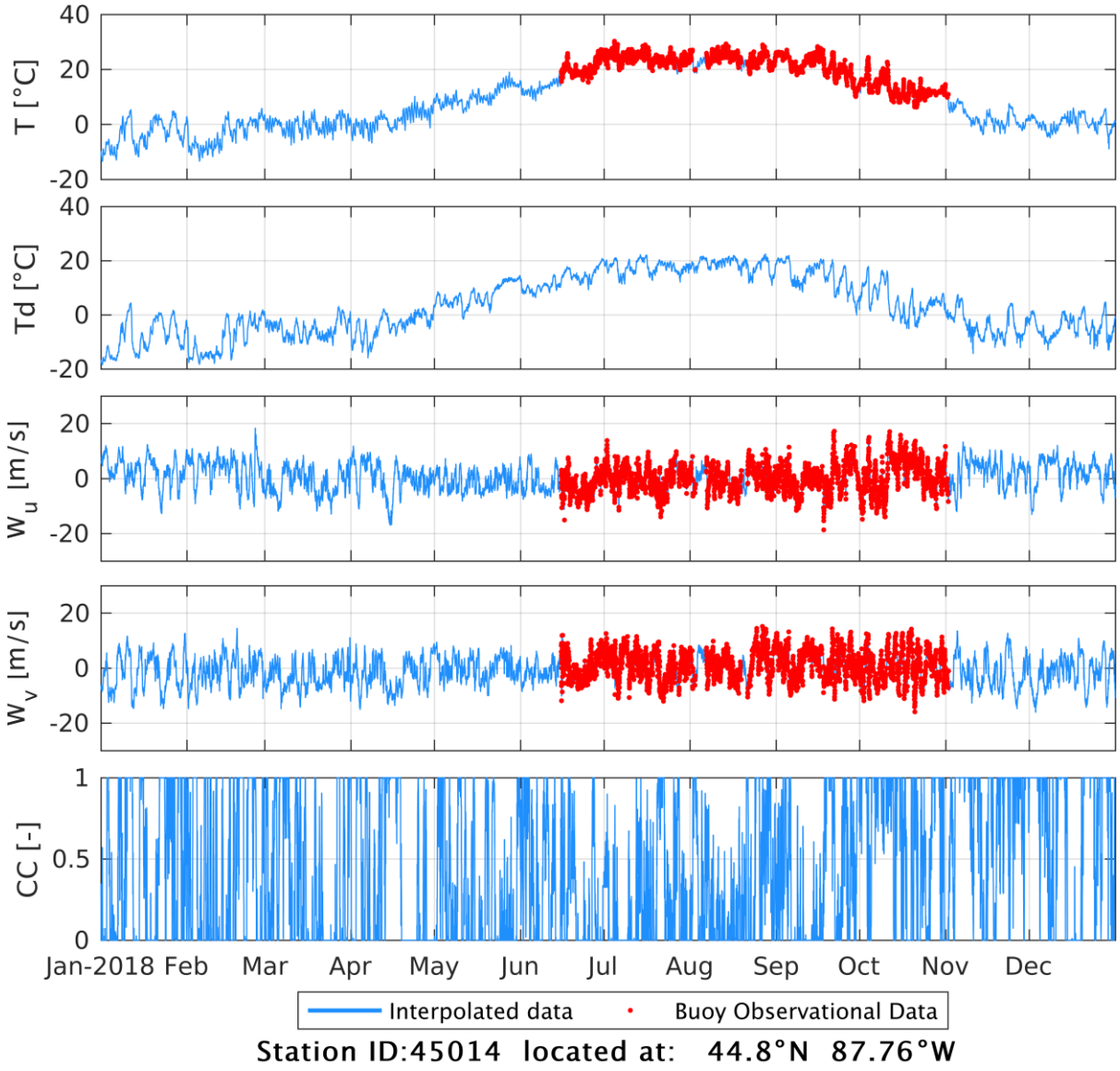

Figure B.1. Validations of the meteorological forcing at the location of the southern Green Bay buoy 45014 in 2018. T and Td are air temperature and dew point temperature, Wu and Wv are zonal and meridional wind speeds, and CC is cloud cover.

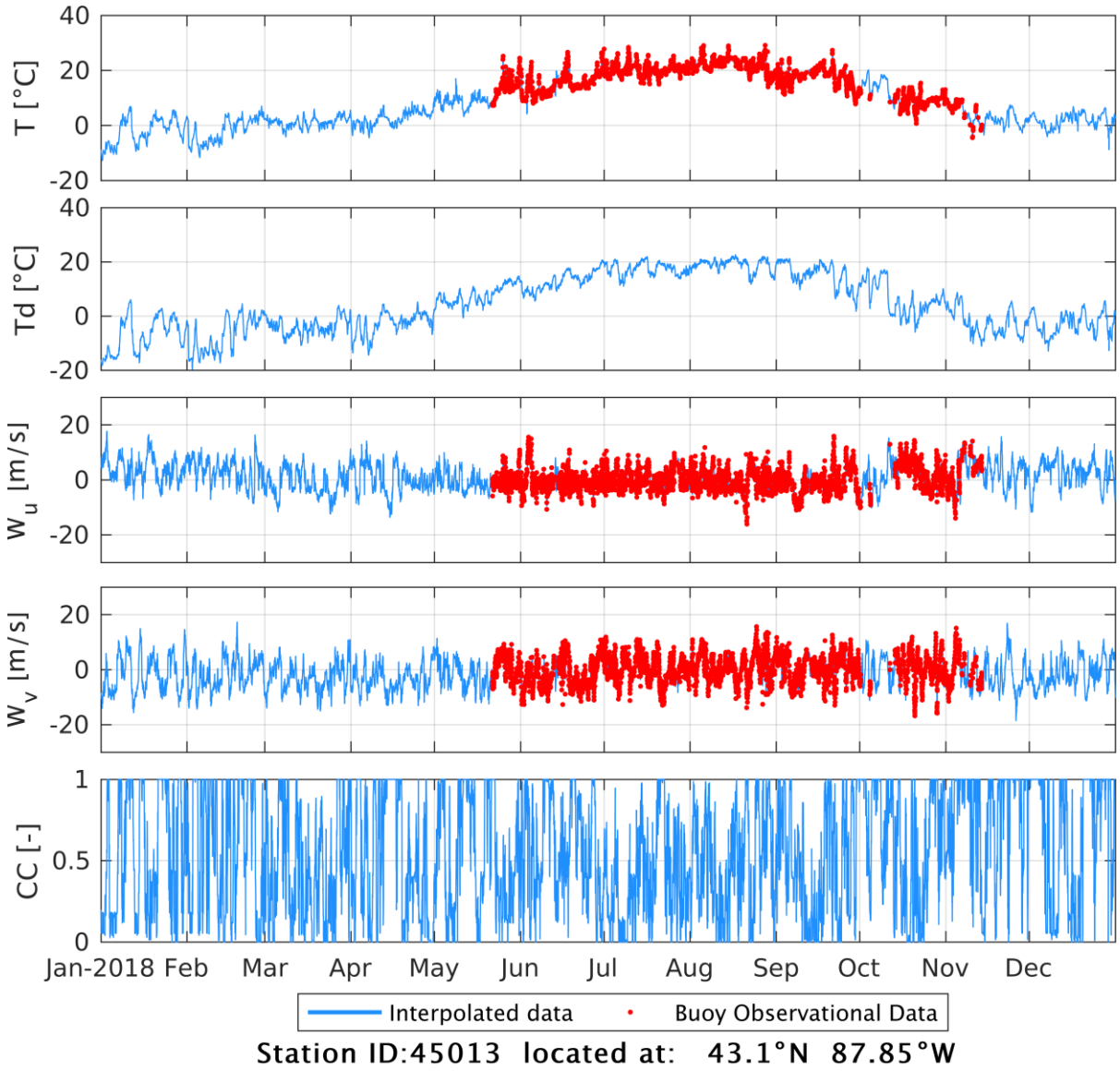

Figure B.2. Validations of the meteorological forcing at the location of the Milwaukee Atwater Beach buoy 45013 in 2018. T and Td are air temperature and dew point temperature, Wu and Wv are zonal and meridional wind speeds, and CC is cloud cover.

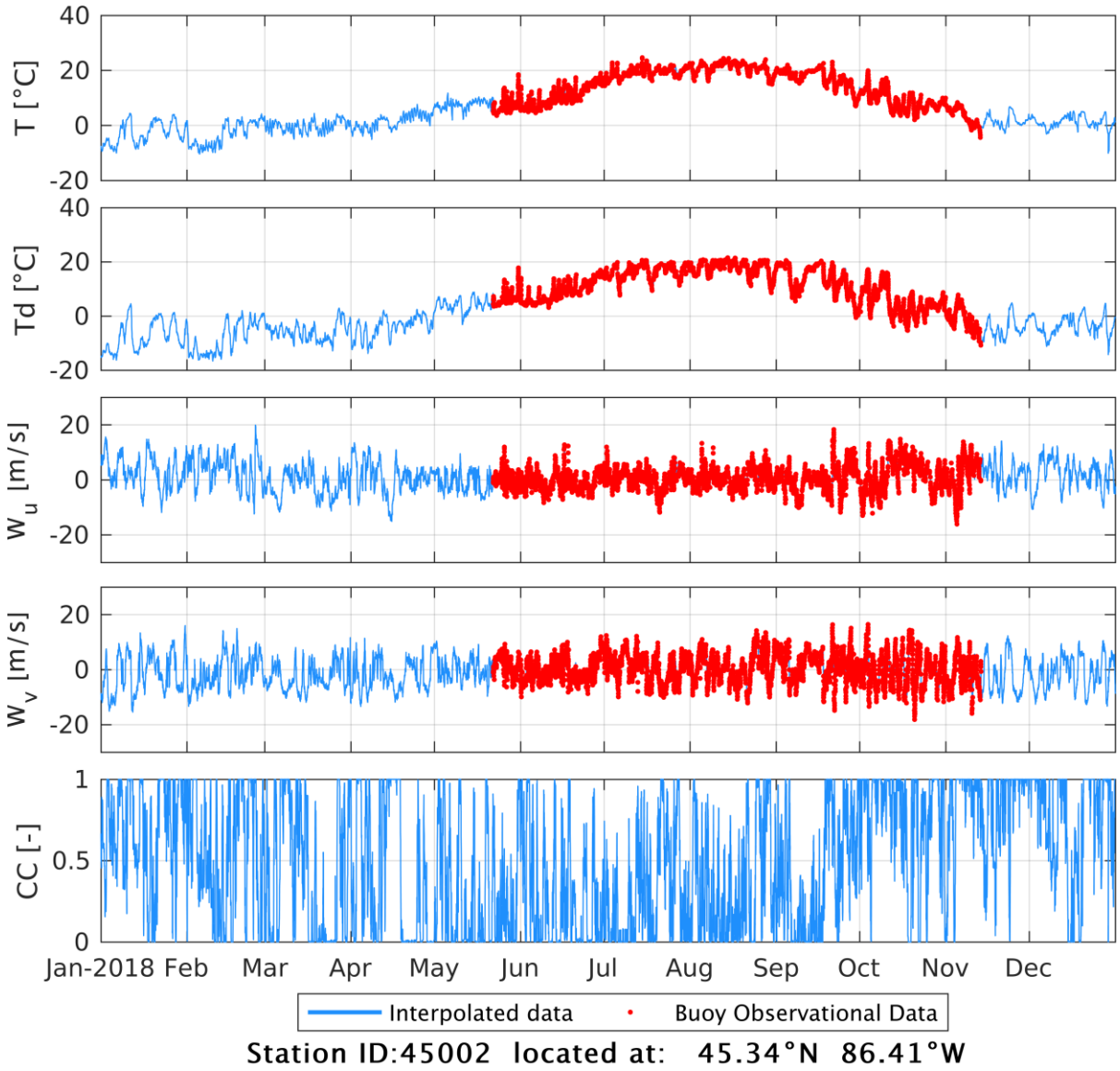

Figure B.3. Validations of the meteorological forcing at the location of the Northern Lake Michigan buoy 45002 in 2018. T and Td are air temperature and dew point temperature, Wu and Wv are zonal and meridional wind speeds, and CC is cloud cover.

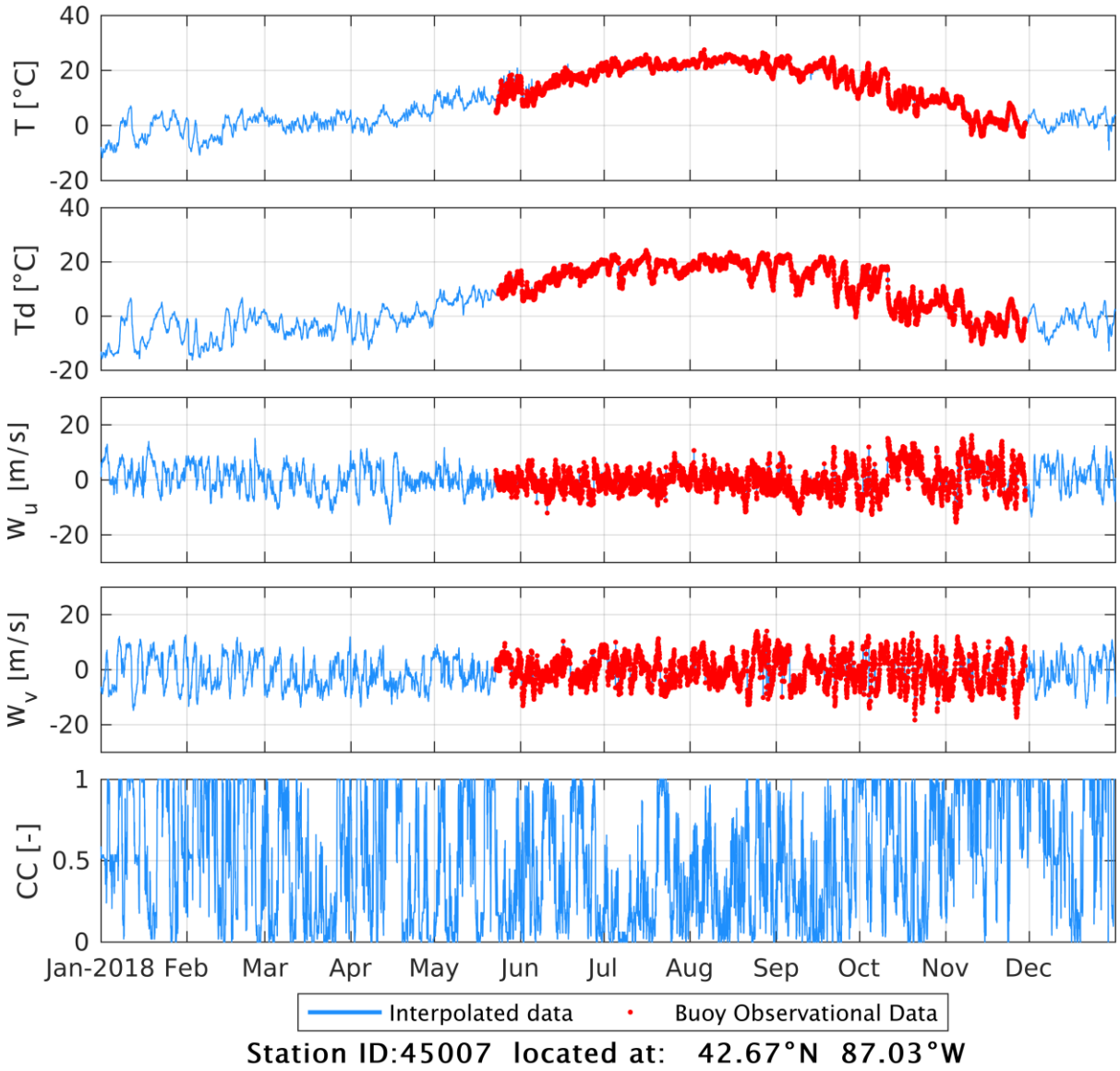

Figure B.4. Validations of the meteorological forcing at the location of the Southern Lake Michigan buoy 45007 in 2018. T and Td are air temperature and dew point temperature, Wu and Wv are zonal and meridional wind speeds, and CC is cloud cover.

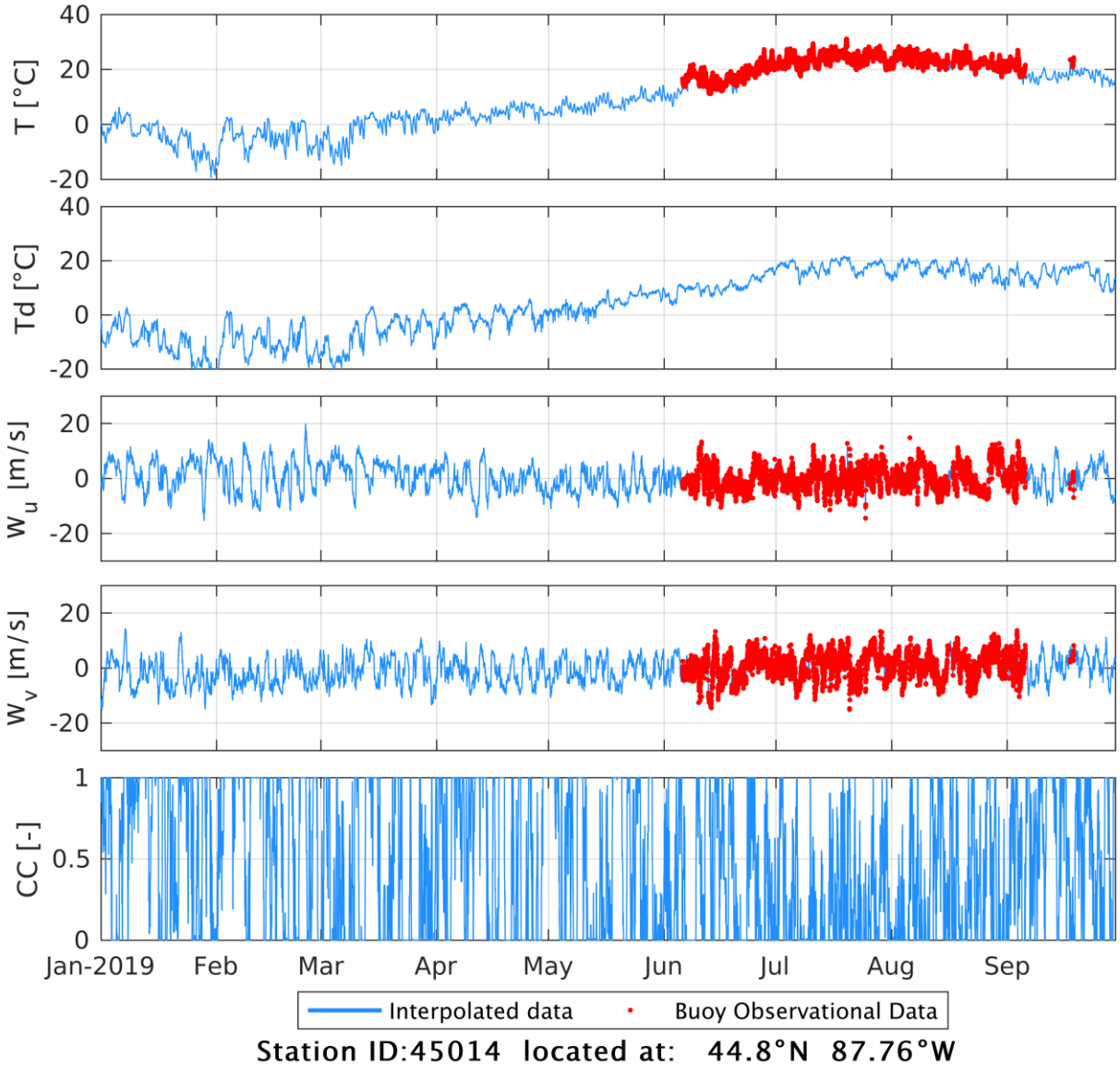

Figure B.5. Validations of the meteorological forcing at the location of the southern Green Bay buoy 45014 in 2019. T and Td are air temperature and dew point temperature, Wu and Wv are zonal and meridional wind speeds, and CC is cloud cover.

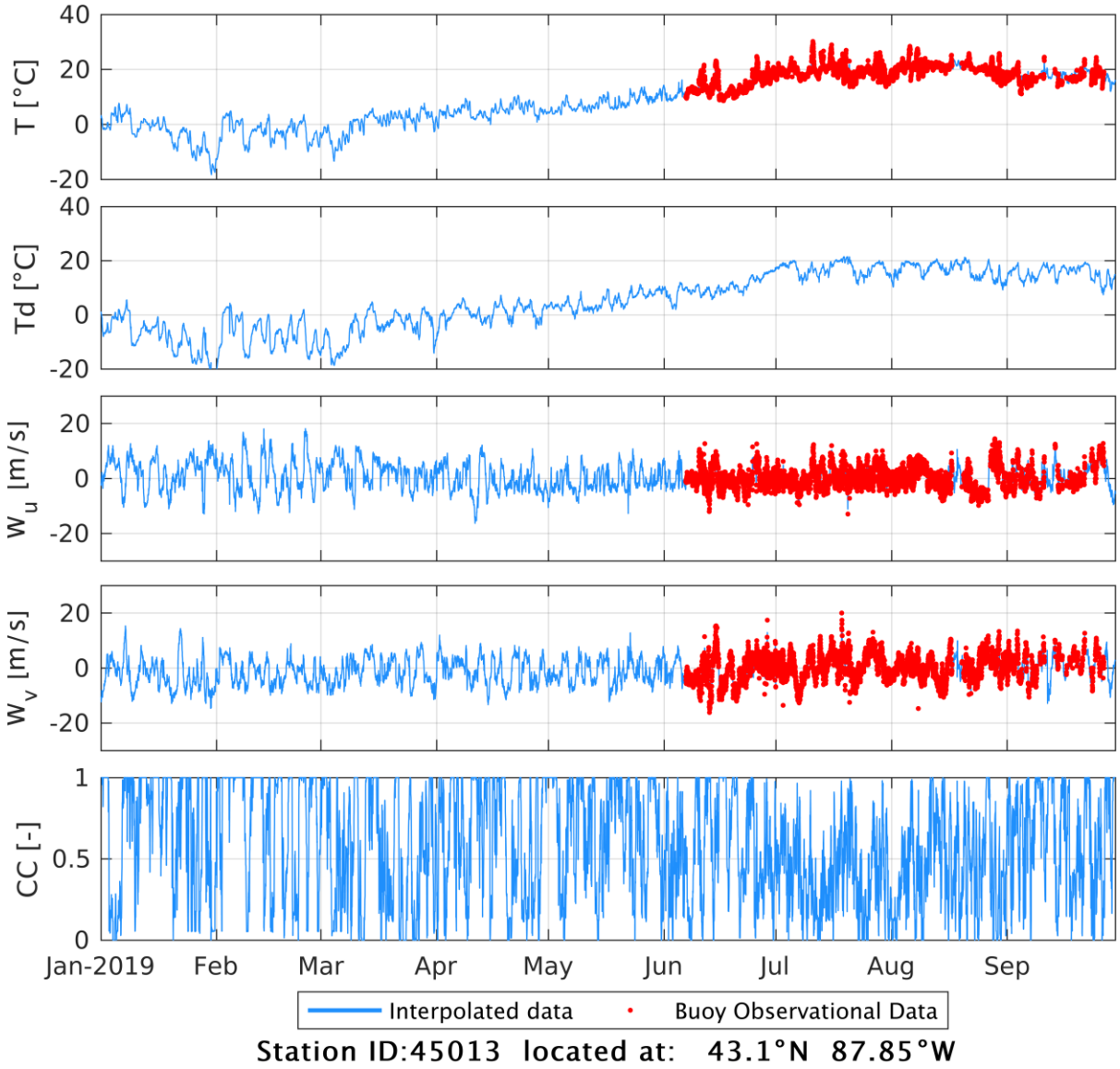

Figure B.6. Validations of the meteorological forcing at the location of the Milwaukee Atwater Beach buoy 45013 in 2019. T and Td are air temperature and dew point temperature, Wu and Wv are zonal and meridional wind speeds, and CC is cloud cover.

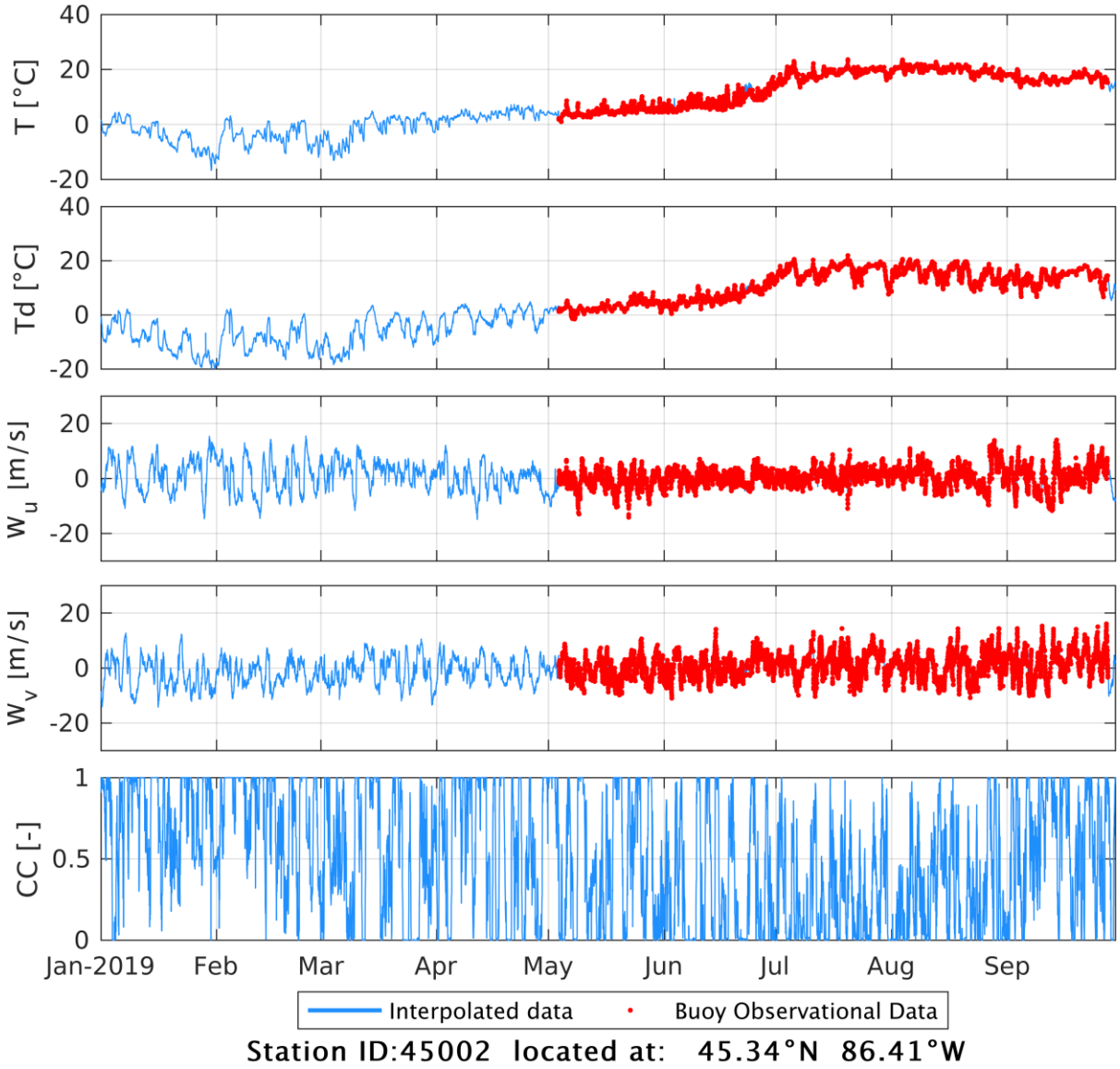

Figure B.7. Validations of the meteorological forcing at the location of the Northern Lake Michigan buoy 45002 in 2019. T and Td are air temperature and dew point temperature, Wu and Wv are zonal and meridional wind speeds, and CC is cloud cover.

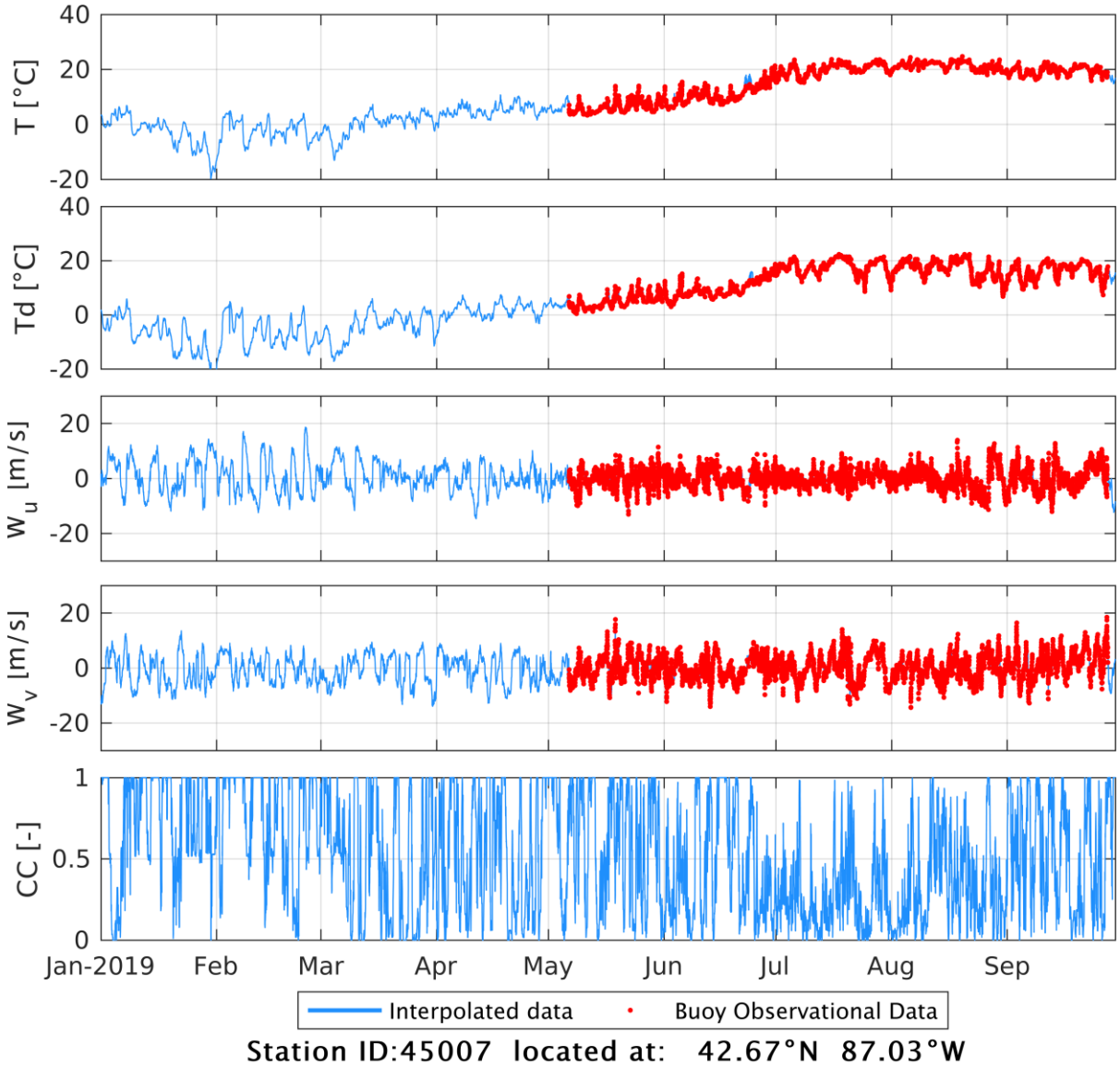

Figure B.8. Validations of the meteorological forcing at the location of the Southern Lake Michigan buoy 45007 in 2019. T and Td are air temperature and dew point temperature, Wu and Wv are zonal and meridional wind speeds, and CC is cloud cover.

CURRICULUM VITAE

Bahram Khazaei

Civil & Environmental Engineering Department
University of Wisconsin-Milwaukee

Education

2015-2020 **Ph.D.,** Civil & Environmental Engineering
University of Wisconsin-Milwaukee, WI, USA **(GPA: 4/4)**

2015-2017 **Graduate Certificate,** Geographic Information Systems
University of Wisconsin-Milwaukee, WI, USA **(GPA: 4/4)**

2009-2012 **M.Sc.,** Civil Engineering
Ferdowsi University of Mashhad, Mashhad, Iran **(GPA: 3.72/4)**

2005-2009 **B.Sc.,** Civil Engineering
Ferdowsi University of Mashhad, Mashhad, Iran **(GPA: 3.23/4)**

Academic Experiences

2019-2020 **Research Assistant,** Civil and Environmental Engineering
University of Wisconsin-Milwaukee

2018-2019 **Dean's Scholar,** College of Engineering and Applied Sciences
University of Wisconsin-Milwaukee

2017-2018 **Teaching Assistant,** Civil and Environmental Engineering
University of Wisconsin-Milwaukee

2015-2017 **Research Assistant,** Civil and Environmental Engineering
University of Wisconsin-Milwaukee

2012-2015 **Lecturer,** Civil Engineering Department
Atrak Institute of Higher Education

2009-2012 **Teaching and Research Assistant,** Civil Engineering Department
Ferdowsi University of Mashhad

Research Interests

- Water quality modeling, sediment transport, and coupled physical and biogeochemical models
- Physical oceanography and limnology with focus on modeling physical processes of the lake systems
- Application of GIS and remote sensing in modeling water systems
- Hydroclimatology and impacts of climate change on water resources systems
- Eco-hydrology with focus on impacts of vegetation dynamics on the hydrological cycle and aquatic systems
- Water balance and watershed modeling

Computer Skills

- **General:** Windows, Linux
- **Programming:** MATLAB, Python, Fortran, IDL, R
- **GIS and Remote Sensing:** ArcGIS, ERDAS, IDRISI, AQUAVEO SMS
- **Water Resources Modeling:** Bentley (WaterCAD, StormCAD, SewerCAD, FlowMaster)

Awards

2019	CUAHSI Hydroinformatics Conference Travel Award
2019	UWM Chancellor's Graduate Student Award
2018	CUAHSI Biennial Colloquium Travel Award
2018	UWM College of Engineering and Applied Sciences Dean's Fellowship
2017	UWM Chancellor's Graduate Student Award
2016	UWM Chancellor's Graduate Student Award
2016	First Place Student GIS Project Competition, GIS Day
2013	Atrak IHE Excellence in Teaching Award
2012	Outstanding Graduate Student, Civil Engineering Depertment, FUM

Publications

Dissertation

1. **Khazaei, B**. 2012. Improving the Accuracy of Water Balance Equation Using Fuzzy Logic Approach. *M.Sc. Thesis report*, Mashhad: Ferdowsi University of Mashhad. (In Farsi)

Journal Papers

2. Bravo, H.R., Hamidi, S.A., Anderson, E.J., Klump, J.V. and **Khazaei, B**. 2019. Timescales of transport through lower Green Bay. *Journal of Great Lakes Research,* under review.
3. Bravo, H.R., Bootsma, H.A. and **Khazaei, B.** 2019. Fate of phosphorus from a point source in the Lake Michigan nearshore zone, *Journal of Great Lakes Research,* 45 (6): 1182-1196.
4. **Khazaei, B.,** Khatami, S., Alemohammad, S.H., Rashidi, L., Wu, C., Madani, K., Kalantari, Z., Destouni, G. and Aghakouchak, A. 2019. Climatic or regionally induced by humans? Tracing hydro-climatic and land-use changes to better understand the Lake Urmia tragedy, *Journal of Hydrology,* 569: 203-217.
5. Hamidi, S.A., Hosseiny, H., Ekhtari, N. and **Khazaei, B**. 2017. Using MODIS remote sensing data for mapping the spatio-temporal variability of water quality and river turbid plume, *Journal of Coastal Conservation,* 21: 939-950.
6. **Khazaei, B.** and Hosseini, S.M. 2015. Improving the performance of water balance equation using fuzzy logic approach, *Journal of Hydrology,* 524: 538–548.
7. Khatami, S. and **Khazaei, B.** 2014. Benefits of GIS application in hydrological modeling: A brief summary, *Journal of Water Management & Research, Swedish Association for Water*, 70 (1): 41–49.

Peer-Reviewed Conference Papers

8. **Khazaei, B.,** Anderson, E.J., Klump, J.V., Miller, T.R. and Bravo, H.R. 2020. Restoration of Green Bay ecosystem: investigating sediment dynamics of lower Green Bay based on a 3D physical sediment transport model. Submitted to the 6th International EcoSummit Conference, Gold Coast, Australia, Jun 21-25.
9. **Khazaei, B.,** Anderson, E.J., Miller, T.R., Klump, J.V. and Bravo, H.R. 2020. Understanding the patterns of sediment dynamics in lower Green Bay, WI. Accepted for presentation at the World Environmental and Water Resources Congress, Henderson, NV, May 17-21.
10. Hamidi, S.A. and **Khazaei**, **B.** 2020. A frequency domain analysis on the Great Lakes water level fluctuations and rivers inflows. Accepted for presentation at the World Environmental and Water Resources Congress, Henderson, NV, May 17-21.
11. **Khazaei, B.,** Anderson, E.J., Klump, J.V. and Bravo, H.R. 2019. Development of an FVCOM-based 3D sediment transport model for Green Bay, Lake Michigan. 38th International Association of Hydraulic Research World Congress, Panama City, Panama, 1–6 Sep.

12. **Khazaei, B.,** Anderson, E.J., Klump, J.V. and Bravo, H.R. 2019. Development of hydrodynamic and sediment transport model for Green Bay, Lake Michigan. World Environmental and Water Resources Congress, Pittsburg, PA, 19–23 May.
13. **Khazaei, B.**, Nabizadeh, A. and Hamidi, S.A. 2018. An empirical approach to estimate total suspended sediment using observational data in Fox River and southern Green Bay, WI. World Environmental and Water Resources Congress, Minneapolis, MN, 3–7 Jun.
14. **Khazaei, B.** and Wu, C. 2018. Estimation of vegetation coverage based on seasonal variabilities in MODIS-based vegetation indices. World Environmental and Water Resources Congress, Minneapolis, MN, 3–7 Jun.
15. Bravo, H.R., Bootsma, H.A. and **Khazaei, B.** 2017. Modeling the transport and fate of phosphorus from a point source in the Lake Michigan nearshore zone. 37th International Association of Hydraulic Research World Congress, Kuala Lumpur, Malaysia, 13–18 Aug.
16. **Khazaei, B.** and Hosseini, S.M. 2013. New method in determination of fuzzy numbers for hydrological parameters based on estimation errors. 7th National Congress on Civil Engineering, University of Sistan & Baluchestan, Zahedan, Iran, 7–8 May. (In Farsi)
17. **Khazaei, B.** and Hosseini, S.M. 2013. Interval analysis of water balance equation using fuzzy logic approaches. 7th National Congress on Civil Engineering, University of Sistan & Baluchestan, Zahedan, Iran, 7–8 May. (In Farsi)
18. **Khazaei, B.**, Abedzadeh, A., Mirabi, M. and Kashefi, S. 2012. Development of a linear rainfall–runoff relationship using fuzzy modeling. 2nd National Conference on Innovative Findings in Civil Engineering, IAUN, Najafabad, Iran, 5–6 Dec. (In Farsi)
19. **Khazaei, B.**, Kashefi, S., Mirabi, M. and Seyedi, S.F. 2012. Increasing water treatment efficiency using fuzzy linear programming optimization algorithm. 2nd National Conference on Innovative Findings in Civil Engineering, IAUN, Najafabad, Iran, 5–6 Dec. (In Farsi)
20. **Khazaei, B.**, Eshraghi, S.S. and Mirabi, M. 2012. Comparison of crisp and fuzzy models in benefit analysis of reservoir operations. 2nd Dam & Tunnel Conference & Exposition, Tehran University, Tehran, Iran, 15–17 Oct. (In Farsi)
21. **Khazaei, B.** and Hosseini, S.M. 2012. Increasing the accuracy of water balance equation using fuzzy regression. 9th International Congress on Civil Engineering, Isfahan University of Technology, Isfahan, Iran, 8–10 May. (In Farsi)

Conference Abstracts/Presentations

22. **Khazaei, B.**, Anderson, E.J., Klump, J.V., Miller, T.R. and Bravo, H.R. 2019. Application of the Finite Volume Community Ocean Model (FVCOM) to the analysis of sediment processes in Green Bay, Lake Michigan. Accepted for presentation at the Ocean Sciences 2020 Meeting, San Diego, CA, 16-21 Feb.

23. **Khazaei, B.**, Anderson, E.J., Klump, J.V., Miller, T.R. and Bravo, H.R. 2019. Analysis of sediment processes in the Fox River/Green Bay estuarine system, Lake Michigan. American Geophysical Union 2019 Fall Meeting, San Francisco, CA, 9-13 Dec.
24. **Khazaei, B.**, Bootsma H.A. and Bravo, H.R. 2019. Using a 3D model to investigate the spatial patterns of algal growth in western Lake Michigan. CUAHSI 2019 Hydroinformatics Conference, Provo, UT, 29–31 Jul.
25. **Khazaei, B.,** Khatami, S., Alemohammad, S.H., Wu, C., Madani, K., Kalantari, Z., Destouni, G. and Aghakouchak, A. 2019. Using observed hydro-climatic and land-use changes to explain the desiccation of Lake Urmia. European Geosciences Union 2019, Vienna, Austria, 7–12 Apr.
26. **Khazaei, B.,** Bajgiran, A.H., Bartlett, S.L. and Bravo, H.R. 2018. Monitoring water quality in Green Bay using MODIS imagery data. American Geophysical Union 2018 Fall Meeting, Washington, D.C., 10–14 Dec.
27. Bajgiran, A.H., **Khazaei, B.**, Khatami, S. and Parolari, A. 2018. Anomaly detection in hydro-climatic time series of Lake Urmia. American Geophysical Union 2018 Fall Meeting, Washington, D.C., 10–14 Dec.
28. Khazaei, H., **Khazaei, B.** and Davary, K. 2018. Long-term monitoring of groundwater quality and quantity in Neyshabur basin, Iran. American Geophysical Union 2018 Fall Meeting, Washington, D.C., 10–14 Dec.
29. **Khazaei, B.** and Hamidi, S.A. 2018. Application of learning systems in water quality monitoring of Green Bay estuary, US. CUAHSI 2018 Biennial Colloquium, National Conservation Training Center in Shepherdstown, WV, 29 Jul–1 Aug.
30. Bravo, H.R., Bootsma, H.A. and **Khazaei, B.** 2018. Assimilation of phosphorus from a point source in the Lake Michigan nearshore zone. International Association for Great Lakes Research 2018 Meeting, Toronto, Canada, 18–22 Jun.
31. **Khazaei, B.**, Hamidi, S.A., Houghton, S., Bartlett, S. and Bravo, H.R. 2018. On the relation between sediment concentration and water quality parameters in the Green Bay of Lake Michigan. Association for the Sciences of Limnology and Oceanography 2018 Summer Meeting, Victoria, Canada, 10–15 Jun.
32. **Khazaei, B.**, Bravo, H.R. and Bootsma H.A. 2017. Using a hydrodynamic and biogeochemical model to investigate the effects of nutrient loading from a wastewater treatment plant into Lake Michigan. American Geophysical Union 2017 Fall Meeting, New Orleans, LA, 11–15 Dec.
33. **Khazaei, B.,** Hamidi, S.A., Hosseiny, H. and Ekhtari, N. 2017. A satellite imagery approach to monitor turbidity and total suspended sediments in Green Bay, WI. American Geophysical Union 2017 Fall Meeting, New Orleans, LA, 11–15 Dec.
34. **Khazaei, B.**, Khatami, S., Rashidi, L. and Madani, K. 2016. Hydro-climatic investigation of Lake Urmia shrinkage using remote sensing. American Geophysical Union 2016 Fall Meeting. San Francisco, Calif., 12–16 Dec.

Professional Activities & Other Skills

Invited Seminars & Presentations

2017	Modeling the transport and fate of phosphorus from a point source in the Lake Michigan nearshore zone, FUM
2013	Civil & Environmental Engineering in the New World, FUM

Professional Affiliations

2019-present	Committee Member, AGU Hydrology Section Student Subcommittee (H3S)
2017-present	Member, American Society of Civil Engineers
2017-present	Member, European Geosciences Union
2016-present	Member, American Geophysical Union
2017-2020	President, Water Environment Federation student chapter at UWM
2010-2012	Member, Science Committee, GIS Association at FUM

Skills

2019	PADI Open Water Scuba Diving